T.C.

AKDENİZ ÜNİVERSİTESİ

İÇME SUYU DAĞITIM ŞEBEKELERİNDE İLERİ BASINÇ YÖNETİMİ İLE SU KAYIPLARININ AZALTILMASINA YÖNELİK MODELLEME ÇALIŞMASI: ANTALYA-KALEİÇİ BÖLGESİ UYGULAMASI

Mustafa S. M. BOLBOL

FEN BİLİMLERİ ENSTİTÜSÜ

ÇEVRE MÜHENDİSLİĞİ

ANABİLİM DALI

YÜKSEK LİSANS TEZİ

HAZİRAN 2019

ANTALYA

T.C.

AKDENİZ ÜNİVERSİTESİ

FEN BİLİMLERİ ENSTİTÜSÜ

**İÇME SUYU DAĞITIM ŞEBEKELERİNDE İLERİ BASINÇ YÖNETİMİ İLE
SU KAYIPLARININ AZALTILMASINA YÖNELİK MODELLEME
ÇALIŞMASI: ANTALYA-KALEİÇİ BÖLGESİ UYGULAMASI**

Mustafa S. M. BOLBOL

ÇEVRE MÜHENDİSLİĞİ

ANABİLİM DALI

YÜKSEK LİSANS TEZİ

Bu tez 11/06/2019 tarihinde jüri tarafından Oybirliği / ~~Oyçokluğu~~ ile kabul edilmiştir.

Prof. Dr. Habib MUHAMMETOĞLU (Danışman)

Prof. Dr. Ayşe Burcu Altan SAKARYA

Dr. Öğr. Üyesi Firdes YENİLMEZ

ÖZET

İÇME SUYU DAĞITIM ŞEBEKELERİNDE İLERİ BASINÇ YÖNETİMİ İLE SU KAYIPLARININ AZALTILMASINA YÖNELİK MODELLEME ÇALIŞMASI: ANTALYA-KALEİÇİ BÖLGESİ UYGULAMASI

Mustafa S. M. BOLBOL

Yüksek Lisans, Çevre Mühendisliği Anabilim Dalı

Danışman: Prof. Dr. Habib MUHAMMETOĞLU

Haziran 2019; 190 sayfa

Her ülkedeki içme suyu idareleri, hizmetlerinin gelirini ve kapasitesini artırmak için içme suyu dağıtım şebekelerindeki su kayıplarını en aza indirmeye çalışmaktadır. Basınca bağlı bir akış olan sızıntı, içme suyu dağıtım şebekelerinde önemli bir su kaybı türüdür. Bu nedenle, basınç yönetimi (BY), su kayıplarını azaltmada kullanılan ana yöntemlerden biridir. Klasik BY, su basıncını her zaman sabit bir seviyeye düşürmeyi amaçlamaktadır ve istisnai su taleplerinin etkilerini göz ardı etmektedir; örneğin yangın ihtiyacı. Diğer yandan, ileri BY, içme suyu dağıtım şebekesinde kritik noktalardaki (KN) basıncı her zaman izin verilen en düşük seviyede tutmayı ve olağanüstü su taleplerini karşılamayı amaçlamaktadır. Buna istinaden, ileri BY, sızıntıyı klasik BY'den daha fazla azaltır. Hidrolik modelleme, su kayıplarını azaltmak için BY uygulanmasında temel bir araçtır. Bu tez çalışmasında, Kaleiçi içme suyu dağıtım şebekesinin hidrolik modellemesi, Hazen-Williams denklemi kullanılarak EPANET 2.0 yazılımı ile yapılmıştır. Her boru boyunca eşit olarak dağılmış bir sızıntı varsayılarak, toplam sızıntı, her bir düğüm noktasına bağlı boruların yarı uzunlukları tarafından belirlenen sızıntı katsayıları ile tanımlanmış ve modeldeki tüm düğüm noktalarına dağıtılmıştır. Bu yöntemle, sızıntı miktarı mekânsal ve zamansal olarak tahmin edilmiştir. Pürüzlülük katsayısı ve basınç katsayısı gibi bazı parametrelerin model sonuçları üzerindeki etkisi incelenmiştir. Boru pürüzlülük katsayısı tüm borular için tek bir değer için (57,6) kalibre edilmiş ve doğrulanmıştır. Doğrulanan pürüzlülük değerine istinaden, ileri BY ile elde edilen sızıntı azalmasının, yaz ve kış aylarında iki simülasyon dönemi boyunca sırasıyla 6,82 m^3/s ve 5,79 m^3/s olacağı tahmin edilmiştir. Son olarak, ileri BY ile sızıntı azalmasına ilişkin iki senaryo incelenmiştir. İlk senaryoda gelecekteki sızıntı olmayan akış değişimi ±%25 oranında varsayılırken, diğer senaryoda sızıntının su kayıpları ekonomik seviyesine (SKES) düşürüldüğü varsayılmaktadır. Mekânsal ve zamansal sızıntı tahminleri elde edilerek her senaryonun KN'deki basınç tahminleri üzerindeki etkisi gösterilmiştir. Hidrolik modellemenin, sızıntının mekânsal ve zamansal tahmini için önemli bir araç olduğu bulunmuştur.

ANAHTAR KELİMELER: Antalya, EPANET, hidrolik modelleme, ileri basınç yönetimi, mekânsal ve zamansal sızıntı tahminleri, sızıntı modelleme.

JÜRİ: Prof. Dr. Habib MUHAMMETOĞLU

       Prof. Dr. Ayşe Burcu Altan SAKARYA

       Dr. Öğr. Üyesi Firdes YENİLMEZ

ABSTRACT

ORIENTED MODELLING FOR REDUCING WATER LOSSES IN DRINKING WATER DISTRIBUTION NETWORKS BY ADVANCED PRESSURE MANAGEMENT: ANTALYA – KALEİÇİ CASE STUDY

Mustafa S. M. BOLBOL

MSc Thesis in Environmental Engineering

Supervisor: Prof. Dr. Habib MUHAMMETOĞLU

June 2019; 190 Pages

The water utilities in each country strive to minimize water losses in their water distribution networks (WDNs) to increase the revenue and the capacity of their services. Leakage, which is a flow driven by pressure, is an important type of water losses in WDNs. Hence, pressure management (PM) is one of the principal techniques used for leakage reduction. The classical PM aims at reducing water pressure to a fixed level all the time and ignores the impacts of exceptional water demands, e.g. fire demands. The advanced PM aims at keeping the pressure at the critical points (CPs) in the WDN at the minimum allowable levels all the time besides satisfying the extraordinary water demands as well. Therefore, the advanced PM reduces leakage more than classical PM. Hydraulic modeling is a fundamental tool in applying PM for leakage reduction. In this thesis study, hydraulic modeling of Kaleiçi WDN has been carried out by EPANET 2.0 software using Hazen-Williams equation. Volume of leakage was determined by the standard water balance. Assuming a uniformly distributed leakage along each pipe, the total leakage has been distributed to all junctions in the model by defining the leakage coefficients, which are determined by the half-length of the pipes connected to each junction. Consequently, the leakage has been predicted spatially and temporally. The impact of several parameters such as roughness coefficient and leakage exponent on the precision of modeling has been investigated. The pipe roughness coefficients have been calibrated and verified for a value of 57.6. Depending on the verified roughness value, the leakage reduction by an advanced PM technique has been predicted over two simulation periods in summer and winter to be 6.82 m^3/h and 5.79 m^3/h, respectively. Finally, two scenarios related to leakage reduction by advanced PM have been examined. The first scenario assumes a future change of non-leakage flow by ±%25, while the other scenario assumes that leakage is reduced to the economic leakage level (ELL). The spatial and temporal leakage predictions and the impact of each scenario on the predicted pressure at the CP have been shown in the results. It has been found that hydraulic modeling is an essential tool for spatial and temporal prediction of leakage.

KEYWORDS: Advanced pressure management, Antalya, EPANET, hydraulic modeling, leakage modeling, leakage prediction in space and time.

COMMITTEE: Prof. Dr. Habib MUHAMMETOĞLU

Prof. Dr. Ayşe Burcu Altan SAKARYA

Asst. Prof. Firdes YENİLMEZ

ÖNSÖZ

Bu tez çalışması kapsamında, içme suyu dağıtım şebekesindeki su kayıplarının ileri basınç yönetimi ile azaltılması ve hidrolik modelleme uygulaması ile incelenmesi hedeflenmiştir. Çalışmada dünyada yaygın olarak kullanılan EPANET hidrolik modeli uygulanarak, Kaleiçi çalışma bölgesi içinde oluşan sızıntı debisinin mekânsal ve zamansal olarak içme suyu dağıtım şebekesindeki tüm düğüm noktalarındaki dağılımı tahmin edilmiştir. Bu uygulamada kullanılan ileri basınç yönetimi tekniği ile fiziki su kayıplarının kontrolü gerçekleştirilebilmektedir. Bu tez çalışmasında kullanılan veri seti, Prof. Dr. Habib MUHAMMETOĞLU'nun yürütücüsü olduğu ve yakın süre önce tamamlanmış olan 114Y168 nolu TÜBİTAK projesi veri tabanından elde edilmiştir.

AKADEMİK BEYAN

Yüksek Lisans Tezi olarak sunduğum "İçme Suyu Dağıtım Şebekelerinde İleri Basınç Yönetimi İle Su Kayıplarının Azaltılmasına Yönelik Modelleme Çalışması: Antalya-Kaleiçi Bölgesi Uygulaması" adlı bu çalışmanın, akademik kurallar ve etik değerlere uygun olarak yazıldığını belirtir, bu tez çalışmasında bana ait olmayan tüm bilgilerin kaynağını gösterdiğimi beyan ederim.

11/06/2019

Mustafa S. M. BOLBOL

İÇİNDEKİLER

SİMGELER VE KISALTMALAR

Simgeler

%	: Yüzde
γ	: Basınç katsayısı
ε	: Sızıntının tolerans değeri
C	: Sızıntı katsayısı
C_j	: Düğüm noktasının sızıntı katsayısı
C_{net}	: Sistemin toplam sızıntı katsayısı
$C_{net}{}^f$	: Son kalibre edilen toplam sızıntı katsayısı
L_j	: (j) düğüm noktasının göreceli önem faktörü
l_i	: (i) borusunun uzunluğu
l_j	: (j) düğüm noktasıyla bağlantılı tüm boruların yarı uzunluktaki toplamı
m^3/h	: Saatte bir metreküp
m^3/y	: Yılda metreküp
P_j	: Düğüm noktasındaki basınç
P_{net}	: Sistemin ortalama basıncı
Q_A	: İzinli tüketim
Q_{AL}	: İdari kayıplar
Q_{BA}	: Faturalandırılmış İzinli Su Tüketimi
Q_{BDj}	: Düğüm noktasının su talebi
Q_I	: Sisteme giren su miktarı
Q_j	: Düğüm noktasındaki sızıntı
Q_L	: Su kayıpları
$Q_{net,model}$	: Tahmin edilen toplam dağılmış sızıntı
$Q_{net,real}$	: Hesaplanan toplam gerçek sızıntı
Q_{RL}	: Fiziki kayıplar

Q_{UA} : Faturalandırılmamış İzinli Su Tüketimi

R_i : Sürtünme katsayısı denemesi

Kısaltmalar

ALC   : Active Leakage Control

ASAT   : Antalya Su ve Atıksu İdaresi

AWWA : American Water Works Association

BÖN   : Basınç Ölçüm Noktası

BY   : Basınç Yönetimi

DMA   : Alt Bölge (District Metered Area)

GGS   : Gelir Getirmeyen Su

IWA   : International Water Association

İDŞ   : İçme suyu Dağıtım Şebekesi

KN   : Kritik Nokta

mSS   : Metre Su Sütunu

NRW   : Gelir getirmeyen su (Non-Revenue Water)

OHM   : Ortalama Mutlak Hata

PI   : Performans indikatörü (Performance Indicator)

PRV   : Basınç düşürücü vana (Pressure Reducing Valve)

SCADA : Supervisory Control and Data Acquisition

SKES   : Su Kayıpları Ekonomik Seviyesi

SSD   : Standart Su Dengesi

TÜİK   : Türkiye İstatistik Kurumu

USEPA : United States Environmental Protection Agency

WHO   : Dünya Sağlık Örgütü (World Health Organisation)

ŞEKİLLER DİZİNİ

ÇİZELGELER DİZİSİ

1. GİRİŞ

Dünya Sağlık Örgütü'ne (WHO) göre, dünya nüfusunun yalnızca % 71'ine günlük yaşam için güvenli ve sürekli su temin edilmektedir. Ayrıca, dünya nüfusunun birçok bölgesinin 2025 yılına kadar su kıtlığıyla karşı karşıya kalacağı beklenmektedir (WHO 2015). Su kaynaklarının tükenmesini ve su yetersizliğini önlemek için ana faktörlerden biri, su temini sistemlerindeki su kayıplarını azaltmaktır.

Teknik olarak, herhangi bir içme suyu dağıtım şebekesindeki (İDŞ) su kayıpları iki gruba ayrılır; idari (görünmeyen) su kaybı ve fiziki (gerçek) su kaybı. İdari su kayıpları izinsiz su tüketimi, veri işleme hataları ve sayaç endeks okuma hatalarıdır ve bunların azaltılmasıyla gelir getiren su miktarı artar. Fiziki su kaybı (başlıca sızıntılar) basınca bağlı su kaybı türüdür ve genel olarak tüm dünyadaki su kayıplarının büyük bölümünü oluşturur ve fiziki su kayıplarını azaltmak, herhangi bir İDŞ'de sisteme giren su hacmini azaltır (Muhammetoglu ve Muhammetoglu 2017). Ayrıca, içme suyu idarelerinin İDŞ'lerde gerçek kayıpları mümkün olan en düşük limitlerde tutma çabaları, enerji tüketimini ve su kaynaklarının aşırı kullanımı ile ilgili riskleri azaltmayı hedeflemektedir (Danish Environmental Protection Agency 2018).

Sızıntıyı azaltmak için yaygın olarak kullanılan teknik, basınç yönetimidir (BY). Bu uygulamadaki temel prensip basıncı minimum seviyelerde tutmak ve İDŞ dahilindeki maksimum yasal seviyeleri aşmamaktır. Hidrolik modelleme, basıncın çoğu zaman minimum veya maksimum olduğu kritik basınç noktalarının konumunu tahmin etmek için kullanılır ve BY uygulamasını gerektirir. Bu tez çalışması için Antalya'da bulunan Kaleiçi İDŞ pilot çalışma alanı olarak seçilmiştir. Kaleiçi İDŞ'nin hidrolik modeli, Hazen-Williams denklemine göre EPANET 2.0 yazılımı kullanılarak yapılmıştır (USEPA 2000).

Bu tez çalışmanın temel amacı, her bir düğüm noktasındaki basıncı hidrolik model ile tahmin ederek, sızıntı debisinin mekânsal ve zamansal olarak İDŞ'deki tüm düğüm noktalarındaki dağılımını tahmin etmektir. Kaleiçi İDŞ'deki toplam sızıntı miktarı, daha önce tamamlanan bir araştırma projesi kapsamında standart su dengesi (SSD) tabloları kullanılarak aylık olarak hesaplanmıştır. Tez çalışması amacına ulaşmak için, boruların sürtünme katsayılarının, sızıntı katsayısının ve basınç katsayısının belirlenmesi gerekmektedir. Bu çalışmada SSD'den hesaplanan sızıntı debileri, mekânsal ve zamansal olarak düğüm noktalarına dağıtılmaktadır. Çalışma kapsamında başka hedeflere de ulaşılmıştır; (a) İDŞ'lerle ilgili literatürün su kayıpları, hidrolik modelleme ve ileri BY uygulamalarına ilişkin vaka çalışmaları açısından incelenmesi, (b) Kaleiçi İDŞ için oluşturulan SSD'nin incelenmesi, (c) SSD'den hesaplanan sızıntı debisinin Kaleiçi İDŞ düğüm noktalarına dağıtılması ve hidrolik modelleme uygulaması, (d) hidrolik modelin kalibrasyonu ve doğrulaması, (e) ileri BY uygulaması, (f) ileri BY uygulamasıyla sızıntı azaltımının tahmin edilmesi, (g) ileri BY uygulamalarının iki senaryo koşulu için incelenmesi (1. Senaryo: sızıntı olmayan debide ±% 25 oranında bir değişiklik olması, 2. Senaryo: sızıntının su kayıpları ekonomik seviyesine (SKES) kadar azaltılması).

Tez çalışması beş bölümden oluşmaktadır. Birinci bölümde araştırılan konu belirtilmekte ve tezin amaçları tanımlanmaktadır. İkinci bölümde su kayıpları ve örnek çalışmalar ile ilgili literatür incelenmektedir. Üçüncü bölümde, pilot çalışma alanındaki gerçek su kayıplarını dağıtmak ve ileri BY uygulamak için kullanılan metodoloji açıklanmaktadır. Dördüncü bölümde, uygulanan metodolojinin bulguları ve tartışmaları

sunulmaktadır. Sonuçlar ve gelecek araştırmalar için öneriler ise beşinci bölümde verilmektedir.

2. KAYNAK TARAMASI

2.1. İçme Suyu Temin ve Dağıtım Sistemlerindeki Su Kayıpları

Her İDŞ'de su kaybı genel bir kavram olarak, oluşma çeşidine göre iki ana bölüme ayrılır; fiziki (gerçek) su kaybı ve idari (görünmeyen) su kaybı. Basınca bağlı bir akış olan sızıntı, gerçek su kayıplarının en büyük kısmını oluşturur. Çizelge 2.1'de gösterilen SSD, periyodik olarak su kayıplarının hesaplanması için gerekmektedir. Su kayıplarının her türünün tanımı, sızıntı ve SSD hakkında detaylı bilgiler Ek-1 (sayfa 3-5)'te sunulmuştur (Thornton vd. 2008).

Çizelge 2.1 IWA/AWWA uluslararası standart su dengesi (Fanner vd. 2007a)

Sisteme Giren Su Miktarı (Q$_I$)	İzinli Tüketim (Q$_A$)	Faturalandırılmış İzinli Su Tüketimi (Q$_{BA}$)	Faturalandırılmış Ölçülmüş Kullanım	Gelir Getiren Su Miktarı
			Faturalandırılmış Ölçülmemiş Kullanım	
		Faturalandırılmamış İzinli Su Tüketimi (Q$_{UA}$)	Faturalandırılmamış Ölçülmüş Kullanım	Gelir Getirmeyen Su Miktarı (GGS)
			Faturalandırılmamış Ölçülmemiş Kullanım	
	Su Kayıpları (Q$_L$)	İdari Kayıplar (Q$_{AL}$)	İzinsiz Tüketim	
			Sayaçlardaki Ölçüm Hataları ve Veri İşleme Hataları	
		Fiziki Kayıplar (Q$_{RL}$)	Temin ve Dağıtım Hatlarında Oluşan Kayıp Kaçaklar	
			Depolarda Meydana Gelen Kaçak ve Taşmalar	
			Servis Bağlantılarında Oluşan Kayıp Kaçaklar	

2.1.1. Gelir getirmeyen suyun (GGS) dünyadaki ve Türkiye'deki durumu

Uluslararası literatürde, GGS, İDŞ'de dağıtılan ancak faturalandırılması yapılmayan suları açıklamak için kullanılan yenilikçi bir ifadedir. GGS, su kayıpları ve faturalandırılmamış izinli su tüketiminin toplamıdır (Lambert 2003). Dünya genelinde, gerçek su kayıplarının yüzdesi yaklaşık %60 ve geri kalan kısım ise idari su kayıpları (%40) olarak kabul edilmektedir. Su kayıpları hiçbir zaman sıfır olamaz ancak mümkün olduğunca en aza indirilebilmektedir (Muhammetoglu ve Muhammetoglu 2017). Şekil 2.1'de gösterildiği gibi, GGS gelişmiş ülkelerde %10 seviyesinin altında iken gelişmekte

olan ülkelerde %50'nin üstüne çıkmaktadır. Türkiye'de, 2004-2016 yılları arasında, GGS yaklaşık %60'tan %36'ya kadar indirilmiştir (Şekil 2.2). Diğer ülkeler ve Türkiye'deki GGS hakkında detaylar Ek-1 (sayfa 5-10)'da verilmiştir.
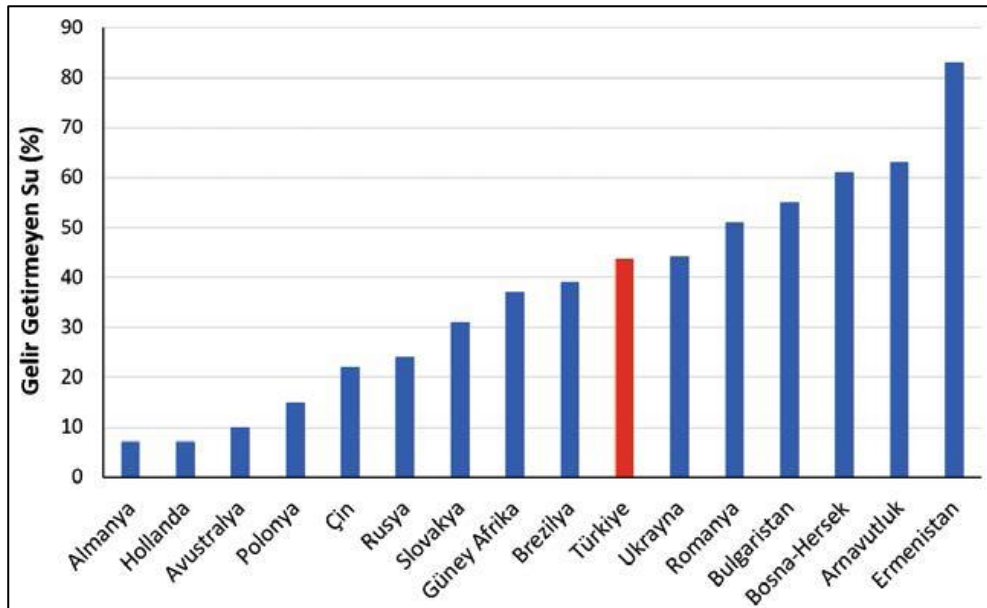
Şekil 2.1. 2010 yılı için bazı ülkelerde Gelir Getirmeyen Su seviyeleri (Muhammetoglu ve Muhammetoglu 2017)
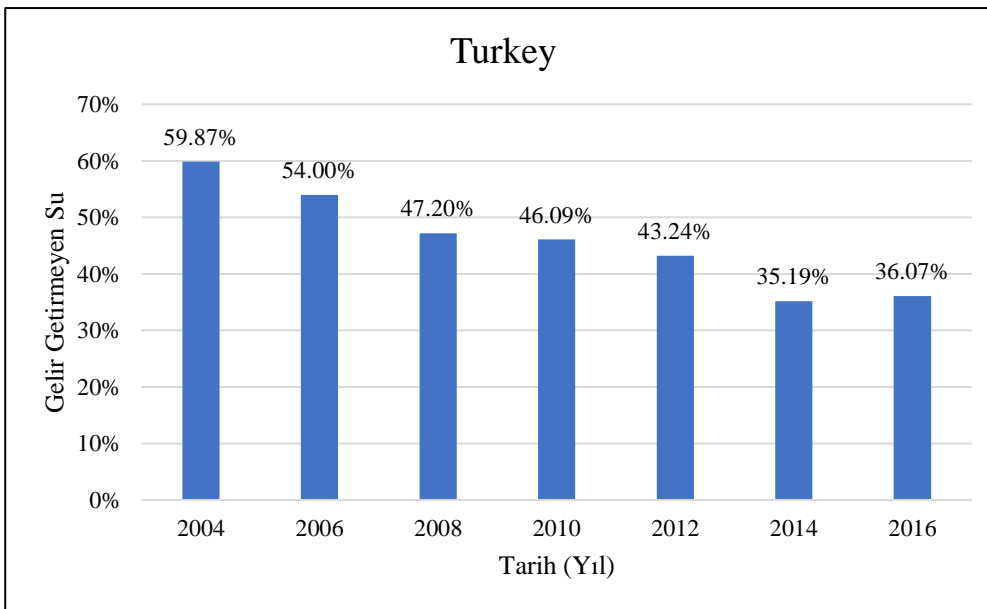
Şekil 2.2. Türkiye'de 2004-2016 yılları için GGS seviyeleri (TÜİK 2018)

2.2. Sızıntı Yönetim Teknikleri

Herhangi bir İDŞ'deki su kayıplarını değerlendirmek amacıyla, Uluslararası Su Kuruluşu (IWA) ve Amerikan Su İşleri Kuruluşu (AWWA) bir metodoloji önermektedir.

Bu metodoloji iki aşamadan oluşmaktadır. İlk aşamada periyodik olarak SSD hesaplanır ve ikinci aşamada ise seçilen bir su kaybı performans indikatörü (PI) kullanılarak farklı büyüklükteki İDŞ'ler için su kayıpları değerlendirilir. Belirtilen metodoloji ve PI'ler hakkında ayrıntılı bilgiler Ek-1 (sayfa 11-12)'de verilmiştir. Sızıntıyı daha iyi anlamak için, sızıntı tipleri, sızıntı tespit teknikleri ve sızıntı tespitini etkileyen faktörlere ilişkin detaylar Ek-1 (sayfa 12 – 18)'de sunulmuştur. IWA, fiziki su kayıplarını azaltmak için Şekil 2.3'te sunulan dört temel yöntemi önermektedir. 'te sunulan alt bölge (DMA) oluşumu, İDŞ'nin yönetilmesi için önemli altyapısal prensiplerden biridir. Alt bölgeler hakkında daha fazla bilgi Ek-1 (sayfa 15 – 18)'de verilmiştir.
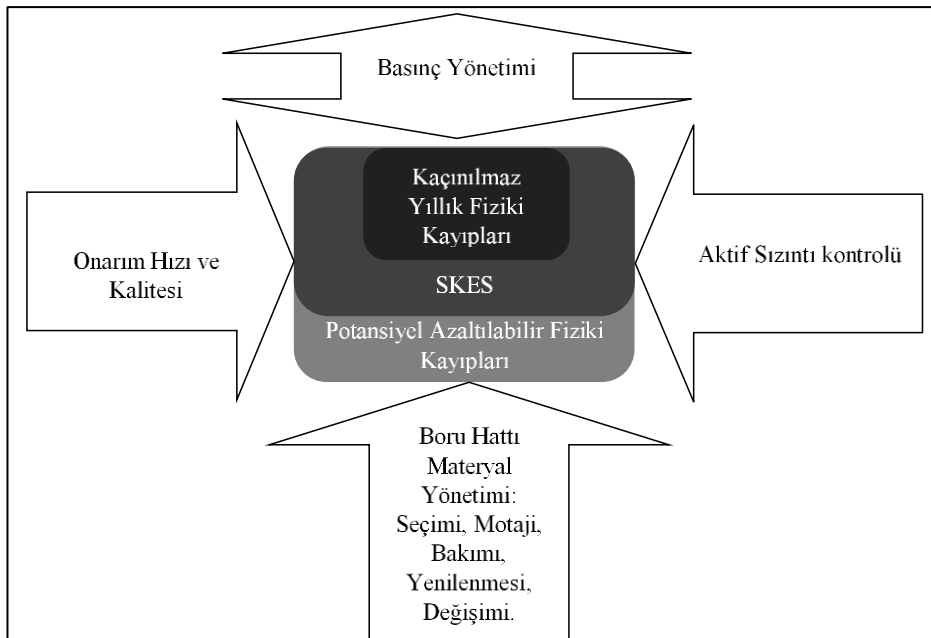
Şekil 2.3. Fiziki su kayıplarının yönetimi için dört temel teknik (Pilcher vd. 2007)
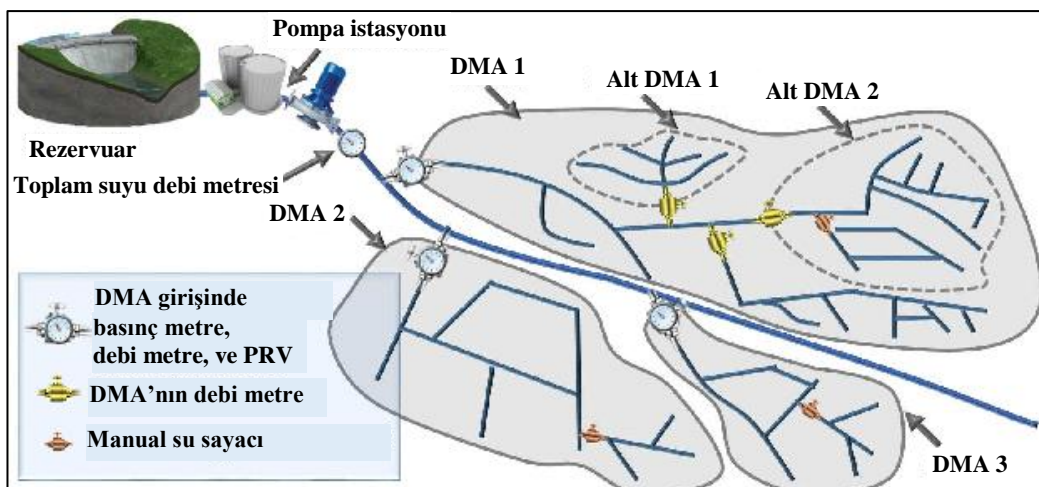
Şekil 2.4. DMA oluşumu ve her DMA girişinde takılan vanaların genel düzeni (Kartakis vd. 2015)

2.2.1. Basınç yönetimi (BY)

Sızıntı basınçla akan bir debi olduğundan, su idareleri tarafından sızıntı azaltması için gerçekleştirilebilecek en önemli teknik BY'dir. Şekil 2.5' te gösterilen BY kavramına göre, İDŞ'deki tüm düğüm noktalarında özellikle en düşük su basıncına sahip olan kritik noktalardaki (KN) basıncın her zaman minimum seviyelerde tutulması hedeflenmektedir. BY, klasik yöntemleri ve ileri yöntemleri içermektedir. Bu tez çalışmasında, hidrolik model uygulaması ile birlikte ileri bir BY tekniği uygulanmıştır. Klasik ve ileri BY teknikleri ile ilgili detaylı bilgiler Ek-1 (sayfa 19 – 23)'te verilmiştir.
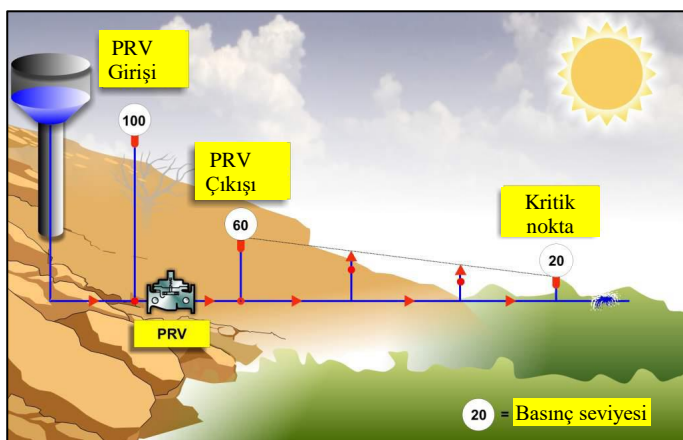
Şekil 2.5. BY ile kritik noktadaki su basıncının 20 mSS seviyesinde tutulması (Mckenzie ve Wegelin 2009)

2.3. İçme Suyu Dağıtım Şebekelerinde Hidrolik Modelleme

Hidrolik modelleme, kompleks ve büyük içme suyu temin ve dağıtım sistemlerinin yönetilmesinde ve herhangi bir İDŞ için uygun BY tekniğin tanımlanması için önemlidir. Herhangi bir hidrolik modelleme çalışması, İDŞ'nin tüm unsurlarını içeren boruları, pompaları, rezervuarları, basınç düşürücü vanaları (PRV) ve su tüketimi verilerini içermelidir. İyi bir hidrolik model oluşturmak için araştırılan İDŞ'in bileşenleri hakkında yüksek düzeyde ayrıntıya, basınç kontrol prosesleri için geri bildirim olarak kullanılan tüm veri kaynaklarına ve çıktılara erişim gereklidir. Gelecekteki koşullara ilişkin analizler ve iyileştirmeler için kayıtların tutulması ve uzun süreli modelleme için güçlü simülasyon ekipmanı ve araçlarına ihtiyaç duyulmaktadır (Mpiana vd. 2017). Hidrolik model BY uygulamasında İDŞ'nin kritik noktalarını tespit etmek için kullanılabilmektedir. Su kalitesi ve hidrolik modellemesi için kullanılan yazılımlardan bir EPANET'tir (Koker ve Altan-Sakarya 2016)(Köker ve Altan-Sakarya 2015). BY uygulamasında hidrolik modelin nasıl kullanılacağı hakkında daha ayrıntılı bilgiler Ek-1 (sayfa 23 – 24)'te verilmiştir.

2.4. Örnek Çalışmalar

İDŞ'lerde hidrolik modelleme uygulaması, özellikle su kayıpları modellemesi konusunda, su kuruluşlarındaki karar vericilerin ve teknik personelin karar vermesine yardımcı olmaktadır. Schwaller ve van Zyl (2014)'a ait bir araştırmada İDŞ'de çok sayıda rastgele olarak dağılmış sızıntılar hidrolik model ile simüle edilmiştir. Bahsedilen

çalışmanın amacı, saha çalışmalarında belirlenen basınç katsayısının, modelde aynı davranışı sağlayıp sağlayamayacağını belirlemektir. Çalışmanın sonucunda, ortalama basınç katsayısının büyük su temini sistemlerinde yaklaşık 1 olduğu ve bu katsayının sistem basıncından çok fazla etkilendiği ortaya konulmuştur. EPANET yazılımı, su kayıplarının tespit edilmesinde, gerçek sızıntı senaryosuna göre Barcelona İDŞ'de bulunan bir alt bölgede kullanılmıştır. Barcelona'da bulunan alt bölge için gerçekleştirilen gerçek zamanlı hidrolik modelleme çalışması ile gerçek arıza senaryosunun tatmin edici sonuçlar verdiği görülmüş ve sızıntı tespitinde hidrolik modellerin kullanılmasının etkinliği ve güvenilirliği vurgulanmıştır (Ramon vd. 2014). Konuya ilişkin daha fazla örnek çalışmalara ait ek bilgiler Ek-1 (sayfa 24 – 27)'de verilmiştir.

3. MATERYAL VE METOT

3.1. Çalışma Sahası ve Özelikleri, Antalya – Kaleiçi

Antalya Su ve Atık Su idaresi (ASAT), Antalya ilinde yer alan 19 ilçede içme suyu temini ve atıksu bertarafı sistemlerinin yönetiminden sorumludur. Çalışma sahası olan Kaleiçi bölgesi, Muratpaşa ilçesinde bulunmaktadır. Kaleiçi İDŞ'de 2014-2018 yılları arasında Prof. Dr. Habib MUHAMMETOĞLU'nun yürütücülüğünde "Turistik Bölgelerde Otomatik Okuma Sayaçları Kullanılarak Fiziki Su Kayıplarının Yüksek Hassasiyetle Belirlenmesi ve Yönetimi: Antalya-Kaleiçi Uygulaması" başlıklı bir TÜBİTAK araştırma projesi yürütülmüştür. Proje kapsamında Kaleiçi bölgesinde bulunan abonelerin bir kısmı için günlük ve saatlik su tüketimleri belirlenmiş, aylık ve yıllık SSD tabloları oluşturulmuş, PI'ler ve su kayıpları ekonomik seviyesi (SKES) hesaplanmıştır. Kaleiçi İDŞ, bir alt bölge (DMA) olarak inşa edilmiştir ve Antalya'daki diğer İDŞ'lerden hidrolik olarak bağımsızdır. Kaleiçi İDŞ girişinde mevcut olan bir SCADA online izleme istasyonu ile gerçek zamanlı olarak bazı veriler izlenebilmektedir. Bu sistem ile DMA girişindeki debi ve su basıncı değerleri beş dakika zaman aralığında sürekli ölçülmekte ve kaydedilmektedir. Ek olarak, Şekil 3.1'de gösterildiği gibi, TÜBİTAK projesi kapsamında İDŞ içinde seçilen yedi farklı basınç ölçüm noktasında (BÖN) yerleştirilen taşınabilir basınç ölçüm cihazları ile beş dakika zaman aralığında su basıncı değerleri sürekli olarak izlenmiş ve kaydedilmiştir. TÜBİTAK projesinde klasik BY ve su tasarrufu ile ilgili öneriler sunulmuştur (Muhammetoğlu 2017). Antalya ili, çalışma sahasının özellikleri ve TÜBİTAK araştırma projesi hakkında daha ayrıntılı bilgiler Ek-1 (sayfa 29 – 32)'de verilmiştir. TÜBİTAK projesi kapsamında elde edilen veri setleri ve proje sonuçları, yüksek lisans tez çalışmasında gerçekleştirilen uygulamalar ve hesaplamalar için temel referans kaynaklardır.
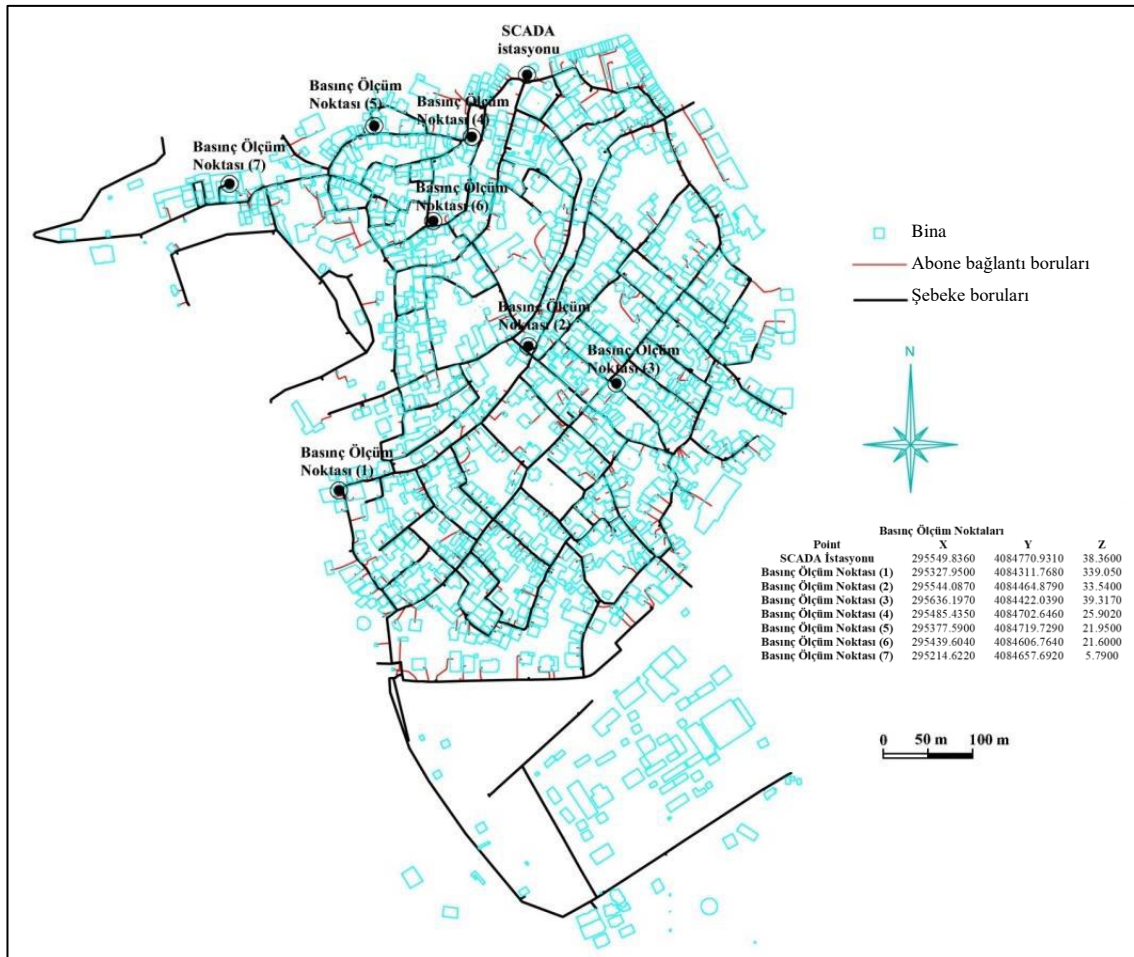
Şekil 3.1. Çalışma sahasında basınç ölçüm noktalarının konumları (Not: Z: Basınç ölçüm noktasının kotu, koordinatlar UTM cinsindendir) (Muhammmetoğlu 2017'den alınmıştır)

3.2. Sızıntı Modelleme Yaklaşımı

Kaleiçi İDŞ'sinin hidrolik modellemesi için EPANET yazılımı kullanılmıştır. DMA girişinde kaydedilen sisteme giren su miktarı, sızıntı ve sızıntı olmayan debi olarak ayrılmıştır. EPANET'te, her düğüm noktası için sonuçlarda rapor edilen gerçek talep, hem düğüm noktasındaki su tüketimini (sızıntı olmayan debi), hem de sızıntıyı içermektedir. Sızıntı debisi, Eşitlik 3.1'de gösterildiği gibi deşarj katsayısı, düğüm noktasının basıncı ve basınç katsayına bağlıdır:

$$q = Cp^{\gamma} \tag{3.1}$$

Bu eşitlikte q: sızıntı debisi, C: sızıntı katsayısı, p: düğüm noktasının basıncı, γ: basınç katsayısı (Rossman 2000).

Hidrolik olarak, sızıntı olmayan debinin artması, düğüm noktasındaki basıncın azalmasına sebep olmakta ve buna bağlı olarak daha az sızıntı meydana gelmektedir (Muhammetoglu ve Muhammetoglu 2017). Eşitlik 3.1 kullanılarak, sızıntı debisi her düğüm noktasında basınca bağlı bir akış olarak modellenmektedir. Bu arada, Cobacho Jordán vd. (2015) tarafından geliştirilen bir yaklaşımda, EPANET yazılımı kullanılarak

9

mekânsal ve zamansal sızıntı modellemesi için, sızıntının boru uzunluğuna eşit olarak dağıldığı varsayılmıştır. Bu yaklaşımı uygulayabilmek için öncelikle üç parametrenin tanımlanması gereklidir. Bu parametreler, toplam İDŞ sızıntı debisi, boru sürtünme katsayısı ve basınç katsayısıdır. Sızıntı ve sızıntı olmayan akışlar, basınç değerleri ve önerilen yaklaşımla ilgili bir şema ve detaylar Ek-1 (sayfa 32 – 33)'te sunulmuştur.

Önerilen yaklaşım, mekânsal ve zamansal sızıntı simülasyonunu iki aşamada elde etmektedir. Bu aşamalar İDŞ'deki toplam sızıntının mekânsal dağılımı ve her bir düğüm noktasındaki sızıntı katsayısının hesaplanmasıdır. Bu yaklaşım tez çalışması kapsamında Kaleiçi İDŞ'ye uyarlanmıştır.

3.2.1. Toplam sızıntının mekânsal dağılımı

Hem sızıntı debisinin, hem de sızıntı olmayan debinin boru uzunluğu ile eşit dağıldığı varsayımı matematiksel olarak bu aşamada gerçekleştirilmektedir. Eşitlik 3.2'de, (l_i), (j) düğüm noktasıyla bağlantılı olan (i) borusunun uzunluğunu ifade etmekte ve (l_j), (j) düğüm noktasıyla bağlantılı olan tüm boruların yarı uzunluktaki toplamını ifade etmektedir. (L_j), her bir düğüm noktasının, İDŞ'deki toplam sızıntıya kıyasla sızıntı açısından göreceli önemini belirten bir faktörü temsil etmektedir. (L_j), Eşitlik 3.3 kullanılarak hesaplanmaktadır.

$$l_j = \sum_{i=1}^{m_j} \frac{l_i}{2} \tag{3.2}$$

$$L_j = \frac{l_j}{\sum l_i} = \frac{l_j}{l_{net}} \tag{3.3}$$

3.2.2. Sızıntı katsayılarının kalibrasyonu

Bu aşamada, her bir düğüm noktasındaki sızıntı katsayısı (C) deneme yanılma yöntemiyle aşamalı olarak kalibre edilmektedir. Öncelikle, İDŞ'deki toplam sızıntı katsayısının ($C_{Net}^{(1)}$) hesaplanmasıyla ilk iterasyon başlamaktadır (Eşitlik 3.4):

$$C_{Net}^{(1)} = \frac{Q_{Net,real}}{P_{Net}^{\gamma}} \tag{3.4}$$

Bu eşitlikte $Q_{Net,real}$: simülasyon süresinde İDŞ için belirlenen toplam sızıntı, P_{Net}: simülasyon süresi boyunca tüm düğüm noktalarının ortalama basıncı, γ: basınç katsayısıdır. P_{Net} yalnızca ilk iterasyonda İDŞ'nin sızıntı katsayısının ($C_{Net}^{(1)}$) hesaplanması için kullanılmaktadır.

($C_{Net}^{(1)}$) ve (L_j) ile bir sonraki aşamada İDŞ'nin düğüm noktalarının sızıntı katsayısı aşağıdaki eşitlikle hesaplanmaktadır (eşitlik (3.5))

$$C_j^{(h)} = C_{Net}^{(h)} \times L_j \tag{3.5}$$

Bu eşitlikte $C_j^{(h)}$: (h) nolu iterasyonda (j) düğüm noktasının sızıntı katsayısı, $C_{Net}^{(h)}$: (h) nolu iterasyonda İDŞ'nin sızıntı katsayısı, L_j: (j) düğüm noktasının göreceli önemini belirten faktördür.

Hidrolik model kullanılarak simülasyon periyodu boyunca düğüm noktalarına dağıtılan toplam sızıntı tahmin edilmektedir. Son aşamada, model ile tahmin edilen toplam dağılmış sızıntı ($Q_{Net,model}^{(h)}$) hesaplanan toplam gerçek sızıntı ($Q_{Net,real}$) ile karşılaştırılmaktadır (Eşitlik (3.6)):

$$\left| Q_{Net,model}^{(h)} - Q_{Net,real} \right| \leq \varepsilon \qquad (3.6)$$

Cobacho Jordán vd. (2015) tarafından uygulanan bir örnekte $\varepsilon = 0.005$ tolerans değeri önerilmektedir. Ancak bu değer akış birimi, şebeke hacmi, sisteme giren su miktarı vb. gibi çeşitli faktörlere bağlı olduğundan, farklı bir değer de kullanılabilir.

Bir sonraki iterasyonda ($C_{Net}^{(h+1)}$) katsayısı, tahmin edilen toplam dağılmış sızıntı ve toplam gerçek sızıntı arasındaki farka göre ayarlanmaktadır. Yakınsama kriterlerini yerine getirene kadar proses devam etmektedir. Uygulanan deneme yanılma yönteminin şematik gösterimi Şekil 3.2'de sunulmaktadır. Uygulanan yöntem ile ilgili ayrıntılar Ek-1 (sayfa 33 – 35)'te verilmiştir.
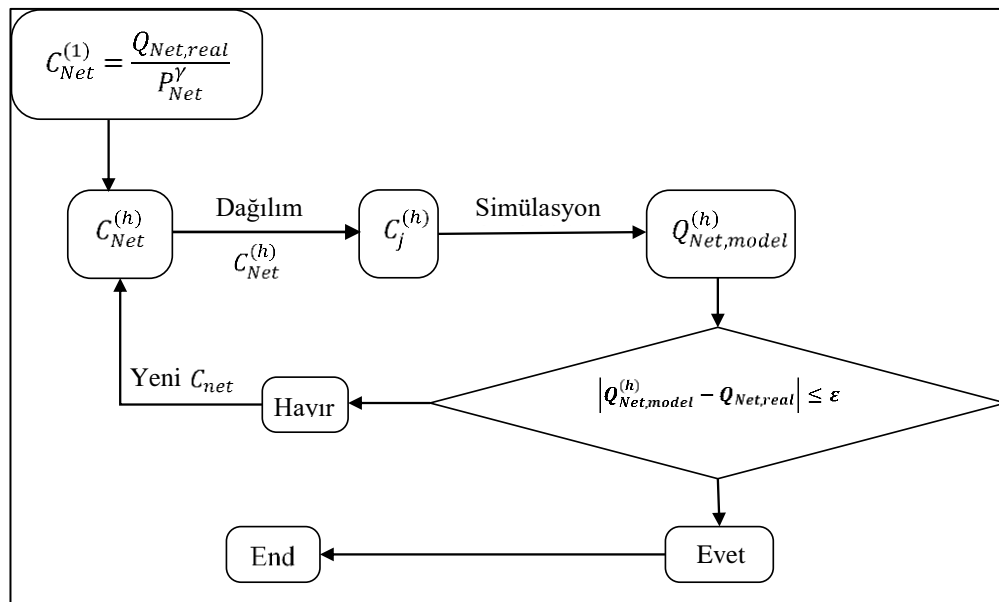
Şekil 3.2. Sızıntı katsayısının kalibrasyonu için uygulanan deneme yanılma yönteminin şematik gösterimi (Cobacho Jordán vd. 2015)

3.3. Temel Örnek Çalışma (M1)

Cobacho Jordán vd. (2015) tarafından önerilen mekânsal ve zamansal sızıntı simülasyonu yaklaşımı Şekil 3.3'te gösterilen İDŞ'de sayısal bir örnek olarak uygulanmıştır. Bu örnek M1 olarak kodlanmıştır ve bu uygulamada hidrolik modelleme yöntemi ve önerilen yaklaşım genelleştirilebilmek amacı ile test edilmiştir.

Model (M1)'in giriş veri setleri:
- Sisteme giren su miktarı = 5100 m³/gün (59,03 L/sn)
- Toplam sızıntı olmayan debi = 3500 m³/gün (40,5 L/sn)
- Toplam sızıntı debisi = 1600 m³/gün (18,52 L/sn)
- γ= 1,1
- Boru sürtünme katsayısı, R= 0.1 mm (Darcy-Weisbach)
- Ortalama İDŞ basıncı = 40 m
- Düğüm noktaları ve boruların özelikleri Ek-1 (sayfa 36)'da verilmiştir.
- Düğüm noktalarının debi değişim profili Ek-1 (sayfa 36)'da verilmiştir.

M1 uygulamasında kullanılan İDŞ Cobacho Jordán vd. 2015'ten alınmıştır.
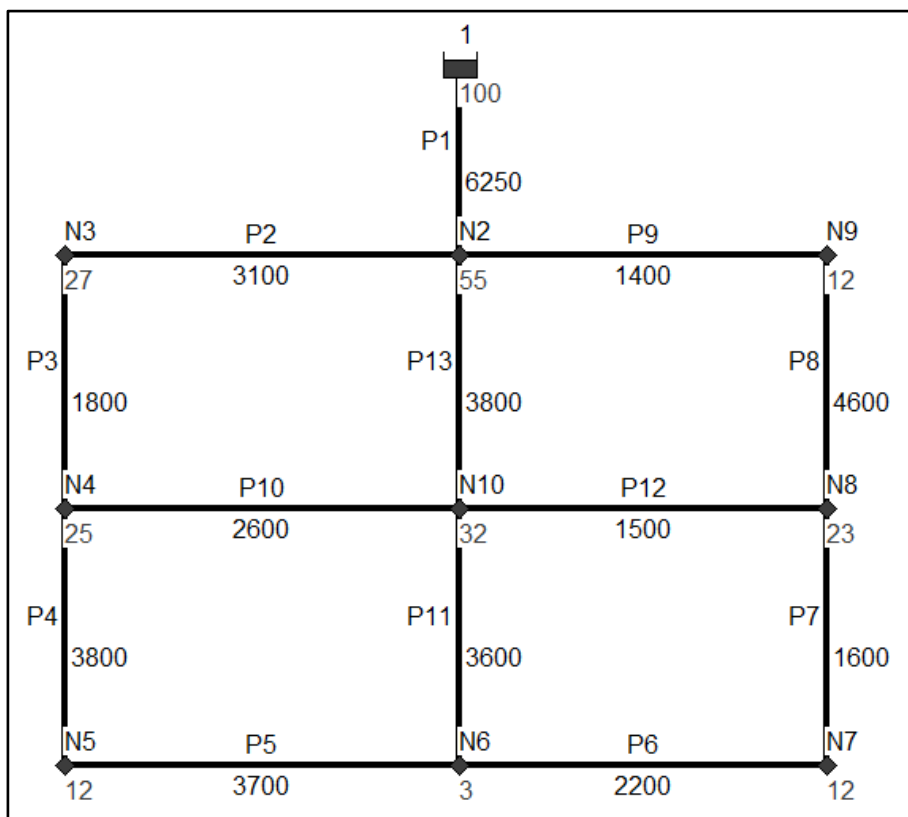
Şekil 3.3. Temel çalışma örneğinin (M1) İDŞ'si (Cobacho Jordán vd. 2015)

Simülasyon periyodu boyunca sisteme giren su debisi, toplam sızıntı olmayan debi ve tahmin edilen toplam dağıtılmış sızıntı Şekil 3.4'te gösterilmektedir. Gösterildiği gibi sızıntı olmayan debi azalınca, sızıntı artmakta; sızıntı olmayan debi artınca sızıntı azalmaktadır. Uygulamaya ilişkin ayrıntılar Ek-1 (sayfa 36 – 41)'de sunulmuştur.
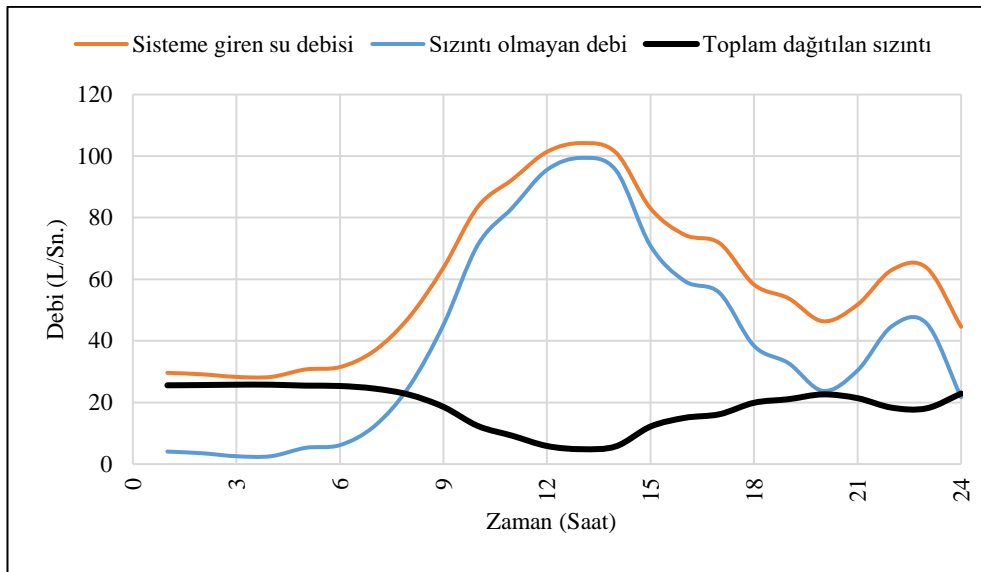
Şekil 3.4. Sisteme giren su debisi, sızıntı olmayan su debisi ve tahmin edilen toplam dağıtılmış sızıntı debisi (Cobacho Jordán vd. 2015'ten uyarlanmıştır)

3.4. Modelin Giriş Varsayımlarından Dolayı Sızıntı Katsayılarının Hassasiyeti

Mekânsal ve zamansal sızıntı simülasyonu için önerilen yaklaşımda üç parametrenin bilindiği varsayılmaktadır. Parametreler, İDŞ'nin ortalama basıncı, basınç katsayısı ve sızıntı katsayısıdır. Bu parametrelerin sızıntı simülasyonu üzerindeki etkileri aşağıda sunulduğu şekilde incelenmiştir:

- İDŞ ortalama basıncının (P_{net}) sızıntı katsayılarının nihai değerine (C_{net}^f) ve dolayısıyla model tahminlerine etkisi (Ek-1 sayfa 41 – 42).

- Boru pürüzlülüğünün İDŞ için tahmin edilen ortalama basınç (P_{net}), nihai sızıntı katsayıları (C_{net}^f) ve dolayısıyla model tahminleri üzerindeki etkisi (Ek-1 sayfa 42 – 43).

- Basınç katsayısının (γ) İDŞ için tahmin edilen ortalama basınç (P_{net}), nihai sızıntı katsayıları (C_{net}^f) ve dolayısıyla model tahminleri üzerindeki etkisi (Ek-1 sayfa 43 – 44).

- Basınç katsayısı ve pürüzlülük katsayısının hassasiyet analizi Ek-1 (sayfa 44 – 45)'te sunulmaktadır.

3.5. Kaleiçi İDŞ için Hesaplanan Yıllık ve Aylık SDD'ler

Kaleiçi İDŞ girişinde bulunan SCADA izleme istasyonunda, 5 dakika zaman aralığında ve sürekli olarak sisteme giren su hacmini ve su basıncını ölçen yüksek hassasiyetli bir elektromanyetik debimetre ve basınç metre bulunmaktadır. Ölçüm verileri SCADA istasyonundan ASAT SCADA Merkezi'ne aktarılmakta ve kaydedilmektedir. Kaleiçi bölgesindeki su aboneleri ASAT Abone İşleri Dairesi'nden alınan bilgiler doğrultusunda iyi bir şekilde belirlenmiş ve aylık su tüketimleri ASAT Tahakkuk Birimi'nden temin edilmiştir. SSD hesaplamaları, 21 Mayıs 2015 – 21 Mayıs 2016

tarihleri arasındaki dönem için yapılmış olup Çizelge 3.1'de sunulmuştur (Muhammetoğlu 2017).

Çizelge 3.1. Kaleiçi DMA'da 21 Mayıs 2015 – 21 Mayıs 2016 tarihleri arasında hesaplanan SSD (Muhammetoğlu 2017)

Sisteme Giren Su Miktarı Q_I = 839,288 m³ (%100)	İzinli Tüketim Q_A= 640,820 m³ (%76,4)	Faturalandırılmış İzinli Su Tüketimi Q_{BA} = 290,147 m³ (%34,6)	Faturalandırılmış Ölçülmüş Kullanım 290,147 m³ (%34,6)	Gelir Getiren Su Miktarı 290,147m³ (%34,6)
			Faturalandırılmış Ölçülmemiş Kullanım 0 m³ (%0)	
		Faturalandırılmamış İzinli Su Tüketimi Q_{UA} = 350,673 m³ (%41,8)	Faturalandırılmamış Ölçülmüş Kullanım 348,729 m³ (%41,6)	Gelir Getirmeyen Su Miktarı (GGS) 549,141 m³ (%65,4)
			Faturalandırılmamış Ölçülmemiş Kullanım 1,944 m³ (%0,2)	
	Su Kayıpları Q_L = 198,468 m³ (%23,6)	İdari Kayıplar Q_{AL} = 54,404 m³ (%6,5)	İzinsiz Tüketim 3,294 m³ (%0,4)	
			Sayaçlardaki Ölçüm Hataları ve Veri İşleme Hataları 51,110 m³ (%6,1)	
		Fiziki Kayıplar Q_{RL} = 144,064 m³ (%17,2)	Temin ve Dağıtım Hatları ile Servis Bağlantılarında Oluşan Kayıp-Kaçaklar 144,064 m³ (%17,2)	

Kaleiçi İDŞ için oluşturan SSD bileşenlerinin hesaplanması ve üç aylık dönemler için oluşturulan SSD'ler Ek-1 (sayfa 45-50)'de verilmiştir. Aylık olarak oluşturulan SSD verileri, hidrolik model kalibrasyonu ve doğrulaması prosesleri ve ileri BY uygulamaları için kullanılmıştır.

3.6. Kaleiçi İDŞ için Hidrolik Model Uygulaması

Tez kapsamında Kaleiçi İDŞ'nin hidrolik modellemesi EPANET yazılımıyla Hazen-Williams eşitliği kullanılarak gerçekleştirilmiştir. Sisteme giren su debisi, sızıntı ve sızıntı olmayan debi olarak ayrılmış, mekânsal ve zamansal olarak düğüm noktalarına dağıtılmıştır. Değişim profili zaman ayarları beş dakika olarak alınmıştır. Sızıntı olmayan su debisi, izinli tüketimini ve idari kayıpları içermektedir. Kaleiçi İDŞ'de özel düğüm noktası talebi ve debi değişim profili iki düğüm noktası için tanımlanmıştır. Bu noktalardan biri halka açık olan parkın sulama sistemi, diğeri ise itfaiyeye ait olan bir alandır. Kaleiçi İDŞ için basınç katsayısı (γ=1) olarak alınmıştır. Boruların sürtünme

katsayısı, hidrolik model kalibrasyonu aşamasında deneme yanılma yöntemiyle elde edilmiştir. Kaleiçi İDŞ'nin hidrolik modellemesi ile ilgili ayrıntılı bilgiler Ek-1 (sayfa 50)'de bulunmaktadır.

3.7. Kaieiçi Çalışma Bölgesi için Boru Sürtünme Katsayısının Kalibrasyonu

Kaleiçi İDŞ için hidrolik model kalibrasyon işlemi, boru pürüzlülük katsayısının farklı denemelerinde basınç ölçüm noktalarında (BÖN) ölçülen basınç değerleri ile hidrolik model ile tahmin edilen basınç değerleri karşılaştırılarak gerçekleştirilmiştir. Basınç değerleri için en düşük ortalama mutlak hatayı (OMH) veren boru pürüzlülük katsayısı, çalışma bölgesindeki tüm borular için kalibre edilmiş pürüzlülük katsayısı olarak kullanılmıştır.

Sızıntı katsayıları, önerilen sızıntı simülasyonu yaklaşımında açıklandığı gibi, pürüzlülük katsayısı belirlemek üzere yapılan her bir deneme için hesaplanmıştır. Sızıntı katsayılarının deneme yanılma yöntemini başlatmak için BÖN'lerde ölçülen ortalama su basıncı değerleri kullanılmıştır. Kalibrasyon prosesi farklı iki simülasyon periyodu üzerinde gerçekleştirilmiştir. Simülasyon periyotları, yaz ve kış mevsimlerini temsil etmektedir. Boru sürtünme katsayısı kalibrasyonu için Eşitlik 3.7 kullanılmaktadır. Kalibrasyon prosesi ile ilgili ayrıntılılar Ek-1 (sayfa 51 – 52)'de sunulmaktadır.

$$R = \frac{R_s \times N_{PMPs} \times N_{ms} + R_2 \times N_{PMPw} \times N_{mw}}{(N_{PMPs} \times N_{ms}) + (N_{PMPw} \times N_{mw})} \tag{3.7}$$

Bu eşitlikte:

R_s, R_w: sırasıyla yaz ve kış mevsimleri için kalibre edilen boru sürtünme katsayıları

N_{PMPs}, N_{PMPw}: sırasıyla yaz ve kış mevsimleri için aktif BÖN sayıları

N_{ms}, N_{mw}: sırasıyla yaz ve kış mevsimlerinde her BÖN noktasındaki basınç ölçümlerinin sayısıdır.

Yaz ve kış mevsimlerine ait sürtünme katsayısı kalibrasyonu ile ilgili giriş veri setleri Ek-1 (sayfa 52 – 58)'de bulunmaktadır.

3.8. Çalışma Bölgesi için Kalibre Edilen Sürtünme Katsayısının Doğrulanması

Doğrulama işleminin amacı, Kaleiçi İDŞ için kalibre edilmiş boru pürüzlülük katsayısının geçerliliğini başka bir simülasyon döneminde test etmektir. Kaleiçi İDŞ için hidrolik model doğrulama aşamasında kalibre edilen boru pürüzlülük katsayısı, tüm borulara tanımlanmış olup modelden elde edilen basınç verileri için OMH hesaplanmıştır. Boru sürtünme katsayısı doğrulamasıyla ilgili giriş veri setleri Ek-1 (sayfa 58 – 61)'de bulunmaktadır.

3.9. İleri BY Uygulanması

Doğrulanan pürüzlülük katsayısı, Kaleiçi İDŞ hidrolik modelindeki tüm borular için, kapalı devre basınç kontrolünün ileri BY tekniği uygulaması için kullanılmıştır. İleri BY uygulaması ile elde edilen sızıntı azalması, yaz ve kış simülasyon dönemleri için

tahmin edilmiştir. İlk olarak, simülasyon periyodu boyunca şebekede en düşük basınç oluşan kritik nokta tespit edilmiş ve bu noktada izin verilen minimum basınç seviyesinin (ilgili yönetmelikte tanımlanan değer 20 mSS'dir) üstündeki basınç değerleri tahmin edilmiştir. Daha sonra, kritik noktadaki su basıncını her zaman 20 mSS'de tutmak için alt bölge girişindeki fazla basınç zamana göre değişen farklı seviyelerde indirilmiştir. Son olarak, basınç ve sızıntıdaki ortalama azalma hesaplanmıştır. Çalışma bölgesindeki yüksek zemin kot farklılıkları nedeniyle, ileri BY uygulaması yapılmadan önce ve yapıldıktan sonra kritik noktalar için elde edilen su basıncı değerleri, şebekede izin verilen maksimum su basıncı seviyesi (ilgili yönetmelikte tanımlanan değer 60 mSS'dir) ile karşılaştırılmıştır.

3.10. Sızıntı Azalım Senaryoları

Kaleiçi İDŞ için iki sızıntı azalım senaryosu incelenmiştir. İlk senaryoda, sadece sızıntı olmayan debinin, mevcut duruma göre %25 artmış veya azalmış olması ve sızıntı katsayılarının bu senaryodan etkilenmediği varsayılmaktadır. Bu senaryo ile sızıntı olmayan debinin artması veya azalmasının, sızıntı üzerindeki etkisi incelenmiştir. İkinci senaryoda, sadece sızıntının SKES'ye düşürüldüğü varsayılmaktadır. İleri BY, basınç düşüşünün bir sonucu olarak elde edilebilecek sızıntı azalmasını bulmak için her senaryo için uygulanmıştır.

3.10.1. Sızıntı olmayan debinin değişimine yönelik senaryo (Senaryo-1)

Bu senaryoda, Kaleiçi İDŞ'de sızıntı olmayan debinin ±%25 değişiminin sızıntıya olan etkisi incelenmiştir. Sızıntı olmayan debi bileşenleri içinde yer alan faturalandırılmamış ölçülmemiş izinli tüketim ve izinsiz tüketimin değişmeyeceği varsayılırken, diğer bileşenlerin ±%25 oranında değiştiği kabul edilmektedir. Senaryo uygulamasında daha önce tanımlanmış olan sızıntı katsayıları, basınç katsayısı ve kalibre edilmiş boru pürüzlülüğü katsayısı değerleri aynen kullanılmıştır. Senaryo-1 ile ilgili ayrıntılar Ek-1 (sayfa 61 – 65)'te bulunmaktadır.

3.10.2. Sızıntı değişimine yönelik senaryo (Senaryo-2)

Kaleiçi İDŞ için su kayıpları ekonomik seviyesi (SKES) Gülaydın (2017) tarafından aynı yıl için belirlenmiştir. 2015-2016 yılları arasında Kaleiçi İDŞ için tespit edilen SKES değeri, aynı yıl için hazırlanan SSD tablosu ile hesaplanan su kayıplarının %41,4'ünü oluşturmaktadır. Bu senaryoda, sızıntı katsayıları, yeni tanımlanan sızıntı debisi için yeniden hesaplanmıştır. Buna göre Senaryo 2'de yaz ve kış simülasyon dönemlerindeki SKES, hesaplanan su kayıplarının %41,4'üne eşittir. İleri BY, belirlenen SKES altında elde edilebilecek basınç düşüşünden kaynaklanan sızıntı azalımını tahmin etmek için uygulanmıştır. Senaryo-2 ile ilgili ayrıntılar Ek-1 (sayfa 65)'te bulunmaktadır.

4. BULGULAR VE TARTIŞMA

Kaleiçi çalışma bölgesine ait İDŞ hidrolik modelleme sonuçlarını elde etmek için her simülasyon dönemi başında 24 saatlik ısınma süresi tanımlanmıştır. Isınma süresine ait model sonuçları, kalibrasyon ve doğrulama prosesleri ile ileri BY uygulaması ve senaryolara ait bulguların elde edilmesinde dikkate alınmamıştır.

### 4.1. Sürtünme Katsayısının Kalibrasyonu

Kalibrasyon prosesi, yaz ve kış simülasyon dönemleri için gerçekleştirilmiştir. Şekil 4.1 ve Şekil 4.2'de gösterildiği gibi, en düşük OMH değerleri sırasıyla R= 55 ve R=60 pürüzlülük katsayıları için elde edilmiştir. Buna bağlı olarak, pürüzlülük katsayısının kesin olarak belirlenmesi için ikinci aşamada R için 55, 56, 57, 58, 59 ve 60 değerleri tanımlanarak simülasyonlar yapılmıştır. Yaz ve kış mevsimleri için tahmin edilen su basıncı değerleri dikkate alındığında en düşük OMH değerleri sırasıyla R=57 ve R=58 için bulunmuştur (Şekil 4.1 ve Şekil 4.2). Kalibrasyon çalışmasına ait bulguların detayları Ek-1 (sayfa 67 – 78)'de verilmiştir.

Yaz ve kış mevsimlerine ait simülasyonlar için kalibre edilen pürüzlülük katsayısı değerleri Eşitlik 3.7'de kullanılarak R için kalibrasyon değeri 57,6 olarak hesaplanmıştır. 24 saatlik ısınma süresi göz önünde bulundurularak, yaz ve kış simülasyon dönemlerinde her BÖN'de kaydedilen basınç değerlerinin sayısı sırasıyla 1122 ve 1144'tür.

$$R = \frac{57 * 1122 * 4 + 58 * 1144 * 5}{1122 * 4 + 1144 * 5} = 57.6$$
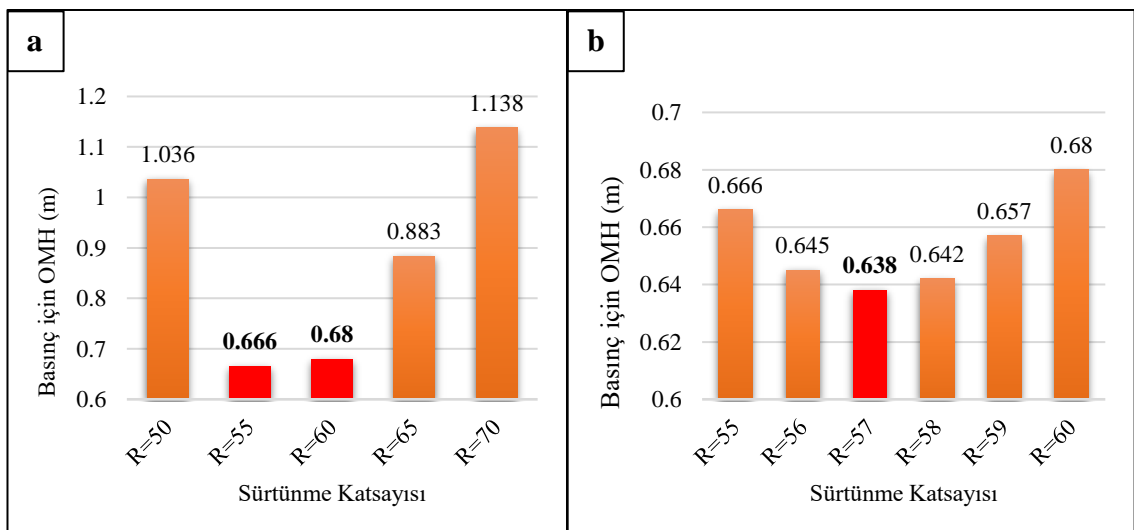
Şekil 4.1. (a) R= [50, 55, 60, 65, 70] ve (b) R= [55, 56, 57, 58, 59, 60] değerleri için tüm BÖN'lerdeki basınç tahminlerine ait OMH değerleri (21 – 25 Ağustos 2015)
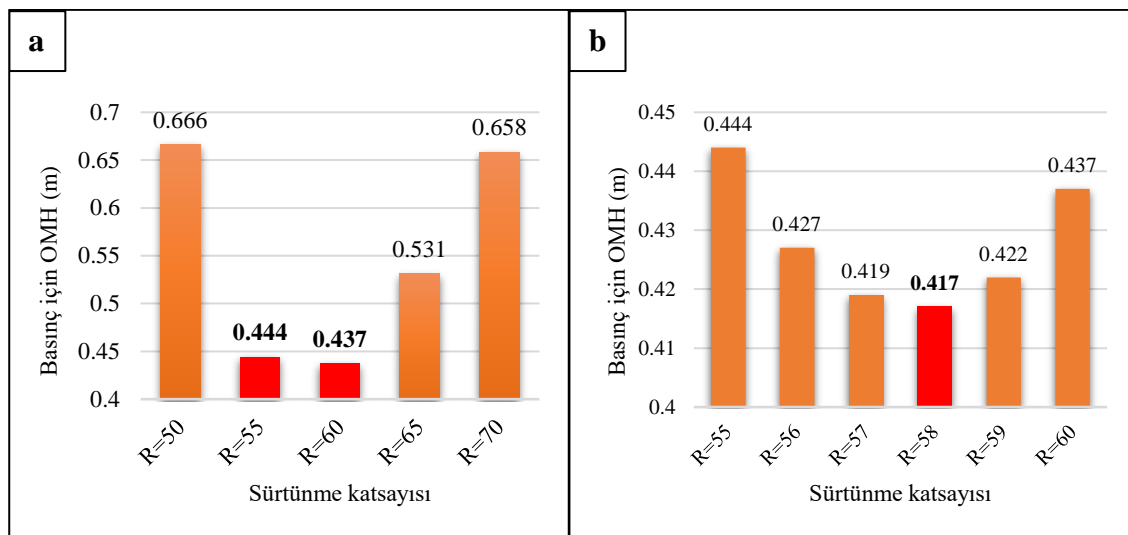
Şekil 4.2. (a) R= [50, 55, 60, 65, 70] ve (b) R= [55, 56, 57, 58, 59, 60] değerleri için tüm BÖN'lerdeki basınç tahminlerine ait OMH değerleri (15 – 19 Ocak 2016)

4.2. Sürtünme Katsayısının Doğrulanması

Kalibre edilen sürtünme katsayısı değeri (R= 57,6) hidrolik modelde tüm borular için tanımlanarak, farklı bir simülasyon dönemi doğrulama çalışması yapılmıştır. Doğrulama dönemine ait veriler ile hidrolik model uygulaması gerçekleştirilmiş, modelden elde edilen basınç tahminleri ile sahada ölçülen basınç değerleri karşılaştırılarak, OMH değerleri hesaplanmıştır. Doğrulama dönemine ilişkin model verileri Çizelge 4.1'de gösterilmektedir. Kaleiçi İDŞ için hidrolik model doğrulama aşamasında, kalibre edilmiş olan sürtünme katsayısı R=57,6 değeri doğrulanmıştır. Doğrulama çalışmasına ait ayrıntılar Ek-1 (sayfa 78 – 81)'de bulunmaktadır.

Çizelge 4.1. Kalibrasyon çalışması ile elde edilen R= 57,6 değeri için doğrulama dönemine ait model tahminleri ve OMH değeri (1 – 6 Haziran 2016)

Parametre	Model Tahminleri
C_{net}	0,634
Ortalama $\Sigma Q_{(sızıntı\ olmayan\ debi)+(sızıntı)}$ (m^3/saat)	111,55
Ortalama Toplam dağıtılan sızıntısı (m^3/saat)	26,93
ε (m^3/saat)	0,060
Basınç OMH'sı (m)	0,659

## 4.3. İleri BY Uygulamasına Ait Bulgular

Kaleiçi İDŞ'de ileri BY tekniği olarak kapalı devre basınç kontrolü uygulanmıştır. Genel olarak, ileri BY uygulandıktan sonra ortaya çıkan ortak bulgular aşağıda özetlenmektedir:

- Basınç düşürme vanası (PRV) çıkışında tahmin edilen basınç değerleri, yapay olarak oluşturulan yüksek su tüketimi anında (yangın hidrantının açılması) belirgin bir artış

göstermektedir. Bu bulgu, olağanüstü su talebine karşılık basınç artışı ile PRV'nin reaksiyonunu göstermektedir.

- İleri BY uygulamasından önce basınç değerleri 60 mSS'nin üzerinde tahmin edilen tüm düğüm noktaları, ileri BY uygulamasından sonra 60 mSS'den daha düşük basınç seviyesine inmiştir.

        Şekil 4.3'te, yaz mevsiminde PRV girişinde ölçülen su basıncı değerleri ile ileri BY uygulamasıyla PRV çıkışı için tahmin edilen su basıncı değerleri gösterilmektedir. İleri BY uygulaması ile basınç seviyesi düşürülmektedir. Yaz mevsimi için ileri BY uygulaması ile elde edilen ortalama basınç düşüşü ve ortalama sızıntı azalması Çizelge 4.2'de sunulmaktadır. Kış mevsimi için PRV girişinde ölçülen ve PRV çıkışı için tahmin edilen basınçları değerleri Şekil 4.4'te, tahmin edilen ortalama basınç düşüşleri ve ortalama sızıntı azalması Çizelge 4.3'te sunulmaktadır. İleri BY uygulamasına ait bulguların detayları Ek-1 (sayfa 82 – 88)'de bulunmaktadır.
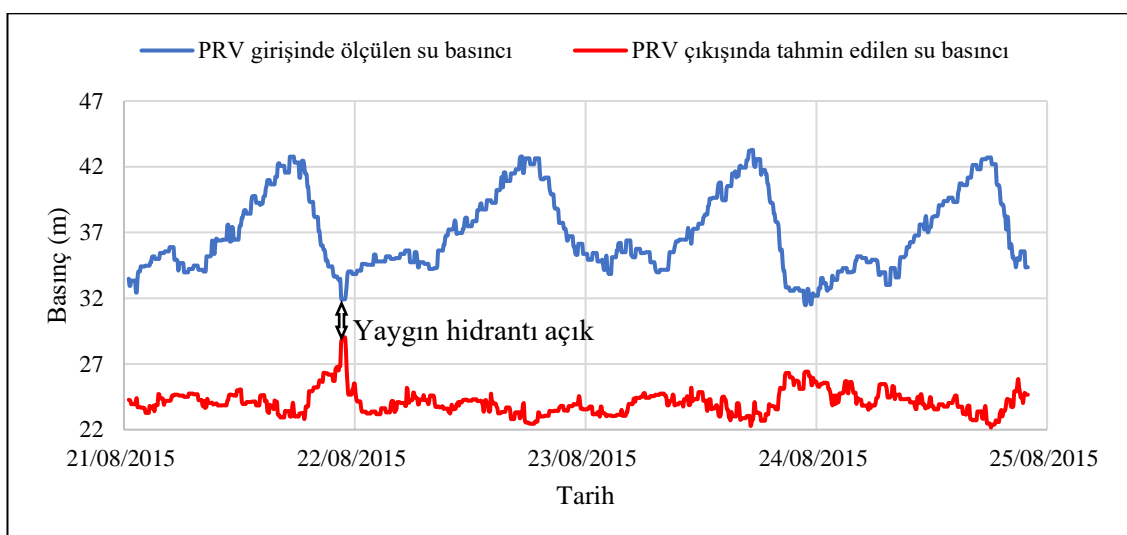
Şekil 4.3. Kaleiçi alt bölgesi için PRV girişinde ölçülen su basıncı ve PRV çıkışında tahmin edilen su basıncı değerleri (21 – 25 Ağustos 2015)

Çizelge 4.2. Yaz simülasyonu döneminde Kaleiçi İDŞ'de ileri BY uygulaması için tahmin edilen ortalama basınç düşüşü ve ortalama sızıntı azalması

| Parametre		İleri BY uygulamasından önce	İleri BY uygulamasından sonra
İDŞ'deki Ortalama Basınç (m)		41,2	28,6
Ortalama Basınç Düşüşü (m)		12,6	
Ortalama $\Sigma Q_{(sızıntı\ olmayan\ debi)+(sızıntı)}$ (m³/saat)		109,47	102,65
Ortalama Sızıntı Azalması	m³/saat	6,82	
	m³/ay	5074,08	

19
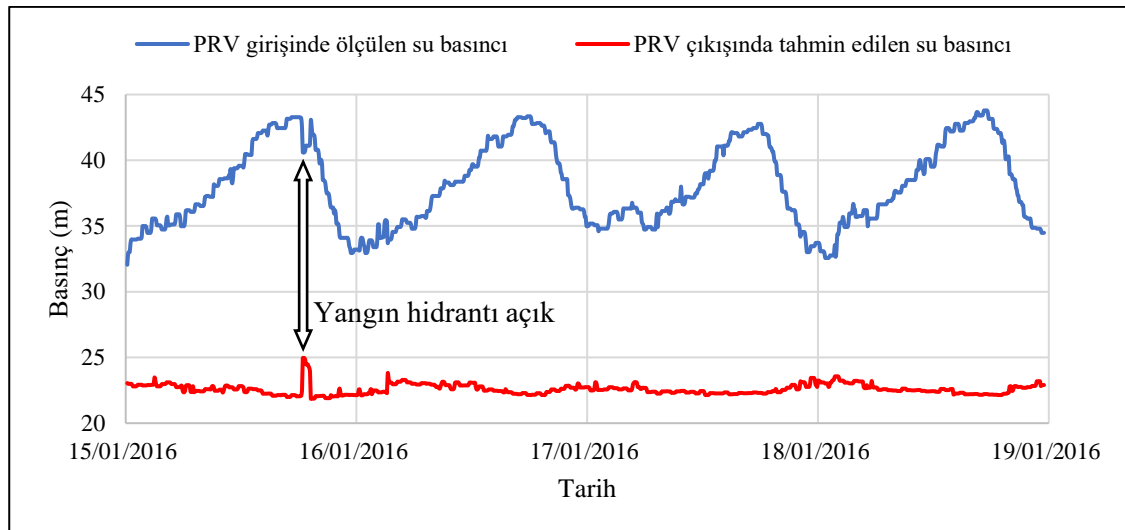
Şekil 4.4. Kaleiçi alt bölgesi için PRV girişinde ölçülen su basıncı ve PRV çıkışında tahmin edilen su basıncı değerleri (15 – 19 Ocak 2016)

Çizelge 4.3. Kış simülasyonu döneminde Kaleiçi İDŞ'de ileri BY uygulaması için tahmin edilen ortalama basınç düşüşü ve ortalama sızıntı azalması

Parametre		İleri BY uygulamasından önce	İleri BY uygulamasından sonra
İDŞ'deki Ortalama Basınç (m)		43,77	28,87
Ortalama Basınç Düşüşü (m)		14,9	
Ortalama $\Sigma Q_{(sızıntı\ olmayan\ debi)+(sızıntı)}$ (m³/saat)		78,01	72,22
Ortalama Sızıntı Azalması	m³/saat	5,79	
	m³/ay	4307,76	

## 4.4. Sızıntı Olmayan Debideki ±% 25 Değişimin Sızıntıya Olan Etkileri

Sızıntı olmayan debi, Kaleiçi İDŞ'de sistem giriş debisinin ana bölümünü oluşturmaktadır. Bu nedenle bu debideki herhangi bir değişiklik, düğüm noktalarındaki basıncı değiştirir ve dolayısıyla Kaleiçi İDŞ'deki sızıntılar etkilenir. Kaleiçi İDŞ için sızıntı olmayan debinin ±%25 oranında değiştirilmesinin (Senaryo-1) yaz ve kış simülasyon periyotları için etkileri Şekil 4.5'te gösterilmiştir. Yaz ve kış mevsimlerinde sızıntı olmayan debinin ±%25 oranında değiştirilmesi ve ileri BY uygulaması ile ortalama sızıntı azalmasının 4099,44 – 5431,2 m³/ay arasında olacağı tahmin edilmiştir. Senaryo-1'e ait bulgular ile yaz ve kış sezonu boyunca ileri BY uygulamasına ilişkin detaylı sonuçlar Ek-1 (sayfa 88 – 99)'da sunulmuştur.
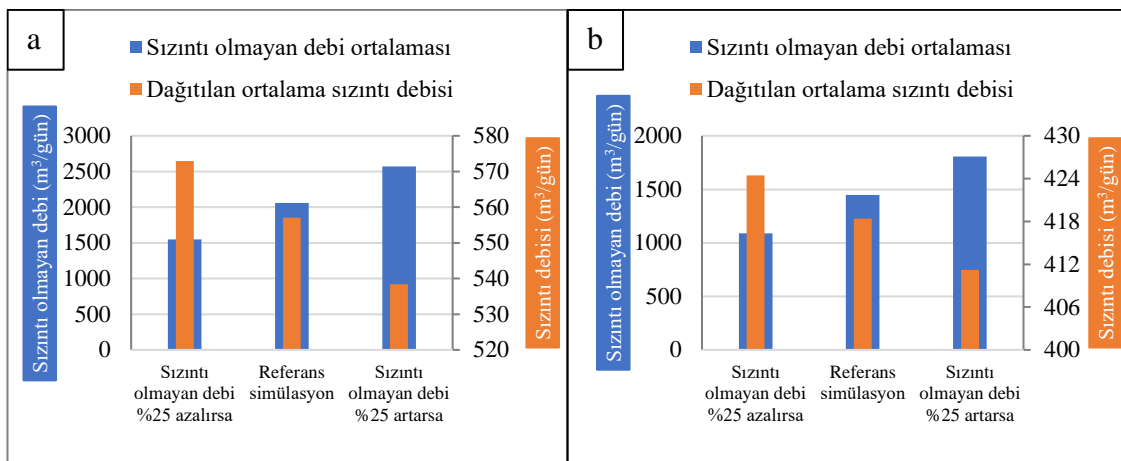
Şekil 4.5. (a) Yaz mevsimi ve (b) kış mevsiminde, sızıntı olmayan debinin değişmesi durumunda Kaleiçi İDŞ'de sızıntı debisindeki değişimler

## 4.5. Sızıntının SKES Düzeyine Kadar Azaltılması Senaryosunda İleri BY Uygulaması

Sızıntının SKES düzeyine kadar azaltılması senaryosunda (Senaryo-2), sızıntı katsayıları yeniden hesaplanmıştır. Sızıntı olmayan debi ve model tarafından SKES düzeyinde dağıtılan sızıntının toplamı ile elde edilen toplam debi ($\Sigma Q_{(Sızıntı\ olmayan\ debi)+(SKES)}$) tahmini ve Kaleiçi İDŞ girişinde ölçülen basınç değerleri yaz ve kış mevsimleri için sırasıyla Şekil 4.6 ve Şekil 4.7'de gösterilmektedir. İleri BY uygulaması ile yaz ve kış mevsimleri için tahmin edilen ortalama basınç düşüşü ve ortalama sızıntı azalması sırasıyla Çizelge 4.4 ve Çizelge 4.5'te sunulmaktadır. Senaryo-2 ile ilgili ayrıntılı sonuçlar Ek-1 (sayfa 99 – 107)'de bulunmaktadır.
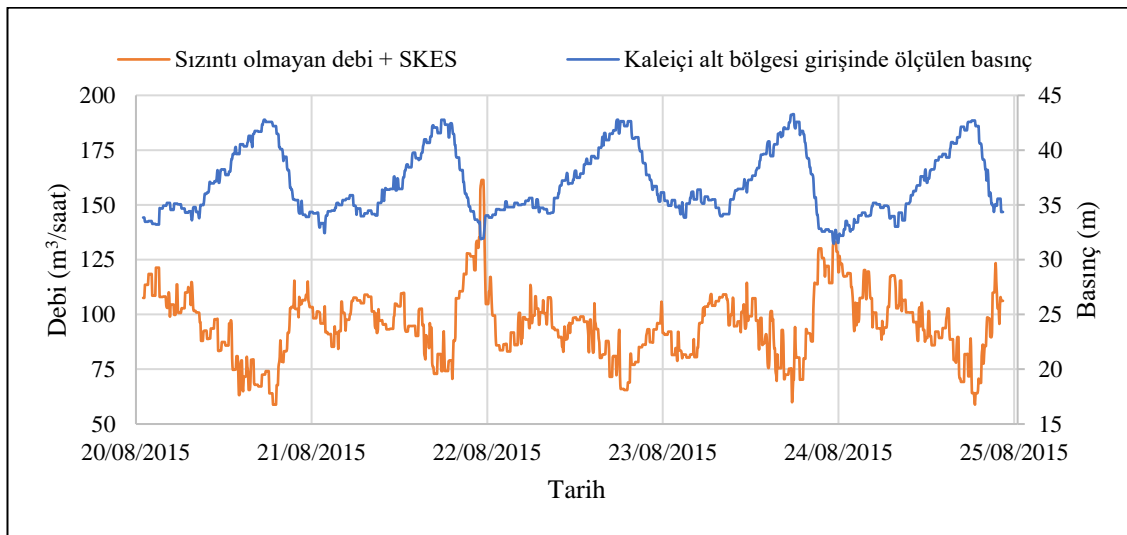
Şekil 4.6. Kaleiçi alt bölgesi için İDŞ girişinde ölçülen basınç değerleri ve tahmin edilen toplam debinin ($\Sigma Q_{(Sızıntı\ olmayan\ debisi)+(SKES)}$) değişimi (21 – 25 Ağustos 2015)

Çizelge 4.4. Yaz simülasyonu döneminde Kaleiçi İDŞ'de ileri BY uygulaması için tahmin edilen ortalama basınç düşüşü ve ortalama sızıntı azalması

| Parametre		İleri BY uygulamasından önce	İleri BY uygulamasından sonra
İDŞ'deki Ortalama Basınç (m)		41,89	28,32
Ortalama Basınç Düşüşü (m)		13,57	
Ortalama $\Sigma Q_{(sızıntı\ olmayan\ debi)+(sızıntı)}$ (m^3/saat)		95,64	92,72
Ortalama Sızıntı Azalması	m^3/saat	2,92	
	m^3/ay	2172,48	

Şekil 4.7. Kaleiçi alt bölgesi için İDŞ girişinde ölçülen basınç değerleri ve tahmin edilen toplam debinin ($\Sigma Q_{(Sızıntı\ olmayan\ debisi)+(SKES)}$) değişimi (15 – 19 Ocak 2016)
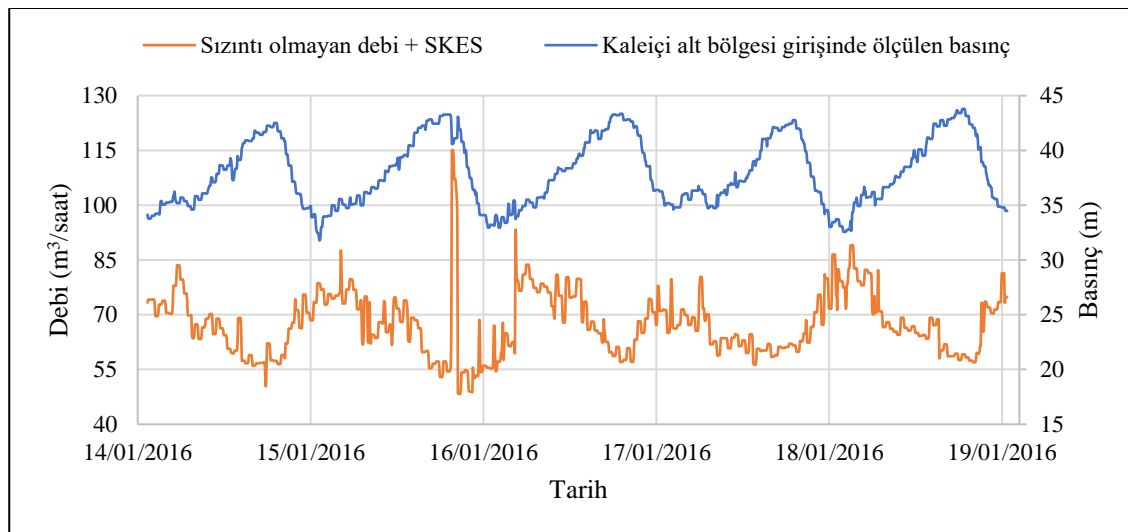
Çizelge 4.5. Kış simülasyonu döneminde Kaleiçi İDŞ'de ileri BY uygulaması için tahmin edilen ortalama basınç düşüşü ve ortalama sızıntı azalması

Parametre		İleri BY uygulamasından önce	İleri BY uygulamasından sonra
İDŞ'deki Ortalama Basınç (m)		44,19	28,76
Ortalama Basınç Düşüşü (m)		15,43	
Ortalama $\Sigma Q_{(sızıntı\ olmayan\ debi)+(sızıntı)}$ (m^3/saat)		67,58	65,18
Ortalama Sızıntı Azalması	m^3/saat	2,4	
	m^3/ay	1785,6	

## 4.6. Mekânsal Sızıntının Tahmin Edilmesi

Tezin çok önemli bir bulgu, sızıntı debilerinin mekânsal olarak tahmin edilmesidir. Bu kapsamda Kaleiçi İDŞ'de herhangi bir düğüm noktasındaki sızıntı simülasyon süresi boyunca tahmin edilmektedir. Örnek olarak Şekil 4.8'de Kaleiçi İDŞ'de tüm düğüm noktalarındaki ortalama su basıncı ile birlikte yaz simülasyon periyodu boyunca seçilen bazı düğüm noktalarındaki sızıntı miktarları gösterilmektedir. Seçilen düğüm noktalarındaki basınç değerleri farklı olduğundan, sızıntı miktarları da birbirinden farklıdır. Mekansal sızıntı tahminine ilişkin bulguların detayları Ek-1 (sayfa 107 – 108)'de sunulmaktadır.
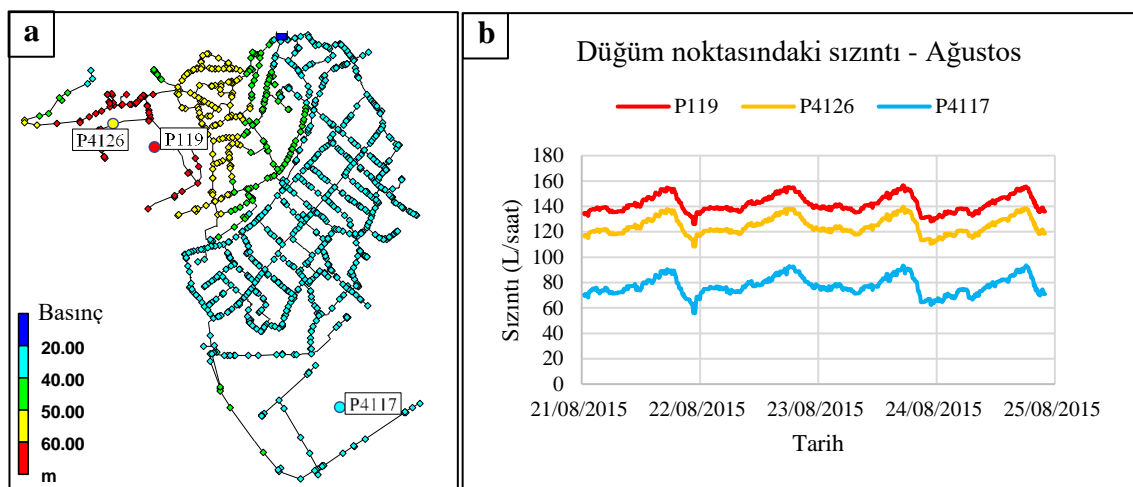

Şekil 4.8. (a) Düğüm noktalarındaki ortalama basınç, (b) P119, P4126 ve P4117 nolu düğüm noktalarındaki sızıntılar (21 – 25 Ağustos 2015)

4.7. Uygulanan Senaryoların Fazla Basınç Üzerindeki Etkisi

Model ile dağıtılan sızıntı ve sızıntı olmayan debinin toplamı ($\Sigma Q_{(Sızıntı\ olmayan\ debi)+(Sızıntı)}$) sızıntı olmayan debisin değiştirilmesi veya SKES düzeyine kadar sızıntının azaltılmasını içeren senaryo koşullarından etkilenmiştir. $\Sigma Q_{(Sızıntı\ olmayan\ debi)+(Sızıntı)}$, düğüm noktalarındaki basınçla ters orantılıdır. Yaz döneminde, Kaleiçi İDŞ'de kritik nokta için tahmin edilen fazla basınç değerlerinin, referans simülasyon ve senaryo koşulları için elde edilen model tahminleri ile karşılaştırması Şekil 4.9 ve Şekil 4.10'da sunulmaktadır. Bu bölüme ilişkin uygulama detayları Ek-1 (sayfa 108 – 109)'de verilmiştir.
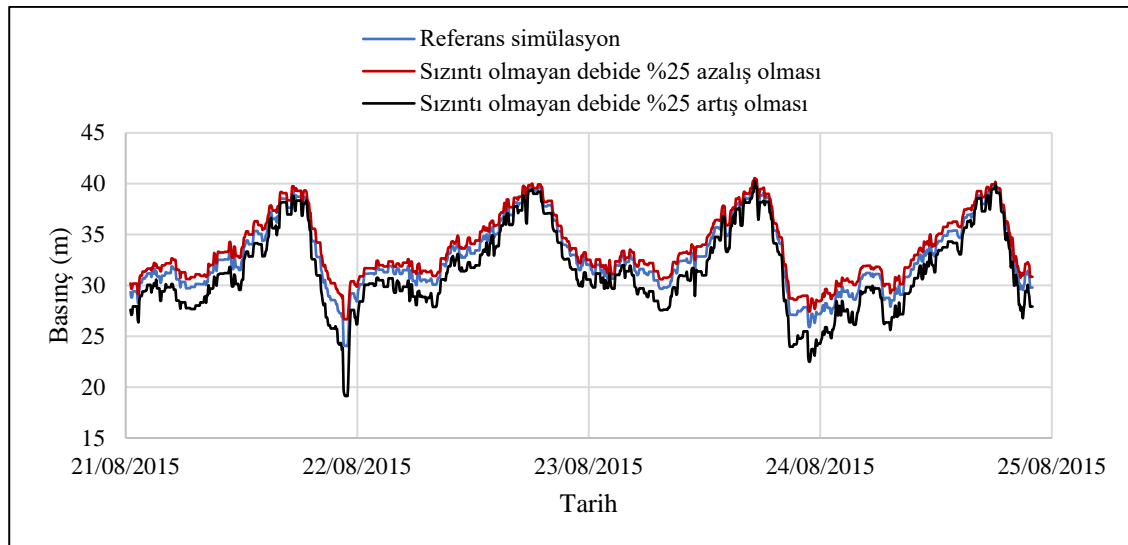
Şekil 4.9. Referans simülasyon ve sızıntı olmayan debide ± %25 oranında değişim olması (Senaryo-1) durumunda Kaleiçi İDŞ'deki kritik nokta için tahmin edilen basınç (21 – 25 Ağustos 2015)
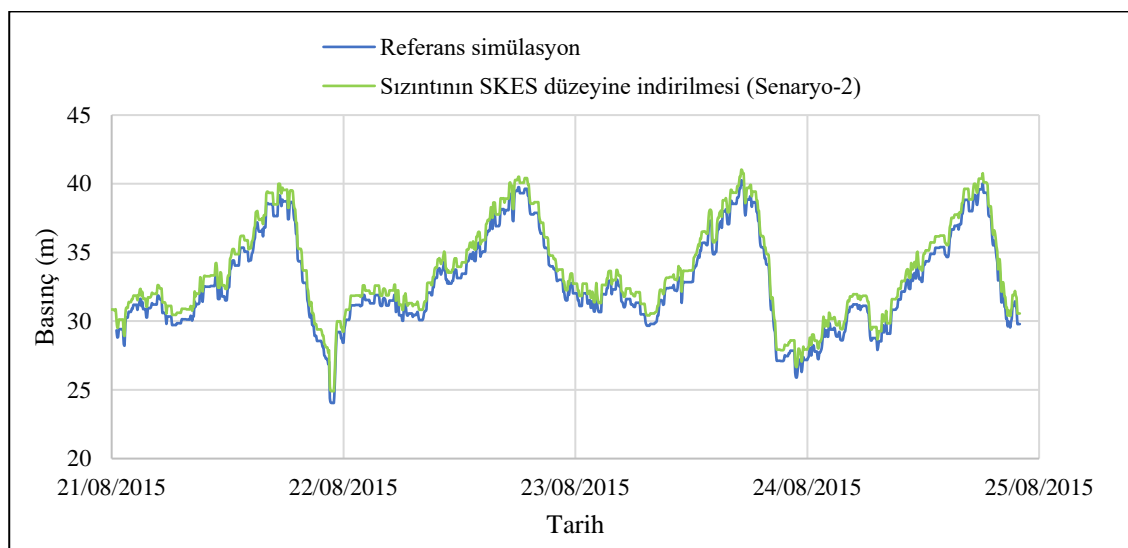
Şekil 4.10. Referans simülasyon ve sızıntının SKES düzeyine kadar indirilmesi (Senaryo-2) durumunda Kaleiçi İDŞ'deki kritik nokta için tahmin edilen basınç (21 – 25 Ağustos 2015)

5. SONUÇLAR

İçme suyu temin ve dağıtım sistemi, her şehir için temel altyapılardan birisidir. Her içme suyu idaresi, içme suyunu uygun kalite ve basınçta kullanıcılara ulaştırmayı hedeflemektedir. Ancak İDŞ'de meydana gelen su kayıpları, içme suyu idarelerinin karşılaştığı önemli bir sorundur. Herhangi bir İDŞ'deki su kayıplarını azaltmak, suyu pompalamak ve arıtmak için gereken enerjiyi azaltmakta olup İDŞ'nin kullanım kapasitesinin artmasına olanak sağlar. Bu nedenle, her su idaresi, su kayıplarını azaltmak veya belirli seviyelerde tutmak için su kayıpları yönetim planları geliştirmelidir. Su kayıpları yönetim programları, su kayıplarının su tüketim hacmine olan oranını hesaplamak ve SSD bileşenlerini periyodik olarak belirlemekle başlar. Sızıntıları da içeren fiziki su kayıpları, herhangi bir İDŞ'de meydana gelen su kayıplarının önemli bir bölümünü oluşturmaktadır. Sızıntı, basınca bağlı olarak oluşan bir debidir ve sızıntıların bulunması son tüketicilere ulaşan suyun basıncını etkilemektedir. Buna istinaden, sızıntının modellenmesi, su kayıplarının yönetimi için gerekli bir işlemdir.

Herhangi bir su temin sistemindeki sızıntı problemini çözmek için en verimli tekniklerden biri, basınç yönetimidir (BY). Hem klasik, hem de ileri yöntemlerle uygulanır. İleri BY yaklaşımı şebekedeki kritik noktanın tespit edilmesi ile başlar, daha sonra, kritik noktadaki basıncın minimum izin verilen değere düşürülmesi koşuluna göre İDŞ girişindeki fazla basınç kırılır. Kritik noktanın tespit edilmesi için kalibre edilmiş bir hidrolik model kullanımı gerekmektedir. EPANET, İDŞ'lerin hidrolik modellemesi için basit ve kullanışlı bir yazılımdır. Bu tez çalışmasında EPANET modelinde Hazen-Williams eşitliği kullanılarak Kaleiçi İDŞ'nin hidrolik modellemesi yapılmıştır. Hidrolik model uygulamasında sisteme giren su hacmi, emitör katsayıları kullanılarak sızıntı debisine ve düğüm noktasındaki su talebi olarak sızıntı olmayan debi bileşenlerine dağıtılmıştır. EPANET yazılımı ile sızıntının mekansal modellemesine yönelik yaklaşım, tez çalışması kapsamında incelenmiş olup bu yaklaşım Kaleiçi İDŞ'deki toplam sızıntının düğüm noktalarına dağılımını tahmin etmek için uygulanmıştır. Hidrolik model, tek bir boru pürüzlülük katsayısı değeri (57,6) için kalibre edilmiş ve doğrulanmıştır. Kalibrasyonu ve doğrulaması gerçekleştirilen model, ileri BY uygulayarak sızıntı azalmasını tahmin etmek için kullanılmıştır. Ek olarak, iki senaryo koşulu için ileri BY uygulaması gerçekleştirilmiştir. İlk senaryoda, sızıntı olmayan debinin ±%25 oranında değiştiği, ikinci senaryoda ise sızıntının SKES düzeyine kadar azaltılacağı varsayılmaktadır. Tez çalışmasından elde edilen bulgular, hidrolik modellemenin su kayıplarını ve özellikle de sızıntıları kontrol etmek için önemli bir araç olduğunu göstermiştir. Tez çalışmasında hidrolik modelleme yapılarak çalışma bölgesindeki her bir düğüm noktası için mekânsal olarak sızıntı tahmini gerçekleştirilmiştir.

Kalibrasyon proseslerinin her biri, ileri BY uygulaması, senaryoların incelenmesi, yaz ve kış mevsimlerini temsil eden iki farklı simülasyon dönemi boyunca gerçekleştirilmiştir. İleri BY uygulaması ile Kaleiçi İDŞ'de fazla basıncın düşürülmesine bağlı olarak önemli düzeyde sızıntı azalması (4307,76 – 5074,08 m^3/ay) önceden tahmin edilmiştir. Bahsedilen konuya ilişkin detaylı sonuçlar Ek-1 (sayfa 111 – 114)'te verilmiştir.

Gelecek Araştırmalar için Öneriler

Hidrolik modelin, sızıntının tahmin edilmesi için kısa zaman periyotları (örneğin 24 saat) için kullanılması önerilmektedir. Bu şekilde, hidrolik model sızıntının mekânsal ve zamansal değişimlerini tespit etmek için yardımcı olabilir.

İleri BY tekniğinin sahada uygulanması için, PRV'nin alt bölge girişine ve basınç sensörlerinin de model çıktılarına göre belirlenen yerel kritik noktalarda ayarlanması önerilir. Buna bağlı olarak, kapalı devre basınç kontrolü, şebekedeki basıncı her zaman minimum seviyede tutabilir ve yangın ihtiyacı gibi olağanüstü su taleplerine cevap verebilir.

Kullanılan sızıntı modelleme yaklaşımı, sızıntı debisinin bilinmesini ve boru uzunluğu boyunca eşit bir şekilde dağıtılmasını gerektirmedir. Sızıntı miktarının otomatik okuma sayaçları (AMR) içeren sistemler tarafından sağlanması ise çok yararlı olabilmektedir. Gelecek uygulamalar için modelin doğrudan SCADA ve AMR sistemlerine bağlanarak, geçmiş veri modellemesi yerine sızıntıyı zamansal olduğu kadar mekânsal olarak da gerçek zamanlı tahmin edebilmesi önemli bir gelişme sağlayabilir. Önerilen bu yaklaşım, programlama dilleri kullanılarak EPANET yazılımının tool (araç) kitler ile SCADA sistemlerine bağlantısının sağlanması ile gerçekleştirilebilir (Cheng vd. 2014).

6. KAYNAKLAR

Anonymous 1: Danish Environmental Protection Agency: Identify sources of water loss. 2018. https://eng.mst.dk/nature-water/water-at-home/water-loss/ [Son erişim tarihi: 04.08.2018].

Anonymous 2: USEPA: EPANET Application for Modeling Drinking Water Distribution Systems. 2000. https://www.epa.gov/water-research/epanet [Son erişim tarihi: 04.08.2018].

Anonymous 3: WHO. World Health Organization - Drinking water. 2015. http://www.who.int/news-room/fact-sheets/detail/drinking-water [Son erişim tarihi: 03.08.2018].

Anonim 1: TÜİK. 2018. http://www.tuik.gov.tr/PreTablo.do?alt_id=1019 [Son erişim tarihi: 06.08.2018].

Cheng, W. P., Yu, T. C., and Xu, G. 2014. Real-Time Model of a Large-Scale Water Distribution System. *Science Direct*, 89: 457 – 466.

Cobacho Jordán, R., Arregui De La Cruz, F., Soriano Olivares, J. and Cabrera Rochera, E. 2015. Including leakage in network models: an application to calibrate leak valves in EPANET. *Journal of Water Supply: Research and Technology - Aqua*, 64(2):130-138.

Fanner, P., Thornton, J., Sturm, R. and Liemberger, R. 2007a. Evaluating Water Loss and Planning Loss Reduction Strategies. *AwwaRF and AWWA*, 289 p, Denver, Colorado.

Gülaydın, O. 2017. İçme Suyu Dağıtım Şebekelerinde Ekonomik Su Kayıpları Seviyesinin Belirlenmesi: Antalya Kaleiçi Örneği. Yüksek lisans tezi, Akdeniz Üniversitesi, Antalya, 135 s.

Kartakis, S., Abraham, E. & McCann, J. A., 2015. WaterBox: A Testbed for Monitoring and Controlling Smart Water Networks, CySWater'15.

Koker, E. and Altan-Sakarya, A. B. (2016), Optimization of Leakage in Water Distribution Networks Using Pressure Reducing Valves. *EURO 2016, 28th European Conference on Operational Research*, Poznan.

Köker, E. and Altan-Sakarya, A. B. (2015), Chance Constrained Optimization of Booster Chlorination in Water Distribution Networks. *CLEAN, Soil, Air Water*, 43, p.717-726.

Lambert, A. 2003. Assessing Non-Revenue Water and its Components: A Practical Approach. *IWA water loss task force*, 21: 50 – 51.

Mckenzie, RS. and Wegelin, W. 2009. Implementatıon of Pressure Management In Munıcıpal Water Supply Systems. *IWA*, 1 – 18.

Mpiana, LA., Hamam, Y. and Abu-Mahfouz, A. 2017. Graph based Hydraulic Modelling of Pressure in Water Distribution Networks. *IEEE*, 1558 - 1563.

Muhammetoğlu, H. 2017. Turistik Bölgelerde Otomatik Okuma Sayaçları Kullanarak Fiziki Su Kayıplarının Yüksek Hassasiyetle Belirlenmesi ve Yönetimi: Antalya-Kaleiçi Uygulaması. ANTALYA.

Muhammetoğlu, H. ve Muhammetoğlu, A. 2017. İçme Suyu Temin Ve Dağıtım Sistemlerindeki Su Kayıplarının Kontrolü El Kitabı. Orman ve Su İşler Bakanlığı, 164 s, Antalya.

Pilcher, R., Hamilton, S., Chapman, H., Field, D., Ristovski, B., Stapely, S. 2007. Leak Location and Repair: Guidance Notes. *IWA water loss task force*, 1st version, 67 P.

Ramon, P. et al. 2014. Leak Localization in Water Networks. Model-Based Methodology Using Pressure Sensors Applied to a Real Network in Barcelona. *IEEE*, 24 - 36.

Rossman, L A. 2000. EPANET 2 USERS MANUAL. Environmental Protection Agenci (EPA), 200 p.

Schwaller, J. and VanZyl J. E. 2014. Modeling the Pressure-Leakage Response of Water Distribution Systems Based on Individual Leak Behavior. *ASCE*, 04014089: 1–8.

Thornton, J., Sturm, R, and Kunkel, G. 2008. Water Loss Control. *McGraw-Hill*, 2nd edition, 632 p, New York.

7. EKLER

7.1. EK-1 Tezin İngilizce versiyonu

T.C.

AKDENİZ UNIVERSITY

ORIENTED MODELLING FOR REDUCING WATER LOSSES IN DRINKING WATER DISTRIBUTION NETWORKS BY ADVANCED PRESSURE MANAGEMENT: ANTALYA – KALEİÇİ CASE STUDY

Mustafa S. M. BOLBOL

GRADUATE SCHOOL OF NATURAL AND APPLIED SCIENCES

DEPARTMENT OF ENVIRONMENTAL ENGINEERING

MASTER THESIS

JUNE 2019

ANTALYA

T.C.

AKDENİZ UNIVERSITY

GRADUATE SCHOOL of NATURAL and APPLIED SCIENCES

ORIENTED MODELLING FOR REDUCING WATER LOSSES IN DRINKING WATER DISTRIBUTION NETWORKS BY ADVANCED PRESSURE MANAGEMENT: ANTALYA – KALEİÇİ CASE STUDY

Mustafa S. M. BOLBOL

DEPARTMENT OF ENVIRONMENTAL ENGINEERING

MASTER THESIS

This thesis was accepted by the jury committee on 11/06/2019

Prof. Dr. Habib MUHAMMETOĞLU (Supervisor)

Prof. Dr. Ayşe Burcu Altan SAKARYA

Dr. Öğr. Üyesi Firdes YENİLMEZ

ABSTRACT

ORIENTED MODELLING FOR REDUCING WATER LOSSES IN DRINKING WATER DISTRIBUTION NETWORKS BY ADVANCED PRESSURE MANAGEMENT: ANTALYA – KALEİÇİ CASE STUDY

Mustafa S. M. BOLBOL

MSc Thesis in Environmental Engineering

Supervisor: Prof. Dr. Habib MUHAMMETOĞLU

June 2019; 190 Pages

The water utilities in each country strive to minimize water losses in their water distribution networks (WDNs) to increase the revenue and the capacity of their services. Leakage, which is a flow driven by pressure, is an important type of water losses in WDNs. Hence, pressure management (PM) is one of the principal techniques used for leakage reduction. The classical PM aims at reducing water pressure to a fixed level all the time and ignores the impacts of exceptional water demands, e.g. fire demands. The advanced PM aims at keeping the pressure at the critical points (CPs) in the WDN at the minimum allowable levels all the time besides satisfying the extraordinary water demands as well. Therefore, the advanced PM reduces leakage more than classical PM. Hydraulic modeling is a fundamental tool in applying PM for leakage reduction. In this thesis study, hydraulic modeling of Kaleiçi WDN has been carried out by EPANET 2.0 software using Hazen-Williams equation. Volume of leakage was determined by the standard water balance. Assuming a uniformly distributed leakage along each pipe, the total leakage has been distributed to all junctions in the model by defining the leakage coefficients, which are determined by the half-length of the pipes connected to each junction. Consequently, the leakage has been predicted spatially and temporally. The impact of several parameters such as roughness coefficient and leakage exponent on the precision of modeling has been investigated. The pipe roughness coefficients have been calibrated and verified for a value of 57.6. Depending on the verified roughness value, the leakage reduction by an advanced PM technique has been predicted over two simulation periods in summer and winter to be 6.82 m^3/h and 5.79 m^3/h, respectively. Finally, two scenarios related to leakage reduction by advanced PM have been examined. The first scenario assumes a future change of non-leakage flow by ±%25, while the other scenario assumes that leakage is reduced to the economic leakage level (ELL). The spatial and temporal leakage predictions and the impact of each scenario on the predicted pressure at the CP have been shown in the results. It has been found that hydraulic modeling is an essential tool for spatial and temporal prediction of leakage.

KEYWORDS: Advanced pressure management, Antalya, EPANET, hydraulic modeling, leakage modeling, leakage prediction in space and time.

COMMITTEE: Prof. Dr. Habib MUHAMMETOĞLU

Prof. Dr. Ayşe Burcu Altan SAKARYA

Asst. Prof. Firdes YENİLMEZ

ACADEMIC STATEMENT

Thesis name "Oriented Modelling for Reducing Water Losses in Drinking Water Distribution Networks by Advanced Pressure Management: Antalya – Kaleiçi Case Study" is written in accordance with academic rules and ethical values. I declared that I had references all of the information that does not belong to me.

11/06/2019

Mustafa S. M. BOLBOL

TABLE OF CONTENTS

LIST OF SYMBOLS AND ABBREVIATIONS

<u>Symbols</u>

%   : Percentage.

γ   : Pressure exponent, Leakage exponent, Emitter exponent.

ε   : The tolerance value for the difference between the predicted and calculated leakage.

Δ   : Pressure mean absolute error.

C   : Emitter discharge coefficient, Leakage coefficient.

$C_{net}{}^f$: Final value of leakage coefficient.

$C_{net}{}^i$: Initial value of leakage coefficient.

C_j : Junctional leakage coefficient.

C_{net} : The network leakage coefficient.

l_i : Length of i'th pipe.

l_j : Summation of half-length of all pipes connected with the junction (j).

L_j : Relative importance factor of the junction (j).

m^3/h : Cubic meter per hour.

m^3/y : Cubic meter per year.

P_j : Junctional pressure.

P_{net} : Average system pressure.

Q_A : Quantity of authorized consumption.

Q_{AL} : Quantity of apparent losses.

Q_{BA} : Quantity of billed authorized consumption.

Q_{BDj} : Junctional base demand.

Q_I : Quantity of system input volume.

Q_j : Junctional leakage.

Q_L : Quantity of water losses.

$Q_{net,model}$: The predicted leakage.

$Q_{net,real}$: The calculated leakage of any WDN.

Q_{RL} : Quantity of real losses.

Q_{UA} : Quantity of unbilled authorized consumption.

R_i : Trial roughness coefficient.

Abbreviations

AC   : Asbestos Cement.

ACV   : Automatic Control Valve

ALC   : Active Leakage Control.

AMR   : Automatic Meter Reading.

ASAT   : Antalya Water and Wastewater Administration
           (Antalya Su ve Atıksu İdaresi)

AT   : Awareness Time.

AWWA   : American Water Works Association.

CARL   : Current Annual Real Losses.

CP   : Critical Point.

DMA   : Discrete Meter Area.

ELL   : Economic Level of Leakage.

GSM   : Global System for Mobile communications.

ILI   : Infrastructure Leakage Index.

IWA   : International Water Association.

LNF   : Legitimate Night Flow.

LT   : Location Time.

MAE   : Mean Absolute Error.

MNF   : Minimum Nighttime Flow.

MSL   : Mean Sea Level.

NRW   : Non-Revenue Water.

PI   : Performance Indicator.

PM   : Pressure Management.

PMP   : Pressure Measuring Points.

PRV   : Pressure Reducing Valve.

PSA   : Pilot Study Area

RT   : Repair Time.

SCADA   : Supervisory Control and Data Acquisition

SIV   : System Input Volume.

SMS   : Short Message Service.

SWB   : Standard Water Balance

TÜİK   : Turkish Statistical Institute (TÜrkiye İstatistik Kurumu)

UARL   : Unavoidable Annual Real Losses.

UFW   : Uncountable for Water.

UK   : United Kingdom.

USEPA   : United States Environmental Protection Agency

WDN   : Water Distribution Network.

WHO   : World Health Organisation.

LIST OF FIGURES

LIST OF TABLES

1. INTRODUCTION

1.1. Problem Statement

According to World Health Organisation (WHO), out of more than 7 billion of earth residents (Worldmeters 2018), only 71% of them is served with safe and continuous water for daily life, about 850 million are destitute of a basic level of drinking water service. Moreover, it is expected that the global population will face water scarcity in many areas by 2025 (WHO 2015). 24/7 available safe water is important for public health in the fields of drinking and domestic usage, food production, and recreational aims. Therefore, improving water supply systems and managing water resources are essential for countries to grow economically and reduce the levels of indigence within their people.

Technically, water supply systems face a challenging problem of water loss. Water loss is grouped into two types; (a) physical (real) water loss, and (b) commercial (apparent) water loss. The apparent water losses are related to human illegal usage (water theft), data handling errors, or costumer meter inaccuracy. Real water loss is the pressure dependent type of water losses which generally forms the major part of water losses all over the world (Muhammetoglu and Muhammetoglu 2017). Water losses have a much lower level in developed countries than in developing and undeveloped countries due to several reasons such as the good infrastructure and qualified staff of water utilities in developed countries (Water And Waste Water International 2018). Water utilities should work hard to maintain water losses in their networks at the lowest possible limits to lessen the dissipation of energy, the exploitation of groundwater, and risks of aquifer contaminants due to water over-extraction (Danish Environmental Protection Agency 2018). Since physical water loss (leakage) forms the majority of water losses, then it deserves to be maintained at lower limits. Leakage level depends on several factors such as pipe connections, internal or external pipe corrosion, mechanical damage, ground conditions, system pressure, pipe age, and qualification level of handicraft (Puust et al. 2010).

In all WDNs, leakage increases considerably with increasing water pressure. Therefore, the commonly used strategy to reduce leakage is pressure management (PM). The basic idea of PM is to maintain pressure at the minimum legislated levels and not exceeding the maximum legislated levels at all junctions all the time in the WDN. The PM techniques require essentially localizing of the critical point(s) of pressure (CP) where the pressure is minimum or maximum all the time. CPs must be detected by hydraulic modeling of the WDN under investigation. Therefore, hydraulic modeling is the body-subject of the thesis. In Antalya city, Turkey, Kaleiçi WDN has been chosen as a pilot study area (PSA) in order to apply this research. Kaleiçi WDN has been constructed as a discrete meter area (DMA) and has been modeled hydraulically according to Hazen-William equation using EPANET 2.0 software which developed by the United States Environmental Protection Agency (USEPA) (USEPA 2000). The hydraulic model of Kaleiçi WDN has been calibrated and verified, then it has been used to predict the leakage reduction due to applying the closed-loop pressure control as an advanced PM technique. Additionally, two scenarios of applying advanced PM have been tested. The first scenario imposes a possible change of non-leakage flow in the future while the other scenario assumes that leakage was reduced to the economic leakage level (ELL). It has been exhibited in the thesis how hydraulic modeling played an essential role in predicting

leakage reduction by applying advanced PM. Besides, it is found that hydraulic modeling is a vital tool for predicting leakage spatially and temporally.

1.2. Aims and Scope of The Research

The main objective of this study is predicting the distribution of total leakage rate in space and time to all junctions in WDNs through predicting pressure at each junction by hydraulic modeling. Also, the study aims at predicting leakage reduction by advanced PM. Kaleiçi has been chosen as a PSA to apply this study. The total leakage rate in Kaleiçi WDN has been calculated monthly in standard water balance (SWB) tables within the scope of a previous research project. To achieve the aim of this research, the pipe roughness coefficients, the leak coefficient, and the leakage exponent must be determined. Then the calculated leakage through the SWB is distributed to the junctions in space and time. The scopes of the study are summarized as follows:

1. Surveying the literature related to WDNs in terms of hydraulic modeling, water losses modeling, water losses lessening, and case studies of advanced PM application, hydraulic modeling, and physical water losses calculations.

2. Investigating the monthly calculated SWB of Kaleiçi WDN and the water pressure through the network.

3. Distributing the calculated leakage rate through SWB to the nodes of the WDN in space and time by carrying out hydraulic modeling.

4. Calibration of the hydraulic modeling of Kaleiçi WDN for the determination of pipe friction coefficient. Checking the model reliability by verification processes.

5. Applying advanced pressure management.

6. Predicting leakage reduction as a result of applying advanced pressure management.

7. Investigating two scenarios of applying advanced PM; the first scenario assumes that non-leakage flow changes in future by ±25%, while the second scenario assumes that leakage is reduced to ELL.

1.3. Thesis Outline

The study consists of five chapters. Chapter one states the problem under research and identifies the objectives of the thesis. Chapter two investigates the literature related to water losses in terms of definitions, the national and international situation, leakage reduction strategies, and related case studies. Chapter three demonstrates the methodology used to model physical water losses in the study area (Kaleiçi). Also, applying advanced pressure control technique and investigating two scenarios related to the future possible change of consumption or leakage in the study area are included in this chapter. Chapter four discusses the results of calibration and verification processes of the hydraulic model of Kaleiçi WDN, the predicted leakage reduction by applying advanced PM. Moreover, it contains the results of tested scenarios and leakage reduction by advanced PM application on each scenario. Finally, the conclusions and recommendations are provided in chapter five.

2. LITERATURE REVIEW

2.1. Water Losses in Water Supply Systems

All over the world, the losses of water in any water supply system happens either by subscribers or in piping network. Water loss as a general term is divided according to the position of occurrence into two main parts:

1- Physical (real) water loss: it is the water leaked from pipes, joints, or fittings inside WDN. The overfilling of the reservoir, the leaks or overflowing of tanks, or any accidental damage of the system are also considered as real losses.

2- Commercial (apparent) water loss: it is a loss of water due to the imprecision of customer metering systems (records of consumption are below the real value), the data handling error, or any unauthorized consumption. It is considered as losses since its revenue cannot be gathered by water utilities (Thornton et al. 2008).

Kingdom et al. (2006) state that leakage forms the paramount part of physical losses. Therefore, physical losses are the term used basically for defining leakage since tank overflow or reservoir leakage are usually numerous events and often can be detected easier than pipe leaks (AWWA 2009). Leakage is considered as the technical loss of water since the input volume of water is not delivered totally to the end-users. Based on that, leakage occurs technically in three forms; reported, unreported, and background leakage (Figure 2.1).
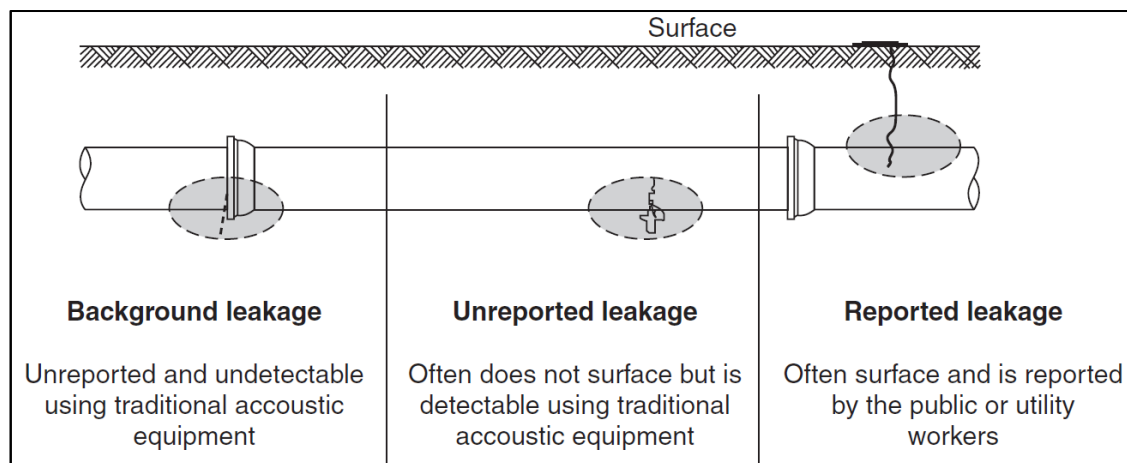
Figure 2.1. Forms of leakage (Thornton et al. 2008)

The reported leakage is the burst events. Since it appears to the surface, reported leaks are usually found out immediately after occurrence. Unreported leaks usually buried underground and take a far longer time until being detected. Background leakage is hard to be detected and runs continuously for long period until being the detectable type of leakage, that is why background leakage is considered as the greatest share of physical water losses in any WDN. The only technique to reduce background leaks is PM, otherwise renewing WDN is the final solution (Thornton et al. 2008).

Leakage cannot be avoided at all in any water supply system. Even in the newly installed WDN, a minimum leakage flow exists (Unavoidable real loss). There are many causes of leakage occurrence in any WDN; the improper setup of the pipe due to unqualified workmanship, insufficient quality of materials, wrong backfill, pressure transients, pressure fluctuation, excess pressure, material corrosion, vibration and traffic loading, environmental conditions, and improper maintenance programme (Thornton et al. 2008).

2.1.1. The Standard Water Balance (SWB)

The first step to estimate water losses is establishing of water balance tables at regular intervals (usually yearly) for the water supply system under study. Water balance is a worldwide used approach because of being accredited by many countries and utilities (FALLIS 2011). The elements of SWB are shown in Table 2.1 (Fanner, et al., 2007a).

Generally, SWB is read from left to right starting from System input volume (SIV) through the different types of consumption and losses ending with revenue and non-revenue water (NRW). According to this arrangement, the elements of SWB are explained as follows:

1- System Input volume (SIV): the total quantity of treated water pumped to WDN whatever the water is self-sourced or imported across operational boundaries.

2- Authorized consumption: the volume of metered and unmetered water consumed by the subscribers who are registered officially as customers in the responsible water utility. It may include water consumption for special purposes such as firefighting, infrastructure maintenance, recreational places like parks or fountains, etc. The authorized consumption may be billed or unbilled.

3- Water losses: the difference between SIV and authorized consumption. It consists of real and apparent losses.

4- Billed authorized consumption: the part of authorized consumption which provides revenue through bills whatever the consumption is metered or unmetered (Also it is called Revenue Water).

5- Unbilled authorized consumption: it is legal consumption of water but not billed. This part includes the water used for firefighting, system flushing, street cleaning, watering of municipal gardens, etc. Or it may include the water consumed in governmental institutions or worship places (mosque, church, etc) (Muhammetoglu and Muhammetoglu 2017). Also, it includes unbilled metered consumption or unbilled unmetered consumption.

6- Apparent losses: the water lost due to customer meter inaccuracies or errors while meter reading and billing, and the unauthorized consumption.

7- Real losses: are the leaks from pipes, fittings, or transmission, reservoir overflow, or leakage from tanks or reservoir.

4

8- Non-revenue water (NRW): the sum of all components which are not billed and do not produce revenue, i.e. the unbilled authorized consumption and water losses. (Fanner et al. 2007a)

The SWB used in the Turkish regulation merge the leakage in transmission and distribution mains with the leakage on service connections in one component (Muhammetoglu and Muhammetoglu 2017)

Table 2.1. IWA/AWWA international standard water Balance (Fanner et al. 2007a)

System input volume (Q_I)	Authorized Consumption (Q_A)	Billed Authorized Consumption (Q_{BA})	Billed Metered Consumption	Revenue water
			Billed Unmetered Consumption	
		Unbilled Authorized Consumption (Q_{UA})	Unbilled Metered Consumption	Non-revenue water (NRW)
			Unbilled Unmetered Consumption	
	Water losses (Q_L)	Apparent losses (Q_{AL})	Unauthorized Consumption	
			Customer meter inaccuracies and data handling errors	
		Real losses (Q_{RL})	Leakage on transmission and distribution mains	
			Leakage and overflows at storage tanks	
			Leakage on service connections up to point of customer meter	

2.1.2. Non-Revenue Water (NRW), Worldwide

Internationally, NRW is an innovative expression that used to describe the level of water losses in each country. NRW contains any water pumped into the system while its bills cannot be gathered. NRW is defined as the sum of real and apparent water losses and unbilled authorized consumption (Lambert 2003). NRW is considered as an indicator of operational efficiency of WDN. It is the financial differentiation of water inside pipes of any water supply system, so that water utilities cannot operate efficiently if it does not realize all its revenue due to water losses (Mutikanga et al. 2010).

Globally, the percentage of real losses are about 60% and the rest is considered as Apparent losses (40%). Water losses cannot be zero at all but can be minimized as much as possible. According to the World Bank report, global water losses equals 48.6 billion m^3/year, while 32.7 billion m^3 are lost due to leaks in water supply systems and 15.9 billion m^3 are considered as apparent losses. In some low-income countries, water losses are 50-60% with an average estimated regionally at 35% (Kingdom et al. 2006). NRW varies from less than 10% in developed countries to more than 50% in developing counties as shown in Figure 2.2.
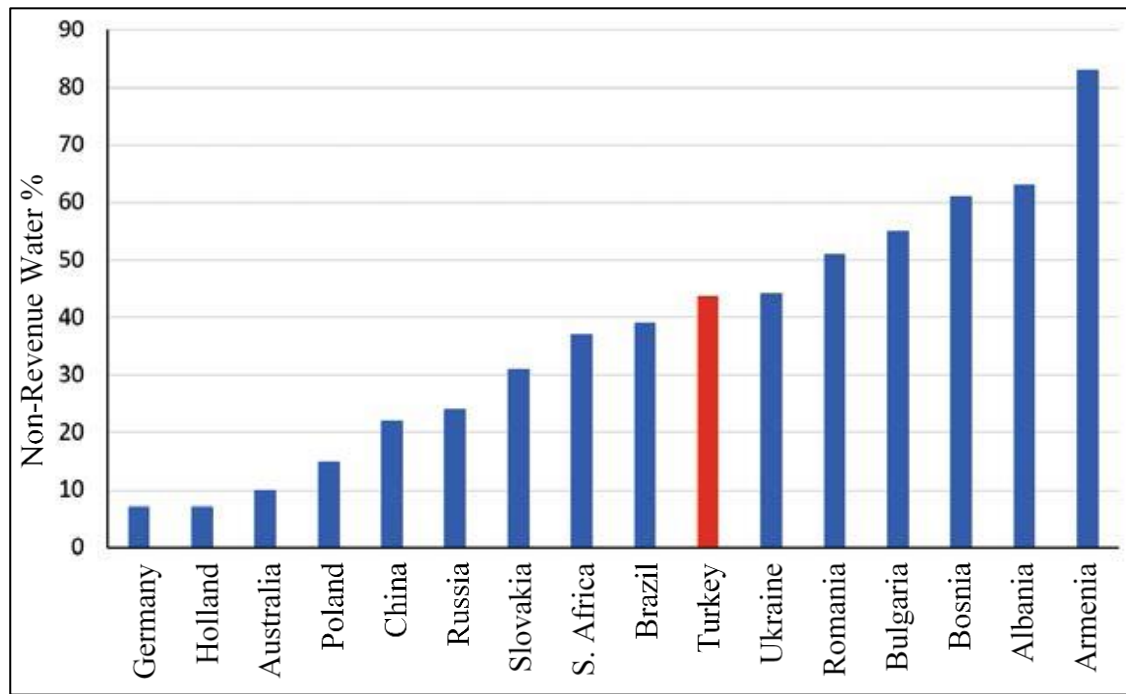
Figure 2.2. Level of Non-Revenue Water in Some countries 2010, adapted from (Muhammetoglu and Muhammetoglu 2017)

The reason for low water losses in developed countries is the level of response strategies and response sensitivity of decision-makers in these countries. Water utilities in developed countries have water loss management plans for reducing the losses to an optimum level (Makaya and Hensel 2015). The European Federation of National Associations of Water and Wastewater Service (EurEau) in the recent report estimates that there are approximately 4.2 million kilometers pipes of water network in all member countries, each inhabitant has a share of water pipes extends from 4.92 m/inhabitant in Spain to 19.55 m/inhabitant in Finland. Inside these water supply systems, NRW is estimated as 23% in all EurEau member countries as shown in Figure 2.3 (EurEau 2017).

In developing countries, the urbanization increases five times faster than in developed countries. Besides that, the population growth in undeveloped and developing countries is estimated to be twice higher than the rate in developed countries. In addition, a significant amount of transmitted water between treatment plants and customers is lost as leaks from transition lines. Moreover, most of water supply systems in developing countries are facing a problem of intermittent supply of water, i.e. water is not provided

24/7, which causes a high level of pressure-based losses, injustice distribution of water, and high level of water contaminants (Dighade et al. 2014).
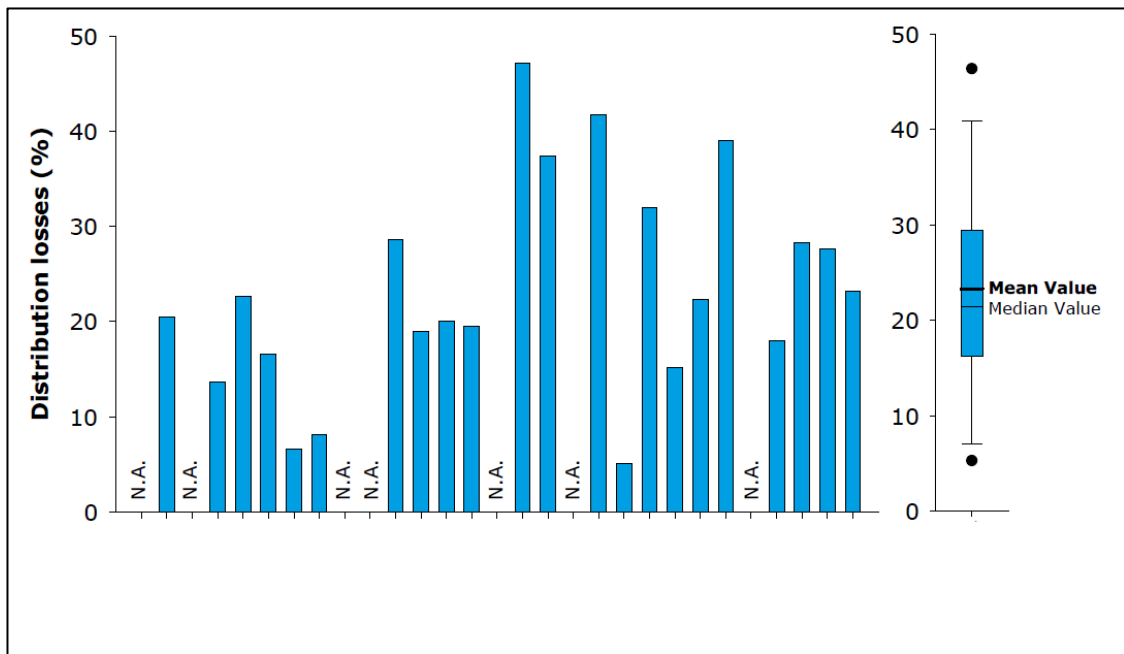
Figure 2.3. Water losses in European countries (EurEau 2017)

2.1.3. Water losses in Turkey – Antalya

In Turkey, there are around 80 million inhabitants living in 81 provinces (TÜİK 2018). Within these provinces the water is consumed in five forms; for governmental institutes, commercial purposes, domestic usage, constructions, and recreational aspects (Öztürk et al. 2007). Municipalities are responsible for management of water supply systems in Turkey. Supervisory Control And Data Acquisition (SCADA) systems are found within the structure of several water utilities in Turkey for monitoring and controlling reservoirs water level, pressure, and flow of water in WDNs. Conversely, there are many municipalities are not provided with any flow or pressure meters for recording purposes. Old infrastructure, improper management, weak maintenance of networks, illegal consumption, and inadequate reliable data for evaluation of WDNs are the main challenges of water losses management in Turkey (Karadirek, 2016).

According to the statistics of the Turkish Statistical Institute (TÜİK), NRW in Turkey between 2004 and 2016 are presented in Figure 2.4 (TÜİK 2018). Determination of NRW requires sensitive flowmeters to measure the system input volume in all water distribution networks which are not found all around Turkey, because of that the NRW level in Turkey is evaluated to be more than levels given by TÜİK (Muhammetoglu and Muhammetoglu 2017).
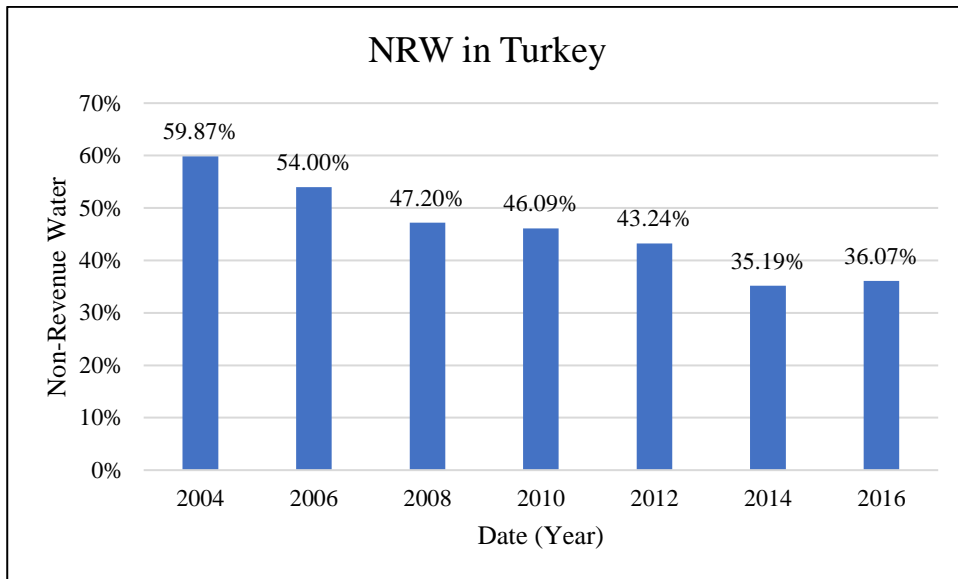
Figure 2.4. Non-Revenue Water in Turkey, 2004 - 2016, (TÜİK 2018)

On the other hand, the Turkish official gazette, where the official decisions are advertised, had published a regulation in 2014. The regulation declared that in the metropolitan municipalities, the water losses must be maximum 30% in the first five years after 2014 and must be lessened to 25% in the following four years. In the other municipalities, the water losses must be maximum 30% within the first nine years after 2014 and must be reduced to 25% in the following five years. The regulations stated important procedures that must be applied to reduce water losses:

1. The system input volume of the WDNs must be measured and saved regularly.
2. The water consumption of all subscribers must be measured by costumer water meters and saved regularly. The age of costumer meters must not be more than 10 years.
3. All water utilities must prepare yearly SWB.
4. Dividing the installed WDNs into discrete meter areas (DMAs) and designing the new WDNs as DMAs.
5. The input flow of each DMA and the critical pressure of each DMA must be measured and saved.
6. The maximum legislated static pressure is 60 m.
7. Geographic Information Systems (GIS) and suitable monitoring systems (e.g. SCADA) must be installed for monitoring and saving the datasets.
8. Using the acoustic instruments for reducing water losses.
9. Hydraulic modeling must be performed for each WDN (Muhammetoglu and Muhammetoglu 2017).

Groundwater, which is the main source of drinking water in Antalya, is naturally very hard but has good quality. Recently, customers were using local storage tanks to sustain a continuous supply of water for domestic purposes because the WDN was facing frequent cuts. Because of that, most of the residents of Antalya were refusing to drink from tap water due to adverse health impact. Nowadays most of such tanks are out of service since the water is provided 24/7, and the customers' satisfaction raised up but still

afraid of using tap water as a direct source of drinking water (Celik and Muhammetoglu 2007).

Because of its location along the Mediterranean coast, Antalya is one of the highest attractive cities in Turkey for tourists. Antalya Water and Wastewater Administration (ASAT) is responsible for the water supply system of the province. The water supply networks are monitored online by SCADA central station found in the structure of ASAT for the purpose of conserving adequate quality and quantity of the water provided to the customers (Akdeniz and Muhammetoğlu 2016).

Based on the regulation announced in 2014 and as an example of good behaviour of the water utility, ASAT prepares annual reports of water losses in Antalya province. The calculated NRW of Antalya province in between 2016 – 2018 is shown in Figure 2.5 and Table 2.2 shows the last published SWB of ASAT for 2018 year for Antalya province. (ASAT 2019).
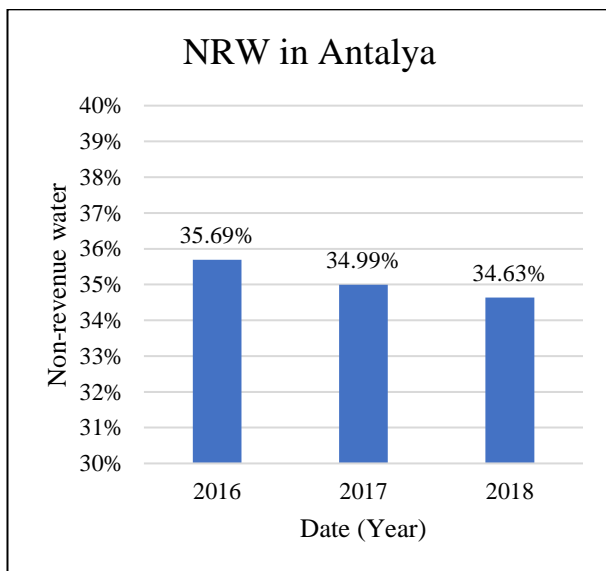
Figure 2.5. Non-revenue water in Antalya province (ASAT 2017a, 2018, 2019)

Table 2.2. SWB of 2018 of Antalya province (ASAT 2019)

System input volume $Q_I =$ 269,693,359 m³/y (100%)	Authorized Consumption $Q_A =$ 176,740,622 m³/y (65.53%)	Billed Authorized consumption $Q_{BA} =$ 176,265,888 m³/y (65.36%)	Billed metered consumption 176,265,888 m³/y (65.36%)	Revenue water 176,265,888 m³/y (65.36%)
			Billed unmetered consumption 0 m³ (0%)	
		Unbilled Authorized consumption $Q_{UA} =$ 456,734 m³/y (0.17%)	Unbilled metered consumption 456,734 m³/y (0.17%)	Non-revenue water 93,402,539 m³/y (34.63%)
			Unbilled unmetered consumption 0 m³ (0%)	
	Water losses $Q_L =$ 92,952,737 m³/y (45.17%)	Apparent losses $Q_{AL} =$ 19,466,020 m³/y (7.22%)	Unauthorized consumption 108,026 m³/y (0.04%)	
			Customer meter inaccuracies and data handling errors 19,357,864 m³/y (7.18%)	
		Real losses $Q_{RL} =$ 73,486,818 m³/y (27.25%)	Leakage on transmission and distribution mains 72,093,818 m³/y (26.73%)	
			Leakage and overflows at storage tanks 1,376,162 m³/y (0.51%)	

2.1.4. Benefits of reducing water losses

Water losses, especially leakage, cause contamination in water pipeline which results in adverse effects on public health (Kouchi et al. 2017), and infrastructure damage (BBC, 2017). There are several economic benefits of reducing the water losses; reducing the physical water losses leads to lessening system input volume of the WDN. Consequently, the depletion of water resources is reduced and energy consumption decreases. Besides that, the NRW decreases, the revenue of the supplied water services increases, and the infrastructure repairing frequency is reduced. Generally, the supplied fresh water is treated to a certain degree before it is pumped to the system, reducing the physical water losses lessens treatment costs of fresh water. In additional to the economic benefits, reducing the physical water losses leads to grater maintaining of the provided water quality (Muhammetoglu and Muhammetoglu 2017). Social benefits are represented in lower price of water services, job creations for workmanship, promotion of social aspects and increasing the customers satisfaction on the freshwater services. Environmental benefits are represented in the reduction of greenhouse gas emission (Xu et al. 2014).

2.2. Leakage Management Techniques

International Water Association (IWA) and the American Water Works Association (AWWA) suggest a methodology to evaluate water losses in any water supply system. The methodology stands for two phases; the first one is establishing of water balance tables periodically (usually yearly) to calculate the usage and losses of water. The second phase is an evaluation of water losses in different sized WDNs using a term of water loss performance indicators (PI). The benefits of the IWA/AWWA methodology can be summarized as follows:

1- It is a standard international best practice for water loss calculations,

2- The methodology assists in the determination of unavoidable annual real losses (UARL) and finding out the non-seen leaks which could be considered as a part of authorized consumption,

3- Discovers other terms to describe water losses than the percent of input flow,

4- Dropped the term of uncountable for water (UFW),

5- Every type of water usage or loss has a specific division in water balance, and

6- An expressive comparison of water audit results can be carried out using PIs, independent from different characteristics of compared WDN.
(Thornton et al. 2008)

SWB has explained above in the previous section. Herein, the performance indicators concept is going to be illustrated briefly.

Water utilities have dissimilar characteristics of their water supply systems in terms of size, intense of customers, the age of networks … etc. Therefore, comparing the performance of water loss management using the volume per year or percentage of SIV

is not the best way because water loss in WDNs of high consumption has a low percentage comparing with those of low consumption. On the other hand, if there is water export from the investigated network, which could be included in water consumption, then water loss expressed in percentage of SIV will be too much low (Thornton et al. 2008).

Lambert et al. (1999) recommend two PIs for comparing water losses of different WDNs; the water loss volume per service connection per day (e.g. L/service connection/day), and the infrastructure leakage index (ILI) which is adapted by IWA (Delgado, 2007). The best-recommended PI is ILI since it is the dimensionless ratio between the current annual real losses (CARL) and UARL, equation (2.1).

$$ILI = \frac{CARL}{UARL} \tag{2.1}$$

The CARL is based on the results of the periodically determined water balance. A component-based approach adopted by IWA to calculating UARL is described in detail by Lambert, et al. (1999). The approach considers the three forms of leakage; background leakage, reported leaks and unreported bursts. Lambert, et al. (1999) have suggested a basic form to determine UARL shown in equation (2.2):

$$UARL = \left(18 * L_m + 0.8 \times N_c + 25 \times L_p\right) * P \tag{2.2}$$

where L_m is the mains length in km, N_c is number of service connections, L_p is the total length in km of the pipes between the edge of street and customer meters, and P is the average operating pressure in meters.

2.2.1. Basics of leakage

It is essential for water loss management staff to recognize the structural characteristics of leakage incidences and suitable techniques to control them. The types of leakage and the factors affecting the leakage detection are summarized in the following sub-sections.

2.2.1.1. The types of leakage

The types of leakage are classified according to the infrastructure elements in WDNs to:

1- Main bursts or pipe fracture

It is the catastrophic pipe failure occurs due to pipe corrosion, unstable or excessive pressure, ground movement or combination of these factors. This type of water loss is reasonably detectable because it appears to the surface usually faster than the other types, also causes a sudden drop in pressure inside WDN.

2- Crack

It is a mechanism of pipe failure which happens due to peripheral or longitudinal failure such as pipe deterioration or ground movements. It may be undetected for some time, but it is generally definite and of high audible frequency.

3- Pinhole

It has the form of leaks that are small circular failures in rigid pipelines. It is formed generally due to the corrosion caused by the lack of protective procedures, or the stress of stones after poor backfill during installation. This kind of leak is usually detectable and generates recognizable noise that differs according to the pressure, pipe material, and backfill.

4- Seepage

Commonly it is found on deteriorated asbestos cement (AC) pipes where the pipe wall becomes semi-porous and water escapes slowly. These types of leaks are extremely difficult to locate as leak noise is minimal.

5- Leakage on packing glands of pumps and valves

These leaks result due to pump deterioration overtime or valve fittings and usually occur when a valve is used after a long period of inactivity. This leakage is detectable and can easily be controlled within a short time.

6- Pipe joint leaks

These are widespread types of leakage, especially on older cast iron and AC pipes where the caulking or joint gasket weakens over time. At the incidents of ground movement, pipe joints usually bear most of the fatigue and often result in leakage, then a fracture case. Welded joints on steel pipes are in fact stronger than the pipe itself but are rarely protected against corrosion after jointing and therefore it is considered as a vulnerable point of corrosive attack. This type of leakage is generally detectable in metallic pipes but oppositely it is hard to be recognized in AC pipes due to the difficulty of noise distinguishing.

7- Leaking service connection pipe

It is the most frequently occurring type of leakage in WDNs. Between the water source and customers, there are many changes of pipe size or material at main and service connection joints, and also at service connection and customer meter joints. These joints are often weak and with frequent fluctuating pressure they are vulnerable to be deteriorated causing leaks. Otherwise, service connections are usually placed very closed to the surface, where they are sensitive to be damaged by traffic load. Leak events at service connections are detectable and often it is possible to recognize the noise generated by them.

8- Leaking fire hydrant, air valves, and scour valves

Leakages that occur in main bursts and pipe fracture, crack, leakage on packing glands of pumps and valves, and leakage on fire hydrants and valves can be included within reported leaks, while pinholes, pipe joint leakage, and service connection types of leakage are contained within unreported leaks. Seepage is considered as background leakage. The background leakage can be minimized by PM techniques or infrastructure replacement. (Thornton et al. 2008)

2.2.1.2. Factors affecting leakage detection

Leaks are discovered in the field through acoustic sensing instruments. The quality of any leak detection process depends essentially on six factors as follows:

1- Pressure

Water pressure is the main factor affects the volume, quality of generated noise accompanying any leakage. Higher pressure leads to higher leakage and therefore higher noise. Pressure is flow related parameter, i.e. consumption during the day is higher than night so that pressure is lower during daytime than the nighttime. Based on that, the best time suggested to search for leaks is 2:00 – 4:00 am when consumption is supposed to be at the lowest level and over-ground noise is minimum.

2- Pipe materials or pipe size

Pipe materials influence the leak in terms of volume and noise transforming along the pipe. In the rigid materials, the leaks hole is smaller and noise travels further distance than in soft materials. On the other hand, metallic materials are protected against corrosion by many means like bitumen or concrete, these materials are voice absorbers and hinder the detection of leaks.

3- Types of leaks noise

Valve packing, pinhole leaks, and small fittings produce higher frequency leak noise than bursts, cracks and some joint leaks. Large leaks generate higher sounds (like rumble) than smaller leaks (like hissing).

4- Backfills over the pipe

The presence of cavities in the medium over the pipe lessens the transmission of leak sound, Therefore, sandy soils and asphalt conduct noise better than clay or concrete.

5- Soil moisture

Raising water in the soil minifies the transmission of leakage noise. Backpressure is created against the leak origin by the saturated soil.

6- Sources of interference with leak noise.

Rather leaks noise many sounds can be generated by other sources like generators, compressors, traffic, pressure reducing valves, vehicles, air conditioners … etc. These sounds contend the leaks noise in any given location and make leak detection more difficult. (Thornton et al. 2008)

2.2.2. Reducing the runtime of leakage

The speed-and-quality-of-repair is one of four intervention tools affect the controlling of leakage in any water distribution network (Figure 2.6). The runtime of any leak consists of three elements as illustrated in Figure 2.7; awareness time (AT), location time (LT), and repair time (RT). Awareness time is counted from the start of the leak to the point of time when leakage is recognized by the operator, its period depends on the level of work under active leakage control program (ALC) and DMA system. Location time is the time used for pinpointing the position of the leak just after being concerned. Repair time begins at the instants when the leak location is detected to the stage when leakage is stopped at that location, (Thornton et al. 2008). Figure 2.7 presents the effect of the runtime of leakage on the total volume of lost water, it is shown that low flow leaks for long period produce more leakage volume than the apparent bursts.
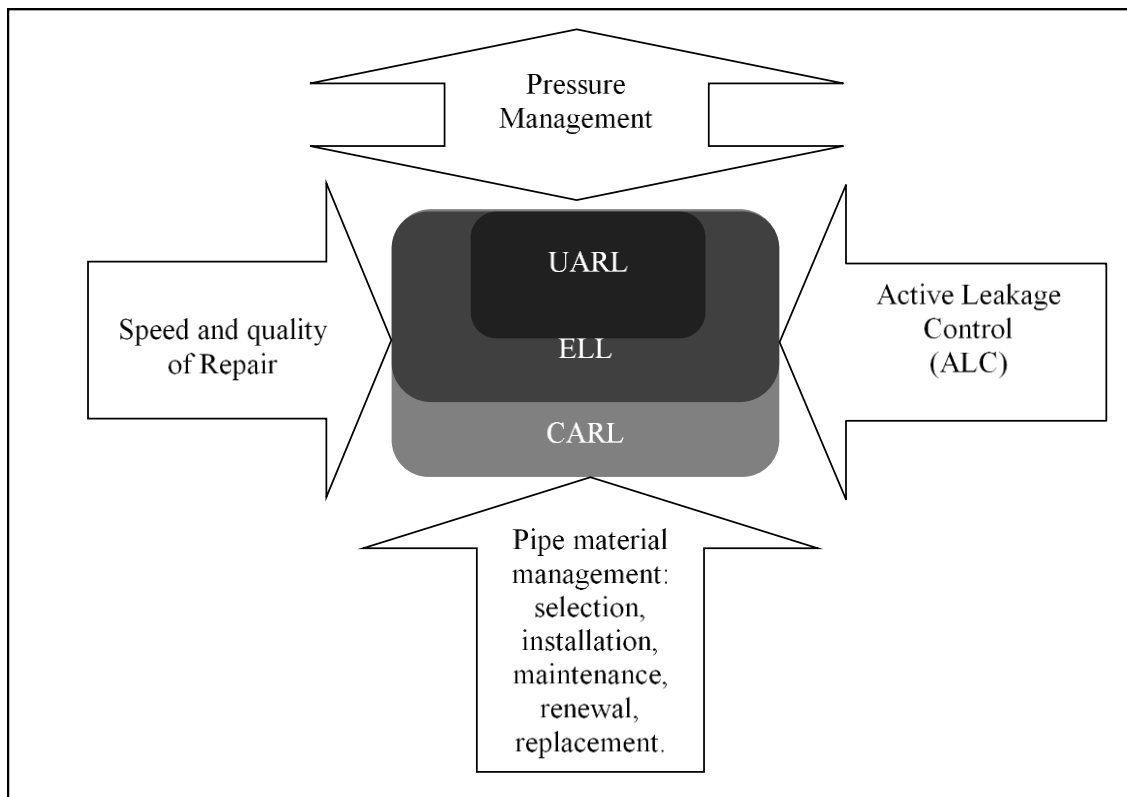
Figure 2.6. The four essential leakage management techniques, (Pilcher et al. 2007)
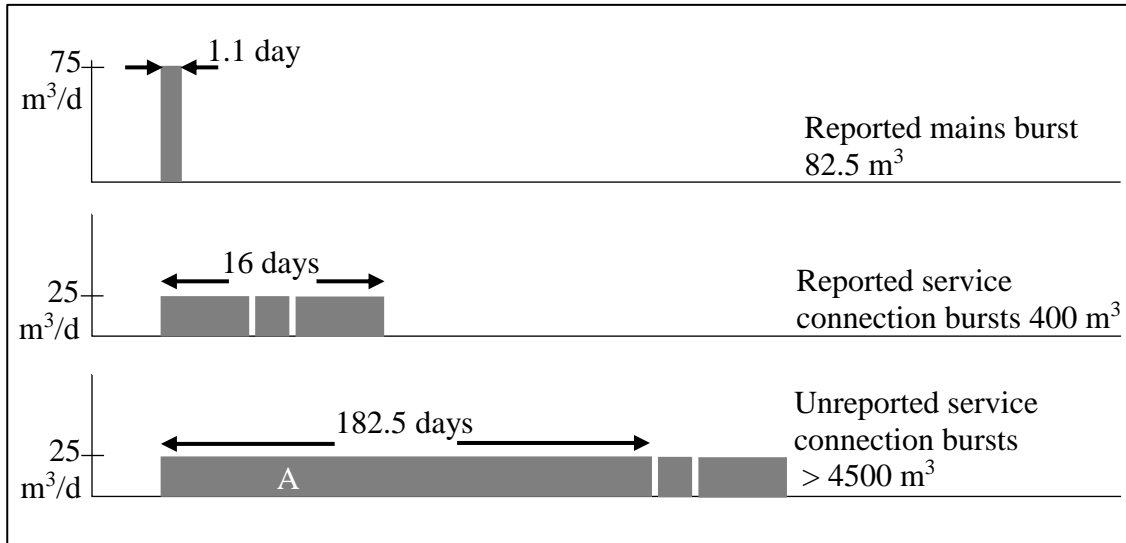
Figure 2.7. The effect of runtime on the volume of leaked water, (Pilcher et al. 2007)

2.2.3. The concept of the discrete meter area (DMA)

The use of DMA principle for management of water supply systems serves in better water losses reduction in terms of lessening the awareness time of leaks. Also, it improves the schedule of ACL program through prioritizing the leaks survey activity to the areas which have the highest level of losses. The awareness time of leakage is reduced by minimum nighttime flow (MNF) analysis of each DMA, therefore leak events can be recognized.

The concept of the economic level of leakage (ELL) is very useful for leakage management within any DMA. ELL is affected by many factors like the cost of water production and personnel or equipment costs used in leak detection. Economic level of leakage is a term describes the point in which the production of 1 m^3 of water has the same cost of reducing 1 m^3 of water losses (Gülaydin 2017).

The main concept of DMA is dividing the water supply system into smaller sections by physical valving or other factors like variable topography and are provided with water by a limited number of feeds (one or more). Each sector is usually quite large with multiple feeds; thus, the localized hydraulic problems are usually not generated due to valve closures. Then at each feeder point there is metering unite records periodically flow, pressure, and/or any quality related parameters of the water provided to DMA (Kara et al. 2015), as shown in Figure 2.8. Sectorization of WDNs which are fed by natural gravity sources usually sectorize by ground level, while WDNs fed by pumps usually sectorize according to levels of elevated tanks or storages (Thornton et al. 2008). Installation of DMAs in any water supply system provides mainly two values:

1- Assists the operators of WDNs to identify the occurrence of unreported leaks through MNF analysis. Therefore, leak detection efforts can be prioritized.

2- Enabling water utility to manage the pressure WDNs at an optimum level (Thornton et al. 2008) (Wright et al. 2014).
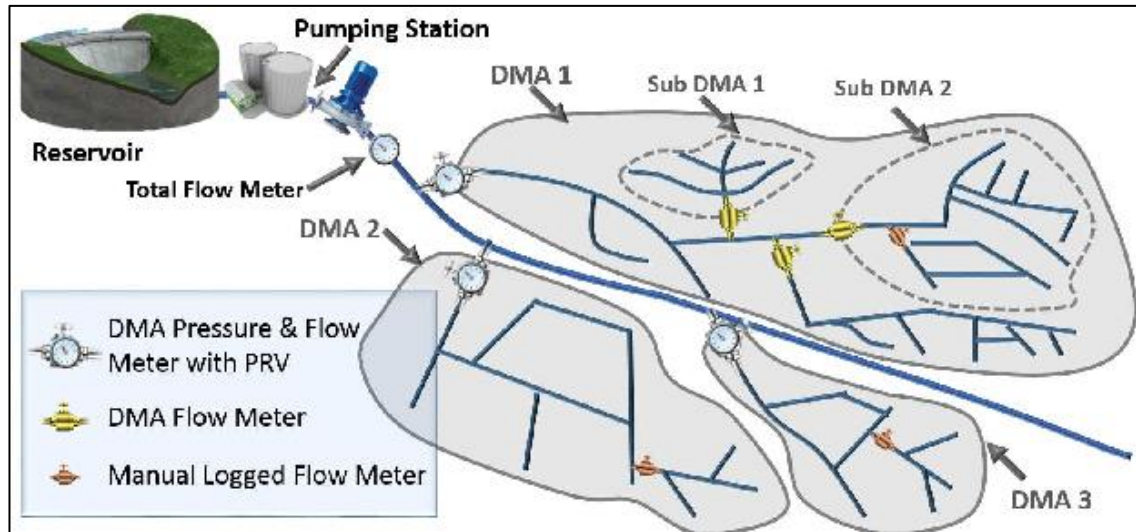
Figure 2.8. DMA layout and the flow meters, pressure meters, and the pressure reducing valves (PRVs) at each feeder point, copied from (Kartakis et al. 2015)

2.2.3.1. DMA monitoring and data analysis

For the purpose of monitoring flow and pressure within each DMA, there are several options such as:

1- Real-time data transmission

The SCADA systems are the most common technique used for online monitoring and controlling of whole elements in water supply systems like pumping station, reservoir sites, pressure reducing valves (PRV), treatment facilities, security, video transmission, and water quality, e.g. Antalya city (Kara et al. 2015).

Real-time monitoring is suitable if the utilities look forward to speedy response to the appearing leak or main break in DMA. Since most of the leaks slowly emerge and small in volume at first, they are not identified at moment. Therefore, it is important to transfer the collected data of these DMAs periodically (e.g. daily) rather than online transferring. For water distribution systems with commonly slowly coming out leaks, the best economical frequency of data collection is once per day (Thornton et al. 2008).

2- Data transmission through GSM telemetry

As a second choice of DMA data monitoring method, the flow and pressure recorded at the feeder point of each DMA are sent periodically (daily, weekly, monthly) by global system for mobile communications (GSM) via short message service (SMS). The advantage of this option is that the capital cost is very low (Thornton et al. 2008).

3- Manual data collection

It is the method of lowest cost of installation since there is no automated communication system required. This approach needs an employee to visit the equipment

periodically. This provides the advantage of frequent visual checks in the field, but the disadvantage is the time and cost ineffectiveness (Thornton et al. 2008).

2.2.3.2. Minimum night-time flow (MNF) analysis

The best analysis of DMA's data is to perform MNF analysis. It stands for the least legal consumptions occurs at the nighttime hours, so that if the legitimate night flow (LNF) is known then MNF = LNF + water losses. In urban areas, MNF usually occurs between 2:00 – 4:00 a.m. MNF analysis is useful for both real losses estimation and prioritizing of leakage detection efforts. Five kinds of data have to be collected for MNF analysis; Length of mains, number of service connections, number of household properties, number and types of nonhousehold properties, and legitimate nighttime consumption. LNF composed of three elements; exceptional night use of water, nonhousehold and household night demand. A leakage modeling for 24 hours based on minimum night flow is shown in Figure 2.9.
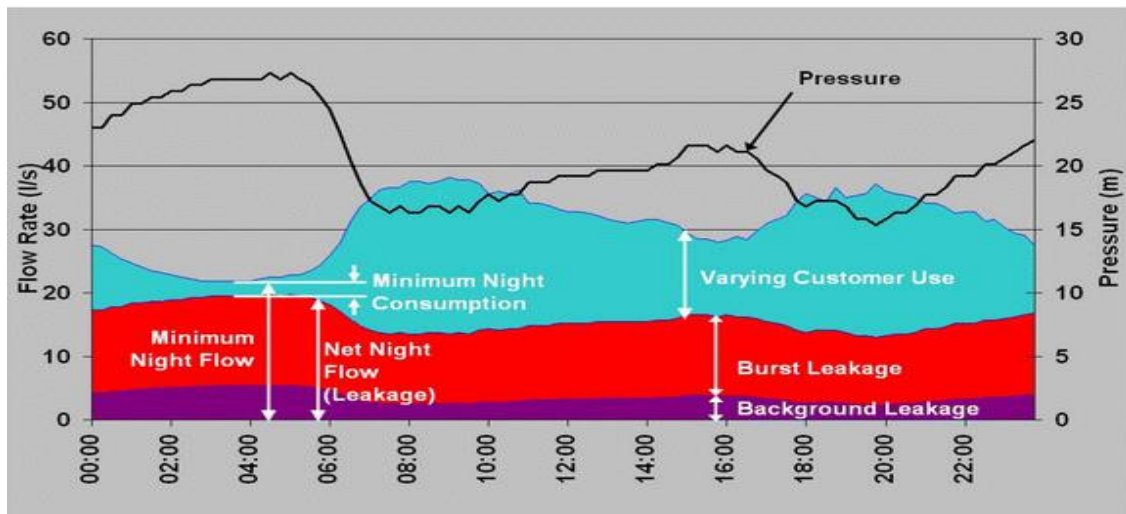
Figure 2.9. Leakage modeling based on MNF, (Pilcher et al. 2007)

2.2.3.3. Impact of DMA on water quality management

Although DMAs have been successfully implemented for water losses reduction in many case studies, it has introduced major operational constraints which influence the quality of water. As a case study of the water company in the United Kingdom (UK), it is found that at one-third of dead-ends resulted in DMAs were defined as discoloration events (Armand et al. 2015).

Sectorization of WDNs to DMAs includes the constant closure of valves in order to achieve a cost-effective leakage management and make pressure control simpler. Armand et al. (2018) state that DMAs may affect the overall quality of water and escalate the discoloration of the water inside the network. Based on this study over 22 DMAs in the UK, the noticed impact of DMAs on water quality was including:

- Water age increasing,

- Increasing of dead-ends nodes by %15,

- Reduction of the diurnal velocity of water,

- A rise in the number of pipes experiencing velocities cause continuous sedimentation by %12 and intermittent sedimentation by %6,

- Diminution in the length of pipes needing self-cleaning velocity by %18,

- A decrease in the length of pipes suffering reverse flow by %10.
  (Armand et al. 2018)

Although the advantages of sectorizing water distribution systems into DMAs for reduction of water losses, it causes real concerns about chlorination. Water losses reduction leads to low flow rates and therefore higher water age. That requires higher chlorine dosing rates to fulfill the relevant chlorine standards in WDN (Akdeniz & Muhammetoğlu 2016).

2.2.4. Pressure management (PM)

Since leakage is a flow driven by pressure, PM represents the most important method can be performed by water utilities for leakage reduction (Figure 2.6). The accurate practice of PM reduces the number of burst events, the hidden background leakage, extends the lifespan of WDN, and in special conditions can cause considerable reduction in the normal consumption (Mckenzie and Wegelin 2009). Vicente et al. (2015) specified the forms of consumptions that can be minimized by PM throughout dividing consumption flow into the pressure-dependent flow and demand driven flow. The pressure-dependent consumption flow, like irrigation systems, showers, and taps, is the only component that may be influenced by the PM process. While the customer consumption, which is a demand driven flow, is affected by PM indirectly.

Pressure management techniques are extending from classical forms like basic sectorization of the gravity system to advanced PM techniques like automatic control valves (ACVs).

2.2.4.1. Classical pressure management

Three basic techniques of PM are going to be summarized in this section; sectorization, pump control and throttled line valves.

Sectorization has been explained in the concept of DMA in upstream sections. Controlling boundary valves of DMAs is the advanced level of pressure management which are explained in the next section.

The usage of pump control for controlling the pressure of WDN depends on the time whenever the pump will be activated or deactivated according to water demand. Pump control is an effective method of pressure control if the lessened level of pumping (mainly at night) can still preserve reservoir levels. If pumps are controlled properly with

variable speed drives, then it can provide a very effective technique of pressure control. But inversely, if the pump is subjected to upstream valve throttling or water demands over of the design limits, then it may be operated outside the designed profile of pumping. On the other hand, insufficient pumps may lead to higher consumption of electricity (Thornton et al. 2008).

The throttled line valve is the least effective method of the pressure controlling in WDNs. Its concept depends on partial closure of gate or butterfly valve at the water feeder point(s) of the water supply system. Closing valves partially create head loss and pressure reduction. But also, the method causes insufficient supply of water, i.e. the pressure will be higher at night when the least pressure is needed and will be lower during the day when high pressure needed for covering customer water demand (Thornton et al. 2008).

Fixed outlet pressure control devices like conventional fixed outlet PRVs are used to maintain the flow through valve with lower downstream pressure, as shown in Figure 2.11a. Thus, using the fixed outlet PRV is an advanced technique of PM.

2.2.4.2.Advanced pressure management

In general, WDN is designed to supply water at some agreed level of service to the customers; i.e. water is provided by which pressure at all nodes in WDN above or equals the minimum limit agreed to the legislation of each utility. This leads to the concept of critical point (CP) at WDN. CP is defined as the node belongs to the lowest pressure in the system at minimum pressure time all over the simulation period (Mckenzie and Wegelin 2009), or the node which has the highest pressure in the system at maximum pressure time all over the simulation period (Muhammetoglu and Muhammetoglu 2017). To apply PM effectively, sensors are installed at CPs to provide the system with feedback about network efficiency (Vicente et al. 2015). On the other hand, there are other terms of the level of service like peak hour and off-peak hour water supply, fire-fighting water flow, time modulated park irrigation … etc. Pressure management should consider all these circumstances in WDN. Figure 2.10 illustrates the concept or PM by which pressure at CP is 20 m at least.

PRV is usually used in WDNs to control the pressure intelligently for leakage reduction purposes (Fontana et al. 2017). Water pressure reduction in WDNs can be accomplished by advanced techniques of pressure control devices like PRV shown in Figure 2.11; Fixed outlet pressure control, Time-modulated pressure control, Flow-modulated pressure control, and closed-loop pressure control (Mckenzie and Wegelin 2009). A brief description of each technique and advantages and disadvantages are summarized in Table 2.3. The appropriate PM method is decided according to available technical competences and budget.
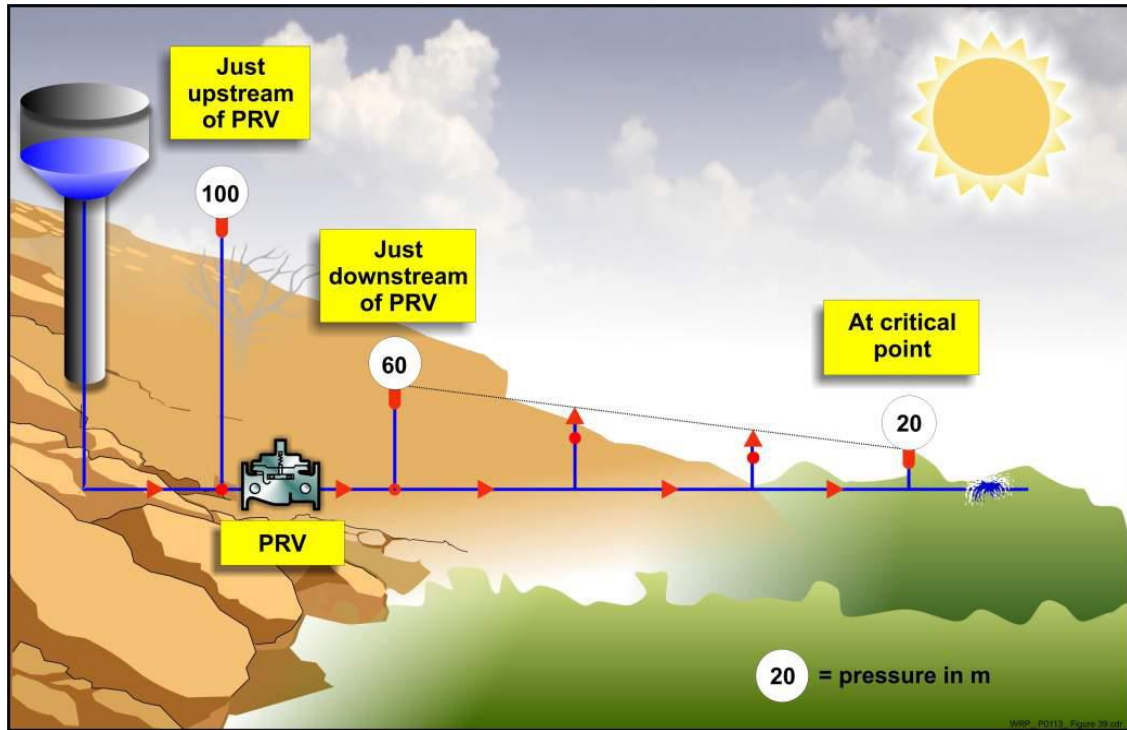
Figure 2.10. Keeping pressure at CP on 20m by PM (Mckenzie and Wegelin 2009)
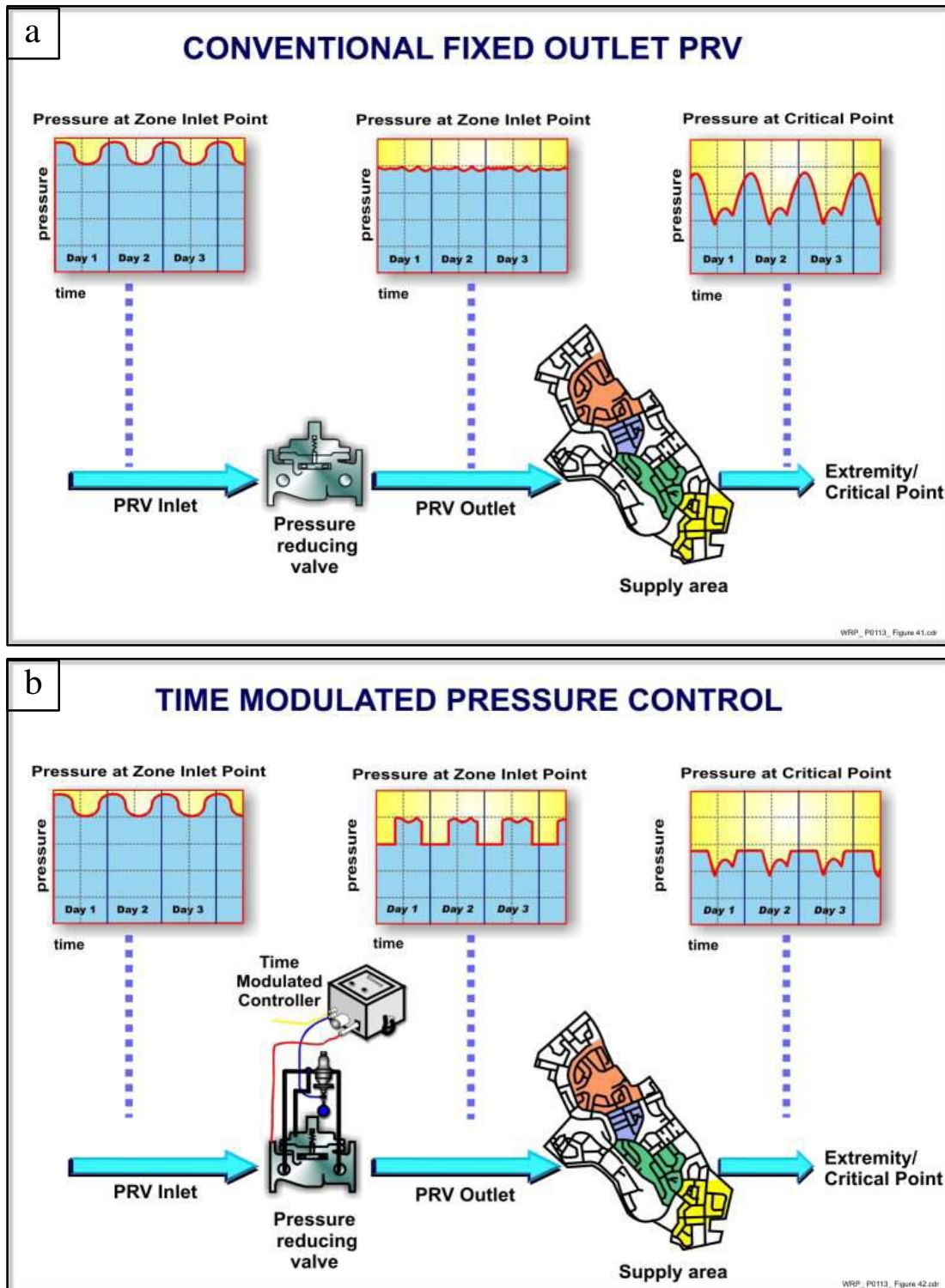
Figure 2.11. Advanced pressure management techniques: a) Fixed outlet pressure control, b) Time-modulated pressure control (Mckenzie and Wegelin 2009)
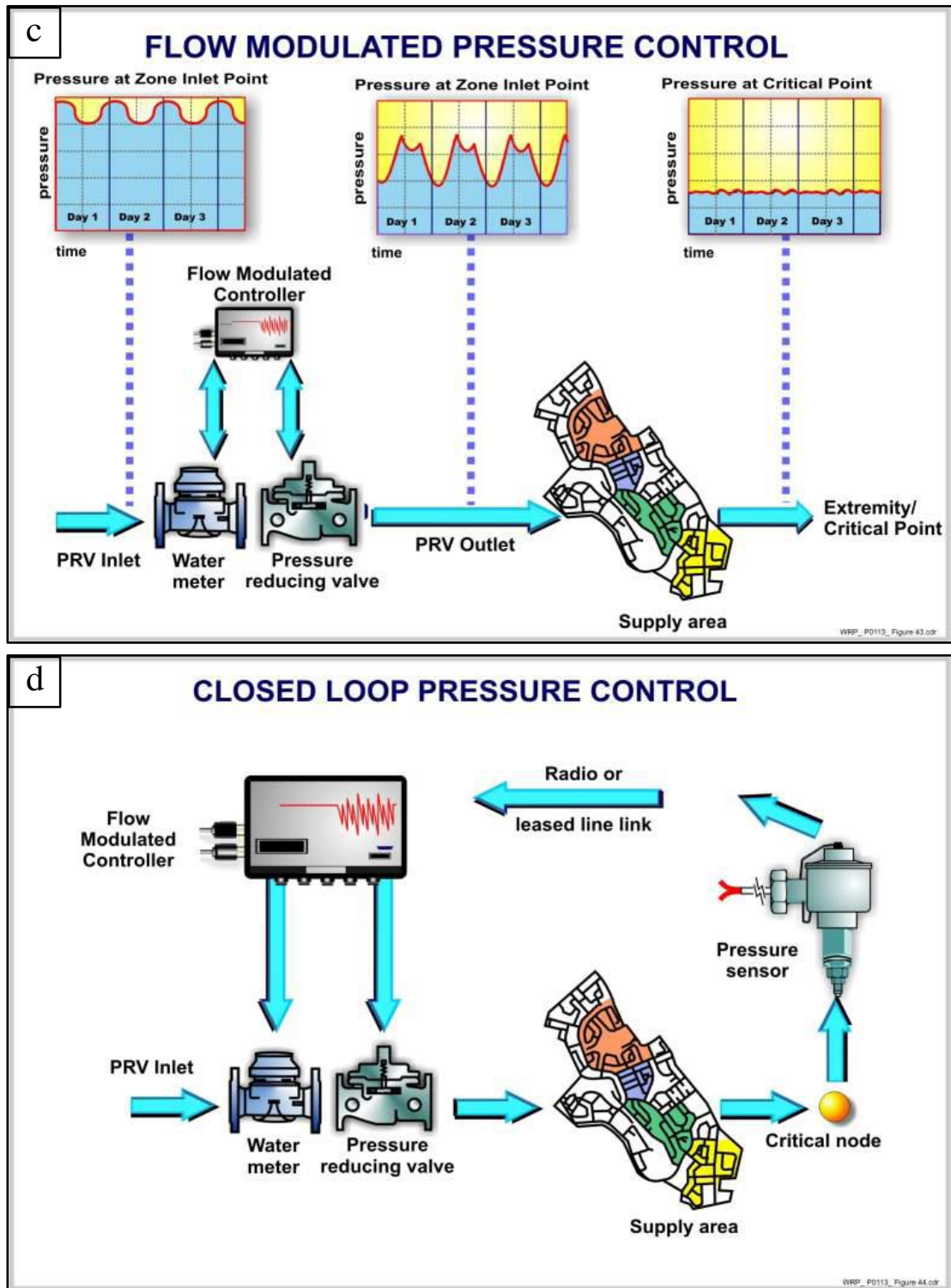
Figure 2.11. (Continued) Advanced pressure management techniques: c) Flow-modulated pressure control, d) Closed-loop pressure control (Mckenzie and Wegelin 2009)

Table 2.3. Advanced Pressure management techniques (Mckenzie and Wegelin 2009)

Technique	Description	Advantages	Disadvantages	Using circumstances
Fixed outlet	PRV controls the max. pressure at the inlet of DMA.	- Simple installation. - low costs. - simple operation and maintenance.	- No flexibility to adapt water pressure by demand change.	- If there are no qualified personnel to operate and maintain the additional assets
Time-modulated	Fixed outlet system in addition to another device for further pressure reduction throughout off-peak periods.	- More flexible in pressure control. - Cheaper electronic controller than the flow-modulated system. - Simple operation. - No need to flow meter.	- no reaction to sudden demand rise, e.g. fire-fighting.	- Useful where water pressures raise up during the off-peak periods.
Flow-modulated	Fixed outlet system in addition to another flow meter and time control device	- Higher control and flexibility. - Higher saving in water losses. - Adapt flow for fire-fighting.	- more expensive. - Requires properly sized meter. - NOT cost effective.	- Useful for fire-fighting events.
Closed-loop system	The pressure sensor at CP sends live data to the PRV at the inlet	- The ultimate level of pressure control. - Maximum leakage reduction.	- The most complicated system. - High chance to equipment fails.	- Useful for areas where flow pattern is not constant all over the year, e.g. touristic area.

2.3. Hydraulic Modelling of Water Distribution Networks

For efficient control of pressure, hydraulic modeling is an essential tool. Managing the complex-wide water supply systems and defining the appropriate methods of PM in any WDN, hydraulic modeling plays a crucial role. Any hydraulic modeling of any WDN should include all elements like pipes, pumps, reservoir, PRVs, and data of

water consumption. A proper hydraulic model needs a high level of details about components of studied WDN, access to all sources of data and outputs which are used as feedback for pressure control process, keeping the records for future analysis and improvements, and powerful simulation equipment and tools for extended period modeling (Mpiana et al. 2017). There are many software programs for implementing the hydraulic or water quality modeling of WDNs. EPANET is an open source simple software developed by USEPA for hydraulic and water quality modeling of WDNs, and it has been used in studying several case studies and researches such as (Köker and Altan-Sakarya, 2015) and (Koker and Altan-Sakarya, 2016)

2.3.1. Detecting of CP for PM applications

Since pressure is the dominant cause of leakage in all forms, then it is necessary to localize the main affecting nodes within WDNs. The system of DMA can usually cause higher average pressure and inconsistency of pressure than larger water supply systems with multiple feeds (Wright et al. 2014).

At the same time, it is necessary for any WDN to provide water service for all customers with adequate pressure, which is generally 20 – 30 m. Based on that, a concept of CP was found to sustain the pressure at the minimum level in all water supply systems including this node where there is a high possibility for pressure to be under minimum limits.

Without needing to field survey to pinpoint CP, available hydraulic modeling software can do such mission by simulating the real WDNs after being calibrated and verified to be reliable, and also for mimicking the pressure control process (Wright et al. 2014).

In the PSA included in this thesis, the methodology of CP detection is going to be illustrated experimentally on real WDN.

2.4. Case Studies

Application of hydraulic modeling principles in water distribution networks assists in the mission of decision makers of water utilities worldwide. Especially in the subject of water losses modeling there are several studies implemented, herein some of them:

Schwaller and van Zyl (2014) modeled the leakage through a large number of randomly distributed leaks in the studied WDN. The aim of the study was to specify if the determined pressure exponent in the field studies can provide the same behavior in the model. Leaks were modeled individually using the FAVAD equation which assumes that pressure and leak area are linearly related. The study found out that mean leakage exponent was around 1 in large water supply systems, and its value is strongly affected by system pressure.

Apulian network in Italy consists of 23 nodes and a reservoir. The WDN need total water demand of 225.6 L/s, while the leakage was estimated to be %25 of demand. Modeling of both demand and leakage was implemented as uniformly distributed along

pipe length. Moreover, a correction of pipe's roughness coefficient has been applied based on the effect of topology in the case study. That effect can be described such that topology simplification creates the distortion in momentum losses which leads to the wrong simulation of leakage. The WDN of the studied area was performed by EPANET and both leakage and demand were considered as uniformly distributed along pipe length with one improvement of the hydraulic resistance correction procedure. Without the correction, the modeled leakage was underestimated (Liu & Yu 2014).

Costanzo et al. (2014) have used the hydraulic modeling in the detection of leaks position in a real WDN in Amantea, Italy. A network containing 39 nodes, 55 pipes, and a reservoir has been modeled. The pipes roughness coefficients have been calibrated in the model by trial-and-error. The study concluded that there is a high possibility to find out the leaks in a real WDN using the calibrated model, but this is dependent on the quality of observed data.

EPANET software has been used in leak localization within one DMA of Barcelona WDN under real leak scenario. The DMA contains 3377 nodes and 3442 pipes supplied with water from two inlets. The inlets and six random selected inner nodes within the DMA are connected with pressure and flow sensors, these sensors are integrated with SCADA central station. The sensors record and send the measurements of pressure and flow every 10 minutes to SCADA, then these records are transferred to the EPANET model in a process of online modeling of the studied DMA. The model is calibrated and verified based on the data sent from sensors. As a result of the online modeling of DMA of Barcelona WDN, the effectiveness and robustness of using modeling in leak pinpointing have been emphasized through the satisfactory results of real faults scenario (Ramon et al. 2014).

Gomes et al. (2013) have studied the benefits yielded by PM through investigating the pressure/leakage relationship from existing leaks. The methodology of modeling depends on the MNF analysis and FAVAD concept. The network which used in the study consists of 42 pipes, 33 nodes, and a reservoir of elevation equals 177m. The author supposed that water consumption is pressure-dependent flow with a pressure exponent of 0.5, while leakage exponent has values between 0.5 and 2.5 based on the type and average system pressure. The results show that PM reduces significantly the water losses, and with lower influence on water consumption. Mainly the pressure exponent plays an important role in achieving the benefits of pressures management.

Old Town DMA (Kaleiçi) which is considered as tourism area in Antalya city, Turkey, has been simulated by EPANET software for the purpose of water supply management. The area of Old town belongs to highly varying topographic levels and significant variation of consumption. The study presents a nodal demand estimation approach for hydraulic modeling of WDNs. The entrance of DMA is provided with SCADA unite for monitoring and recording pressure and flow every five minutes. Also, another 4 pressure loggers were connected with random points inside the DMA. The results show that the model predictions of pressure were in good agreement with the measured pressure at each node connected with pressure logger. (Kara et al. 2016)

Another case study in Antalya city has been investigated. For the water loss management, the water supply system of Konyaalti has been modeled using EPANET

software. The results of the model showed that some DMAs have high pressure and MNF throughout a year. Also, the ILI related to the study area was higher than 20 which indicates a high level of water losses. Based on that, PRV has been installed at one of DMAs. The optimum pressure level (3.0 bar) has been chosen through the hydraulic model of the study area. EPANET model showed a high level of reliability through predicting the water saving of 17 m^3/h which was so closed value to the average water saving calculated by MNF analysis (18.7 m^3/h). This study proofs that hydraulic modeling can be used as an accredited tool for water supply management and prediction the results of applying PM techniques (Karadirek et al. 2012).

2.4.1. Water losses calculations for 32 hours (Kaleiçi – Antalya)

As a part of the research project implemented in Kaleiçi WDN (Muhammetoğlu 2017), calculations of water losses were done for 32 hours (10:00 02.06.2016 – 18:00 02.06.2016), Table 2.4. The system input volume of every 5 minutes measures was gained by the SCADA station at the inlet of Kaleiçi DMA. The consumptions and apparent losses were determined as follows:

- Measures of AMR systems: The consumption of 855 subscribers who are provided with AMR systems in the study area were measured every 4 hours. Besides that, the consumption of fire-fighting and Karaalioğlu park was monitored hourly for the same period of study.

- In site measures: There were 48 customers where their consumption was classified as big level like hotels, motels, stores, schools, …etc. Also, there were no AMR systems assigned to these subscribers. The consumption of these customers was read in the site every 72 hours and converted to 4 hours measures using multipliers determined according to SCADA data sets.

- The consumption of 192 subscribers was gained from ASAT on monthly basis. Additionally, there were 300 AMR subscribers of passive status, their water demand was excluded from the calculations.

- The apparent losses: 8% as flowmeter inaccuracy and 9 m^3 of unauthorized consumption at 06:00 a.m. which consumed in a period of 10 minutes every morning.

Table 2.4. The calculations of water losses for 32 hours (Muhammetoğlu 2017)

Time range	System input volume (m^3)	AMR + Park measures (m^3)	Other consumption (m^3)	Total consumption (m^3)	Flow meter inaccuracies (m^3)	Unauthorized consumption (m^3)	Physical losses (m^3)	Apparent losses (%)	Physical losses (%)
June 02 10:00 – 14:00	479,87	213,45	105,34	318,79	25,30	0	135,77	5,27%	28,29%
June 02 14:00 – 18:00	471,25	211,86	103,45	315,31	25,03	0	130,91	5,31%	27,78%
June 02 18:00 – 22:00	460,06	187,59	100,99	288,58	23,09	0	148,39	5,02%	32,25%
June 02 22:00 – 02:00	432,52	176,24	94,95	271,18	21,69	0	139,64	5,02%	32,29%
June 03 02:00 – 06:00	418,36	150,37	91,84	242,21	19,38	0	156,77	4,63%	37,47%
June 03 06:00 – 10:00	472,30	193,32	103,68	297,00	23,76	9	142,54	6,94%	30,18%
June 03 10:00 – 14:00	485,83	207,25	106,65	313,90	24,91	0	147,02	5,13%	30,26%
June 03 14:00 – 18:00	477,70	213,80	104,87	318,67	25,29	0	133,74	5,29%	28,00%
Total	3697,88	1553,89	811,76	2365,65	188,45	9	1134,78	5,34%	30,69%

This short-term water losses investigations aim to show the relation between leakage flow and consumption flow. The lower the consumption the higher the pressure, i.e. higher leakage. This can be seen clearly in Figure 2.4. When the consumption was the least (02:00 – 06:00 June 03) the leakage was at the highest level. The leakage determination was not implemented under a high level of sensitivity, this leads the researchers to suggest that the consumption of all subscribers in such a touristic area should be metered by online AMR system since there is night consumption in Kaleiçi (Muhammetoğlu 2017).

3. MATERIAL AND METHODOLOGY

ASAT is the department responsible for the management of drinking WDNs and wastewater collection systems of 19 districts in Antalya province. ASAT provides services for 2,426,356 capita who live in 20,177 km2 (ASAT 2019), and 1,214,752 subscribers with 12,909 km pipes (ASAT 2017). Antalya WDNs are monitored by SCADA central station owned by ASAT. SCADA system is connected with 110 monitoring stations contain electromagnetic flow meters and pressure loggers for recording flow and pressure at the inlet of each DMA (Kara et al. 2016).

Geographically, Antalya county mainly consists of five districts; Döşemealtı, Kepez, Konyaaltı, Muratpaşa, and Aksu, as shown in Figure 3.1. This research study was applied to a pilot study area (PSA) namely Antalya Kaleiçi. The PSA is a frequently visited place in Antalya since it combines the historical, natural, and enjoyment aspects of tourism. As shown in Figure 3.2, Kaleiçi is located within Muratpaşa district.

3.1. Description of The Pilot Study Area (PSA)

Kaleiçi WDN was the PSA of a research project for a period of more than two years. As a part of the project activities, the pressure, flow, and MNF over a period of more than twelve months were investigated. Within the scope of the project, the determination of daily and hourly customers water demand, monthly and yearly tables of SWB, PIs, and ELL was performed. The topographic features of the PSA present highly varying characteristics, the elevations over its area of 2.5 km^2 differs between the mean sea level (MSL) and about 40 m above MSL. Kaleiçi WDN is constructed as DMA, i.e. it is hydraulically independent of the rest of WDNs in Antalya. The WDN in the PSA is provided with a monitoring system; at the inlet, there is a SCADA monitoring unit where system input flow and pressure are recorded every five minutes. Moreover, there are seven locations, named as pressure measuring points (PMPs), were installed in the field for recording the pressure at their junctions within the scope of the project as shown in Figure 3.3. Nevertheless, only five portable pressure loggers were available. The attached pressure loggers record the pressure every five minutes. The details of the five PMPs where the pressure loggers were installed are provided in Table 3.1. The majority of water subscribers in Kaleiçi (1394 customer) are connected with automatic meter reading (AMR) system. The WDN in the PSA contains 12 km of mains and about 7.9 km of service connections as shown in Figure 3.3. Finally, classical PM and water saving suggestions were proposed within the research project (Muhammetoğlu 2017).

Being noticed that the data sets and some results of that project are the main references for the calculations implemented in thesis works.

Figure 3.1. The districts of Antalya province (ASAT, 2017)
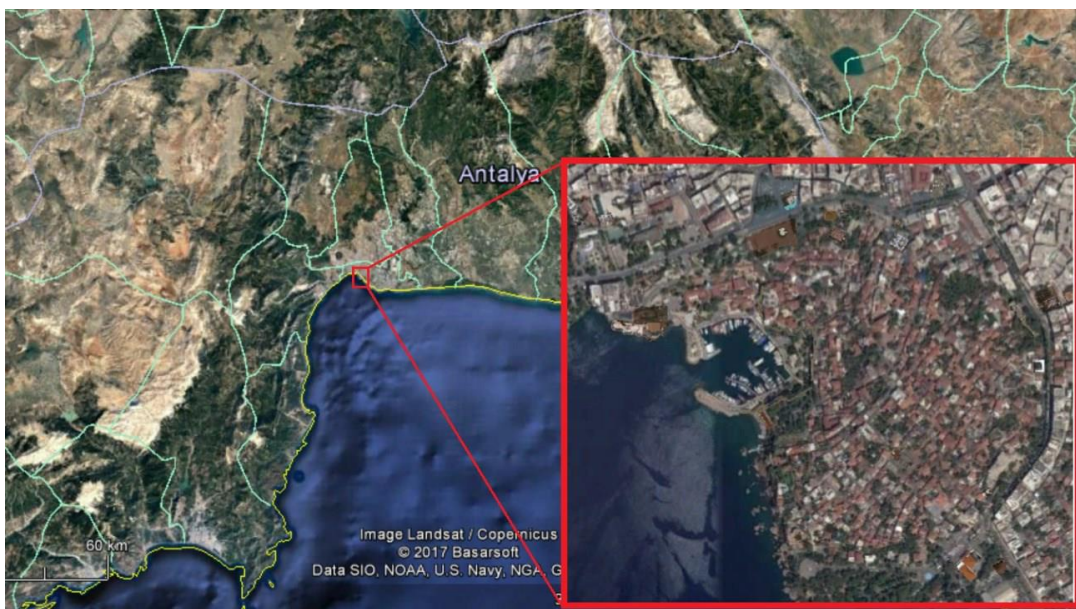
Figure 3.2. The location of the PSA (Kaleiçi) in Antalya county, copied from (Gülaydın 2017)
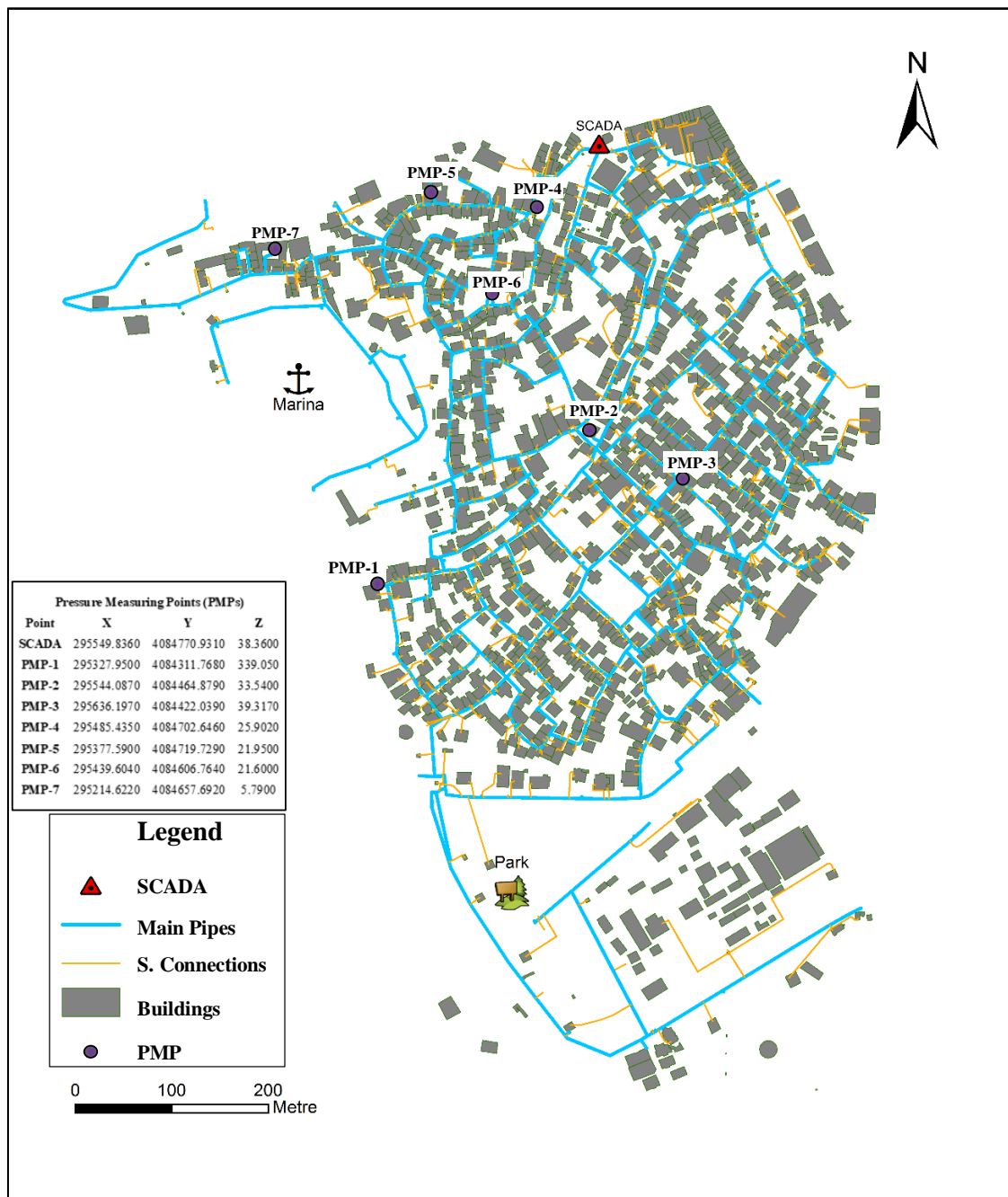
Figure 3.3. A GIS map of the PSA (Kaleiçi) and its details including the locations of PMPs (Note: the X, Y, Z coordinates according to UTM system), adapted from (Muhammetoğlu, 2017)

Table 3.1. Properties of the five PMPs, copied from (Muhammetoğlu, 2017)

Stations	Model Node ID	Node level (m)	Ground level (m)	Asset level (m)
SCADA	-	38.360	39.360	38.360
PMP-1	S492	31.700	32.700	33.905
PMP-2	S232	32.100	33.100	33.540
PMP-3	S623	37.603	38.603	39.317
PMP-4	S468	24.162	25.162	25.902
PMP-7	S490	5.300	5.300	5.790

3.2. Leakage Modeling Approach

EPANET software has been used to perform the hydraulic modeling of Kaleiçi WDN. The system input flow, which is recorded by SCADA, divides into leakage and non-leakage flow. The network leakage is determined based on the water balance and then distributed among the nodes assuming that leakage is uniformly distributed along the pipe network of the PSA. The non-leakage flow has been distributed to the junctions as nodal demand follows multipliers patterns. The nodal demand has been determined by the half-length of the pipes connected to each junction except for the large users namely a park and a firefighting unit. By this way, both leakage and non-leakage flow rates have been assumed as uniformly distributed by the pipe length, and hence, each node has two demands: leakage (pressure dependent) and non-leakage flow (demand-driven). The leakage at each junction has been predicted by determining the leak coefficients and predicting the pressure at each node. Thus, the total network leakage rate has been predicted in space and time.

In EPANET, the actual demand involves both nodal demand (non-leakage flow) plus flow through emitters (leakage). The flow rate through emitters depends on leak coefficients, nodal pressure, and pressure exponent as shown in equation (3.1):

$$q = Cp^{\gamma} \tag{3.1}$$

Where q is the flow rate through the emitter (leak), C is the leak coefficient, p is the nodal pressure and γ is the leakage exponent (Rossman 2000).

The Leakage exponent is influenced mainly by two factors; the pipe material and type of flow through leaks. The pipe material defines the size and shape of leakage orifice and the form of breaks. Also, the shape of the leak specifies the ability of leaks to develop as the pressure gets higher. The type of orifice flow (laminar, transient, or turbulent flow) varies by the Reynold number and orifice's shape (Falls et al. 2011). Leakage exponent value differs from 0.5 for metal (rigid) pipes to 1.5 for plastic (ductile) pipes to as much as 3 for more elastic materials (Mckenzie and Wegelin 2009). A value of 1 could be considered for homogeneous large WDNs with different pipe materials (Falls et al. 2011).

Hydraulically, the more increasing of the non-leakage flow the more decreasing of nodal pressure and accordingly the less leakage rate (Muhammetoglu and

Muhammetoglu 2017). By equation (3.1), the leakage rate is modeled at each junction as a pressure-dependent flow.

Herein, an approach proposed by Cobacho Jordán et al. (2015) for leakage modeling in space and time by EPANET is going to be presented and used for this research study. First of all, to perform this approach three parameters are required; total leakage rate, pipe friction coefficient, and leakage exponent.

In the hydraulic modelling of the WDN by EPANET; leakage exponent is defined in the defaults to be applied for all junctions, but the leakage coefficient must be assigned for each junction specifically. Cobacho Jordán et al. (2015) proposed a method for determining the leakage coefficient assuming that leakage is uniformly distributed by pipe length. The proposed method supposed that leakage flow through any junction equals the water flow leaked along the half-length of the pipes connected with that junction. As shown in Figure 3.4, through each node water flows in two forms; nodal-demand and flow rate through emitters. In Figure 3.4, (j) denotes junction, (Q_{BDj}) the base-demand at junction (j), (P_j) the nodal pressure, (C_j) the nodal-leakage-coefficient, and (Q_j) the leakage out of junction (j).

The proposed approach simulates leakage in space and time through two stages as follows; the spatial distribution of flow rate, and calculation of the leakage coefficient at each junction. This approach has been adapted to the WDN in the PSA.
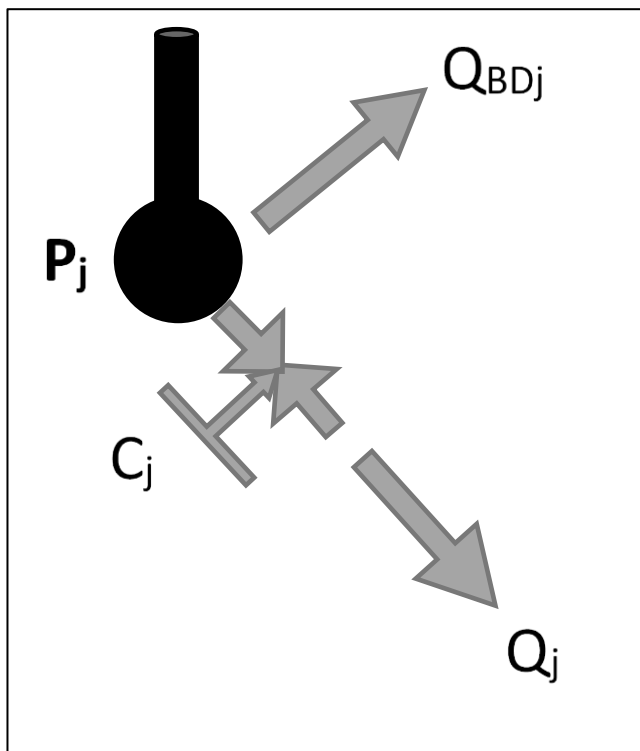
Figure 3.4. The scheme of flow through the junction adapted from (Cobacho Jordán et al. 2015)

3.2.1. Spatial distribution of flow

The assumption that both leakage and non-leakage flow are uniformly distributed by pipe length is performed mathematically through this stage. In equation (3.2), (l_i) denotes the length of the pipe (i) connected with the junction (j), and (l_j) denotes the sum of half-length of all pipes connected with the junction (j). (L_j) represents the relative importance of each junction in terms of flow as compared to the total flow of the WDN. (L_j) equals the ratio between (l_j) and the total length of the pipes in the WDN as shown in equation (3.3).

$$l_j = \sum_{i=1}^{m_j} \frac{l_i}{2} \tag{3.2}$$

$$L_j = \frac{l_j}{\sum l_i} = \frac{l_j}{l_{net}} \tag{3.3}$$

3.2.2. Calibration of the emitter discharge coefficients

In this stage, the leak coefficient (C) at each junction is calibrated by an iterative process. The process starts with the calculation of the leakage coefficient of the whole WDN ($C_{Net}^{(1)}$), as a first iteration, by equation (3.4).

$$C_{Net}^{(1)} = \frac{Q_{Net,real}}{P_{Net}^{\gamma}} \tag{3.4}$$

Where $Q_{Net,real}$ is the calculated total network leakage during the simulation period, P_{Net} is the average pressure of all junctions during the simulation period and γ is the leakage exponent.

P_{Net} is used only for the calculation of the network leakage coefficient at the first iteration ($C_{Net}^{(1)}$), its effect on the final calibrated leakage coefficient will be tested in the later sections.

Knowing both ($C_{Net}^{(1)}$) and (L_j), the second step is the distribution of the network leakage coefficient among the junctions for each iteration by equation (3.5).

$$C_j^{(h)} = C_{Net}^{(h)} * L_j \tag{3.5}$$

Where $C_j^{(h)}$ is the leakage coefficient of the junction (j) at the iteration (h), $C_{Net}^{(h)}$ is the network leakage coefficient at the iteration (h) and L_j is the relative importance of the junction (j) as compared to the whole WDN.

The third step consists in modeling the WDN using the estimated leakage coefficients over the simulation period. The final step is to calculate the total distributed leakage as it is predicted by the model ($Q_{Net,model}^{(h)}$). To calculate ($Q_{Net,model}^{(h)}$) by EPANET, the model of the WDN is run during the same simulation period in two phases.

In the first phase, the total non-leakage flow is distributed by the relative importance of each junction, and the estimated network leakage coefficient is distributed to the junctions as in equation (3.5). The model predicts the ($\Sigma Q_{(non\text{-}leakage)+(leakage)}$) at this phase. In the second phase, only the non-leakage flow is distributed over the junctions, then the model predicts ($\Sigma Q_{(non\text{-}leakage)}$). Finally, ($Q_{Net,model}^{(h)}$) is calculated as in equation (3.6).

$$Q_{Net,model}^{(h)} = \Sigma Q_{(non-leakage)+(leakage)}^{(h)} - \Sigma Q_{(non-leakage)}^{(h)} \qquad (3.6)$$

The ($Q_{Net,model}^{(h)}$) is compared with the total leakage rate calculated in the field, e.g. by the SWB, ($Q_{Net,real}$) as shown in equation (3.7).

$$\left| Q_{Net,model}^{(h)} - Q_{Net,real} \right| \leq \varepsilon \qquad (3.7)$$

For solving an example applied by Cobacho Jordán et al. (2015), they suggest a tolerance value of $\varepsilon = 0.005$, but it is not unique value since it depends on several factors like the unit of flow, the network size, SIV …etc.

The leakage coefficient of the whole WDN for the next iteration ($C_{Net}^{(h+1)}$) is adjusted based on the difference $\left| Q_{Net,model}^{(h)} - Q_{Net,real} \right|$, and the sequence is repeated, from the second step on, until satisfying the convergence criteria. Figure 3.5 presents the iterative process.
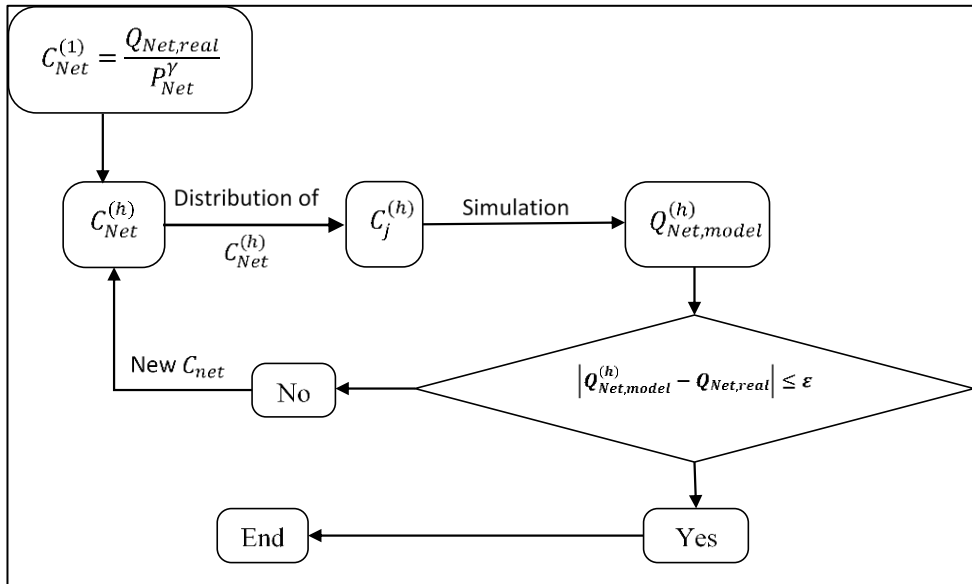
Figure 3.5. Iterative Process to tune the leakage coefficients, adapted from (Cobacho Jordán et al. 2015)

3.3. Base Case Study (M1)

The network shown in Figure 3.6 is a hypothetical WDN adapted from (Cobacho Jordán et al. 2015) which represents a numerical example for applying the proposed

approach for leakage simulation in space and time. This example has been named by M1 and used as a base case model to test the approach.
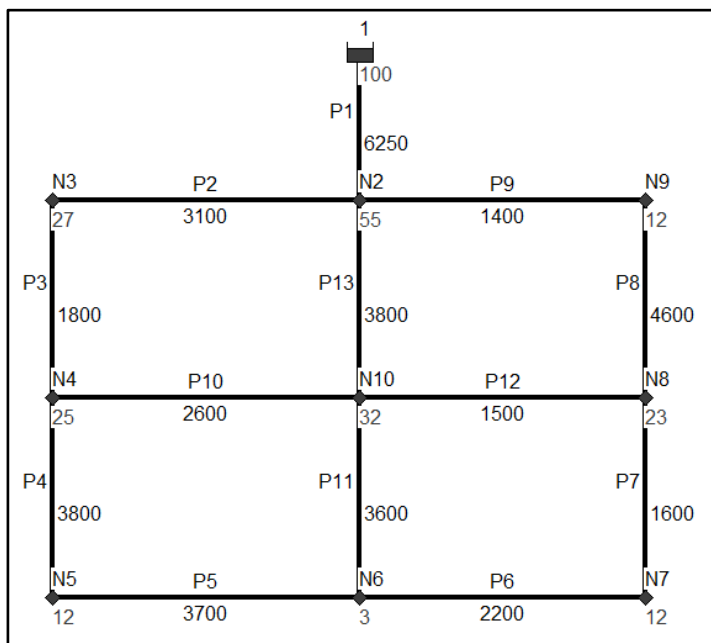
Figure 3.6. Water supply network of the base case study (M1) adapted from (Cobacho Jordán et al. 2015)

The input data set of the base simulation are as follows:

- System input flow = 5,100 m³/day (59.03 L/s),
- Total non-leakage flow = 3500 m³/day (40.5 L/s),
- Total leakage flow = 1600 m³/day (18.52 L/s),
- γ= 1.1,
- Pipes roughness, R= 0.1mm (darcy-weisbach equation has been used),
- Average network pressure = 40 m (assumed value for starting up the leakage simulation),
- Properties of junctions and pipes in Table 3.2, and
- Pattern multipliers of the nodal-base-demands in Table 3.3 and Figure 3.7.
- The modelling time-step is 1 hour.

   Note: the network is copied from (Cobacho Jordán et al. 2015), with one correction has been modified by personal communication with the author which is the base demand of N5 junction as 10.2 L/s instead of 3.4 L/s.

Table 3.2. Junctions and pipes properties adapted from (Cobacho Jordán et al. 2015)

Node ID	Elevation (m)	Base Demand (L/s)	Time Pattern	Pipe ID	Length (m)	Diameter (mm)
N_2	55	1.1	PAT A	P_1	6250	300
N_3	27	4	PAT B	P_2	3100	200
N_4	25	3.4	PAT C	P_3	1800	200
N_5	12	10.2	PAT A	P_4	3800	200
N_6	3	4.5	PAT D	P_5	3700	80
N_7	12	5.6	PAT A	P_6	2200	100
N_8	23	3.4	PAT C	P_7	1600	150
N_9	12	5	PAT D	P_8	4600	150
N_{10}	32	3.4	PAT E	P_9	1400	150
Reservoir	100			P_{10}	2600	100
				P_{11}	3600	80
				P_{12}	1500	200
				P_{13}	3800	250

Table 3.3. Pattern multipliers of the nodal-base-demands, adapted from (Cobacho Jordán et al. 2015)

Time	1	2	3	4	5	6	7	8	9	10	11	12	13	14	15	16	17	18	19	20	21	22	23	24
PAT.A	0.14	0.11	0.06	0.06	0.06	0.07	0.3	0.5	0.9	1.5	1.8	2.2	2.3	2.4	1.8	1.4	1.1	0.7	0.7	0.5	0.9	1.7	1.8	1
PAT.B	0.08	0.07	0.04	0.04	0.04	0.05	0.21	0.55	1.06	1.81	2.17	2.55	2.67	2.49	1.72	1.37	1.38	0.91	0.78	0.46	0.67	1.13	1.16	0.62
PAT.C	0.2	0.2	0.2	0.2	0.6	0.7	0.8	1.2	1.5	1.5	1.5	1.6	1.7	1.7	1.5	1.4	1.3	1	1	1	1	1	1	0.2
PAT.D	0	0	0	0	0	0	0.1	0.3	1.1	2.1	2.5	2.6	2.6	2.5	2.1	2	1.7	1.3	0.8	0.7	0.6	0.5	0.4	0.1
PAT.E	0	0	0	0	0	0	0	1	1.5	2.5	3	3.7	4	2.8	1	0.5	1.9	1.1	1	0	0	0	0	0
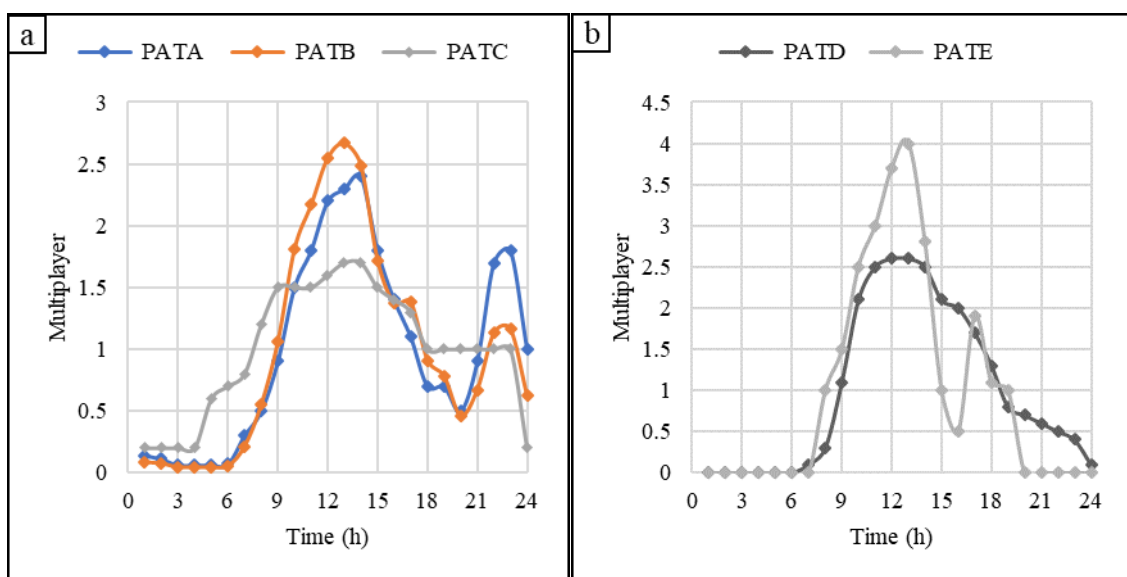
Figure 3.7. Pattern multipliers of the nodal-base-demands, a) PATA, PATB, and PATC. b) PATD and PATE adapted from (Cobacho Jordán et al. 2015)

Table 3.4 presents the iterative process of calibrating leakage coefficients numerically. Since pipe P_1 is connected with the reservoir, l_{N2} involves the full pipe length of P_1 and half-length of the other pipes connected with node N2. The system input flow rate, total non-leakage flow rate, and the total distributed leakage as it is predicted by the model during the simulation period are shown in Figure 3.8. The results of each iteration are numerically summarized in Table 3.5.

Table 3.4. Calibration of the leakage coefficients along with the iterative process

Node ID	l_j	L_j	C_{net}^1	C_{net}^2	C_{net}^3	C_{net}^4	C_{net}^5	C_{net}^6	C_{net}^7	C_{net}^8
			0.32	**0.2**	**0.26**	**0.23**	**0.245**	**0.2525**	**0.2515**	**0.2514**
			C_j^1	C_j^2	C_j^3	C_j^4	C_j^5	C_j^6	C_j^7	C_j^8
N_2	10400	0.260	0.0833	0.0521	0.0677	0.0599	0.0638	0.0657	0.0655	0.0654
N_3	2450	0.061	0.0196	0.0123	0.0159	0.0141	0.0150	0.0155	0.0154	0.0154
N_4	4100	0.103	0.0328	0.0205	0.0267	0.0236	0.0251	0.0259	0.0258	0.0258
N_5	3750	0.094	0.0300	0.0188	0.0244	0.0216	0.0230	0.0237	0.0236	0.0236
N_6	4750	0.119	0.0380	0.0238	0.0309	0.0273	0.0291	0.0300	0.0299	0.0299
N_7	1900	0.048	0.0152	0.0095	0.0124	0.0109	0.0117	0.0120	0.0120	0.0120
N_8	3850	0.096	0.0308	0.0193	0.0251	0.0222	0.0236	0.0243	0.0242	0.0242
N_9	3000	0.075	0.0240	0.0150	0.0195	0.0173	0.0184	0.0190	0.0189	0.0189
N_{10}	5750	0.144	0.0461	0.0288	0.0374	0.0331	0.0353	0.0363	0.0362	0.0362

Table 3.5. The average total distributed leakage rate as it is predicted by the model M1 and the average of ($\Sigma Q_{(non\text{-}leakage)+(leakage)}$) over 24 hours at each iteration

Iteration	Avg. ($\Sigma Q_{(non\text{-}leakage)+(leakage)}$) over 24 h (L/s)	Avg. leakage rate over 24 h (L/s)	ε
1	63.114	22.509	3.989
2	55.853	15.248	3.272
3	59.650	19.045	0.525
4	57.794	17.190	1.330
5	58.733	18.128	0.392
6	59.195	18.590	0.070
7	59.133	18.528	0.008
8	**59.128**	**18.523**	**0.003**
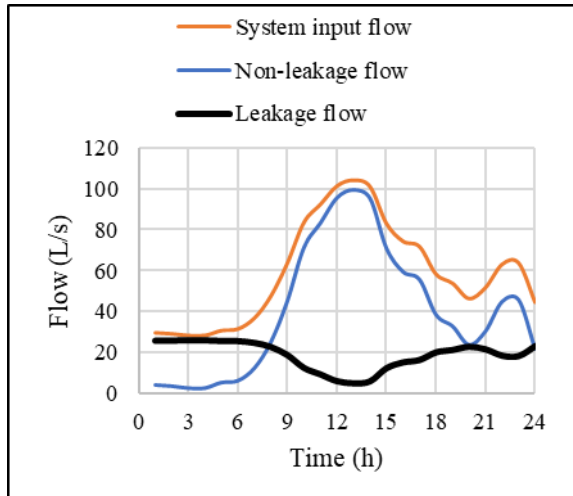
Figure 3.8. The system input flow, the non-leakage flow and the summation of the distributed leakage rate as it is predicted by the model M1, adapted from (Cobacho Jordán et al. 2015)

Higher non-leakage flow causes reduction of nodal pressure. Since leakage is a pressure-dependent flow, then the higher non-leakage flow causes a lower leakage rate as shown in Figure 3.8.

3.4. Assuming that total non-leakage flow is uniformly distributed along each pipe

The base case study (M1) is going to be compared with a scenario (M2), the differences are in the assumed nodal- demands in M2 and the demand patterns. Generally, the nodal demand in WDNs cannot be measured in the field accurately. Therefore, an approach to determining the nodal demand should be used. The basic idea of scenario M2 is assuming that the non-leakage flow is uniformly distributed by the pipe length, and the base demand of each junction is calculated by the half-length of the pipes. Based on that, the nodal-demands in the WDN shown in Figure 3.6 can be re-calculated by multiplying the total non-leakage flow by the relative importance of each junction (Lj). Additionally, the demand multiplier patterns in M2 are assumed to follow the multiplayer pattern of the system input flow as shown in Figure 3.9. The methodology used for nodal demand calculations in this scenario is applicable in certain cases where similar water users, e.g. domestic, commercial, or industrial, are distributed uniformly along the pipes of the WDN. Base on that, the methodology used scenario M2 has been applied in the PSA with corrections related to the high consumption of the park and the fire-fighting unit.

The initial and final values of leakage coefficients and the nodal-base-demands are presented in Table 3.6. The system input flow, the network non-leakage flow and the model prediction of the distributed leakage rate as it is predicted by the model are not different in between base simulation (M1) and scenario (M2) (Figure 3.10). Due to the assumption used in calculating the nodal demand in M2, the spatial prediction of leakage rate varies in between (M1) and (M2) as shown in Figure 3.11. At node N6, the predicted total nodal demand and the non-leakage demand are in the same manner with the system input flow and network non-leakage flow of models (M1) and (M2). The scenario M2 is applicable when the nodal-demands in any WDN cannot be measured.

39
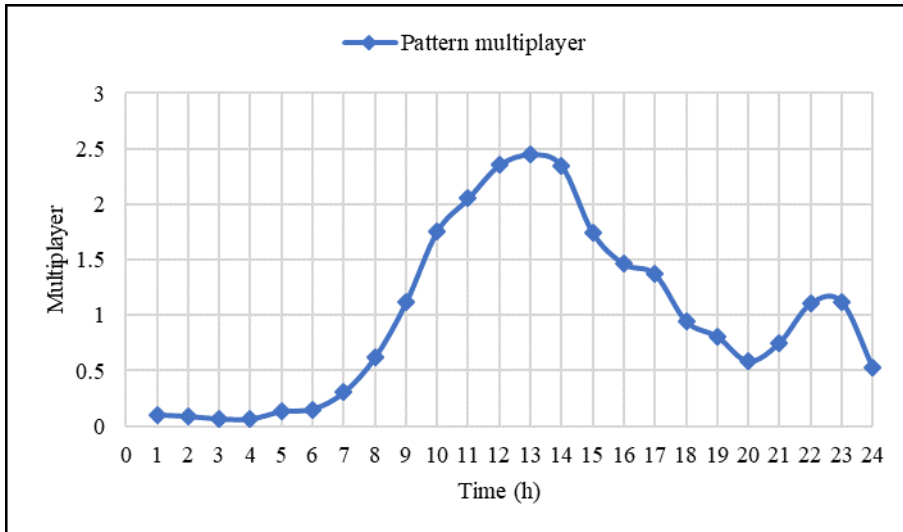
Figure 3.9. The demand pattern multiplayer for all nodes in scenario M2

Table 3.6. Nodal-base-demands and nodal leakage coefficients in first and last iterations

Node ID	l_j	L_j	Consumption	$C_{net}{}^i$	$C_{net}{}^f$
			40.5 L/s	0.32	0.2391
			Base demand	$C_j{}^i$	$C_j{}^f$
N_2	10400	0.260	10.54	0.0834	0.062244
N_3	2450	0.061	2.48	0.0196	0.014663
N_4	4100	0.103	4.16	0.0329	0.024538
N_5	3750	0.094	3.80	0.0301	0.022444
N_6	4750	0.119	4.81	0.0381	0.028429
N_7	1900	0.048	1.93	0.0152	0.011371
N_8	3850	0.096	3.90	0.0309	0.023042
N_9	3000	0.075	3.04	0.0240	0.017955
N_{10}	5750	0.144	5.83	0.0461	0.034414
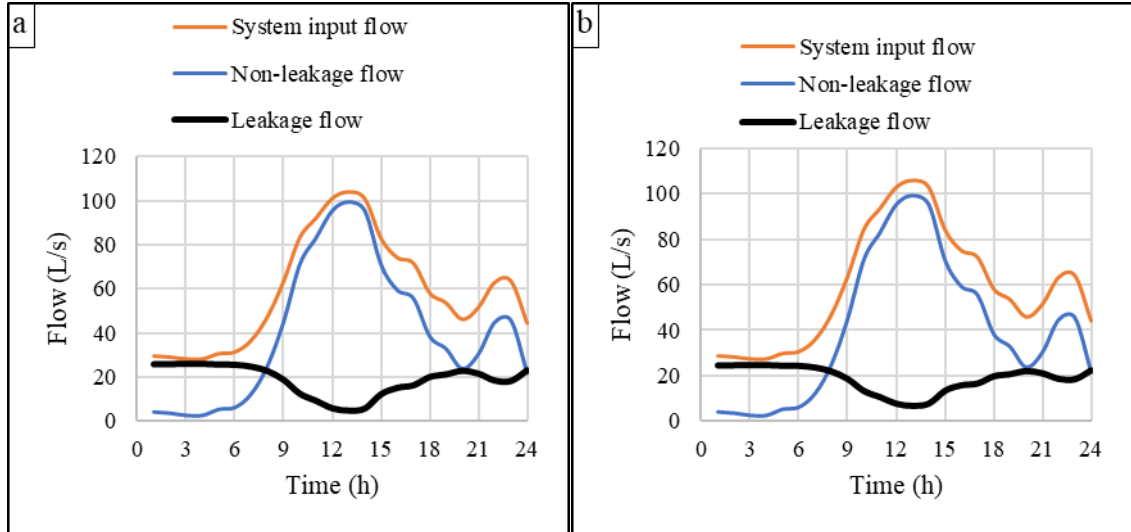
Figure 3.10. The system input flow, the non-leakage flow, and summation of the distributed leakage rate as it is predicted in a) the base simulation (M1) and b) scenario (M2)
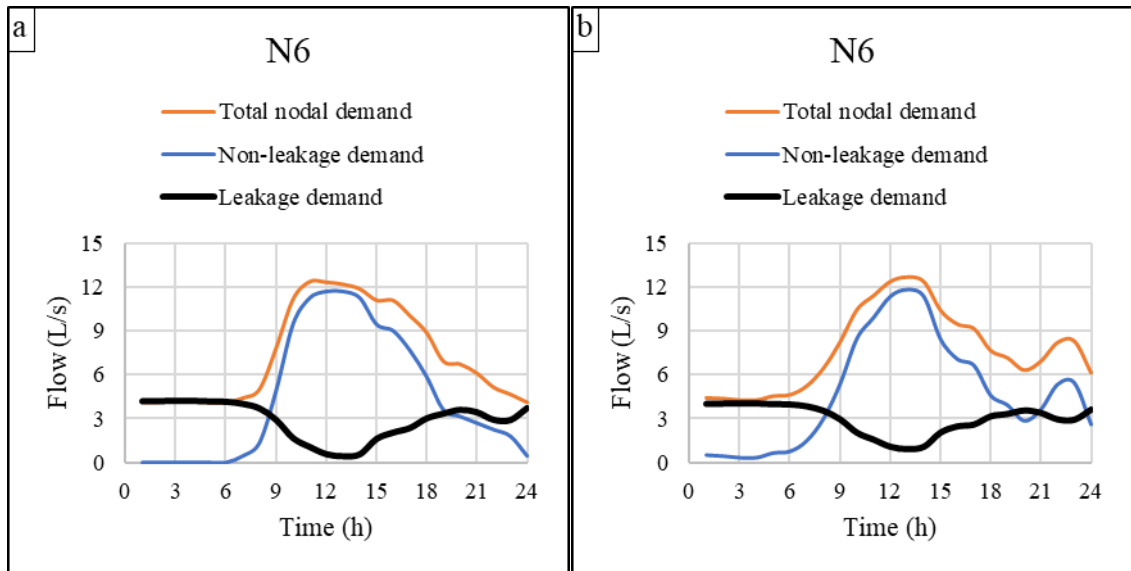
Figure 3.11. The total nodal demand, the non-leakage demand, and the predicted leakage at node N6 by a) the base simulation (M1) and b) scenario (M2)

3.5. The Sensitivity of Model Input Assumptions on Leakage Coefficients

Three input parameters of the proposed approach for leakage simulation in space and time are; (i) the average pressure of all junctions in the WDN over the simulation period, (ii) the leakage exponent, and (iii) the roughness coefficient. The impact of these parameters on leakage simulation has been investigated using the base simulation (M1) as follows:

- Impact of the average pressure of the WDN (P_{net}) on the final value of leakage coefficients (C_{net}) and hence model predictions.

41

- Impact of pipe roughness on the predicted average pressure of WDN (P_{net}), and the final leakage coefficients (C_{net}^f) and hence model predictions.

- Impact of leakage exponent (γ) on the predicted average pressure of WDN (P_{net}), and the final leakage coefficients (C_{net}^f) and hence model predictions.

3.5.1. Impact of the average pressure of the WDN (P_{net}) on C_{net}^f and model predictions

According to equation (3.4), the average pressure of all nodes in the WDN (P_{net}) is a required parameter to start the iterative process for calculating the leakage coefficients at all junctions. In the following analysis, the impact of the assumed P_{net} on the final value of leakage coefficient (C_{net}^f) will be investigated, two values of P_{net} other than the used one in the base simulation M1 (P_{net}= 40m) have been tested; P_{net}=30m and P_{net}=50m.

Table 3.7 exhibits the initial network leakage coefficient (C_{net}^i) and the final coefficient (C_{net}^f) under the tested values of (P_{net}). It can be noticed obviously that C_{net}^f is not affected by the initial assumed P_{net} value which is required for estimating C_{net}^i at the first iteration. If all other parameters ($Q_{net,real}$ and γ) do not change, a <u>unique</u> value of C_{net}^f will be achieved after implementing the iterative process. However, convergence is quicker when the average pressure is taken close to the actual one (e.g. P_{net}=50m in the given example).

Table 3.7. The initial and final leakage coefficients under different P_{net} values, and the average predicted pressure at C_{net}^f

Parameter	P_{net}=30m		P_{net}=40m (M1)		P_{net}=50m	
	C_{net}^i	C_{net}^f	C_{net}^i	C_{net}^f	C_{net}^i	C_{net}^f
Leakage coefficients	0.439347	0.252047	0.32	0.252047	0.250481	0.252047
Average predicted pressure (m)	54.62		54.62		54.62	

3.5.2. Impact of pipe roughness on the predicted average pressure of the WDN and network leakage coefficient (C_{net}^f)

The influence of pipe roughness on the predicted nodal pressure and leakage through emitters has been investigated. Five different roughness coefficients have been tried namely R= [0.001, 0.08, 0.1, 0.12, 0.2] mm, including the input roughness of M1 simulation (R= 0.1 mm). The impact of the variation of roughness coefficient on the predicted average pressure of the WDN and the calculated final leakage coefficient is presented numerically in Table 3.8. As it is shown in Table 3.8, the higher value of the predicted average pressure of the WDN is found against the lower roughness coefficient, then the predicted average pressure decreases gradually by roughness increase. By contrast, C_{net}^f showed a direct relation to the roughness, it increases by roughness increase. Figure 3.12 exhibits the predicted leakage at each junction in the M1 model under each trial of roughness coefficients.

Table 3.8. $C_{net}f$ and the predicted average pressure of the WDN at each trial value of roughness coefficient

Roughness Coefficient	R₁= 0.001 mm	R₂= 0.08 mm	(M1) R₃= 0.1 mm	R₄ =0.12 mm	R₅= 0.2 mm
Network leakage coefficient ($C_{net}f$)	0.234988	0.249159	**0.252047**	0.254773	0.264481
Predicted average network pressure (m)	58.11	55.18	**54.62**	54.10	52.32
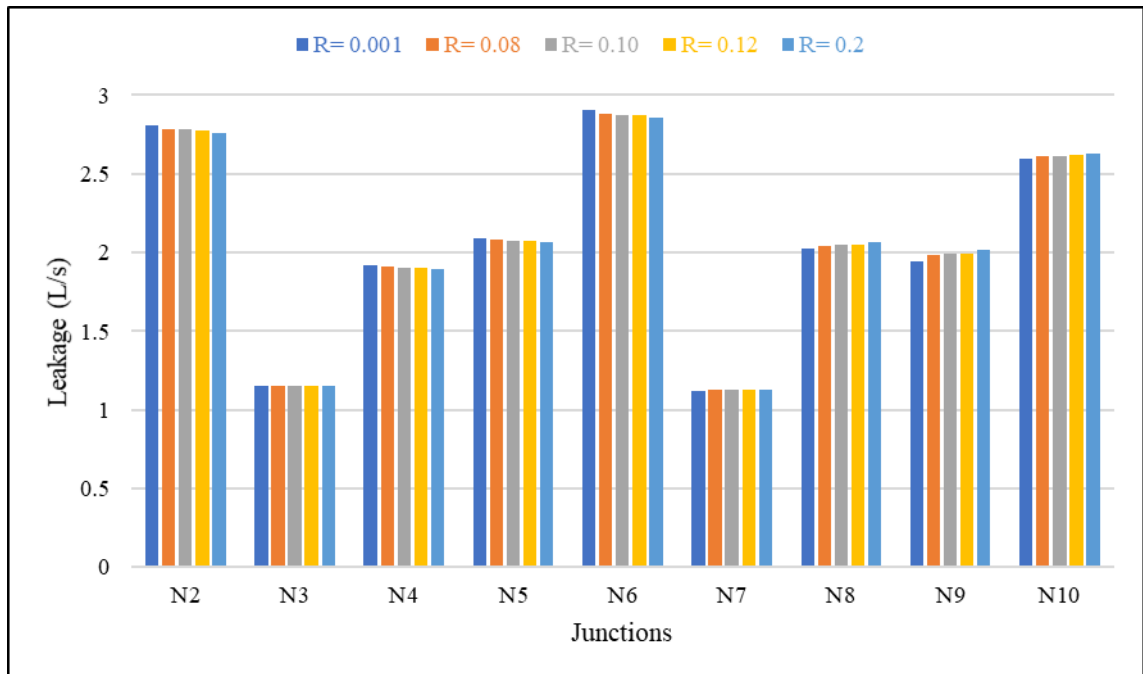
Figure 3.12. The leakage predicted at each junction under different values of roughness coefficient

3.5.3. Impact of leakage exponent (γ) on the predicted average pressure of the WDN and $C_{net}f$

Five trials of leakage exponent have been tested, including the input one (γ= 1.1), to investigate its effect on the predicted average pressure of the WDN and $C_{net}f$. The trials of the leakage exponent are γ= [0.5, 0.88, 1.1, 1.32, 1.4]. The impact of leakage exponent is shown numerically in Table 3.9. As shown, $C_{net}f$ decreases significantly as the leakage exponent increases. Conversely, the predicted average pressure of the WDN increases as the leakage exponent increases. The predicted leakage at each junction in the M1 model under each trial of leakage exponent is shown in Figure 3.11.

Table 3.9. $C_{net}f$ and the predicted average pressure of M1 network at each trial of leakage exponent

Leakage exponent	$\gamma_1 = 0.5$	$\gamma_2 = 0.88$	(Base) γ_3 = 1.1	$\gamma_4 = 1.32$	$\gamma_5 = 1.4$
Network leakage coefficient ($\boldsymbol{C_{net}f}$)	2.756488	0.609892	**0.252047**	0.103577	0.074869
Predicted average network pressure (m)	54.28	54.53	**54.62**	54.69	54.71
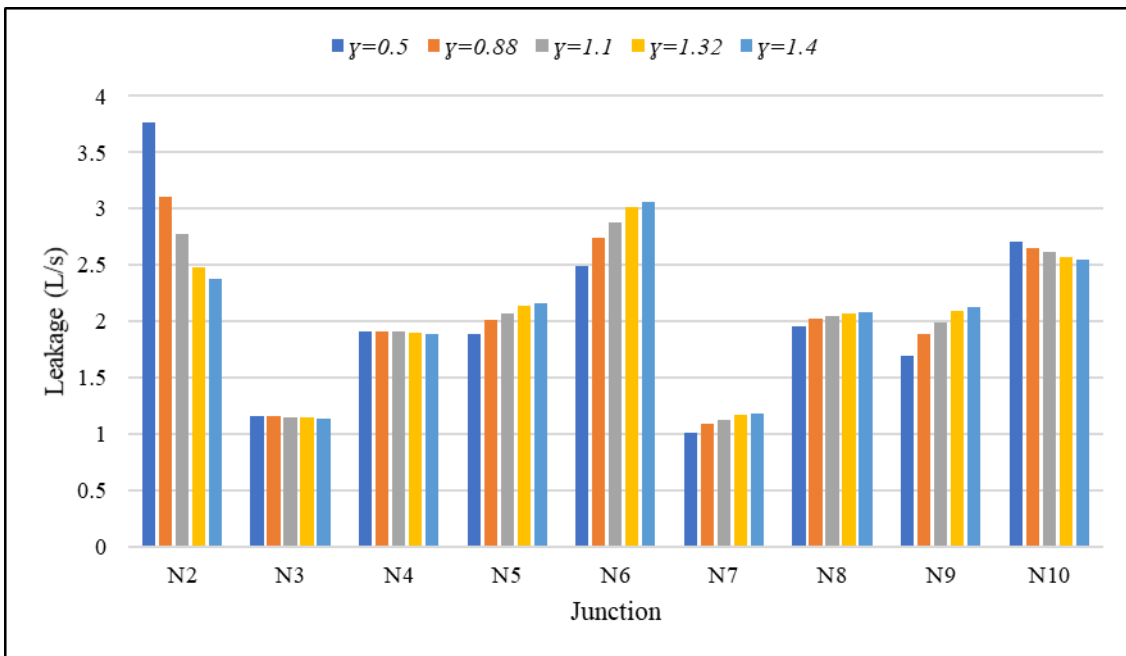
Figure 3.13. The predicted leakage at each junction at each trial of leakage exponent.

3.5.4. Discussion on sensitivity analysis of leakage exponent and roughness coefficient

In the base simulation M1, the pipe roughness coefficient affects the model predictions of the pressure of the WDN as shown in Table 3.8, but its impact on the model prediction of nodal leakage is not highly sensitive as shown in Figure 3.12.

By contrast, the leakage exponent affects the model prediction of nodal leakage as shown in Figure 3.13, but its impact on the model prediction of nodal pressure is not highly sensitive as shown in Table 3.9.

Nodal leakage prediction is directly related to leakage coefficient and nodal pressure. Therefore, the sensitivity of nodal leakage prediction to the leakage exponent and roughness coefficient is shown in Figure 3.14. Additionally, the sensitivity of pressure prediction to the leakage exponent and roughness coefficient is shown in Figure 3.15.
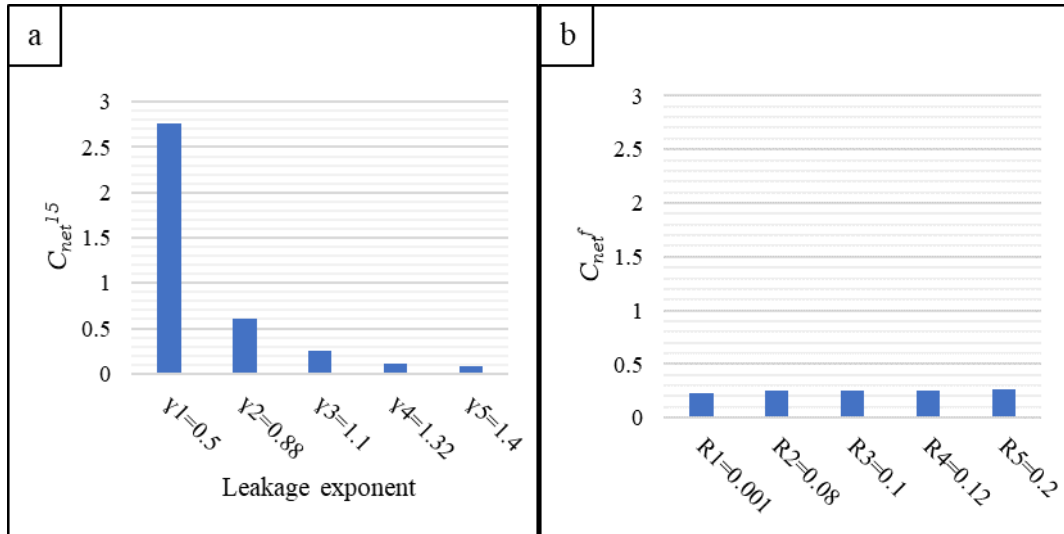
Figure 3.14. The sensitivity of the nodal leakage prediction to a) the leakage exponent and b) the pipe roughness coefficient.
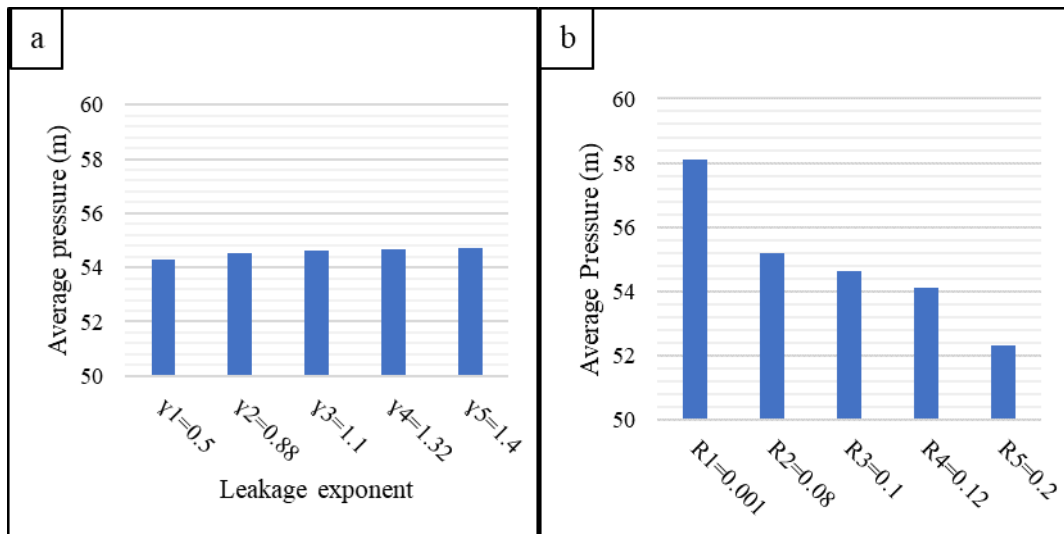
Figure 3.15. The sensitivity of the average pressure of the WDN to a) the leakage exponent and b) the pipe roughness coefficient.

3.6. Determination of Yearly SWB in Kaleiçi WDN

The SCADA station which is found at the inlet of Kaleiçi WDN is provided with a highly accurate electromagnetic flowmeter and pressure logger to measure the SIV and pressure every 5 minutes, then the records are sent to the SCADA central station of ASAT. Additionally, the customers in Kaleiçi are well defined and their water consumptions are recorded monthly by ASAT. Calculations of SWB was made for study period between May 21st, 2015 to May 21st, 2016 as shown in Table 3.10 (Muhammetoğlu 2017).

Table 3.10. The SWB of Kaleiçi DMA calculated for one year, May 21st, 2015 - May 21st, 2016, copied from (Muhammetoğlu 2017)

System input volume Q_I = 839,288 m³ (% 100)	Authorized Consumption Q_A= 640,820 m³ (% 76,4)	Billed Authorized consumption Q_{BA} = 290,147 m³ (% 34,6)	Billed metered consumption 290,147 m³ (% 34,6)	Revenue water 290,147m³ (%34,6)
			Billed unmetered consumption 0 m³ (% 0)	
		Unbilled Authorized consumption Q_{UA} = 350,673 m³ (%41,8)	Unbilled metered consumption 348,729 m³ (%41,6)	Non-revenue water 549,141 m³ (%65,4)
			Unbilled unmetered consumption 1,944 m³ (%0,2)	
	Water losses Q_L = 198,468 m³ (% 23,6)	Apparent losses Q_{AL} = 54,404 m³ (% 6,5)	Unauthorized consumption 3,294 m³ (%0,4)	
			Customer meter inaccuracies and data handling errors 51,110 m³ (%6,1)	
		Real losses Q_{RL} = 144,064 m³ (% 17,2)	Leakage on transmission and distribution mains 144,064 m³ (%17,2)	

Each component of the SWB of Kaleiçi WDN has been calculated as follows:

- System Input Volume Q_I: From the electromagnetic flowmeter which installed at the inlet of Kaleiçi DMA, SIV is measured every five minutes.

- Authorized consumption Q_A: consists of billed and unbilled consumptions of water, each sub-component is determined as follows:

   - Billed Authorized Consumption (Q_{BA}): since un-metered billed consumption is not found in Kaleiçi DMA, then each of Q_{BA} and revenue water equals billed metered consumption. The billed metered consumption includes the water consumed for commercial, domestic, and other purposes. It is calculated from the records of customer meters which is read monthly.

   - Unbilled Authorized Consumption (Q_{UA}) consists of unbilled metered consumption and unbilled un-metered consumption. The unbilled metered consumption has been calculated by the monthly records of customer meters. The unbilled un-metered consumption refers to a park in the Kaleiçi area where no flowmeter attached. The irrigation system of the park consumes 2 m^3 every day in winter and 5 m^3 every day in summer. Besides that, there is an ornamental pool of 15 m^3 volume and its water is in a regular empty-fill activity once every week in summer and once every two

weeks in winter. Based on that, its value was calculated. In the next section, the SWB tables of Kaleiçi within September 2015 and January 2016 are presented in Table 3.11 and Table 3.12, respectively. In Table 3.11, the unbilled unmetered consumption = 5 m^3 × 31 days + 15 m^3 × 4 weeks = 215 m^3/month (in summer). In Table 3.12, the unbilled unmetered consumption = 2 m^3 × 31 days + 15 m^3 × 2 weeks = 92 m^3/month (in winter).

- Water losses ($Q_L = Q_I - Q_A$): consists of apparent losses and real losses. Each sub-component has been determined as follows:

  - Two types of apparent losses are found in Kaleiçi DMA, unauthorized consumption and customers meter inaccuracy.

  a. Unauthorized consumption: It has been observed that shopkeepers in the PSA are using the fire cabinets illegally for cleaning the roads in front of their stores. It has been found that the period of using firewater illegally is not more than 10 minutes every morning. The water used for firefighting purposes is not recorded by any flowmeters. Therefore, this illegal consumption has been calculated by field investigation of all fire cabinets found near stores and estimating of water flow through fire pipes. In Kaleiçi there are 54 fire cabinets are distributed all over the study area. 15 fire cabinets have been detected as being used illegally. During field investigations, it has been determined that average water flows through fire pipe is 0.06 m^3/min. Based on that, total daily unauthorized consumption = 15 × 0.06 m^3/min × 10 min = 9 m^3/d.

  b. According to qualified personal staff working in ASAT, the inaccuracies of flowmeters are %8 of their measurements.

- Real losses Q_R: there are no tanks in Kaleiçi WDN. Therefore, the only source of real losses is the leakage through mains and service connections and the pipe bursts. The real losses equal the SIV minus the authorized consumption and the apparent losses (Muhammetoğlu 2017).

3.6.1. Monthly SWB Calculations

As it is stated before, the proposed methodology by Cobacho Jordán et al. (2015) for simulating leakage in space and time requires essentially a predetermined leakage rate to be distributed to the junctions. Therefore, the SWB which is calculated monthly for Kaleiçi WDN by Muhammetoğlu (2017) has been used to gain the leakage rate. Representing summer and winter seasons, two simulation periods have been chosen for modeling Kaleiçi WDN and later purposes like calibration of the model, PM application, predicting nodal pressure and nodal leakage related to any possible scenarios. Indicating summer, the determined SWB in between August 21 – September 21, 2015 have been used (Table 3.11). Similarly, the SWB which is determined within the period of December 21, 2015 – January 21, 2016 has been used for winter (Table 3.12). And for the verification process, Table 3.13 shows the determined SWB of the period between May 21 – June 21, 2016.

Table 3.11. The SWB of Kaleiçi DMA (August 21 – September 21, 2015), copied from (Muhammetoğlu 2017)

System input volume $Q_I =$ m³ 81855 %100	Authorized Consumption $Q_A=$ 58890 m³ %71.9	Billed Authorized consumption $Q_{BA} = 32093$ m³ %39.2	Billed Metered consumption 32093 m³ % 39.2	Revenue water 32093 m³ % 39.2
			Billed Unmetered consumption 0 m³ % 0	
		Unbilled Authorized consumption $Q_{UA} = 26797$ m³ % 32.7	Unbilled Metered consumption 26582 m³ % 32.5	Non-revenue water 49762 m³ % 60.8
			Unbilled Unmetered consumption 215 m³ % 0.3	
	Water Losses $Q_L = 22965$ m³ % 28.1	Apparent Losses $Q_{AL} = 4973$ m³ % 6.1	Unauthorized consumption 279 m³ % 0.3	
			Customer meter inaccuracies and data handling errors 4694 m³ % 5.7	
		Real Losses $Q_{RL} = 17992$ m³ % 22	Leakage on transmission and distribution mains 17992 m³ % 22	

Table 3.12. The SWB of Kaleiçi DMA (December 21, 2015 - January 21, 2016), copied (Muhammetoğlu 2017)

System input volume Q_I = 57113 m³ 100%	Authorized Consumption Q_A= 41331 m³ 72.4%	Billed Authorized consumption Q_{BA} = 16081 m³ 28.2%	Billed Metered consumption 16081 m³ 28.2%	Revenue water 16081 m³ 28.2%
			Billed Unmetered consumption 0 m³ 0%	
		Unbilled Authorized consumption Q_{UA} = 25251 m³ 44.2%	Unbilled Metered consumption 25159 m³ 44.1%	Non-revenue water 41033 m³ 60.8%
			Unbilled Unmetered consumption 92 m³ 0.2%	
	Water Losses Q_L = 15782 m³ 27.6%	Apparent Losses Q_{AL} = 3578 m³ 6.3%	Unauthorized consumption 279 m³ 0.3%	
			Customer meter inaccuracies and data handling errors 3299 m³ 5.8%	
		Real Losses Q_{RL} = 12204 m³ 21.4%	Leakage on transmission and distribution mains 12204 m³ 21.4%	

Table 3.13. The SWB of Kaleiçi DMA (May 21, 2016 - June 21, 2016), copied from (Muhammetoğlu 2017)

System input volume Q_I = 81165 m³ 100%	Authorized Consumption Q_A= 58218 m³ 71.7%	Billed Authorized consumption Q_{BA} = 24658 m³ 30.4%	Billed Metered consumption 24658 m³ 30.4%	Revenue water 24658 m³ 30.4%
			Billed Unmetered consumption 0 m³ 0%	
		Unbilled Authorized consumption Q_{UA} = 33560 m³ 41.3%	Unbilled Metered consumption 33345 m³ 41.1%	Non-revenue water 56507 m³ 69.6%
			Unbilled Unmetered consumption 215 m³ 0.3%	
	Water Losses Q_L = 22947 m³ 28.3%	Apparent Losses Q_{AL} = 4919 m³ 6.1%	Unauthorized consumption 279 m³ 0.3%	
			Customer meter inaccuracies and data handling errors 4640 m³ 5.7%	
		Real Losses Q_{RL} = 18028 m³ 22.2%	Leakage on transmission and distribution mains 18028 m³ 22.2%	

3.7. Hydraulic Modelling of Kaleiçi WDN

The hydraulic model of Kaleiçi WDN was performed using H-W formulae within the research project of Muhammetoğlu (2017) assuming that the system input flow (including leakage and non-leakage flow) is uniformly distributed along pipe length, and the nodal-demands were determined by the half-length of the pipe except for two subscribers of high consumption which are a park and a fire-fighting unit.

In this thesis research, H-W formulae has been used for hydraulic modeling of Kaleiçi WDN by EPANET software with dividing the system input flow into leakage and non-leakage flow and distributing them in space and time. The leakage (physical water

losses) was determined through the SWB. SIV and pressure at the inlet and the pressure at each PMP have been recorded every five minutes, therefore, the modeling time-step has been set up every five minutes. At each junction, the leakage occurs through emitters and the non-leakage flow is defined by the base-demand at each node and the related multiplier pattern (Rossman 2000).

The non-leakage flow includes SIV minus the leakage (physical water losses). Assuming that they are uniformly distributed by the pipe length as applied in scenario M2, both of the leakage and the non-leakage flow have been distributed by the half-length of the pipes connected to each junction. Taking into consideration that two junctions have special nodal demands and patterns. These two junctions are related to water consumption of a park and fire-defense department in the PSA, their flow measurements were recorded within model simulation periods, thus, their flows have been assigned directly to their nodes and the rest of the total non-leakage flow has been distributed over the other junctions of Kaleiçi WDN.

The approach of spatial leakage simulation, which is proposed by Cobacho Jordán et al. (2015), assumes that the leakage exponent and the pipe roughness coefficient(s) are available. The leakage exponent has been assumed to be (γ=1) since Kaleiçi DMA is considered as a big WDN contains pipes of different types of materials. The pipe roughness coefficient has been calibrated by a process of trial and error (Muhammetoğlu 2017).

3.8. Calibrating The Pipe Roughness Coefficient of PSA

The aim of the calibration is to determine the pipe roughness coefficient. The calibration process has been carried out for Kaleiçi WDN by comparing the measured pressure with the predicted pressure at the PMPs at different trials of the roughness coefficient. The roughness coefficient that reveals the least mean absolute error (MAE) of pressure will be the calibrated roughness coefficient of all pipes.

The roughness coefficient used in the Hazen-Williams equation is a dimensionless factor. During the calibration process, the roughness coefficients have been tested over two stages; in the first stage, the trials of the roughness coefficient are R= [50, 55, 60, 65, 70]. In the second stage, the roughness coefficients are investigated in between the trials against the least and the second least MAE of pressure to find the exactly calibrated roughness coefficient as it is going to be shown in the results.

Leakage coefficients have been determined at each trial of the roughness coefficient as explained in the proposed approach of spatial simulation of leakage. To start up the iterative process of determining leakage coefficient, the average measured pressure at all PMPs has been used. Figure 3.14 presents a flowchart of calculating the MAE of pressure at each trial of the roughness coefficient after determination of the leak coefficients.
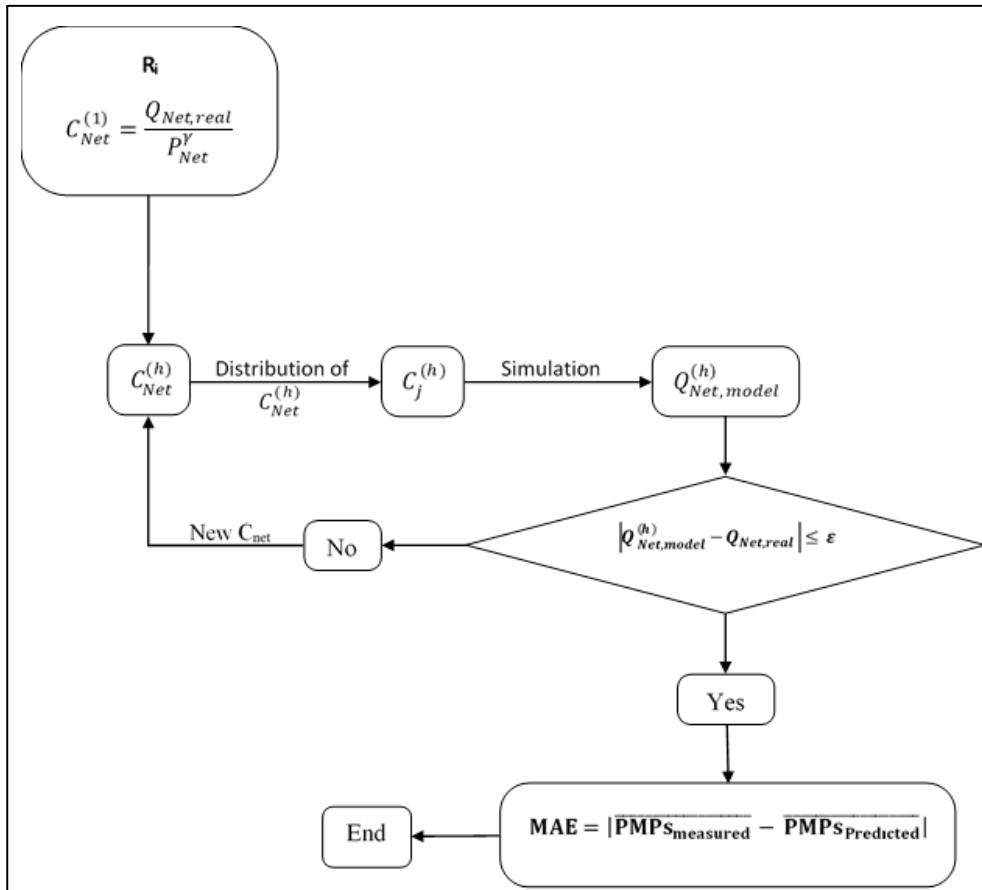
Figure 3.16. Flowchart for calculating the MAE of pressure at each trial of roughness coefficient after determination of leakge coefficients

For the model accreditation purpose, two calibration processes of pipe roughness coefficients have been carried out over two simulation periods. The first simulation period is 117 hours 30 minutes extends from August 20, 2015, at 12:30 PM to August 25, 2015, at 10:00 AM and represents the summer season. The other simulation period is 119 hours 20 minutes in the time between January 14, 2016, at 12:10 PM and January 19, 2016, at 11:30 AM and represents the winter season. When the simulation is run, a one day (24-hours) warming period has been applied at the beginning of the simulation periods. The data of this warming period is not used for analysis.

To study the prediction capability of the model, two artificial high flow events had been executed during simulation period by opening a fire-hydrant valve on August 22, 2015 10:15 – 10:50 AM (for 35 min.) and on January 16, 2016 06:14 – 07:05 AM (for 51 min.) (Muhammetoğlu 2017).

The calibrated pipe roughness coefficient resulted from the two calibration periods is calculated by equation (3.8).

$$R = \frac{R_s \times N_{PMPs} \times N_{ms} + R_2 \times N_{PMPw} \times N_{mw}}{(N_{PMPs} \times N_{ms}) + (N_{PMPw} \times N_{mw})} \tag{3.8}$$

Where:

R_s, R_w: are the roughness calibrated for summer and winter seasons, respectively.

N_{PMPs}, N_{PMPw}: are the number of the considered PMP in summer and winter simulation periods, respectively.

N_{ms}, N_{mw}: are the number of pressure measurements at each PMP in summer and winter simulation periods, respectively.

3.8.1. Calibrating the pipe roughness in the summer season (August 20-25, 2015)

For the summer simulation period, the monthly SWB given in Table 3.11 has been converted to the SWB during the simulation period as follows:

The SIV (12815.3 m³) has been calculated using the records of SCADA station found at the inlet of Kaleiçi DMA. The recorded system input flow and the recorded pressure at the inlet are presented in Figure 3.15. The average of recorded flow related to the park consumption is 31.03 m³/h, and for the consumption of the fire-fighting unit is 0.39 m³/h. The SWB shown in Table 3.11 provides the water volumes of the other components of the SWB within August 21 – September 21, 2015. These volumes are converted for summer calibration simulation period as presented in Table 3.14.
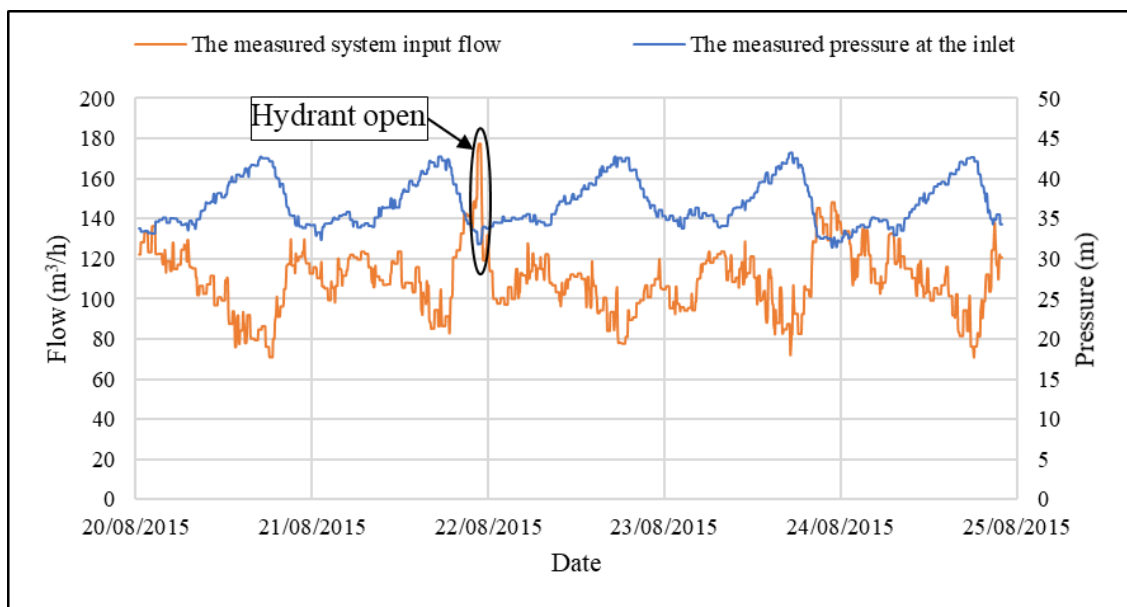
Figure 3.17. The pressure and flow recorded by SCADA station at the inlet of Kaleiçi WDN, (August 20 - 25, 2015)

$$\text{Revenue water} = \text{Authorized billed consumption} = \left(\frac{32093}{31*24}\right) \times 117.5\ \text{h} = 5068.5\ \text{m}^3$$

$$\text{Authorized unbilled metered consumption} = \left(\frac{26582}{31*24}\right) \times 117.5\ \text{h} = 4198\ \text{m}^3$$

$$\text{Authorized unbilled un-metered consumption} = \left(\frac{215}{31*24}\right) \times 117.5\ \text{h} = 34\ \text{m}^3$$

Authorized unbilled consumption = 4198 +34 = 4232 m3

Authorized consumption = 5068.5 + 4232 = 9300.5 m3

Water losses = SIV – Authorized consumption = 12815.3 – 9300.5 = 3514.8 m3

Unauthorized consumption = 9 m3/d × 5 = 45 m3

Customer meter inaccuracies = 0.08 × (4198 + 5068.5) = 741.3 m3

Apparent losses = 741.3 + 45 = 786.3 m3

Real losses = Leakage = 3514.8 – 786.3 = 2728.5 m3

NRW = SIV – Revenue water = 12815.3 – 5068.5 = 7746.8 m3

Table 3.14. The SWB calculated for calibration process in the summer simulation period. (August 20, 2015 at 12:30 PM – August 25, 2015 at 10:00 AM)

System input volume Q_I = 12815.3 m³ %100	Authorized Consumption Q_A= 9300.5 m³ % 72.6	Billed Authorized consumption Q_{BA} = 5068.5 m³ % 39.5	Billed Metered consumption 5068.5 m³ % 39.5	Revenue water 5068.5 m³ % 39.5
			Billed Unmetered consumption 0 m³ % 0	
		Unbilled Authorized consumption Q_{UA} = 4232.0 m³ % 33.0	Unbilled Metered consumption 4198.0 m³ % 32.8	Non-revenue water 7746.8 m³ % 60.5
			Unbilled Unmetered consumption 34.0 m³ % 0.3	
	Water Losses Q_L = 3514.8 m³ % 27.4	Apparent Losses Q_{AL} = 786.3 m³ % 6.2	Unauthorized consumption 45.0 m³ % 0.4	
			Customer meter inaccuracies and data handling errors 741.3 m³ % 5.8	
		Real Losses Q_{RL} = 2728.5 m³ % 21.3	Leakage on transmission and distribution mains 2728.5 m³ **(23.22 m³/h)** % 21.3	

The following parameters are the input data for calibrating the pipe roughness by the model of Kaleiçi WDN in summer season:

The system input flow of Kaleiçi WDN = $\left(\frac{12815.3}{117.5}\right)$ = 109.06 m³/h

The leakage rate in Kaleiçi WDN = $\left(\frac{2728.5}{117.5}\right)$ = 23.22 m³/h

The non-leakage flow = 109.06 – 23.22 = 85.84 m³/h

The nodal-base-demand which is assigned directly at the junction of the park = 31.03 m³/h.

The nodal-base-demand which is assigned directly at the junction of the fire-fighting unit = 0.39 m³/h,

The rest of the non-leakage flow which is going to be distributed uniformly by the half-length of the pipes as nodal-base-demands to the other junctions = 85.84 – 31.03 – 0.39 = 54.42 m³/h.

The average measured pressure at each PMP all over the summer simulation period is presented in Table 3.15, the PMP-1 was out of order during this simulation period. Consequently, the initial leakage coefficient of Kaleiçi WDN is calculated as, $C_{Net}^i = \frac{Q_{Net,real}}{P_{Net}^\gamma} = \frac{23.22}{(47.14)^1} = 0.492575$ m²/h.

Table 3.15. The average measured pressure at each PMP in summer simulation period (August 20 - 25, 2015)

Parameter	PMP-2	PMP-3	PMP-4	PMP-7
Average measured pressure (m)	39.01	33.46	48.96	67.13
Average measured pressure at all PMPs (m)	47.14			

3.8.2. Calibrating the pipe roughness in the winter season (January 14-19, 2016)

For the winter simulation period, the monthly SWB given in Table 3.12 has been converted to the SWB during the simulation period as follows:

The SIV (9292.05 m³) has been calculated using the records of SCADA station found at the inlet of Kaleiçi DMA. The recorded system input flow and the recorded pressure at the inlet are presented in Figure 3.18. The average of recorded flow related to the park consumption is 25.21 m³/h. No recorded consumption of the fire-fighting department in the winter season. The SWB shown in Table 3.12 provides the volumes of the other components of the SWB within December 21, 2015 – January 21, 2016. These volumes are converted for winter calibration simulation period as shown in Table 3.16.
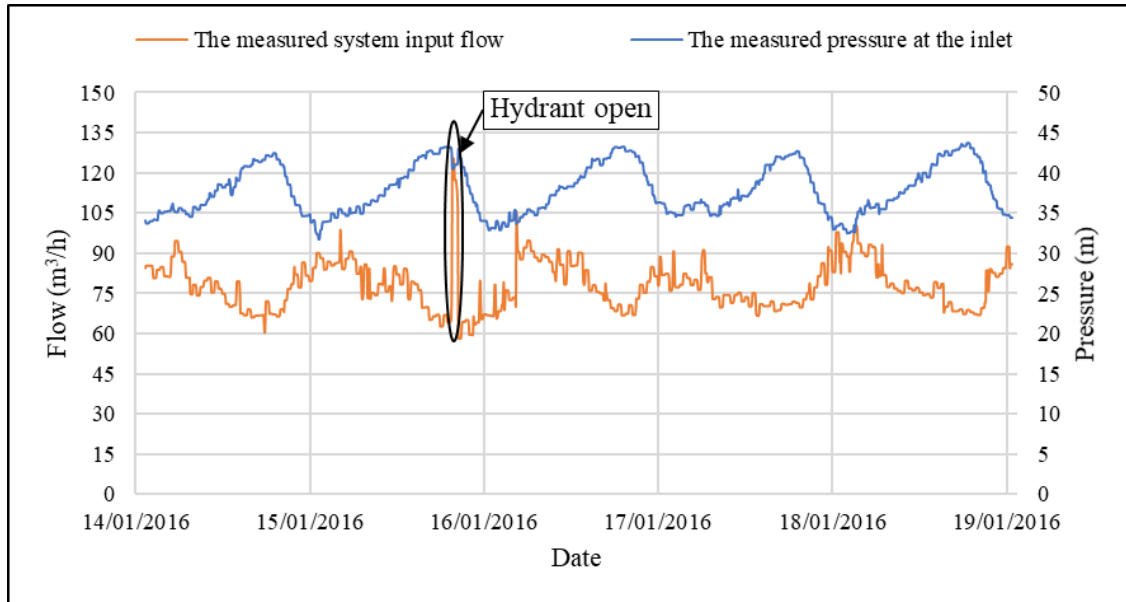
Figure 3.18. The pressure and flow recorded by SCADA station at the inlet of Kaleiçi WDN, (January 14 – 19, 2016)

Revenue water = Billed Authorized consumption = $\left(\frac{16081}{31*24}\right) \times 119.333$ h = 2579.3 m^3

Authorized unbilled metered consumption = $\left(\frac{25159}{31*24}\right) \times 119.333$ h = 4035.36 m^3

Authorized unbilled un-metered consumption = $\left(\frac{92}{31*24}\right) \times 119.333$ h = 14.76 m^3

Authorized unbilled consumption = 4035.36 + 14.76 = 4050.12 m^3

Authorized consumption = 2579.3 + 4050.12 = 6629.42 m^3

Water losses = SIV – Authorized consumption = 9292.05 – 6629.42 = 2662.63 m^3

Unauthorized consumption = 9 m^3/d × 5 = 45 m^3

Customer meter inaccuracies = 0.08 × (4035.36 + 2579.3) = 529.17 m^3

Apparent losses = 529.17 + 45 = 574.17 m^3

Real losses = Leakage = 2662.63 – 574.17 = 2088.46 m^3

NRW = SIV – Revenue water = 9292.05 – 2579.3 = 6712.75 m^3

Table 3.16. The SWB calculated for the calibration process in the winter simulation period. (January 14, 2016 at 12:10 PM – January 19, 2016 at 11:30 AM)

System input volume Q_I = 9292.05 m³ %100	Authorized Consumption Q_A= 6629.42 m³ % 71.3	Billed Authorized consumption Q_{BA} = 2579.3 m³ % 27.8	Billed Metered consumption 2579.3 m³ % 27.8	Revenue water 2579.3 m³ % 27.8
			Billed Unmetered consumption 0 m³ % 0	
		Unbilled Authorized consumption Q_{UA} = 4050.12 m³ % 43.6	Unbilled Metered consumption 4035.36 m³ % 43.4	Non-revenue water 6712.75 m³ % 72.2
			Unbilled Unmetered consumption 14.76 m³ % 0.2	
	Water Losses Q_L = 2662.63 m³ % 28.7	Apparent Losses Q_{AL} = 574.17 m³ % 6.3	Unauthorized consumption 45.0 m³ % 0.6	
			Customer meter inaccuracies and data handling errors 529.17 m³ % 5.7	
		Real Losses Q_{RL} = 2088.46 m³ % 22.4	Leakage on transmission and distribution mains 2088.46 m³ **(17.5 m³/h)** % 22.4	

The following parameters are the input data for calibrating the pipe roughness by the model of Kaleiçi WDN in winter season:

The system input flow of Kaleiçi WDN $= \left(\frac{9292.05}{119.333}\right) = 77.87$ m³/h

The leakage rate in Kaleiçi WDN $= \left(\frac{2088.46}{119.333}\right) = 17.5$ m³/h.

The non-leakage flow = 77.86 – 17.5 = 60.36 m³/h

The base-demand which is assigned directly at the junction of the park = 25.21 m³/h.

The rest of the non-leakage flow which is going to be distributed uniformly by the half-length of the pipes as base-demands to the other junctions = 60.36 – 25.21 = 35.15 m³/h.

The average measured pressure at each PMP all over the summer simulation period is presented in Table 3.17. The initial leakage coefficient of Kaleiçi WDN, $C_{Net}^i = \frac{Q_{Net,real}}{P_{Net}^\gamma} = \frac{17.5}{(48.354)^1} = 0.361914$ m²/h.

Table 3.17. The average measured pressure at each PMP in winter simulation period (January 14 – 19, 2016)

Parameter	PMP-1	PMP-2	PMP-3	PMP-4	PMP-7
Average measured pressure (m)	42.09	42.14	36.67	51.21	69.66
Average measured pressure at all PMPs (m)	48.354				

3.9. Verifying The Calibrated Pipe Roughness Coefficient of PSA

The aim of the verification process is to test the validity of the calibrated roughness coefficient of Kaleiçi WDN through another simulation period. The simulation period for modeling verification of Kaleiçi WDN extends from June 1, 2016, at 12:00 AM to June 6, 2016, at 11:55 PM (144 h). The calibrated roughness coefficient is assigned to all pipes while verifying the model of Kaleiçi WDN, then the MAE of the difference between the measured and the predicted pressure at all PMPs has been determined.

Table 3.13 shows the monthly SWB related to the verification process which has been converted to the SWB during the simulation period as follows;

The SIV (16089.4 m³) has been calculated using the records of the SCADA station found at the inlet of Kaleiçi DMA. The recorded system input flow and the recorded pressure at the inlet are presented in Figure 3.19. The average recorded flow related to the park's consumption is 24.91 m³/h, and for the consumption of the fire-fighting unit is 0.29 m³/h. The SWB shown in Table 3.13 provides the water volumes of the other components of the SWB within May 21 – June 21, 2016. These volumes are converted to SWB for the simulation period of the verification process as presented in Table 3.18.
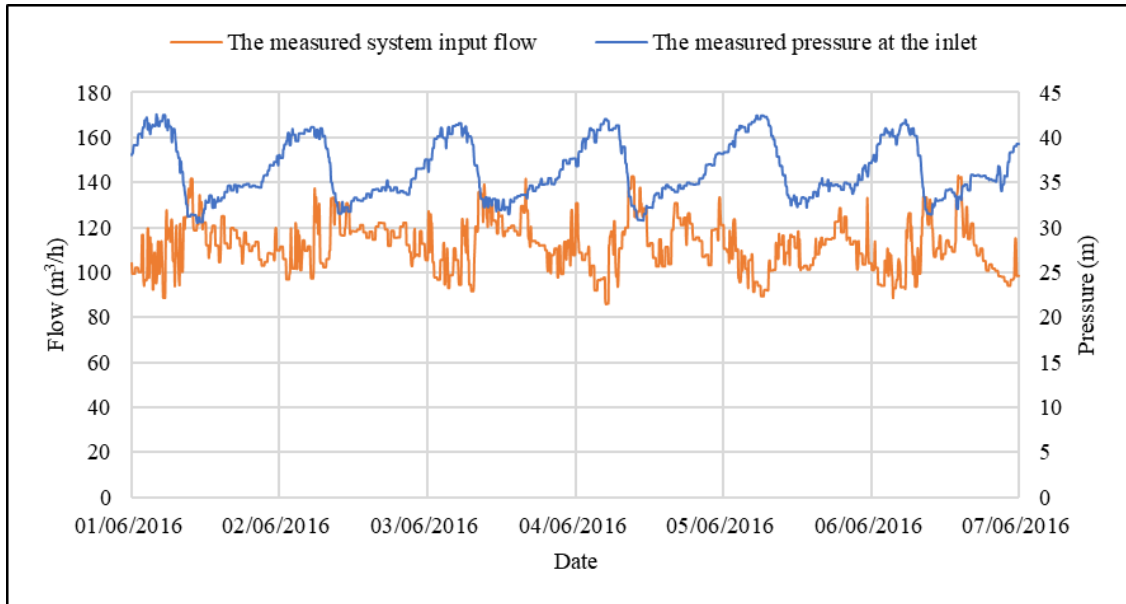
Figure 3.19. The pressure and flow recorded by SCADA station at the inlet of Kaleiçi WDN. (June 1 – 6, 2016)

Revenue water = Billed Authorized consumption = $\left(\frac{24658}{31*24}\right) \times 144$ h $= 4772.5$ m^3

Authorized unbilled metered consumption = $\left(\frac{33345}{31*24}\right) \times 144$ h $= 6453.9$ m^3

Authorized unbilled un-metered consumption = $\left(\frac{215}{31*24}\right) \times 144$ h $= 41.6$ m^3

Authorized unbilled consumption = 6453.9 + 41.6 = 6495.5 m^3

Authorized consumption = 4772.5 + 6495.5 = 11268 m^3

Water losses = SIV – Authorized consumption = 16089.4 – 11268 = 4821.4 m^3

Unauthorized consumption = 9 m^3/d × 6 = 54 m^3

Customer meter inaccuracies = 0.08 × (6453.9 + 4772.5) = 898.1 m^3

Apparent losses = 898.1 + 54 = 952.1 m^3

Real losses = Leakage = 4821.4 – 952.1 = 3869.3 m^3

NRW = SIV – Revenue water = 16089.4 – 4772.5 = 11316.9 m^3

Table 3.18. The SWB calculated for the simulation period of the verification process (June 1, 2016 at 12:00 AM – June 6, 2016 at 11:55 PM).

System input volume Q_I = 16089.4 m³ %100	Authorized Consumption Q_A= 11268.0 m³ % 70.0	Billed Authorized consumption Q_{BA} = 4772.5 m³ % 29.7	Billed Metered consumption 4772.5 m³ % 29.7	Revenue water 4772.5 m³ % 29.7
			Billed Unmetered consumption 0 m³ % 0	
		Unbilled Authorized consumption Q_{UA} =6495.5 m³ % 40.4	Unbilled Metered consumption 6453.9 m³ % 40.1	Non-revenue water 11316.9 m³ % 70.3
			Unbilled Unmetered consumption 41.6 m³ % 0.3	
	Water Losses Q_L = 4821.4 m³ % 30.0	Apparent Losses Q_{AL} = 952.1 m³ % 5.9	Unauthorized consumption 54.0 m³ % 0.3	
			Customer meter inaccuracies and data handling errors 898.1 m³ % 5.6	
		Real Losses Q_{RL} = 3869.3 m³ % 24.0	Leakage on transmission and distribution mains 3869.3 m³ **(26.87 m³/h)** % 24.0	

The following parameters are the input data for the verification process of the calibrated pipe roughness by the model of Kaleiçi WDN:

The input flow of Kaleiçi WDN $= \left(\frac{16089.4}{144}\right) = 111.73$ m³/h

The leakage rate Kaleiçi WDN $= \left(\frac{3869.3}{114}\right) = 26.87$ m³/h

The non-leakage flow = 111.73 – 26.87 = 84.86 m³/h

The nodal-base-demand which is assigned directly at the junction of the park = 24.91 m³/h.

The nodal-base-demand which is assigned directly at the junction of the fire-fighting unit =0.29 m^3/h.

The rest of the non-leakage flow which is going to be distributed uniformly by the half-length of the pipes as nodal-base-demands to the other junctions = 84.86 – 24.91 – 0.29 = 59.66 m^3/h.

The average measured pressure at each PMP all over the simulation period of verification process is presented in Table 3.19. The initial leakage coefficient of Kaleiçi WDN, $C_{Net}^i = \frac{Q_{Net,real}}{P_{Net}^\gamma} = \frac{26.87}{(45.214)^1} = 0.594285$ m^2/h

Table 3.19. The average measured pressure at each PMP during verification simulation period (June 1 – 6, 2016)

Parameter	PMP-1	PMP-2	PMP-3	PMP-4	PMP-7
Average measured pressure (m)	38.69	39.16	33.34	48.20	66.70
Average measured pressure at all PMPs (m)	45.214				

3.10. Application of Advanced PM

Since Kaleiçi contains many tourism aspects, the customers consume water for different purposes even at nighttime hours, especially in summer season. The verified roughness coefficient has been applied for all pipes in the hydraulic model of Kaleiçi WDN to be used in application of closed-loop pressure control as an advanced PM technique by installing the PRV at the inlet and the sensors at the CPs of the WDN in the PSA. Then, the leakage reduction due to advanced PM application has been predicted over the two simulation periods; in summer and in winter.

The first step is detecting the CP of the lowest pressure over simulation period and predicting the excess pressure over the minimum allowable levels there (20 m as legislated) (Muhammetoglu and Muhammetoglu 2017). Then the pressure at the inlet is broken at different levels with time in order to keep the pressure at the CP always at 20 m. Finally, the average reduction in pressure and leakage have been calculated. The CPs of pressure over the maximum legislated level (60 m) have also been investigated before and after applying advanced PM.

3.11. Scenarios of Leakage Reduction

In the following sub-sections, two scenarios of Kaleiçi WDN have been studied. In the first scenario, only the non-leakage flow is assumed to be changed by ± 25% of its measured flow. Then, the effect of increasing or decreasing non-leakage flow on leakage has been studied. The second scenario supposes that only the leakage is reduced to the ELL. The advanced PM has been applied for each scenario to investigate the leakage reduction which can be achieved as a result of pressure reduction.

3.11.1. Scenarios of changes in the non-leakage flow

The impact of changing the non-leakage flow by ± 25% on leakage has been investigated in Kaleiçi WDN in this scenario. The total water consumption increases or decreases according to several factors such as; the intensity of tourists which is changing seasonally, the populations who live in the PSA, and using water more wisely for water saving.

In the components of non-leakage flow, the unbilled un-metered authorized consumption and unauthorized consumption are assumed not to be changed since they are related to a pool and irrigation system of a park and approximated consumption of definite number of fire-water boxes, while the other components are assumed to be changed by ±25%. Additionally, all other factors such as the leakage coefficients, the leakage exponent, the pressure profile at the inlet and the calibrated pipe roughness are assumed to be same as in the base simulation. The nodal base-demands at each assumption of decreasing or increasing the non-leakage flow in the base simulation during summer and winter simulation periods are presented in Table 3.20 and Table 3.21, respectively. For each assumption, the summation of non-leakage flow and leakage rate as it is distributed by the model ($\Sigma Q_{(non\text{-}leakage)+(leakage)}$) and the measured pressure at the inlet are presented in Figures 3.20 & 3.21 for the summer season, and Figures 3.22 & 3.23 for the winter season.

Table 3.20. The assumed increased or decreased volumes of the non-leakage water and the nodal base-demands in the summer simulation period. (August 20 – 25, 2015)

|	(1) **Base simulation**	(2) = (1) × 0.75 **Non-leakage flow decreased by 25%**	(3) = (1) × 1.25 **Non-leakage flow Increased by 25%**
Billed Metered consumption (m³)	5068.5	3801.4	6335.6
Unbilled Metered consumption (m³)	4198.0	3148.5	5247.5
Unbilled Unmetered consumption (m³)	34.0	34.0	34.0
Unauthorized consumption (m³)	45.0	45.0	45.0
Customer meter inaccuracies (m³)	741.3	556	926.65
The average flow of the park (m³/h)	31.03	23.27	38.79
The average flow of the firefighting (m³/h)	0.39	0.29	0.49
The rest of the non-leakage flow (m³/h)	54.42	$\left(\dfrac{3801.4+3148.5+34+45+556}{117.5}\right)$ $- 23.27 - 0.29 = 40.99$	$\left(\dfrac{6335.6+5247.5+34+45+926.6}{117.5}\right)$ $- 38.79 - 0.49 = 67.85$
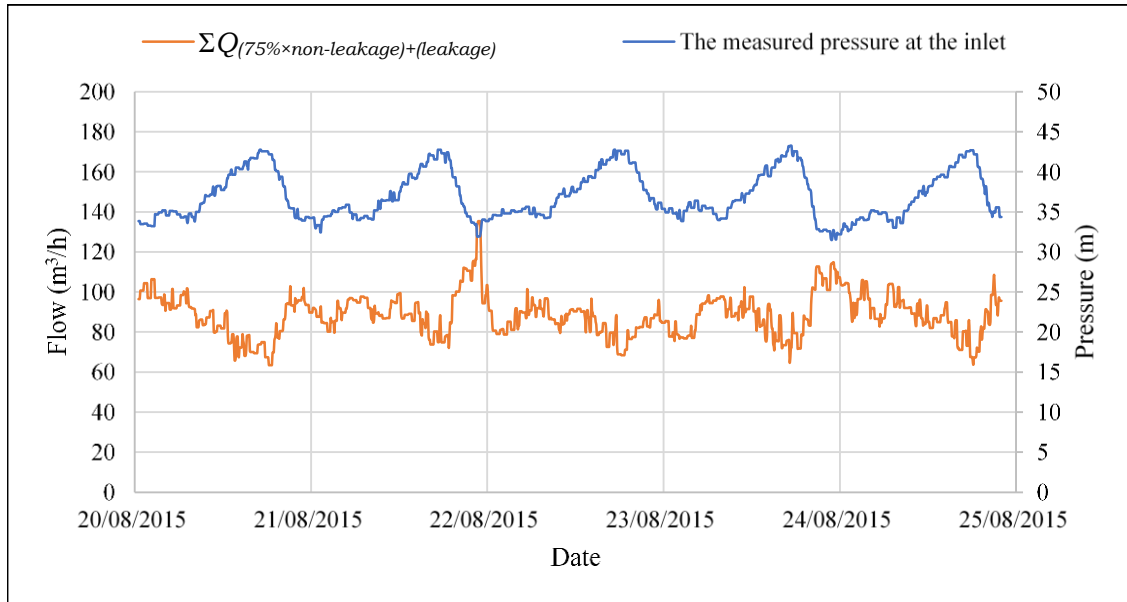
Figure 3.20. The pressure measured at the inlet vs. $\Sigma Q_{(75\% \times non\text{-}leakage)+(leakage)}$, (August 20 – 25, 2015)
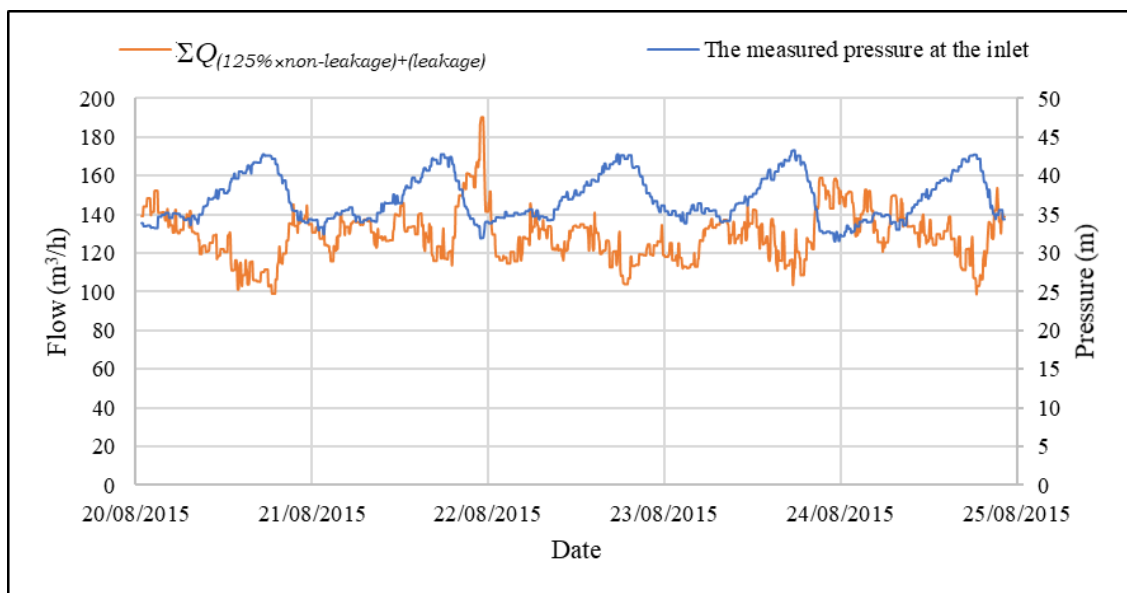

Figure 3.21. The pressure measured at the inlet vs. $\Sigma Q_{(125\% \times non\text{-}leakage)+(leakage)}$, (August 20 – 25, 2015)

63

Table 3.21. The assumed increased or decreased volumes of the non-leakage water and the nodal base-demand in the winter simulation period. (January 14 – 19, 2016)

|	(1) **Exist flow**	(2) = (1) × 0.75 **Non-leakage flow decreased by %25**	(3) = (1) × 1.25 **Non-leakage flow Increased by %25**
Billed Metered consumption (m³)	2579.3	1934.5 m^3	3224.1 m^3
Unbilled Metered consumption (m³)	4035.36	3026.52 m^3	5044.2 m^3
Unbilled Unmetered consumption (m³)	14.76	14.76	14.76
Unauthorized consumption (m³)	45.0	45.0	45.0
Customer meter inaccuracies (m³)	529.17	396.88 m^3	661.5 m^3
The average flow of the park (m³/h)	25.21	18.91 m^3/h	31.51 m^3/h
The rest of the non-leakage flow (m³/h)	35.15	$\left(\dfrac{1934.5+3026.52+14.76+45+396.88}{119.333}\right)$ $- 18.91 = 26.49$	$\left(\dfrac{3224.1+5044.2+14.76+45+661.5}{119.333}\right)$ $- 31.51 = 43.82$
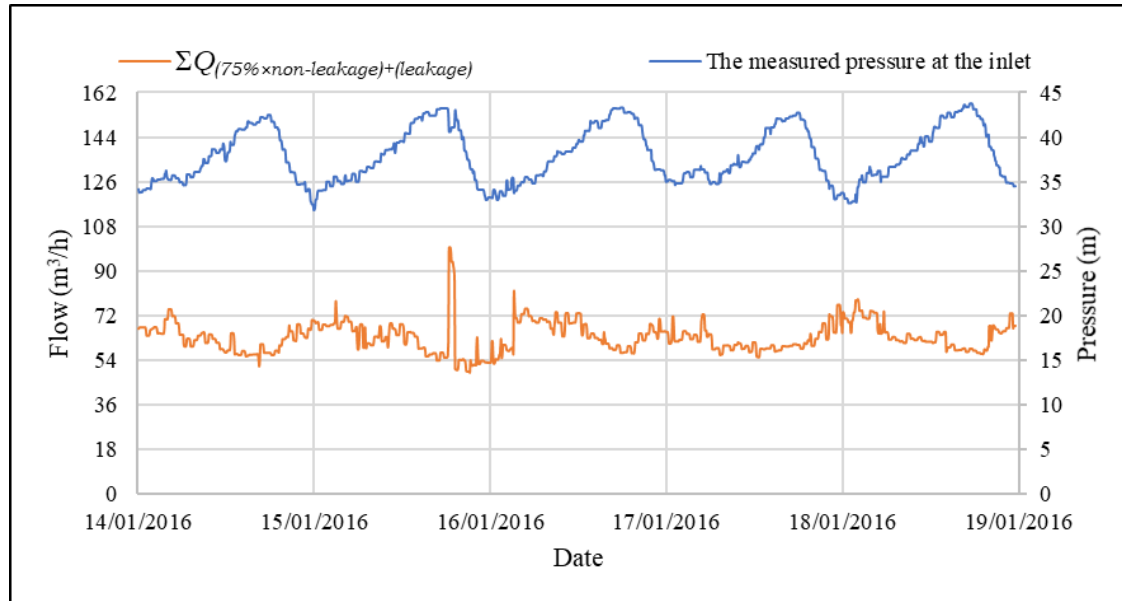
Figure 3.22. The pressure measured at the inlet vs $\Sigma Q_{(75\%\times non\text{-}leakage)+(leakage)}$, (January 14 – 19, 2016)
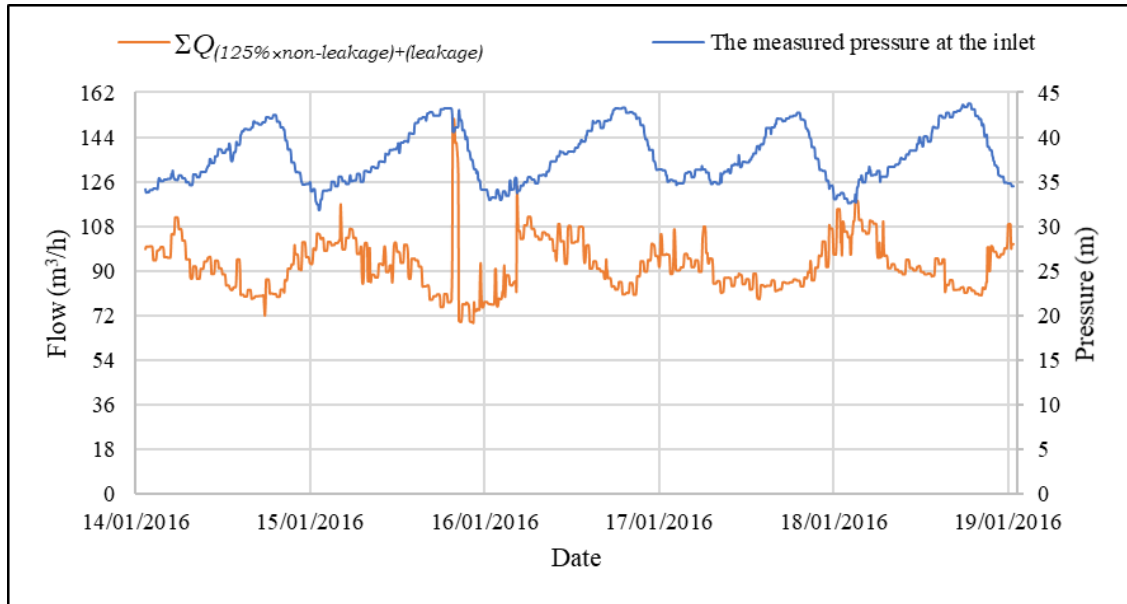
Figure 3.23. The pressure measured at the inlet vs $\Sigma Q_{(125\% \times non\text{-}leakage)+(leakage)}$, (January 14 – 19, 2016)

3.11.2. Scenario of changes in leakage rate

Gülaydın (2017) has determined the ELL of Kaleiçi WDN. The results of this study have been used in the current thesis research as a scenario of future levels of water losses in Kaleiçi. Once the leakage level is reduced to the ELL, it is highly possible to observe the consequent rise of leakage level above ELL within the specified DMA.

According to the SWB prepared by Muhammetoğlu (2017), the calculated annual physical water losses (leakage) of Kaleiçi WDN are 144064 m³/y, which forms %17.2 of SIV. Gülaydın (2017) has determined ELL of Kaleiçi WDN for the same year. ELL of Kaleiçi WDN was determined as 59693.39 m³/y and represents %7.1 of SIV. In other words, the determined ELL of Kaleiçi WDN within 2015-2016 stand for %41.4 of the leakage calculated by SWBs within the same year.

In this scenario, the leakage coefficients have been recalculated for a new leakage flow equals %41.4 of the calculated leakage in summer and winter simulation periods, i.e. the simulated leakage in summer simulation period = 23.22 × 0.414 = 9.613 m³/h and in winter simulation period = 17.5 × 0.414 = 7.245 m³/h. Based on that, the summation of ELL and non-leakage flow as it distributed by the model ($\Sigma Q_{(non\text{-}leakage)+(ELL)}$) will be less than the measured system input flow of Kaleiçi WDN. The following parameters in the model are assumed not to be changed in this scenario; the verified pipe roughness coefficient, the leakage exponent, the non-leakage flow, and the time patterns. After that, the advanced PM has been applied for predicting the leakage reduction due to the pressure reduction that can be achieved under the ELL.

4. RESULTS AND DISCUSSION

Due to the applied 24-hours warming period at the simulation start time, all results are presented excluded the first day of the simulation period.

4.1. Calibrated Roughness Coefficient

4.1.1. Calibrating the pipe roughness in the summer season

PMP-1 was out of order in the summer season. Table 4.1 and Figure 4.1 show the MAE of the difference between the predicted and the measured pressure on the four PMPs while the trials of roughness coefficient are R= [50, 55, 60, 65, 70].

Table 4.1. The model predictions of of C_{net}^f, average ($\Sigma Q_{(non-leakage)+(leakage)}$), average total distributed leakage rate, ε, and the pressure MAE against R= [50, 55, 60, 65, 70], (August 21-25, 2015)

Roughness Coefficient	C_{net}^f	Average ($\Sigma Q_{(non-leakage)+(leakage)}$) (m³/h)	Average total distributed leakage (m³/h)	ε (m³/h)	Pressure MAE (m)
50	0.560	109.429	23.136	0.034	1.036
55	0.5486	109.436	23.142	0.078	0.666
60	0.5410	109.441	23.147	0.073	0.68
65	0.5352	109.446	23.152	0.068	0.883
70	0.5306	109.45	23.156	0.064	1.138
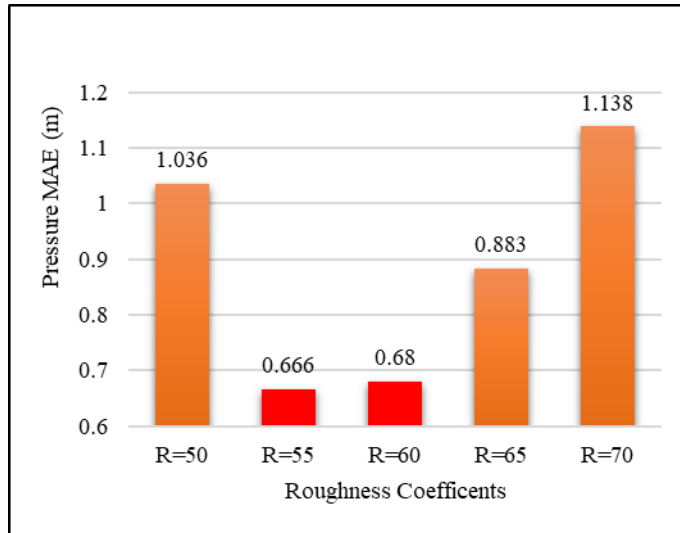
**Figure 4.1.** The pressure MAE at all PMPs against each trail of R= [50, 55, 60, 65, 70]. (August 21-25, 2015)

As shown in Figure 4.1, the least and the second least MAE are found against the roughness coefficients R= 55 and R= 60, respectively. So that the second stage of investigating the exact roughness coefficient has been performed on R= [55, 56, 57, 58, 59, 60] as shown in Table 4.2 and Figure 4.2.

Table 4.2. The model predictions of of $C_{net}f$, average ($\Sigma Q_{(non\text{-}leakage)+(leakage)}$), average total distributed leakage rate, ε, and the pressure MAE against R= [55, 56, 57, 58, 59, 60], (August 21-25, 2015)

| Roughness Coefficient	$C_{net}f$	Average ($\Sigma Q_{(non\text{-}leakage)+(leakage)}$) (m³/h)	Average total distributed leakage (m³/h)	ε (m³/h)	Pressure MAE (m)
55	0.548571	109.436	23.142	0.078	0.666
56	0.546876	109.437	23.133	0.077	0.645
57	0.545306	109.439	23.145	0.075	0.638
58	0.54379	109.440	23.146	0.074	0.642
59	0.542375	109.441	23.147	0.073	0.657
60	0.54099	109.441	23.147	0.073	0.68
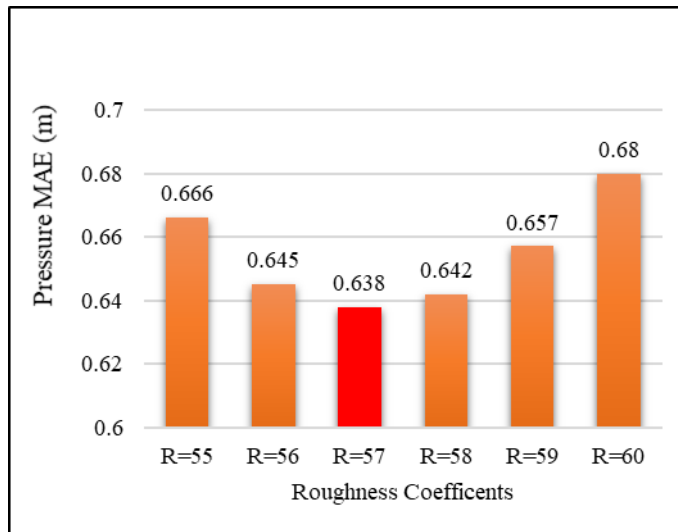
Figure 4.2. The pressure MAE at all PMPs against each trail of R= [55, 56, 57, 58, 59, 60]. (August 21-25, 2015)

As a result, the exactly calibrated value of the roughness coefficient in summer season is **R= 57** since it corresponds to the least pressure MAE. Figure 4.3 presents the roughness coefficients related to the least MAE at each PMP.
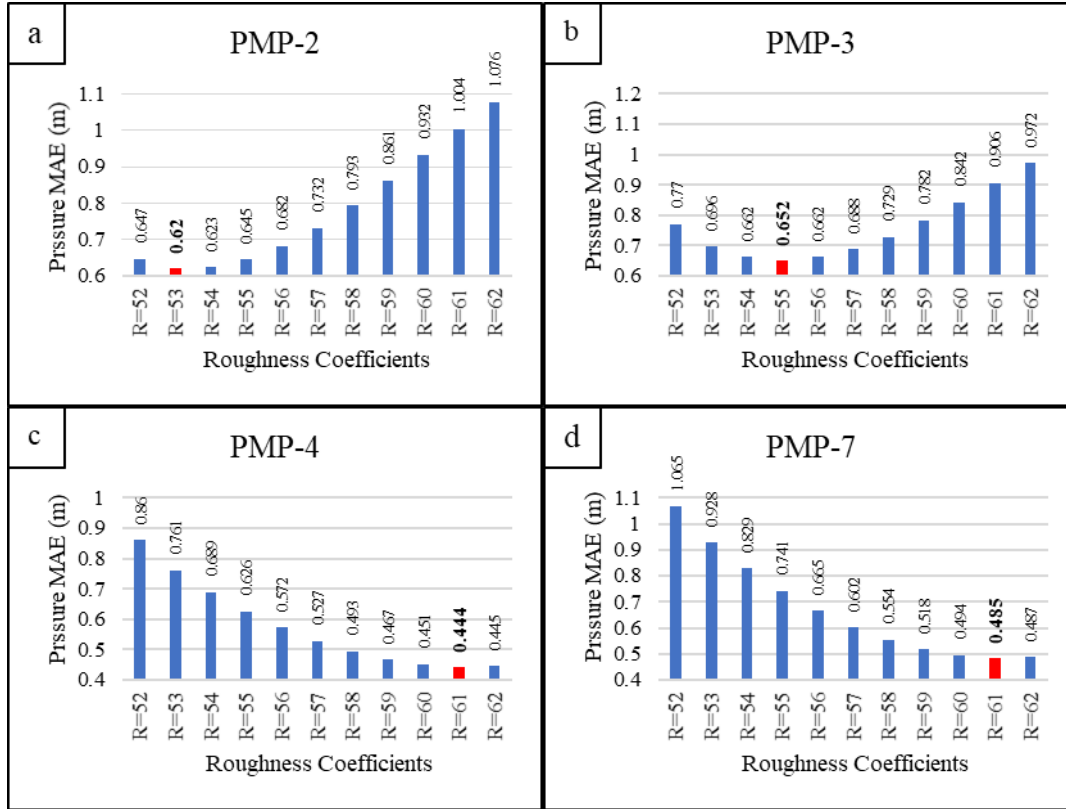
Figure 4.3. Against the range of trails R= [52 – 62], the MAE between the predicted and the measured pressure at a) PMP-2, b) PMP-3, c) PMP-4, d) PMP-7. (August 21-25, 2015)

The measured system input flow and the total of the leakage and the non-leakage flow distributed by the model ($\Sigma Q_{(non-leakage)+(leakage)}$) are not fully fitted with each other as shown in Figure 4.4. The flow MAE has been calculated as 1.67 m^3/h while the RMSE has been calculated as 2 m^3/h. Figure 4.5 presents the total distributed leakage rate as it is predicted by the model versus the total non-leakage flow while the roughness coefficient is **57**. Figure 4.6 presents a comparison between the measured pressure and the predicted pressure at each PMP while the pipe roughness is **57**.
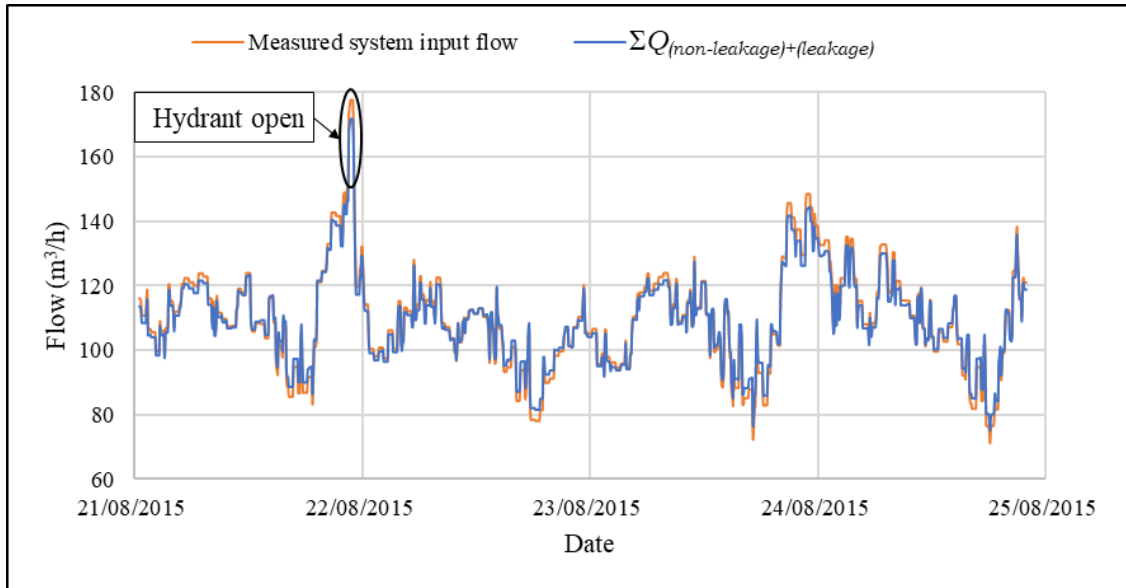
Figure 4.4. The measured system input flow vs. ($\Sigma Q_{(non-leakage)+(leakage)}$) at roughness R= 57, MAE = 1.67m^3/h and RMSE = 2 m^3/h (August 21-25, 2015)
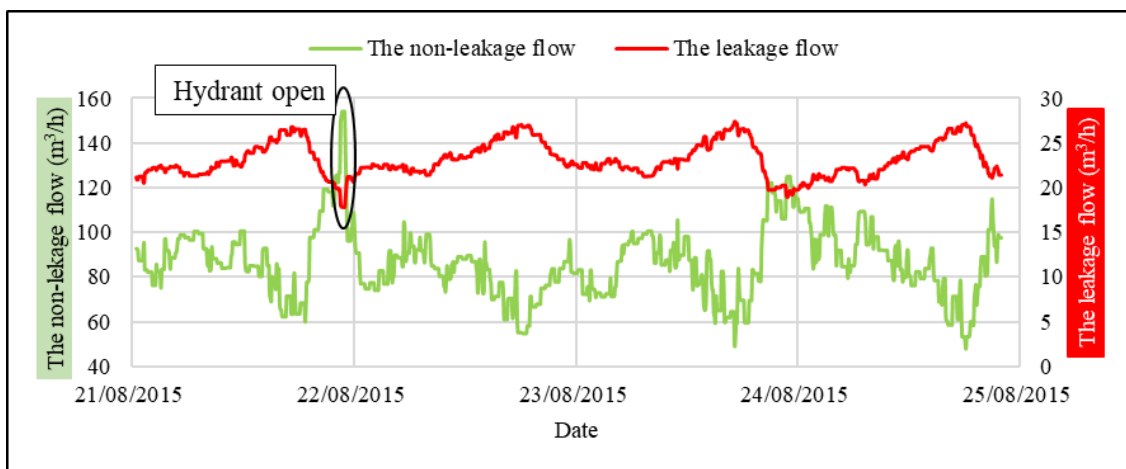

Figure 4.5. The network non-leakage flow vs. the total leakage rate as it is distributed by the model at R= 57. (August 21-25, 2015)
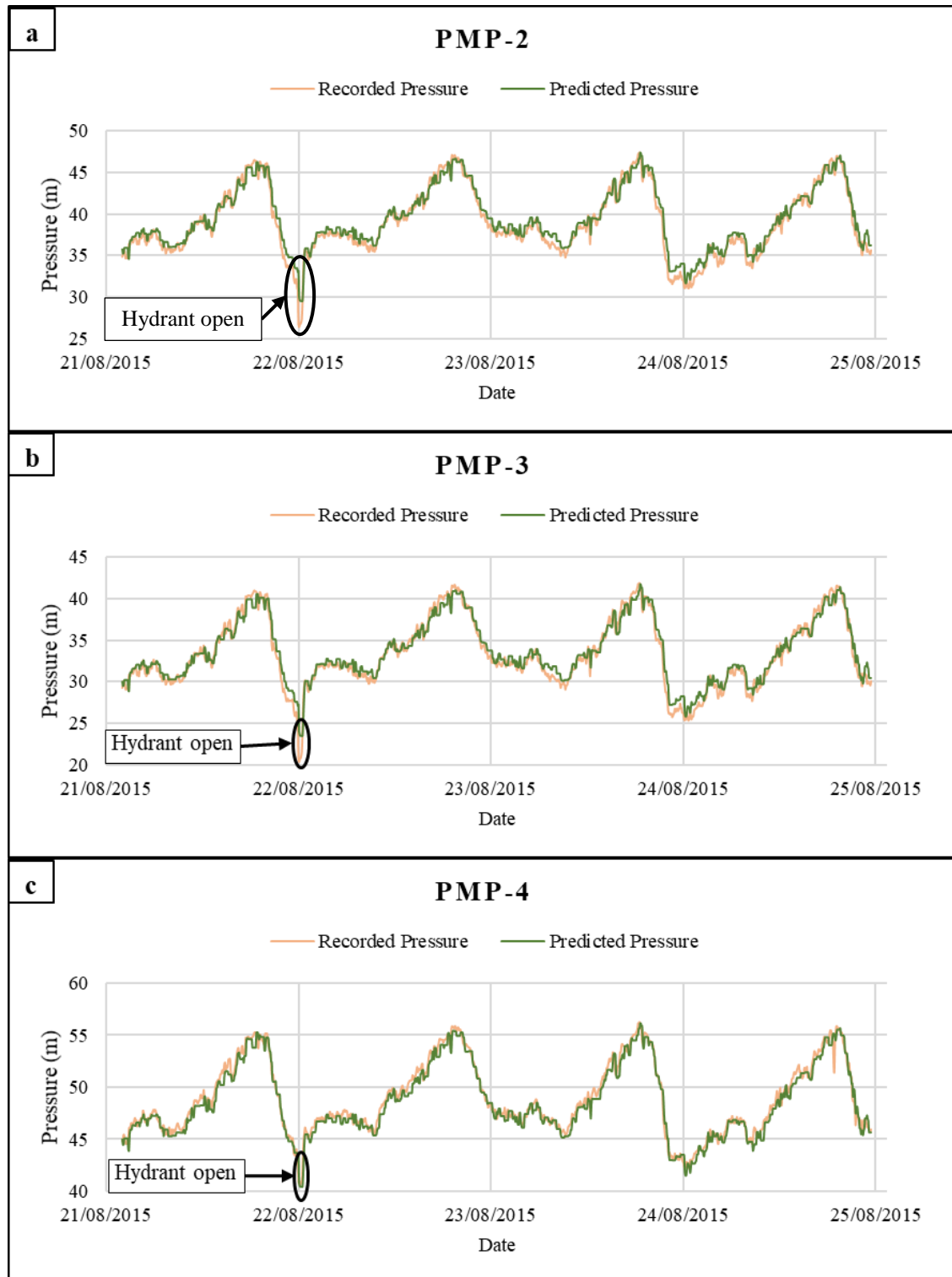
Figure 4.6. The comparison of the measured pressure with the predicted pressure at R=57
a) on PMP-2, b) on PMP-3, c) on PMP-4 (August 21-25, 2015)
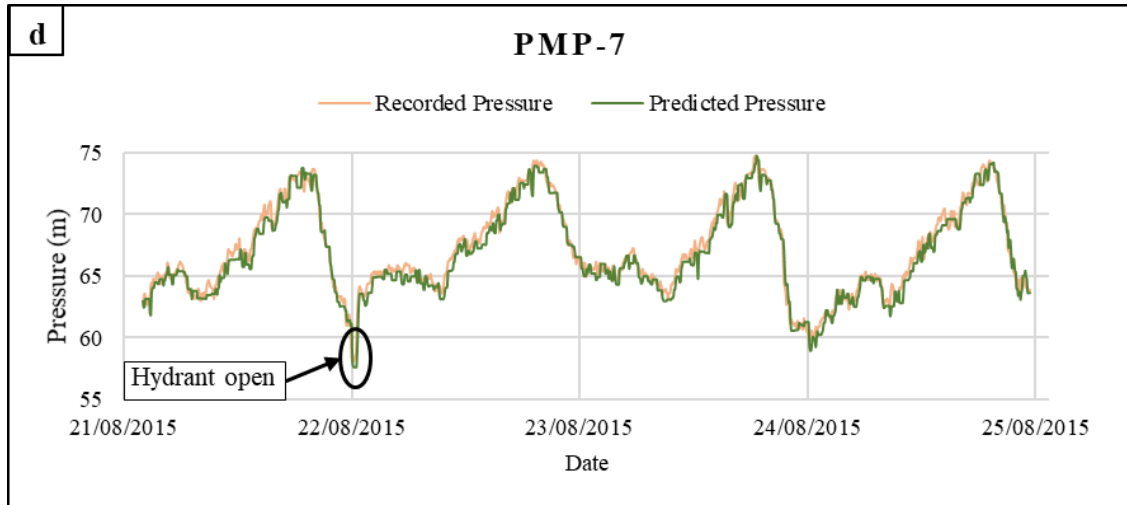
Figure 4.6. (Continued) The comparison of the measured pressure with the predicted pressure at R=57 d) on PMP-7 (August 21-25, 2015)

4.1.2. Calibrating the pipe roughness in the winter season

In the winter season, the pressure was measured at all PMPs. Table 4.3 and Figure 4.7 show the MAE of the difference between the predicted and the measured pressure on all PMPs while the trials of roughness coefficient are R= [50, 55, 60, 65, 70].

Table 4.3. The model predictions of of $C_{net}f$, average ($\Sigma Q_{(non-leakage)+(leakage)}$), average total distributed leakage rate, ε, and the pressure MAE against R= [50, 55, 60, 65, 70], (January 15-19, 2016)

| Roughness Coefficient	$C_{net}f$	Average ($\Sigma Q_{(non-leakage)+(leakage)}$) (m³/h)	Average total distributed leakage (m³/h)	ε (m³/h)	Pressure MAE (m)
50	0.3909	78.02	17.49	0.01	0.666
55	0.3873	78.02	17.49	0.01	0.444
60	0.3846	78.02	17.49	0.01	0.437
65	0.3824	78.02	17.49	0.01	0.531
70	0.3807	78.02	17.49	0.01	0.658
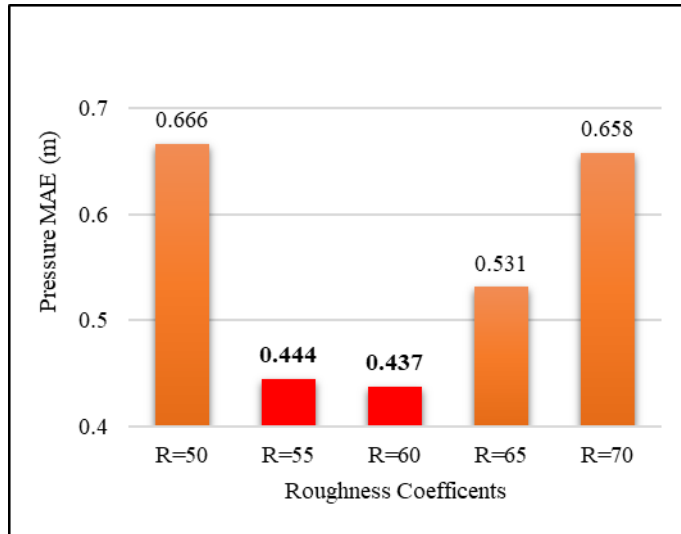
Figure 4.7. The pressure MAE at all PMPs against each trail of R= [50, 55, 60, 65, 70]. (January 15-19, 2016)

As shown in Figure 4.7, the least and the second least MAE are revealed on the roughness coefficients R= 55 and R= 60, respectively. So that the second stage of investigating the exact roughness coefficient has been performed on R= [55, 56, 57, 58, 59, 60] as shown in Table 4.4 and Figure 4.8.

Table 4.4. The model predictions of of $C_{net}f$, average ($\Sigma Q_{(non-leakage)+(leakage)}$), average total distributed leakage rate, ε, and the pressure MAE against R= [55, 56, 57, 58, 59, 60], (January 15-19, 2016)

Roughness Coefficient	$C_{net}f$	Average ∑ (leakage+ non-leakage flow) (m³/h)	Average total distributed leakage flow (m³/h)	ε (m³/h)	Pressure MAE (m)
55	0.3873	78.02	17.49	0.01	0.444
56	0.3867	78.02	17.49	0.01	0.427
57	0.3861	78.02	17.49	0.01	0.419
58	**0.3856**	**78.02**	**17.49**	**0.01**	**0.417**
59	0.3851	78.02	17.49	0.01	0.422
60	0.3846	78.02	17.49	0.01	0.437
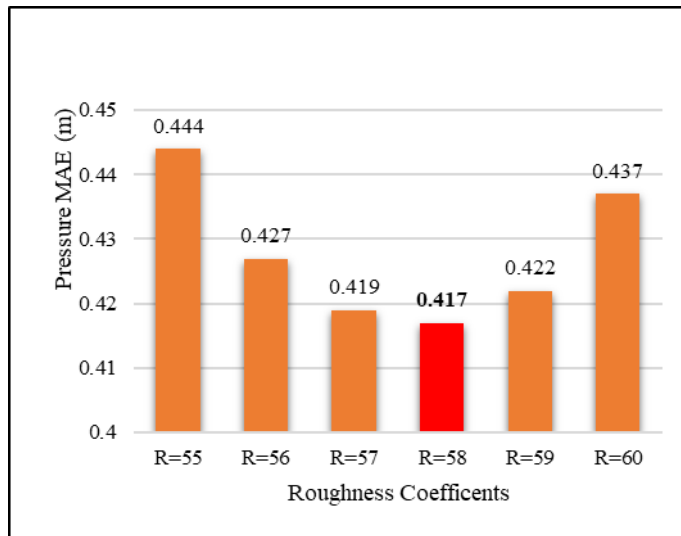
Figure 4.8. The pressure MAE at all PMPs against each trail of R= [55, 56, 57, 58, 59, 60]. (January 15-19, 2016)

The exactly calibrated value of roughness coefficient in winter season is R= **58** since it corresponds to the least pressure MAE. The roughness coefficients related to the least MAE at each PMP are presented in Figure 4.9.
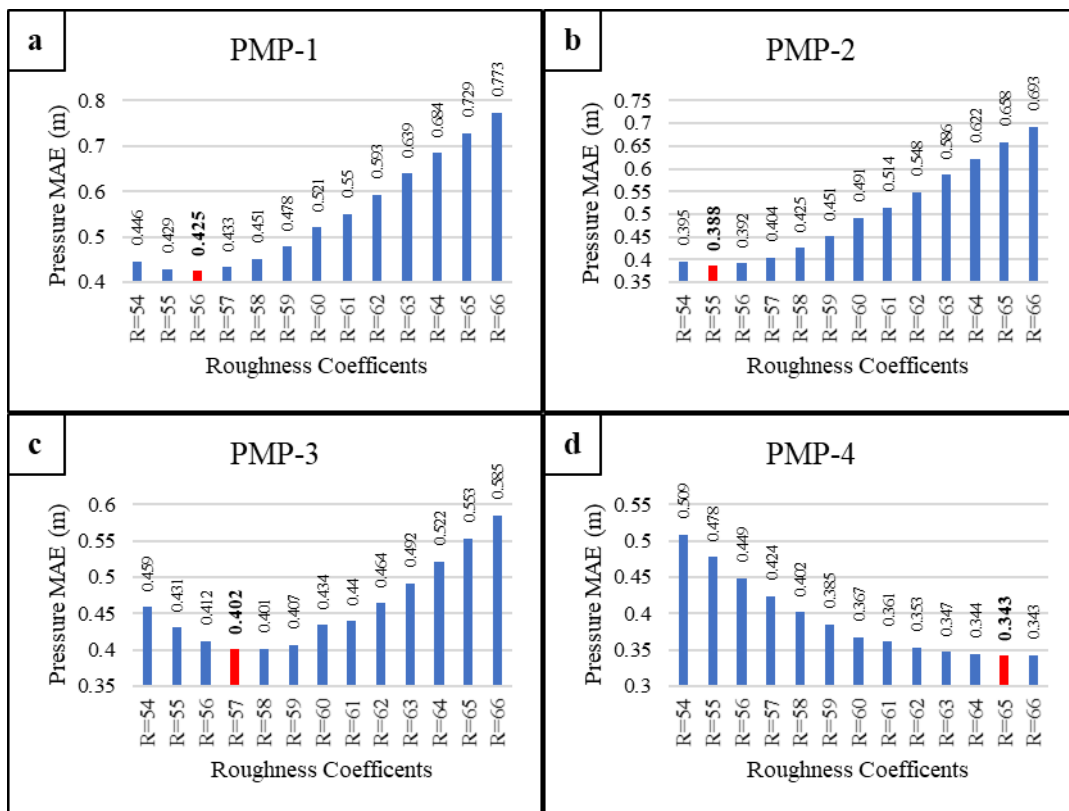
Figure 4.9. Against the range of trails R= [54 – 66], the MAE between the predicted and the measured pressure at a) PMP-1, b) PMP-2, c) PMP-3, d) PMP-4 (January 15-19, 2016)
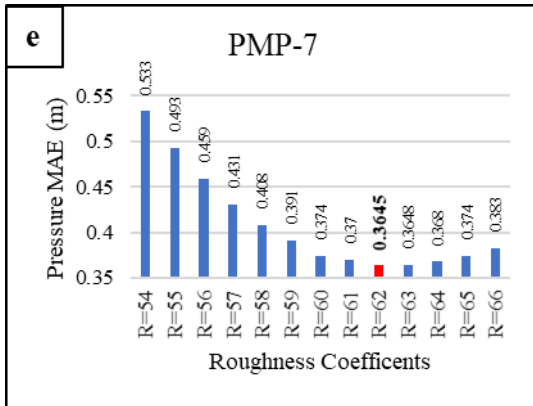
**Figure 4.9.** (Continued) Against the range of trails R= [54 – 66], the MAE between the predicted and the measured pressure at e) PMP-7 (January 15-19, 2016)

The non-fully fitted curve of $\Sigma Q_{(non\text{-}leakage)+(leakage)}$ with the measured system input flow is shown in Figure 4.10. The flow MAE has been calculated as 1.113 m^3/h while the RMSE has been calculated as 1.286 m^3/h. Figure 4.11 presents the total distributed leakage rate as it is predicted by the model versus the total non-leakage flow while the roughness coefficient is **58**. Figure 4.12 presents a comparison between the measured pressure and the predicted pressure at each PMP while the pipe roughness is **58**.
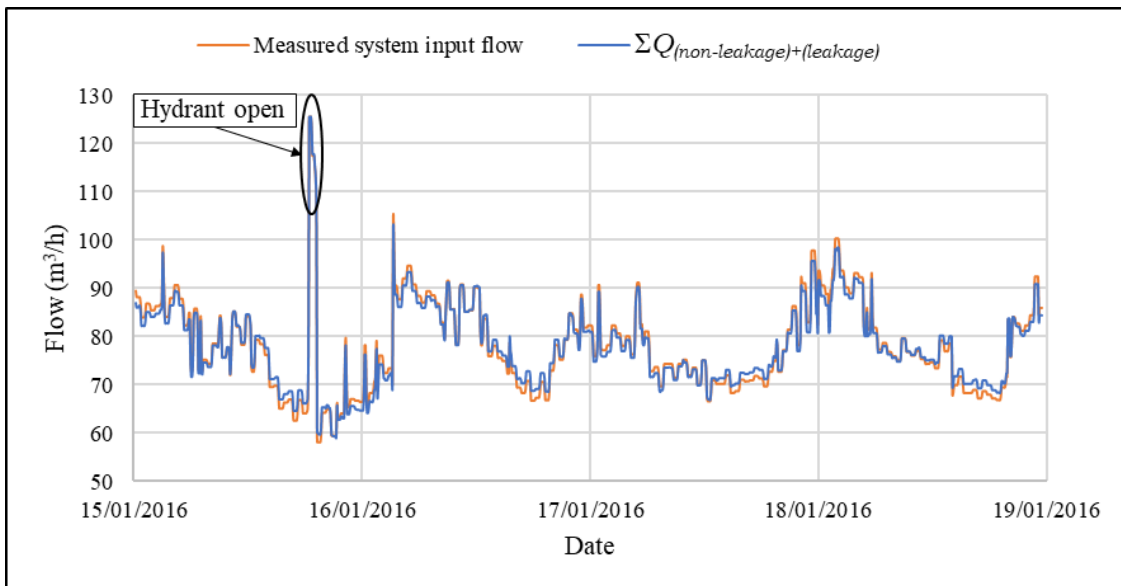
Figure 4.10. The measured system input flow vs. ($\Sigma Q_{(non\text{-}leakage)+(leakage)}$) at roughness R= 58, MAE = 1.113 m^3/h and RMSE = 1.286 m^3/h (January 15 - 19, 2016)
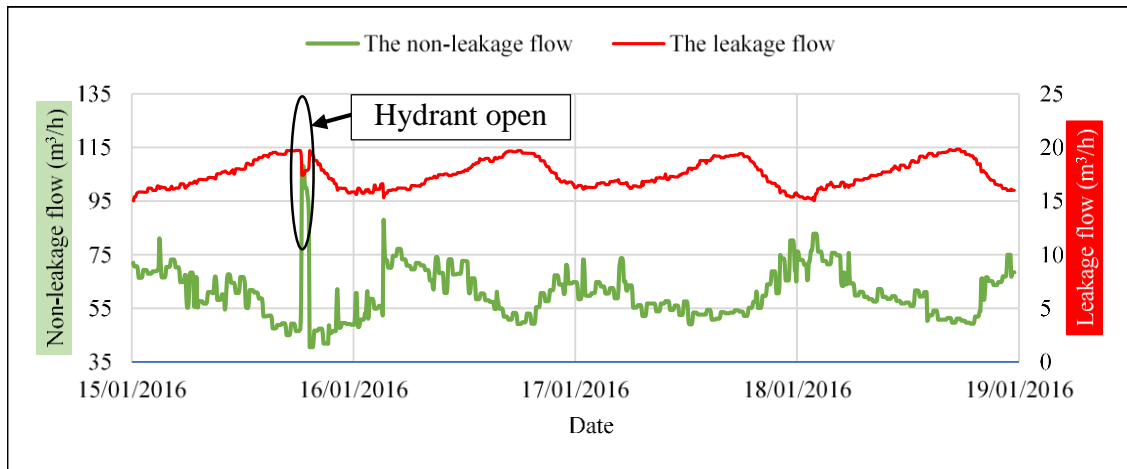
Figure 4.11. The network non-leakage flow vs. the total leakage rate as it is distributed by the model at roughness R= 58. (January 15 - 19, 2016)
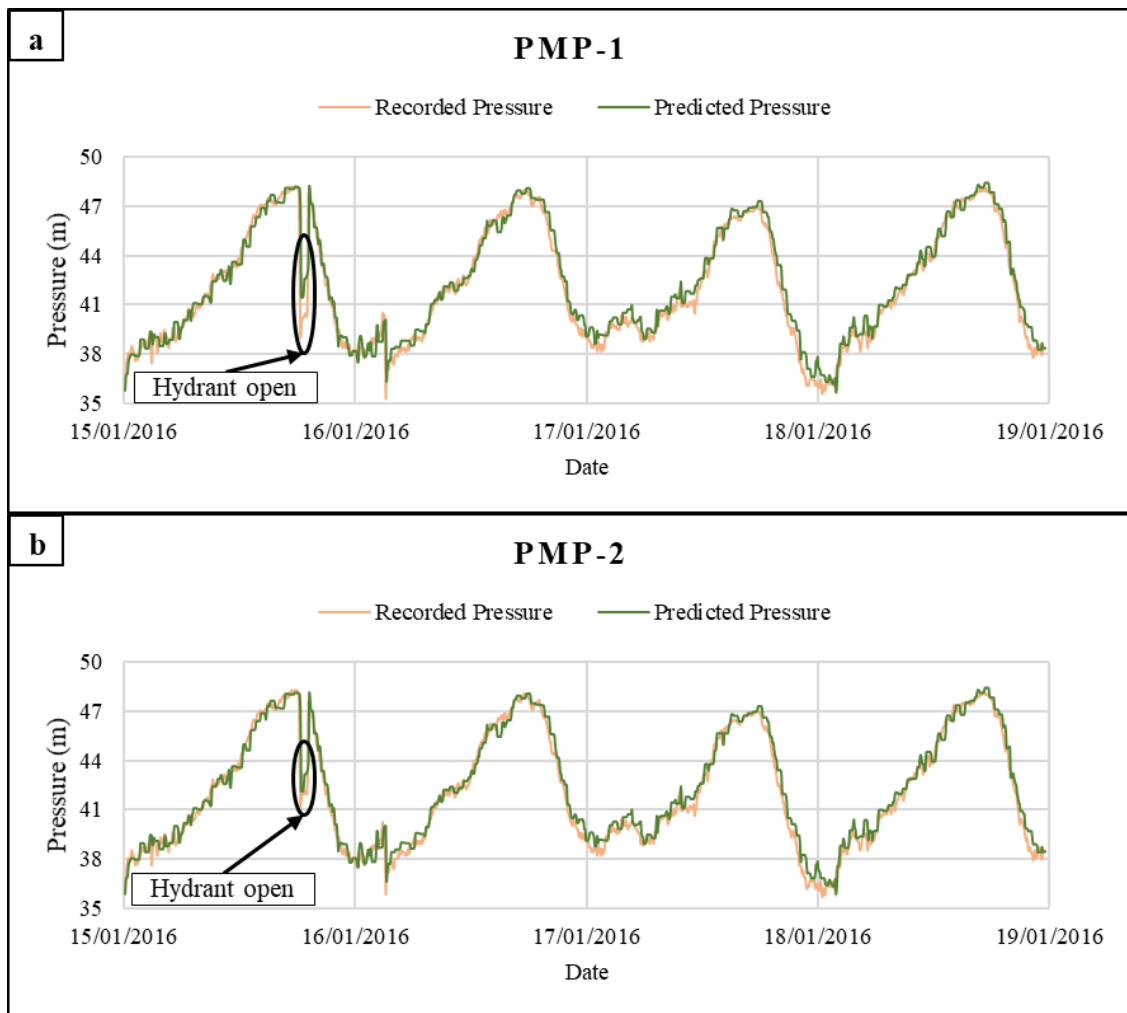
Figure 4.12. The comparison of the measured pressure with the predicted pressure at R=58 a) on PMP-1, b) on PMP-2 (January 14 - 19, 2016)

75
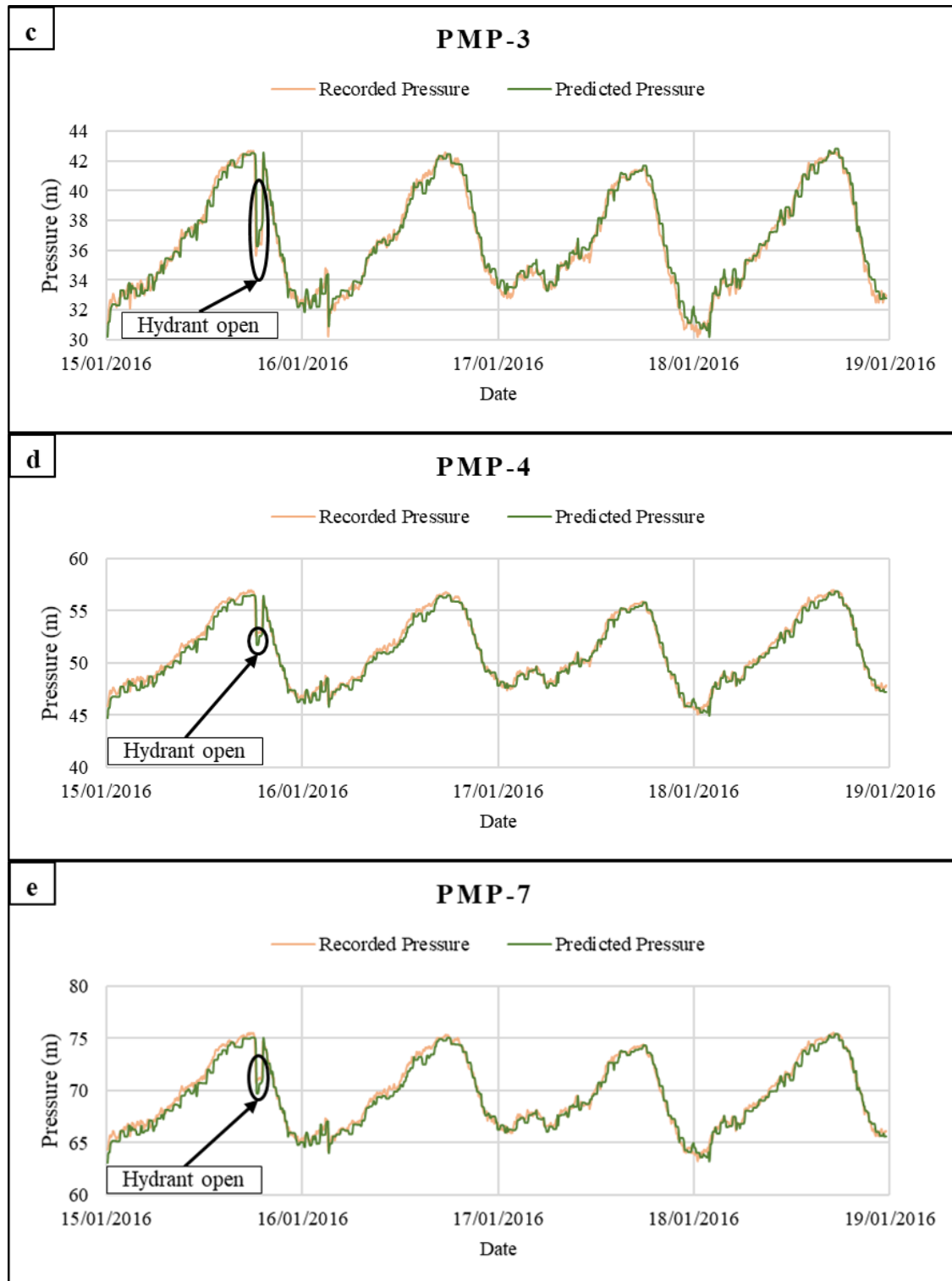
Figure 4.12. (Continued) The comparison of the measured pressure with the predicted pressure at R=58 c) on PMP-3, d) on PMP-4, e) on PMP-7 (January 14 - 19, 2016)

4.1.3. The calibrated pipe roughness coefficient of the PSA

The calibrated pipe roughness coefficient of Kaleiçi WDN which is resulted from the two simulation periods is considered as the weighted average of the calibrated roughness in summer and winter seasons. Considering the warming period of 24 hours, the number of pressure measurements at each PMP within summer and winter simulation periods are 1122 and 1144, respectively. The calibrated pipe roughness coefficient of Kaleiçi WDN has been calculated by equation (3.8) as:

$$R = \frac{57 * 1122 * 4 + 58 * 1144 * 5}{1122 * 4 + 1144 * 5} = 57.6$$

The verification process of the calibrated roughness is presented in the next section.

4.2. Verifying The Calibrated Pipe Roughness Coefficient of PSA

In verification of the calibrated roughness, $\Sigma Q_{(non\text{-}leakage)+(leakage)}$ is not fully fitted with the curve of the measured system input flow is shown in Figure 4.13. The flow MAE has been calculated as 1.962 m³/h and the RMSE has been calculated as 2.204 m³/h. The total distributed leakage rate as it is predicted by the model versus the total non-leakage flow, while the roughness coefficient is **57.6**, are presented in Figure 4.14. Figure 4.15 presents a comparison between the measured pressure and the predicted pressure at each PMP while the pipe roughness is R= 57.6.
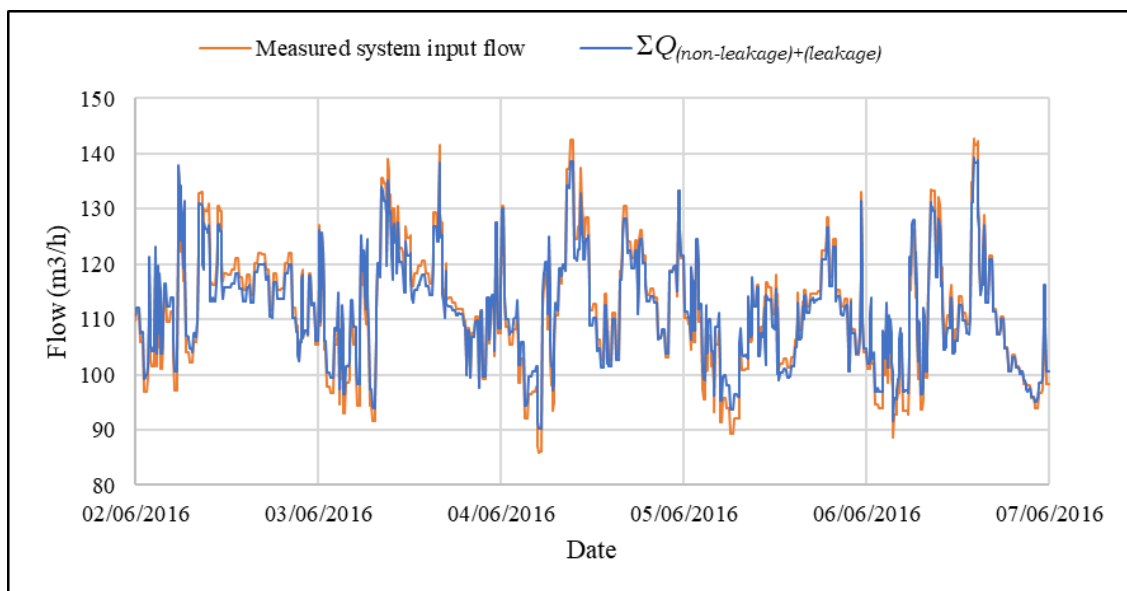
**Figure 4.13.** The measured system input flow vs. $\Sigma Q_{(non\text{-}leakage)+(leakage)}$ at roughness R= 57.6, MAE = 1.962 m³/h and RMSE = 2.204 m³/h (June 1 – 6, 2016)
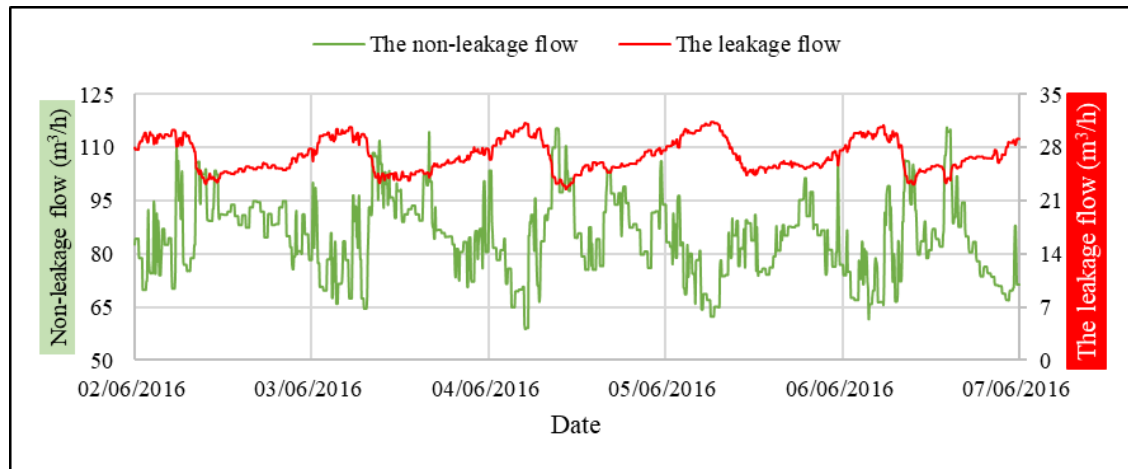
Figure 4.14. The network non-leakage flow vs. the total leakage rate as it is distributed by the model at roughness R= 57.6, (June 1 - 6, 2016)
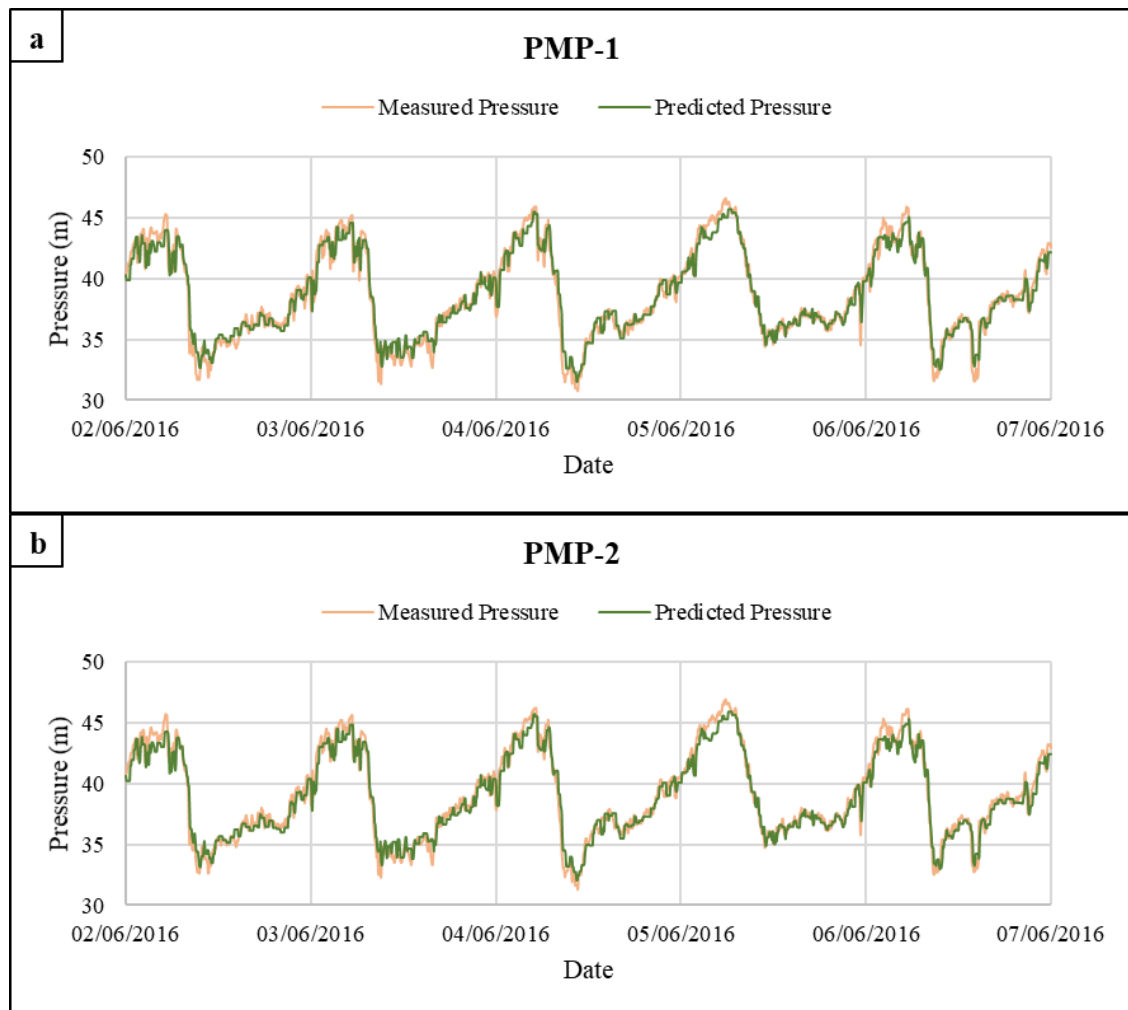

Figure 4.15. The comparison of the measured pressure with the predicted pressure at R=57.6 a) on PMP-1, b) on PMP-2 (June 1 - 6, 2016)
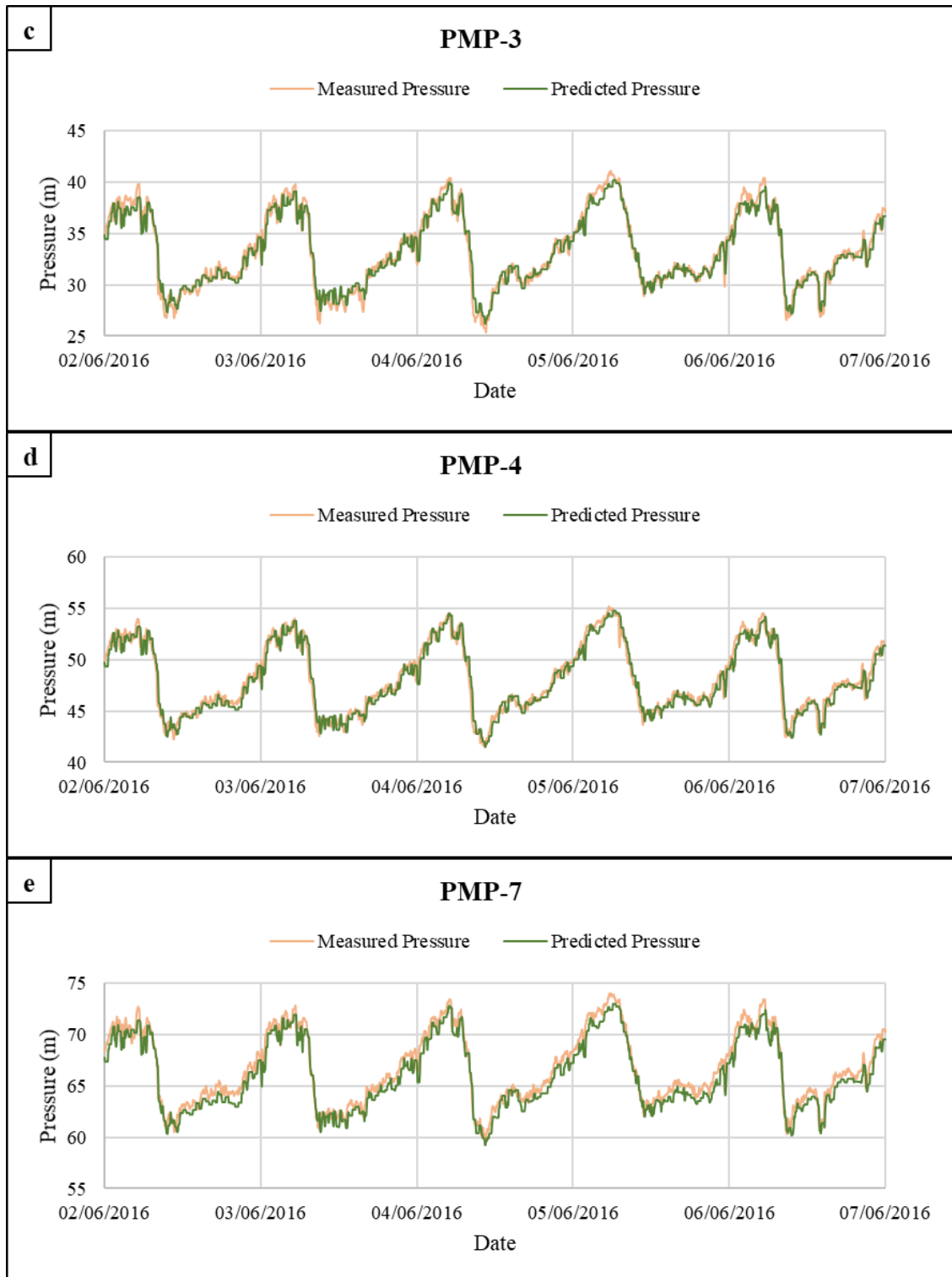
Figure 4.15. (Continued) The comparison of the measured pressure with the predicted pressure at R=57.6 c) on PMP-3, d) on PMP-4, e) on PMP-7 (June 1 - 6, 2016)

Applying the calibrated roughness (R= 57.6), the model determination of $C_{net}f$, the average $\Sigma Q_{(non\text{-}leakage)+(leakage)}$, average total leakage flow, ε, and the MAE of the difference between the measured pressure and the predicted pressure at all PMPs are

presented in Table 4.5. The MAE of pressure against R= 57.6 is acceptable for the model, therefore, the roughness coefficient of **57.6** is verified for the hydraulic modeling of Kaleiçi WDN.

Table 4.5. Against R= 57.56, The model predictions of C_{net}^f, average $\Sigma Q_{(non-leakage)+(leakage)}$, average total distributed leakage flow, ε, and the pressure MAE, (June 1 – 6, 2016)

Parameter	Model determination
C_{net}^f	0.634
Average $\Sigma Q_{(non-leakage)+(leakage)}$ (m^3/h)	111.55
Average total distributed leakage flow (m^3/h)	26.93
ε (m^3/h)	0.060
Pressure MAE (m)	0.659

4.3. Discussing The Calibration and Verification of Roughness Coefficient

A common result appeared during calibrating and verifying the pipe roughness coefficients of Kaleiçi WDN that the model predictions of $\Sigma Q_{(non-leakage)+(leakage)}$ is not fully fitted with the measured system input flow. That is due to the assumption that leakage is uniformly distributed by the pipe length, while it is not in reality.

It is found in the first stage of calibration process in summer and winter simulation periods that the least and the second least pressure MAE was revealed at R= 55 and R= 60, respectively. In the second stage, the calibrated roughness coefficient which reveals the least pressure MAE during summer and winter simulation period has been found in the range R= [55 - 60]. Thus, it was not necessary to investigate the calibrated roughness outside this range.

Although the roughness coefficient (R=57.6) has been verified for modeling Kaleiçi WDN by showing acceptable MAE, it has not revealed the least pressure MAE. Figure 4.16 shows that the least pressure MAE of all PMPs is revealed at roughness coefficient of R=60 during the simulation period of the verification process. But the MAE against R=57.6 still acceptable.
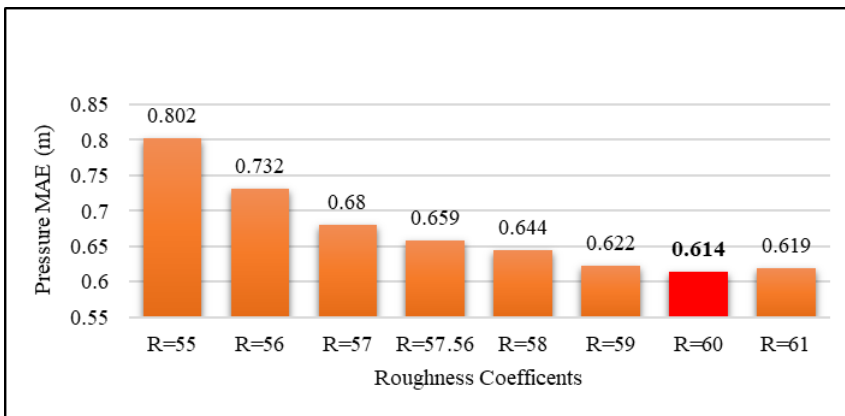

Figure 4.16. The MAE between the predicted and the measured pressure at all PMPs against each trail of R= [55, 56, 57, 57.56, 58, 59, 60, 61]. (June 1 – 6, 2016)

4.4. Applying Advanced PM

The closed loop pressure control as an advanced PM technique has been applied on the WDN in the PSA during summer and winter simulation periods.

4.4.1. In the summer season (August 21 – 25, 2015)

For the summer season, the model determined the location of the CP which has the least predicted pressure in Kaleiçi WDN as illustrated in Figure 4.17 at node number 270, CP (P270). The predicted pressure at the CP (P270), the predicted excess pressure, and the minimum allowable pressure (20 m) prior to advanced PM application are shown in Figure 4.18. The predicted pressure downstream of PRV versus the pressure measured upstream of PRV at the inlet of Kaleiçi WDN are presented in Figure 4.19. Figure 4.20 shows the predicted broken pressure by the PRV at the inlet.
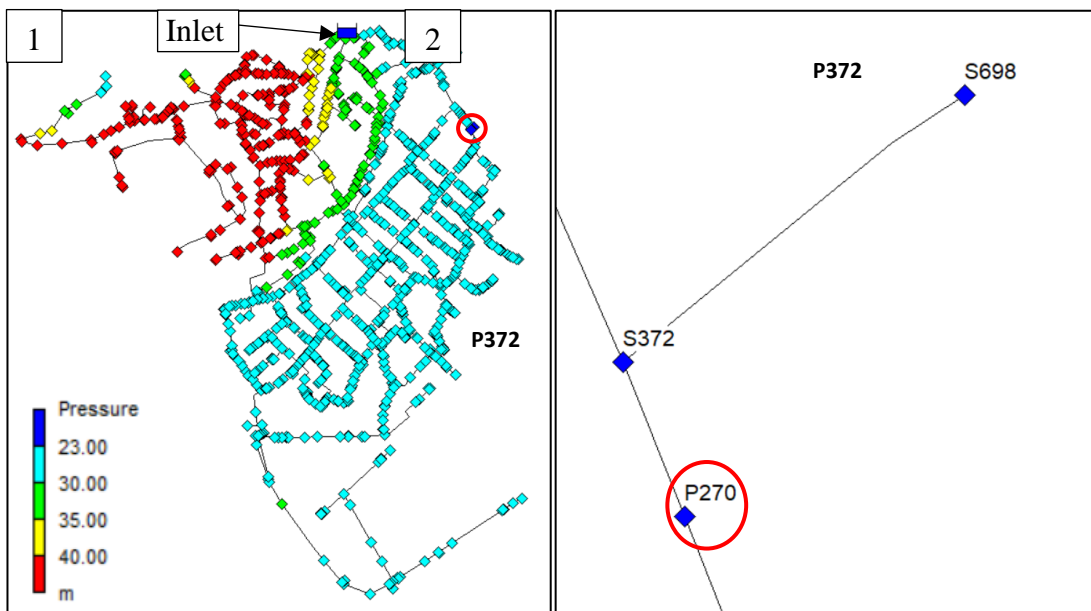
Figure 4.17. The location of the CP related to the least predicted pressure in the PSA during summer season. CP (P270), on 22.08.2015 at 10:45 – 11:00 AM; min. pressure = 22.91 m, system input flow = 177.5 m^3/h and pressure upstream PRV = 31.93 m
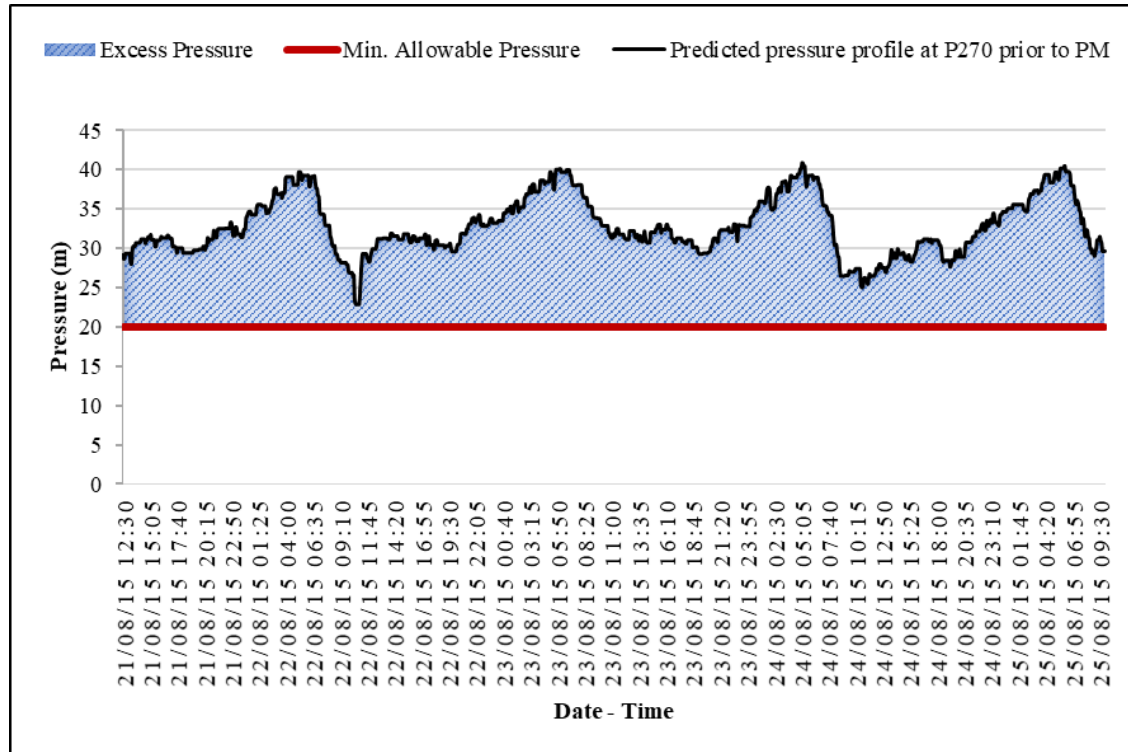
Figure 4.18. The predicted pressure at the CP (P270), the predicted excess pressure, and the minimum allowable pressure level prior to advanced PM application, (August 21-25, 2015)
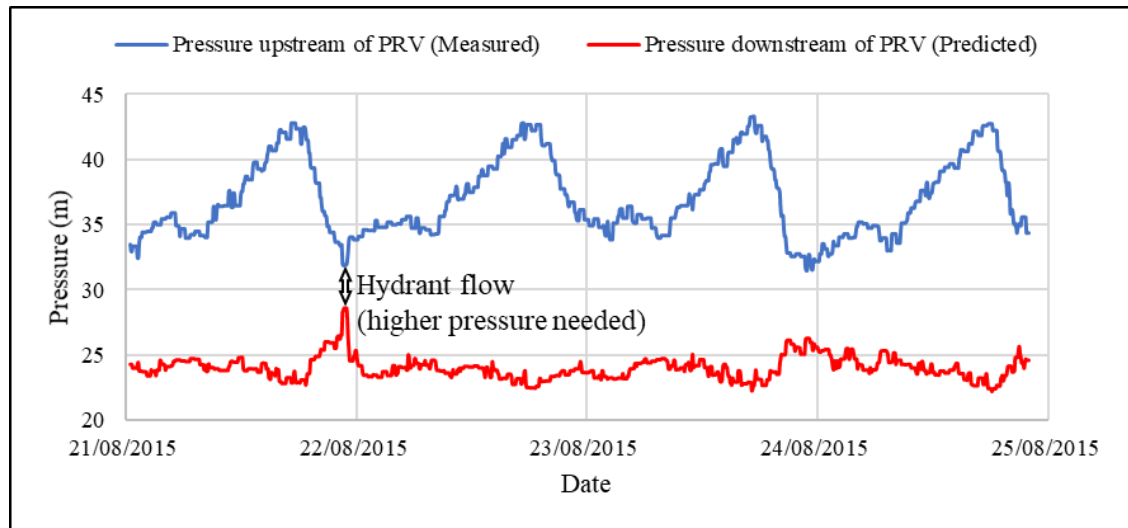
Figure 4.19. The pressure measured upstream of PRV vs. the predicted pressure downstream of PRV (August 21 - 25, 2015)
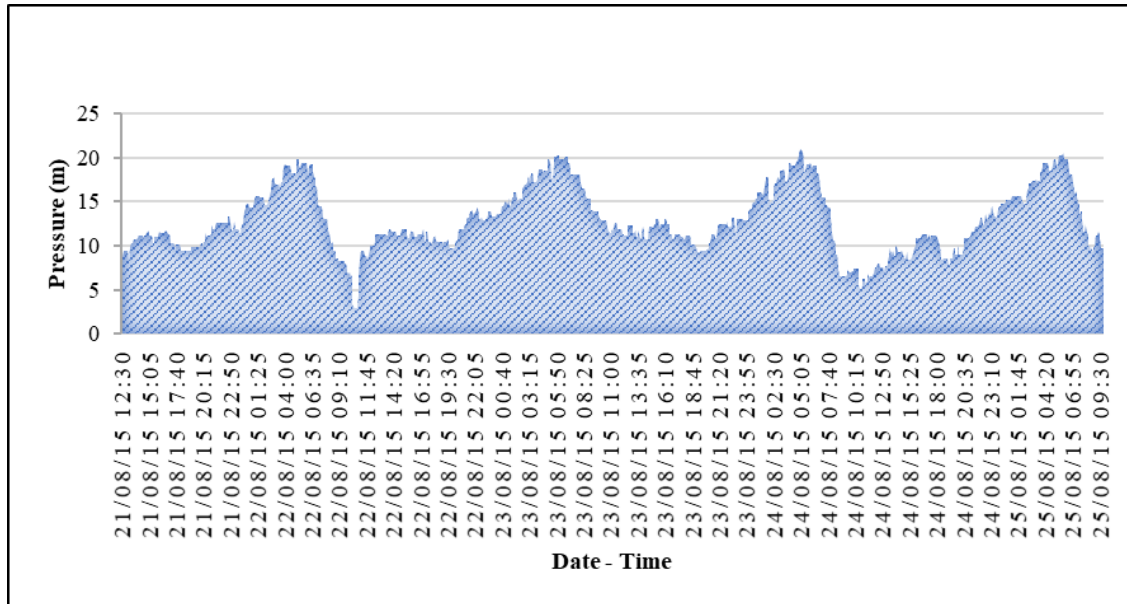
Figure 4.20. The predicted broken pressure by the PRV. (August 21-25, 2015)

The maximum predicted pressure at all nodes before and after applying the advanced PM in the summer season is shown in Figure 4.21. The maximum pressure was predicted as 79.91 m at node (P253) before applying advanced PM, while the maximum predicted pressure at (P253) after applying advanced PM is 60 m. The predicted reduction of the average network pressure and average leakage due to advanced PM application within the summer simulation period are summarized in Table 4.6.
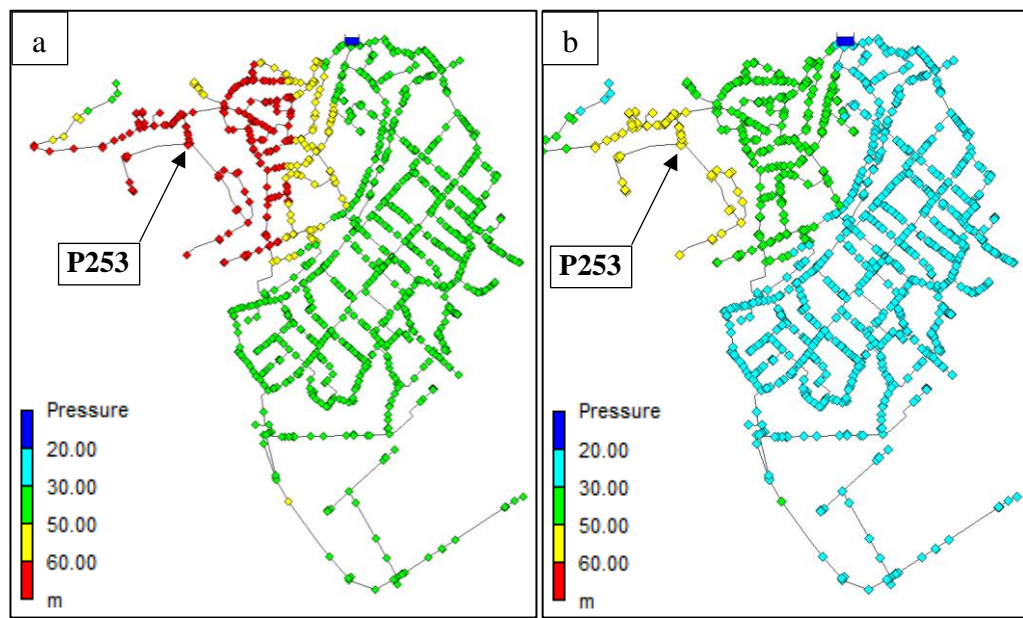
Figure 4.21. The maximum predicted pressure at all nodes in Kaleiçi WDN a) before advanced PM application, b) after advanced PM application during summer simulation period

Table 4.6. The predicted average network pressure reduction and average leakage reduction in Kaleiçi WDN during the summer simulation period. (August 21-25, 2015)

Status		Before Advanced PM Application	After Advanced PM Application
Average Network Pressure (m)		41.2	28.6
Average Pressure reduction (m)		12.6	
Min. Network Pressure (m)		22.91	20
Min. Pressure reduction (m)		2.91	
Max. Network Pressure (m)		79.91	60
Max. Pressure reduction (m)		19.91	
Average $\Sigma Q_{(non\text{-}leakage)+(leakage)}$ (m^3/h)		109.47	102.65
Average Leakage Reduction	m^3/h	6.82	
	m^3/month	5074.08	

4.4.2. In the winter season (January 15 – 19, 2015)

To apply advanced PM during winter simulation period, the model determined the location of the CP which has the least predicted pressure in Kaleiçi WDN as illustrated in Figure 4.22 at node number 704, CP (P704). The predicted pressure at the CP (P704), the predicted excess pressure, and the minimum allowable pressure (20 m) prior to advanced PM application are shown in Figure 4.23. The predicted pressure downstream of PRV versus the pressure measured upstream of PRV at the inlet of Kaleiçi WDN are presented in Figure 4.24. Figure 4.25 shows the predicted broken pressure by the PRV at the inlet.
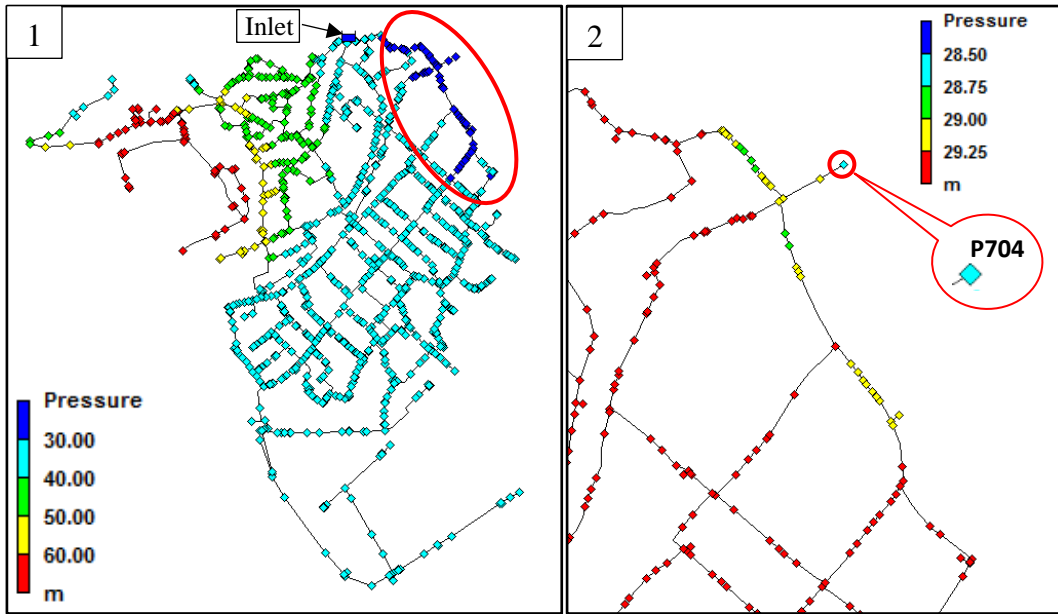
Figure 4.22. The location of the CP related to the least predicted pressure in the PSA during winter season. CP (P704), on 15.01.2016 at 12:00 AM; min. pressure = 28.86 m, system input flow = 89.44 m^3/h and pressure upstream PRV = 32.05 m
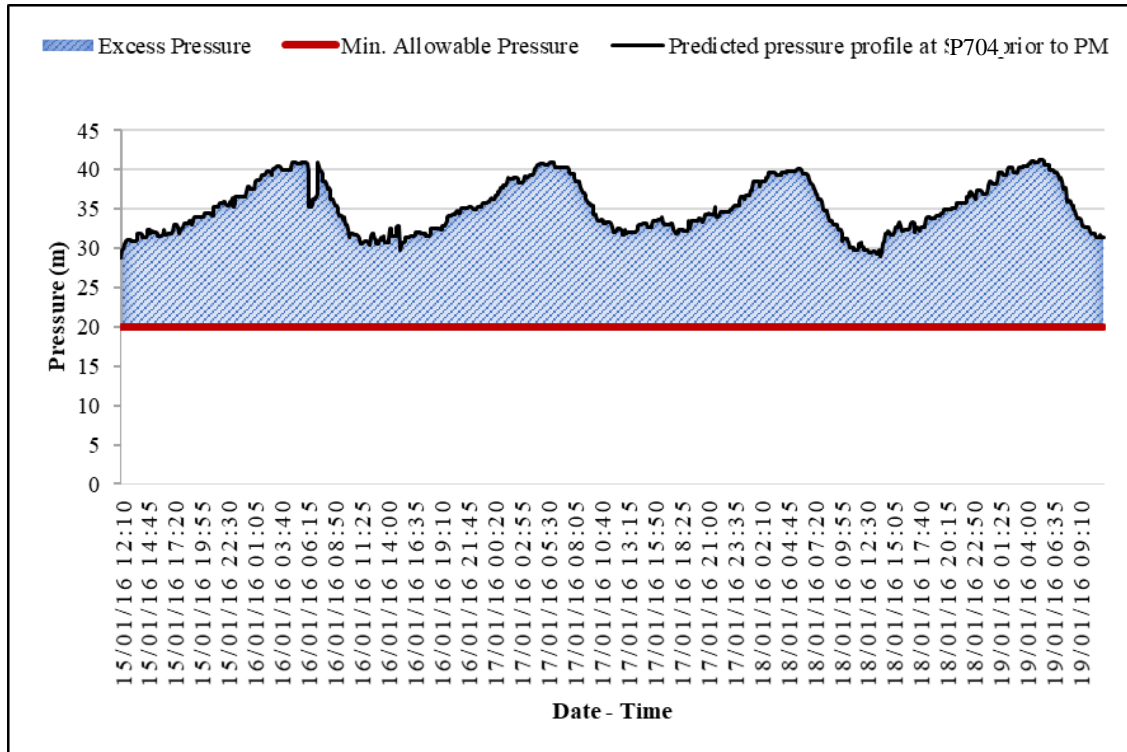
Figure 4.23. The predicted pressure at the CP (P704), the predicted excess pressure, and the minimum allowable pressure level prior to advanced PM application, (January 15 - 19, 2016)
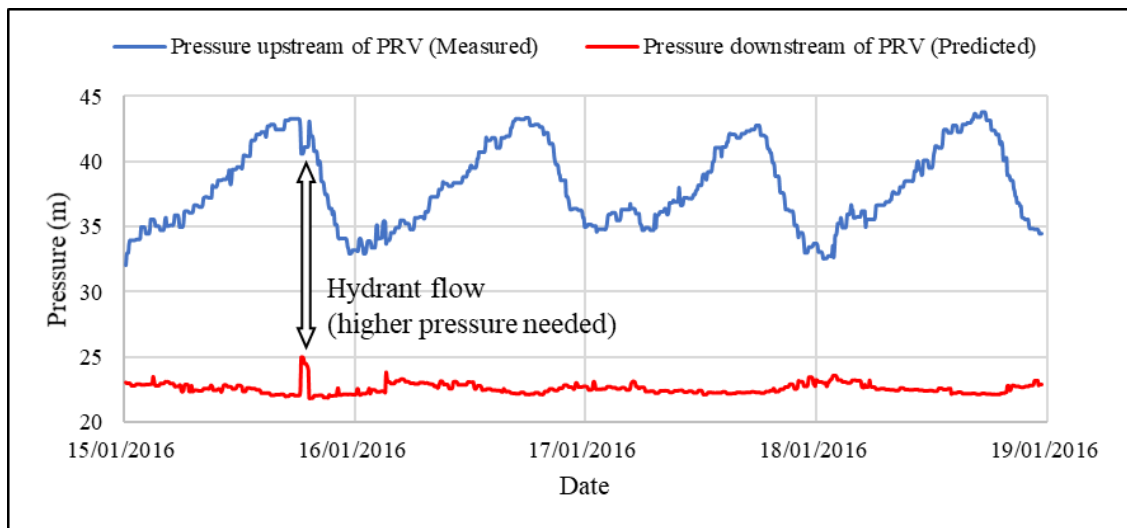

Figure 4.24. The pressure measured upstream of PRV vs. the predicted pressure downstream of PRV (January 14 - 19, 2016)

85
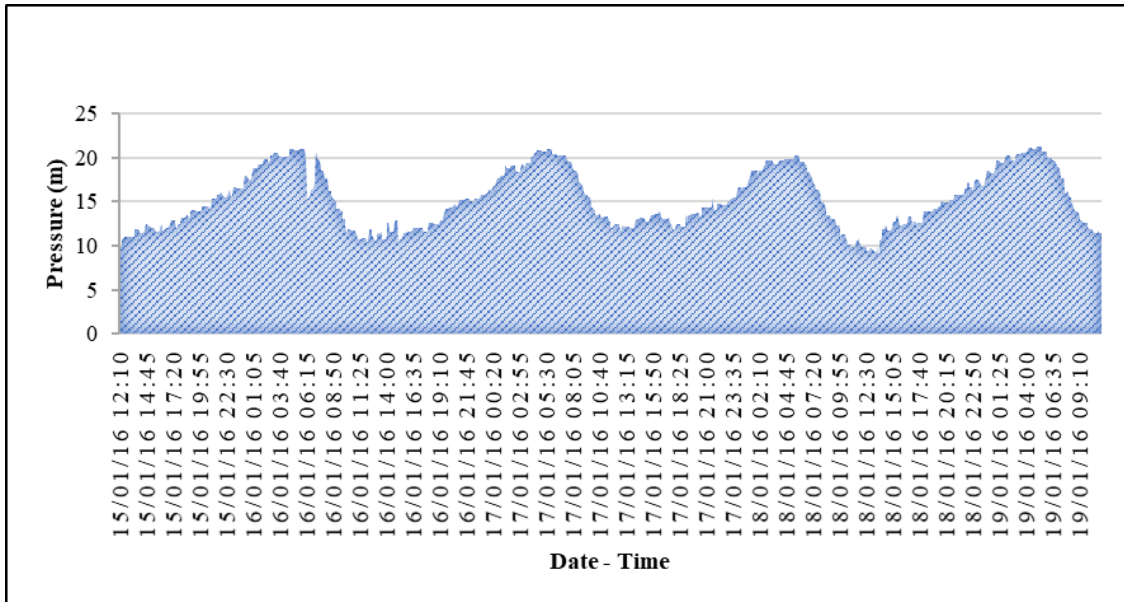
Figure 4.25. The predicted broken pressure by the PRV. (January 15-19, 2016)

The maximum predicted pressure at all nodes before and after applying the advanced PM in the winter season is shown in Figure 4.26. The maximum pressure was predicted as 80.61 m at node (P253) before applying advanced PM, while the maximum predicted pressure at (P253) after applying advanced PM is 59.91 m. The predicted reduction of the average network pressure and average leakage due to advanced PM application within the winter simulation period are summarized in Table 4.7.
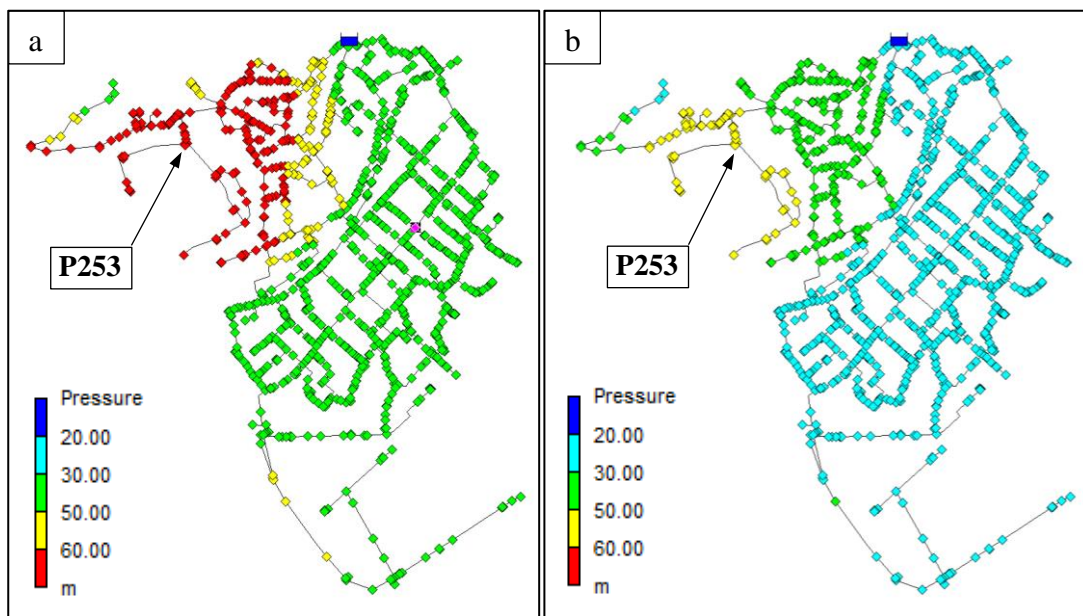
Figure 4.26. The maximum predicted pressure at all nodes in Kaleiçi WDN a) before advanced PM application, b) after advanced PM application during winter simulation period

Table 4.7. The predicted average network pressure reduction and average leakage reduction in Kaleiçi WDN during the winter simulation period. (January 15-19, 2016)

Status		Before Advanced PM Application	After Advanced PM Application
Average Network Pressure (m)		43.77	28.87
Average Pressure reduction (m)		14.9	
Min. Network Pressure (m)		28.86	20
Min. Pressure reduction (m)		8.86	
Max. Network Pressure (m)		80.61	59.91
Max. Pressure reduction (m)		20.7	
Average $\Sigma Q_{(non-leakage)+(leakage)}$ (m³/h)		78.01	72.22
Average Leakage Reduction	m³/h	5.79	
	m³/month	4307.76	

4.5. The Effect of Changing Non-Leakage Flow By ±%25 on The Leakage Rate

The impact of changing the non-leakage flow by ±25% on the flow of leakage in Kaleiçi WDN during the summer and the winter simulation periods are shown in Figure 4.19 and Figure 4.20, respectively. As presented in the figures, the less non-leakage flow the more leakage rate found in the WDN in the PSA.
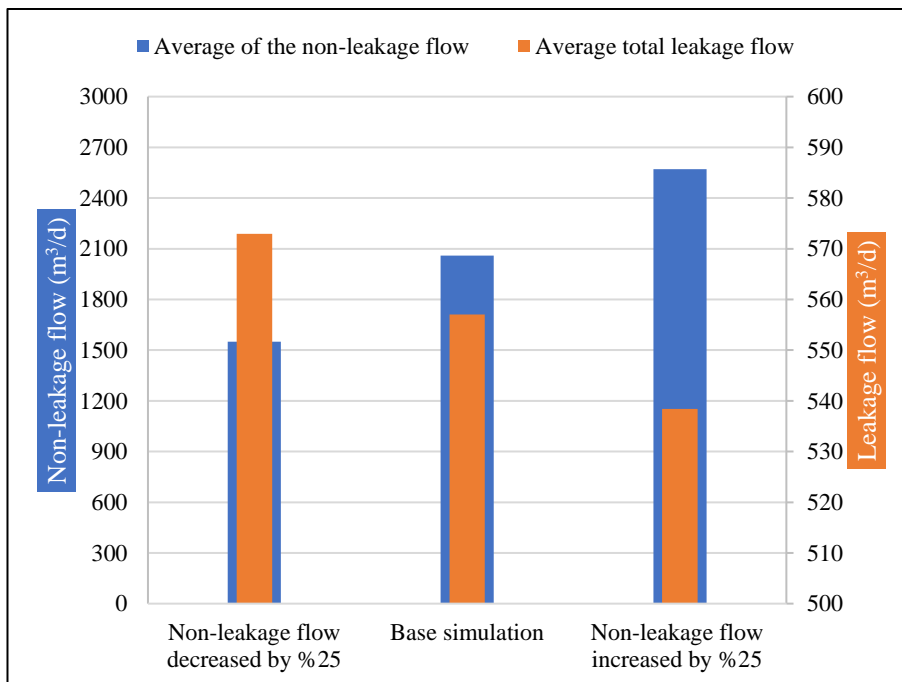
Figure 4.27. The effect of changing the non-leakage flow by ±25% on the leakage rate in Kaleiçi WDN during the summer season (August 21 – 25, 2015)
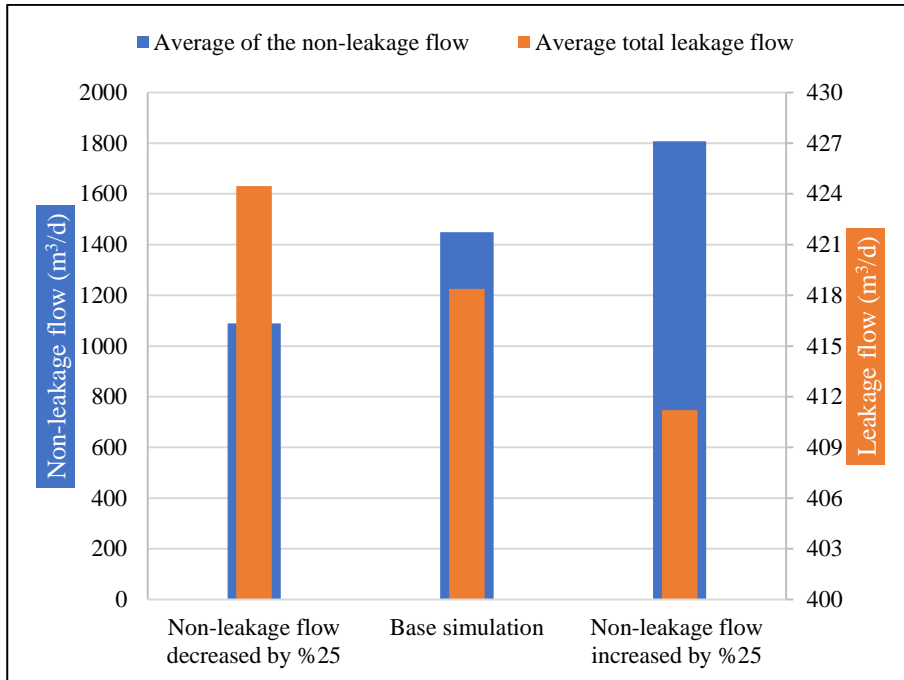
Figure 4.28. The effect of changing the non-leakage flow by ±25% on the leakage rate in Kaleiçi WDN during the winter season (January 15 – 19, 2016)

4.6. Advanced PM Application on Changing The Non-Leakage Flow by ±%25 in Summer Season

Advanced PM has been applied on each assumption of changing the non-leakage flow by ±25% during the summer simulation period as follows:

4.6.1. Assuming a reduction of the non-leakage flow by %25

The model determined the location of the CP which has the least predicted pressure in Kaleiçi WDN as illustrated in Figure 4.29 at node number 704, CP (P704). The predicted pressure at the CP (P704), the predicted excess pressure, and the minimum allowable pressure (20 m) prior to advanced PM application are shown in Figure 4.30. The predicted pressure downstream of PRV versus the pressure measured upstream of PRV at the inlet of Kaleiçi WDN are presented in Figure 4.31. Figure 4.32 shows the predicted broken pressure by the PRV.
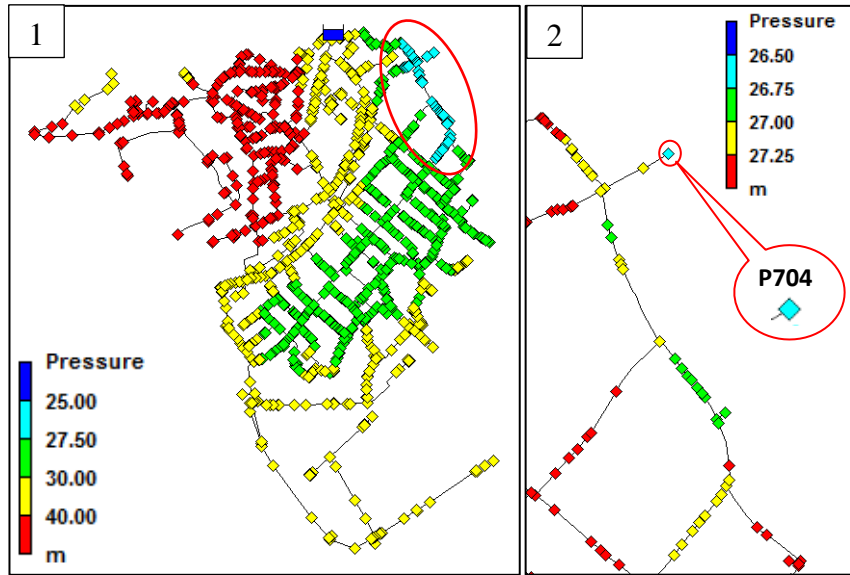
Figure 4.29. The location of the CP related to the least predicted pressure in the PSA (assuming -25% decrease of non-leakage flow) during summer season. CP (P704), on 22.08.2015 at 10:45 – 11:00 AM; min. pressure = 26.07 m, $\Sigma Q_{(75\% \times non\text{-}leakage)+(leakage)}$= 135.4 m^3/h and pressure upstream PRV = 31.93 m
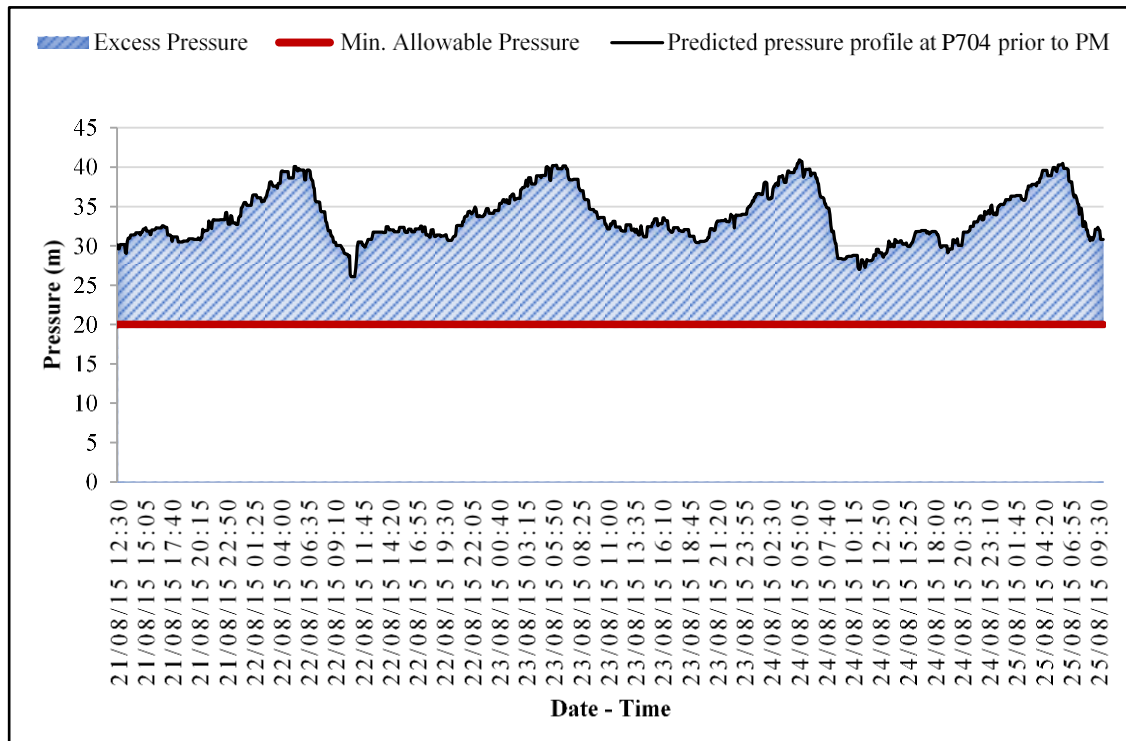
Figure 4.30. The predicted pressure at the CP (P704), the predicted excess pressure, and the minimum allowable pressure level prior to advanced PM application, assuming -25% decrease of non-leakage flow. (August 21-25, 2015)
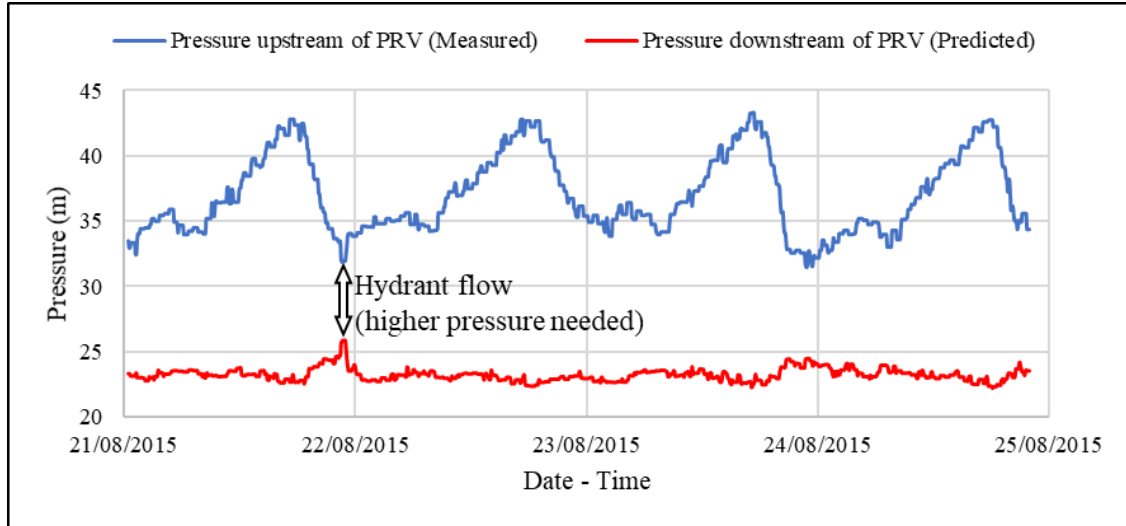
Figure 4.31. The pressure measured upstream of PRV vs. the predicted pressure downstream of PRV, assuming -25% decrease of non-leakage flow. (August 21 - 25, 2015)
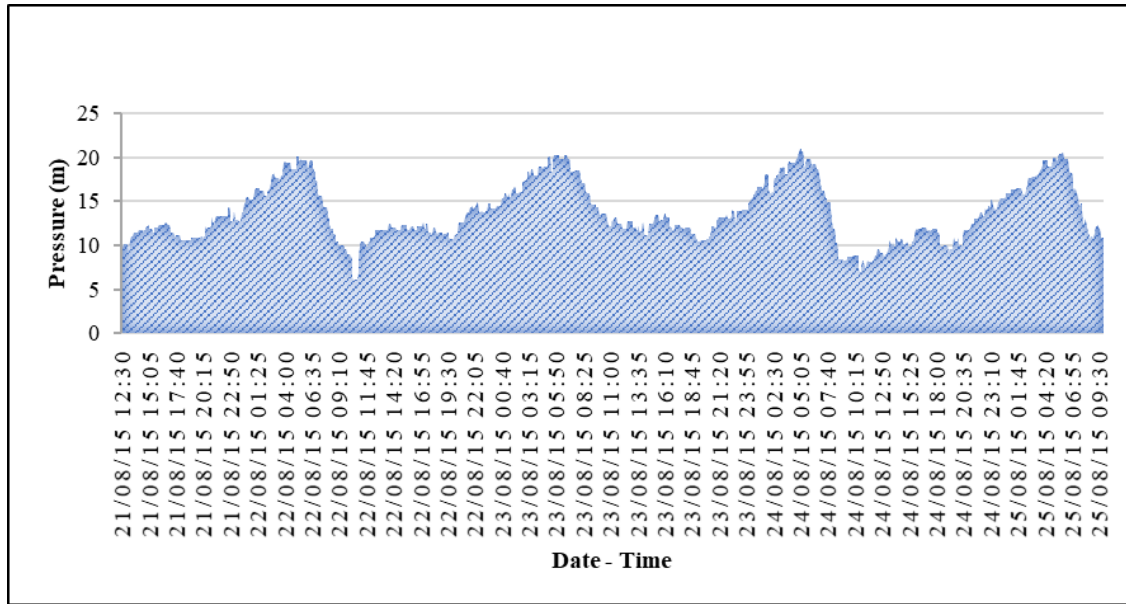
Figure 4.32. The predicted broken pressure by the PRV, assuming -25% reduction of the non-leakage flow. (August 21-25, 2015)

Assuming non-leakage reduction by 25%, the maximum predicted pressure at all nodes before and after applying the advanced PM is presented in Figure 4.33. The maximum pressure was predicted as 80.29 m at node (P253) before applying advanced PM, while the maximum predicted pressure at (P253) after applying advanced PM is 59.9 m. The predicted reduction of the average network pressure and average leakage due to advanced PM application are presented in Table 4.8.
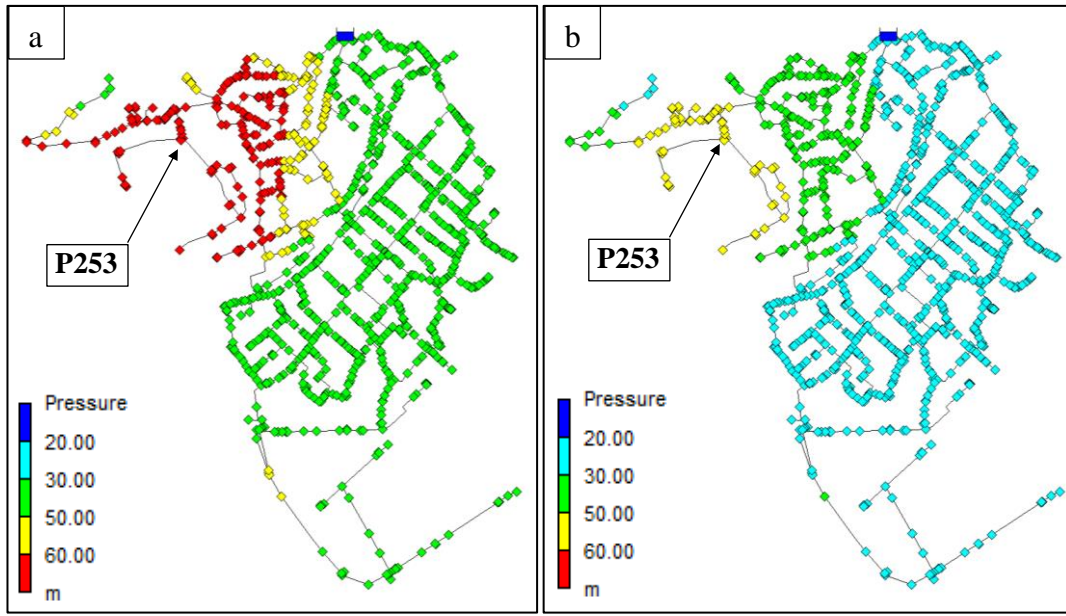
Figure 4.33. The maximum predicted pressure at all nodes in Kaleiçi WDN a) before advanced PM application, b) after advanced PM application, assuming -25% reduction of the non-leakage flow. (August 21-25, 2015)

Table 4.8. The predicted average network pressure reduction and the average leakage reduction, assuming -25% reduction of the non-leakage flow, (August 21 - 25, 2015)

Status		Before Advanced PM Application	After Advanced PM Application
Average Network Pressure (m)		42.35	28.92
Average Pressure reduction (m)		13.43	
Min. Network Pressure (m)		26.07	20
Min. Pressure reduction (m)		6.07	
Max. Network Pressure (m)		80.29	59.9
Max. Pressure reduction (m)		20.39	
Average $\Sigma Q_{(75\% \times non\text{-}leakage)+(Leakage)}$ (m³/h)		88.74	81.44
Average Leakage Reduction	m³/h	7.3	
	m³/month	5431.2	

4.6.2. Assuming an increase of the non-leakage flow by %25

In this assumption, the predicted pressure at many junctions in Kaleiçi WDN were below the minimum allowable pressure of 20 m (Figure 4.34). Therefore, advanced PM is not applicable in this situation.
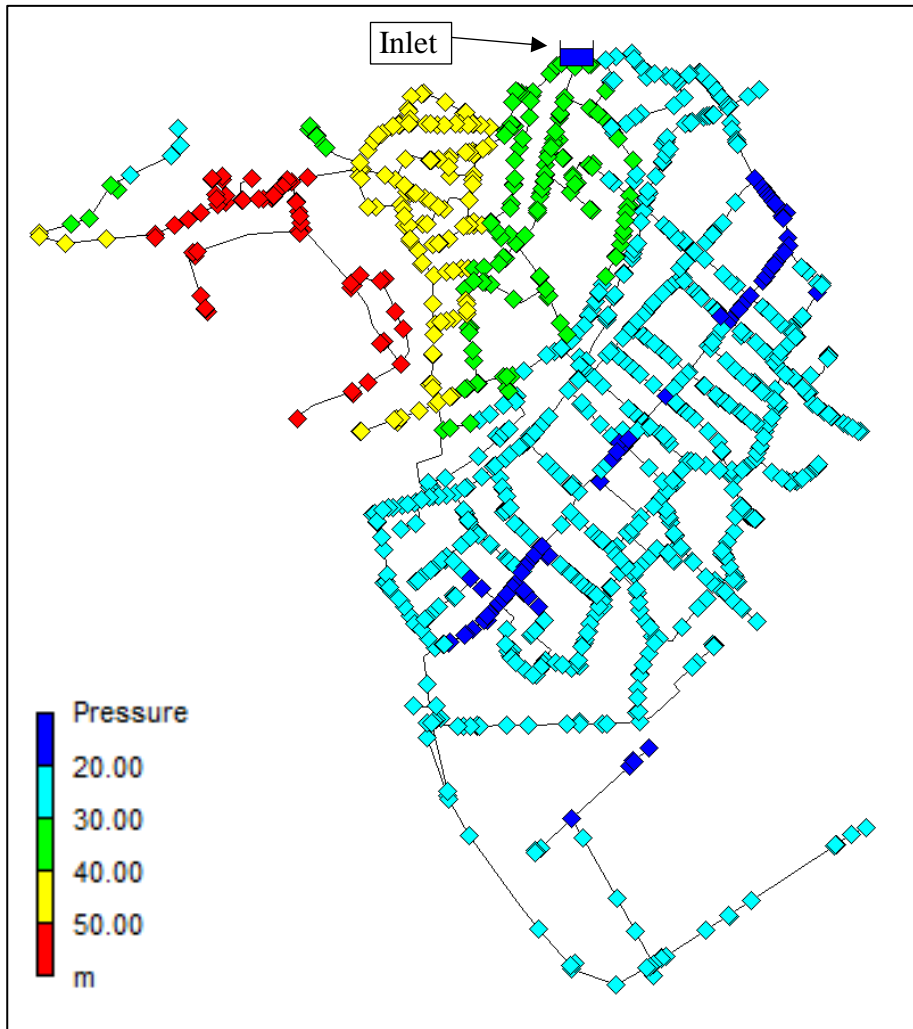
Figure 4.34. Junctions in Kaleiçi WDN have predicted pressure less than 20 m, assuming +25% increase of the non-leakage flow. (August 21 - 25, 2015)

4.7. Advanced PM Application on Changing The Non-Leakage Flow by ±%25 in Winter Season

Advanced PM has been applied to each assumption of changing the non-leakage flow by ± 25% during the winter simulation as follows:

4.7.1. Assuming a reduction of the non-leakage flow by %25

The model determined the location of the CP which has the least predicted pressure in Kaleiçi WDN as illustrated in Figure 4.35 at node number 704, CP (P704). The predicted pressure at the CP (P704), the predicted excess pressure, and the minimum allowable pressure (20 m) prior to advanced PM application are shown in Figure 4.36. The predicted pressure downstream of PRV versus the pressure measured upstream of PRV at the inlet of Kaleiçi WDN are presented in Figure 4.37. Figure 4.38 shows the predicted broken pressure by the PRV.
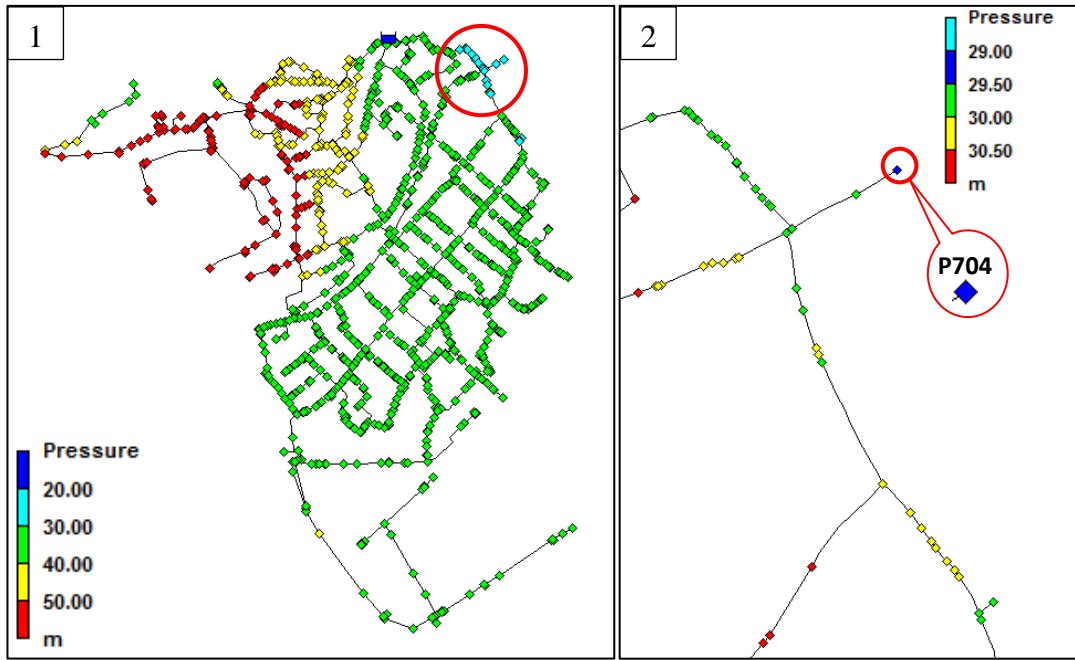
Figure 4.35. The location of the CP related to the least predicted pressure in the PSA (assuming -25% decrease of non-leakage flow) during winter season. CP (P704), on 15.01.2016 at 12:00 AM; min. pressure = 29.60 m, $\Sigma Q_{(75\% \times non\text{-}leakage)+(leakage)}$= 69.46 m^3/h and pressure upstream PRV = 32.05 m
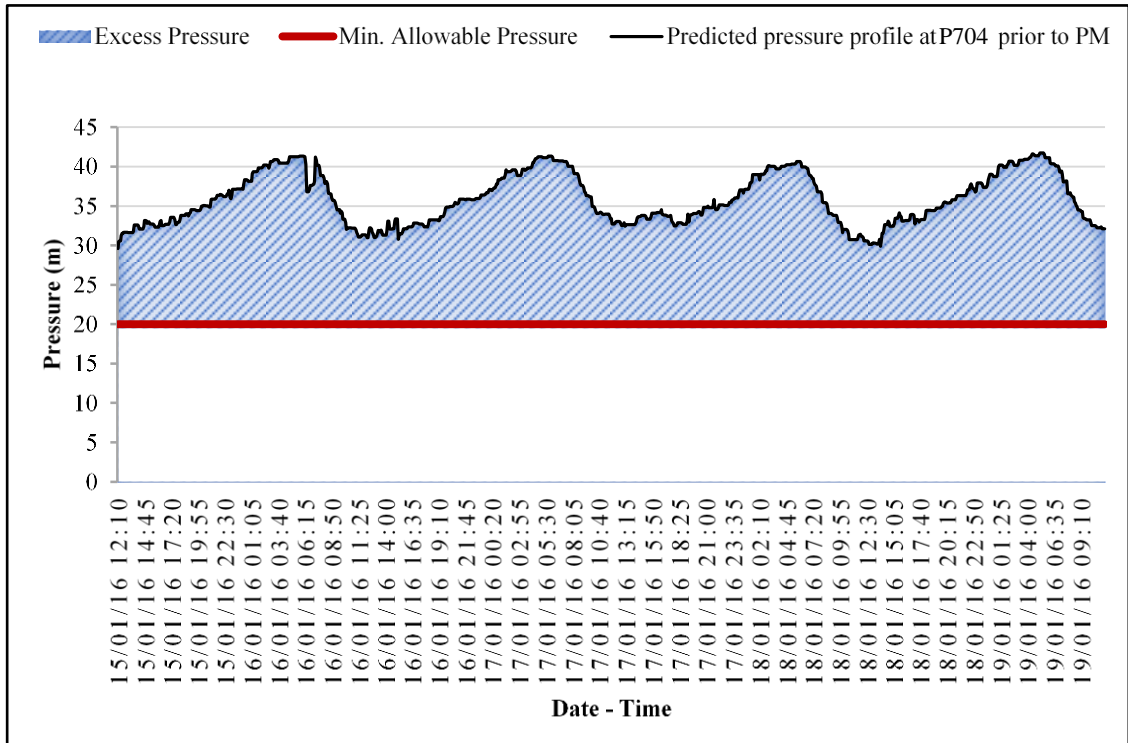
Figure 4.36. The predicted pressure at the CP (P704), the predicted excess pressure, and the minimum allowable pressure level prior to advanced PM application, assuming -25% reduction in the non-leakage flow. (January 14 – 19, 2016)
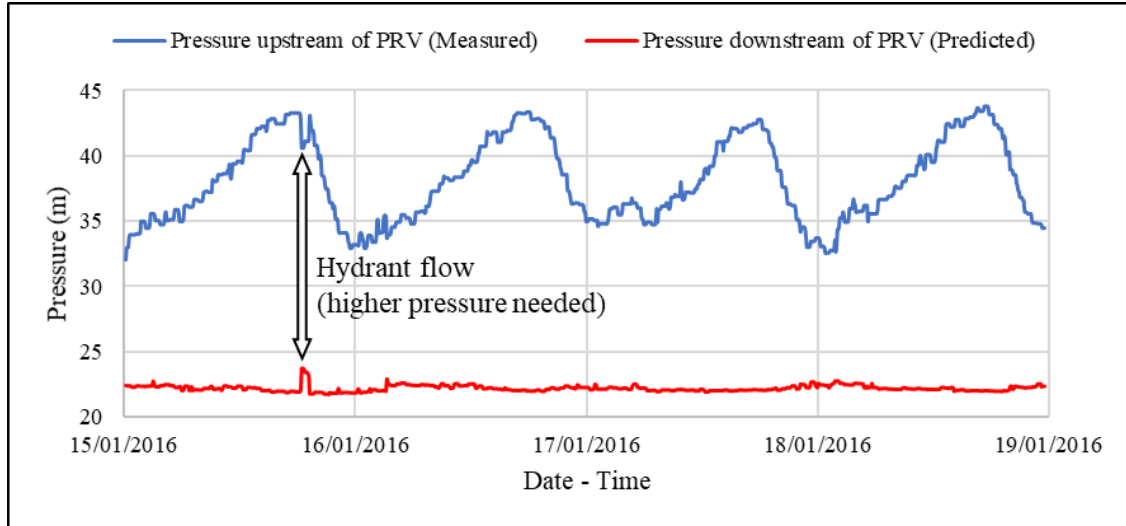
Figure 4.37. The pressure measured upstream of PRV vs. the predicted pressure downstream of PRV, assuming -25% reduction in the non-leakage flow. (January 15 – 19, 2016)
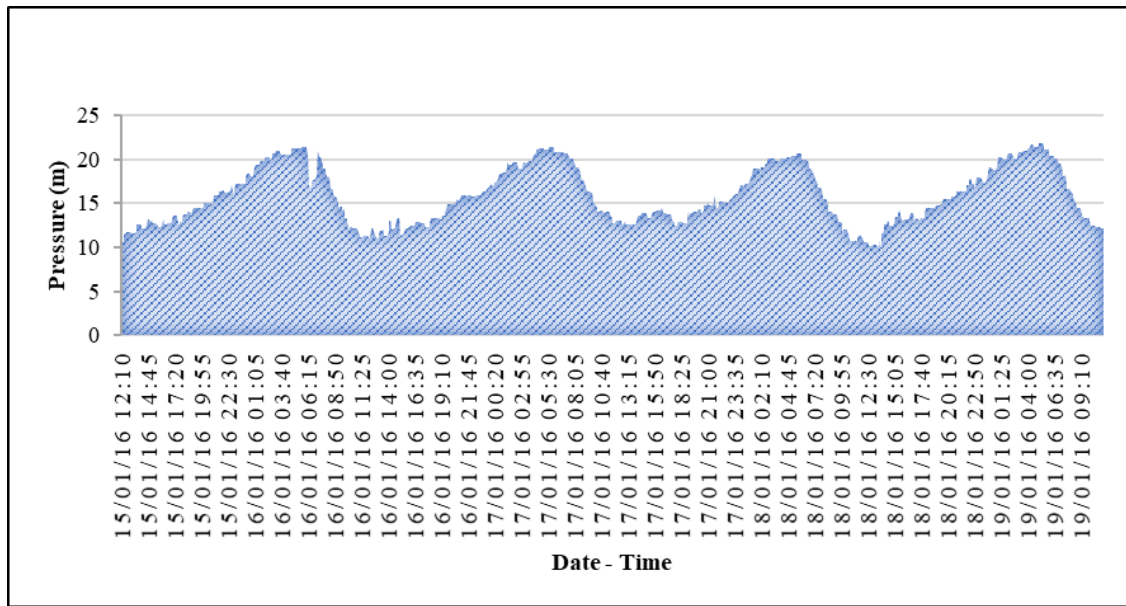
Figure 4.38. The predicted broken pressure by the PRV, assuming -25% reduction in the non-leakage flow. (January 15 – 19, 2016)

Assuming non-leakage reduction by 25%, the maximum predicted pressure at all nodes before and after applying the advanced PM is presented in Figure 4.39. The maximum pressure was predicted as 81.02 m at node (P253) before applying advanced PM, while the maximum predicted pressure at (P253) after applying advanced PM is 59.73 m. The predicted reduction of the average network pressure and average leakage due to advanced PM application are presented in Table 4.9.

94
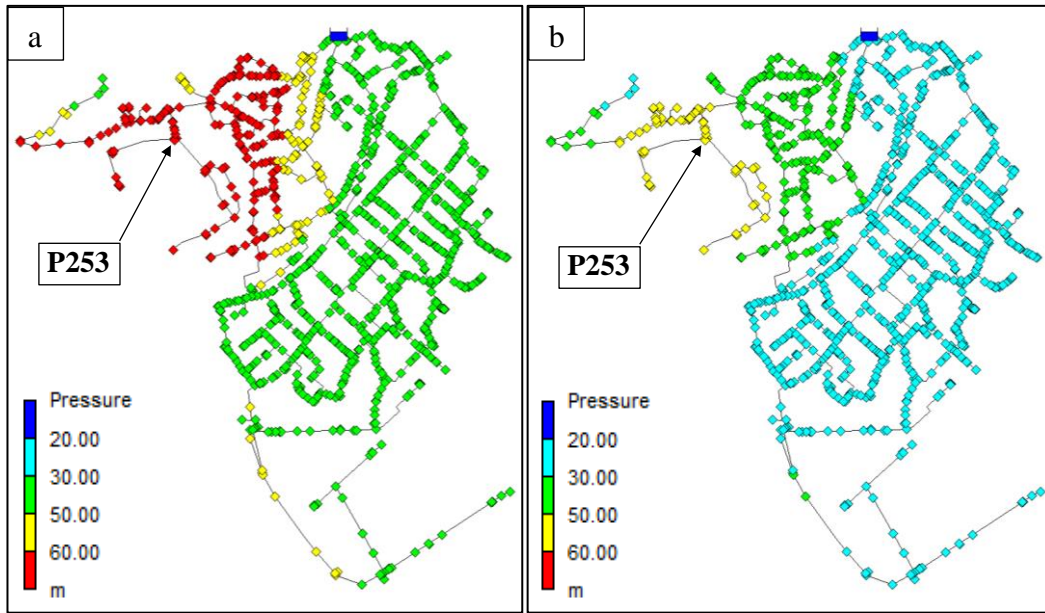
Figure 4.39. The maximum predicted pressure at all nodes in Kaleiçi WDN a) before advanced PM application, b) after advanced PM application, assuming -25% reduction in the non-leakage flow. (January 15 – 19, 2016)

Table 4.9. The predicted average network pressure reduction and the average leakage reduction, assuming -25% reduction in the non-leakage flow, (January 15 – 19, 2016)

Status		Before Advanced PM Application	After Advanced PM Application
Average Network Pressure (m)		44.42	28.91
Average Pressure reduction (m)		15.51	
Min. Network Pressure (m)		29.60	20
Min. Pressure reduction (m)		9.60	
Max. Network Pressure (m)		81.02	59.73
Max. Pressure reduction (m)		21.29	
Average $\Sigma Q_{(75\%\times non\text{-}leakage)+(Leakage)}$ (m³/h)		63.26	57.23
Average Leakage reduction	m³/h	6.03	
	m³/month	4486.32	

4.7.2. Assuming an increase of the non-leakage flow by %25

The model determined the location of the CP which has the least predicted pressure in Kaleiçi WDN as illustrated in Figure 4.40 at node number 704, CP (P704). The predicted pressure at the CP (S704), the predicted excess pressure, and the minimum allowable pressure (20 m) prior to advanced PM application are shown in Figure 4.41. The predicted pressure downstream of PRV versus the pressure measured upstream of PRV at the inlet of Kaleiçi WDN are presented in Figure 4.43. The predicted broken pressure by the PRV is presented in Figure 4.43.
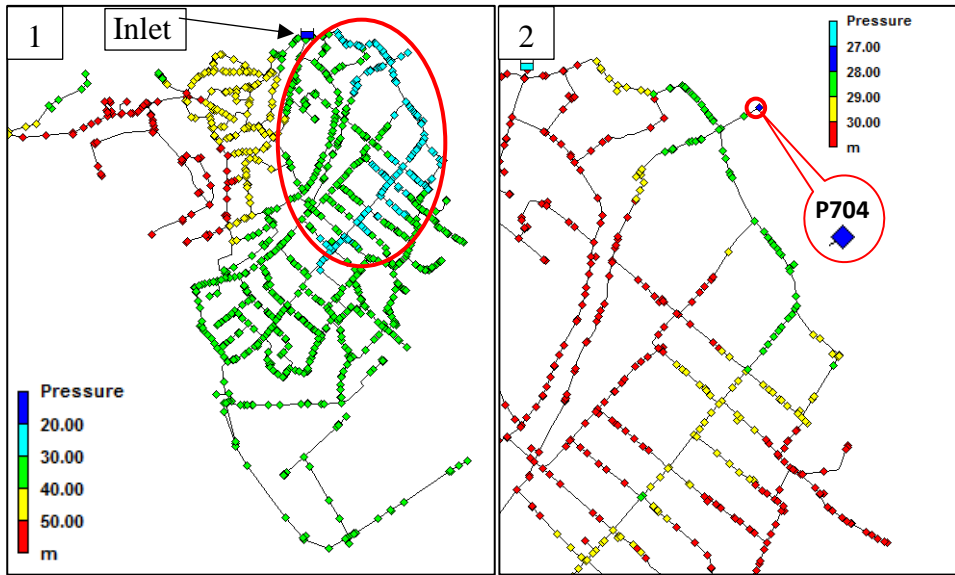
Figure 4.40. The location of the CP related to the least predicted pressure in the PSA (assuming +25% increase of non-leakage flow) during winter season. CP (P704), on 18.01.2016 at 01:50 PM; min. pressure = 27.81 m, $\Sigma Q_{(125\% \times non\text{-}leakage)+(leakage)}$= 117.82 m^3/h and pressure upstream PRV = 32.65 m
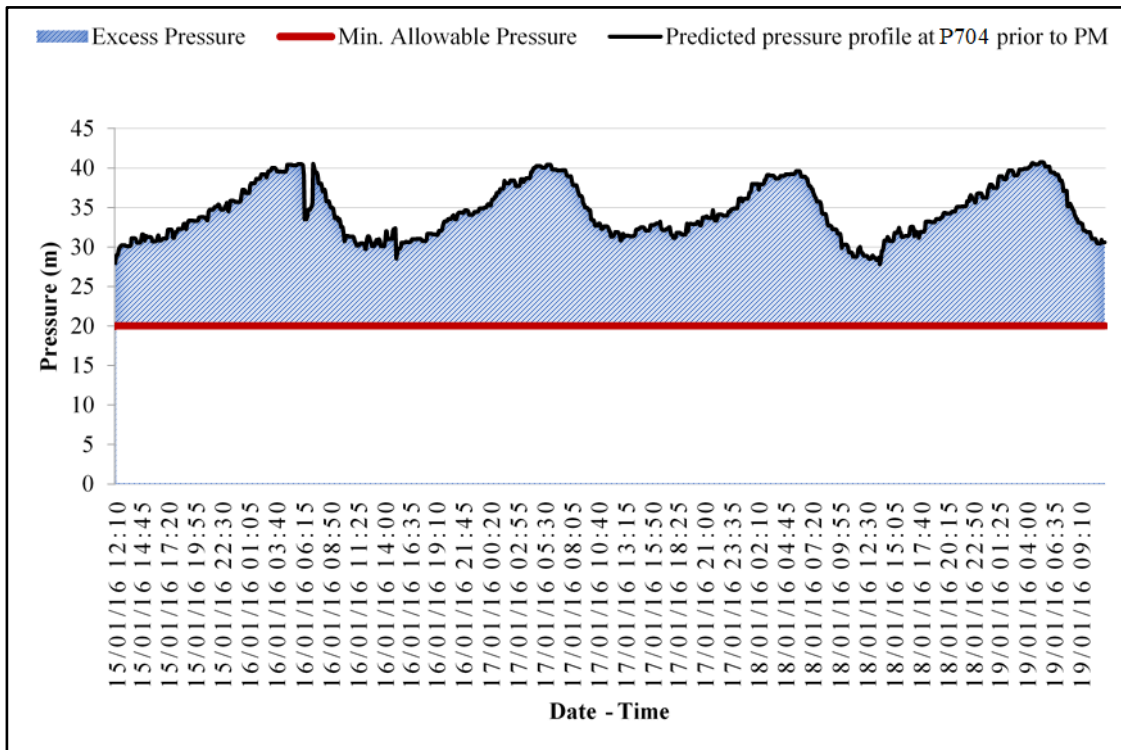
Figure 4.41. The predicted pressure at the CP (P704), the predicted excess pressure, and the minimum allowable pressure level prior to advanced PM application, assuming +25% increase of the non-leakage flow. (January 15 – 19, 2016)
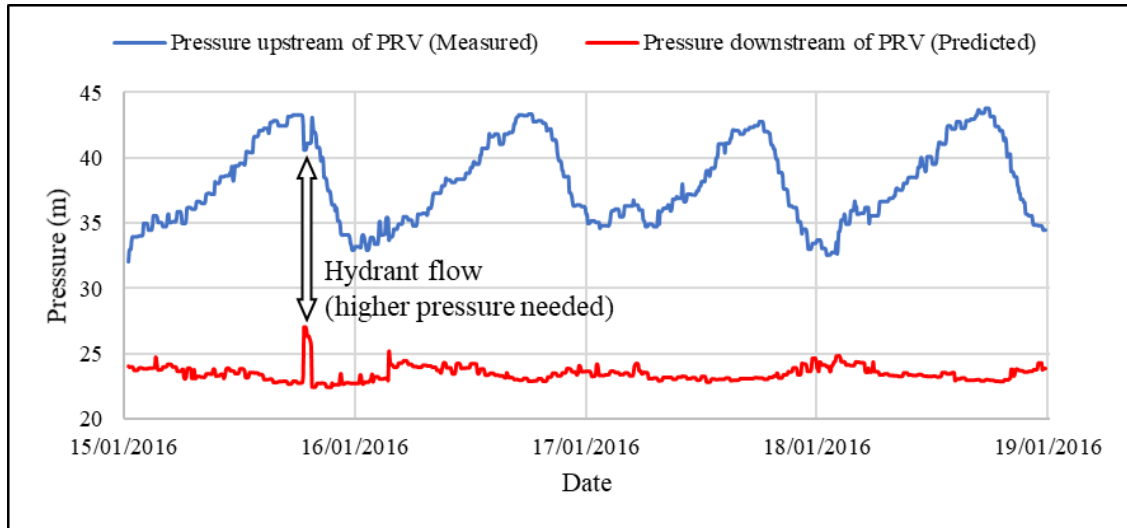
Figure 4.42. The pressure measured upstream of PRV vs. the predicted pressure downstream of PRV, assuming +25% increase of the non-leakage flow. (January 15 – 19, 2016)
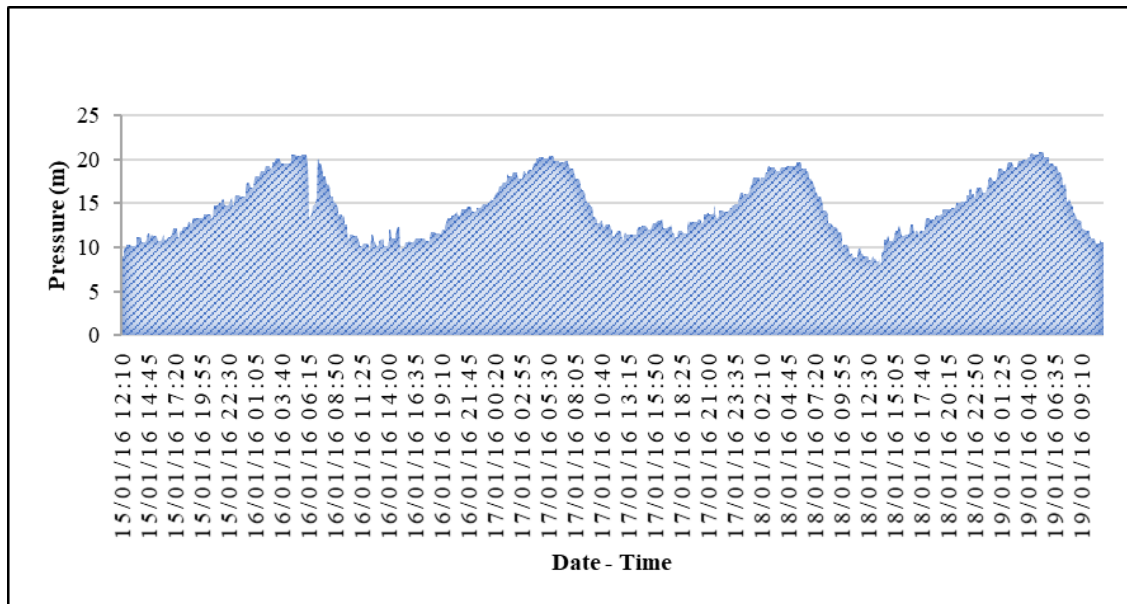
Figure 4.43. The predicted broken pressure by the PRV, assuming +25% increase of the non-leakage flow. (January 15 – 19, 2016)

Assuming non-leakage increase by 25%, the maximum predicted pressure at all nodes before and after applying the advanced PM is presented in Figure 4.44. The maximum pressure was predicted as 80.15 m at node (P253) before applying advanced PM, while the maximum predicted pressure at (P253) after applying advanced PM is 60 m. The predicted reduction of the average network pressure and average leakage due to advanced PM application are presented in Table 4.10.
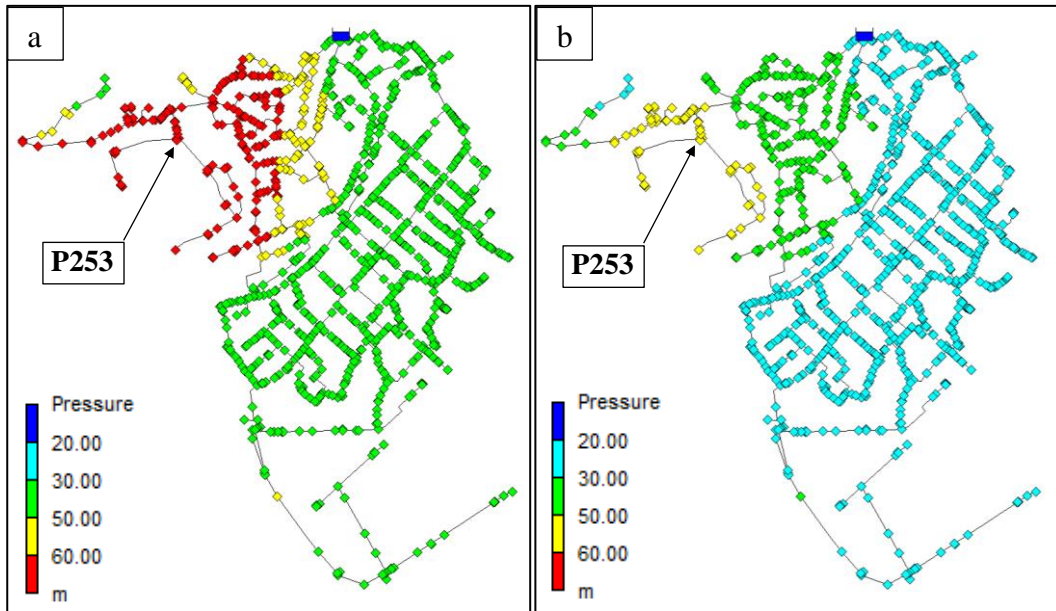
Figure 4.44. The maximum predicted pressure at all nodes in Kaleiçi WDN a) before advanced PM application, b) after advanced PM application, assuming +25% increase of the non-leakage flow. (January 15 – 19, 2016)

Table 4.10. The predicted average network pressure reduction and the average leakage reduction, assuming +25% increase of the non-leakage flow, (January 14 – 19, 2016)

Status		Before Advanced PM Application	After Advanced PM Application
Average Network Pressure (m)		43.0	28.8
Average Pressure reduction (m)		14.2	
Min. Network Pressure (m)		27.81	20
Min. Pressure reduction (m)		7.81	
Max. Network Pressure (m)		80.15	60
Max. Pressure reduction (m)		20.15	
Average $\Sigma Q_{(125\% \times non\text{-}leakage)+(Leakage)}$ (m³/h)		92.72	87.2
Average Leakage Reduction	m³/h	5.51	
	m³/month	4099.44	

4.8. Advanced PM Application on The Scenario of Reducing Leakage to ELL

4.8.1. In the summer season (August 21 – 25, 2015)

The total of non-leakage flow and the ELL flowrate as it is distributed by the model ($\Sigma Q_{(non\text{-}leakage)+(ELL)}$) versus the pressure measured at the inlet of Kaleiçi WDN are presented in Figure 4.45. The model determined the location of the CP which has the least predicted pressure in Kaleiçi WDN as illustrated in Figure 4.46 at node number 270, CP (P270). The predicted pressure at the CP (P270), the predicted excess pressure, and the minimum allowable pressure (20 m) prior to advanced PM application are shown in

Figure 4.47. The predicted pressure downstream of PRV versus the pressure measured upstream of PRV at the inlet of Kaleiçi WDN are presented in Figure 4.48. Figure 4.49 shows the predicted broken pressure by the PRV at the inlet.
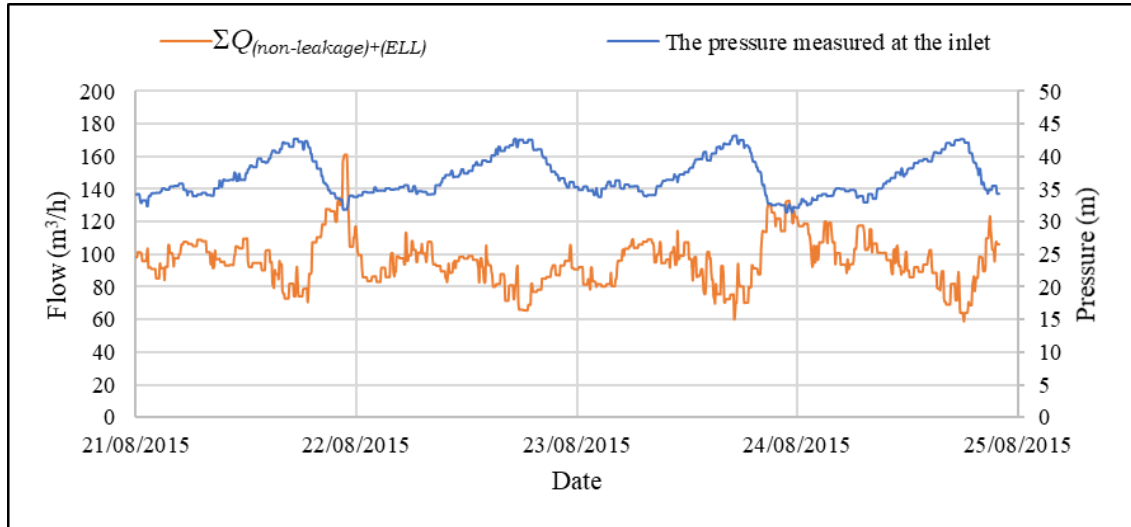

Figure 4.45. The pressure measured at the inlet vs. $\Sigma Q_{(non\text{-}leakage)+(ELL)}$, (August 21 – 25, 2015)
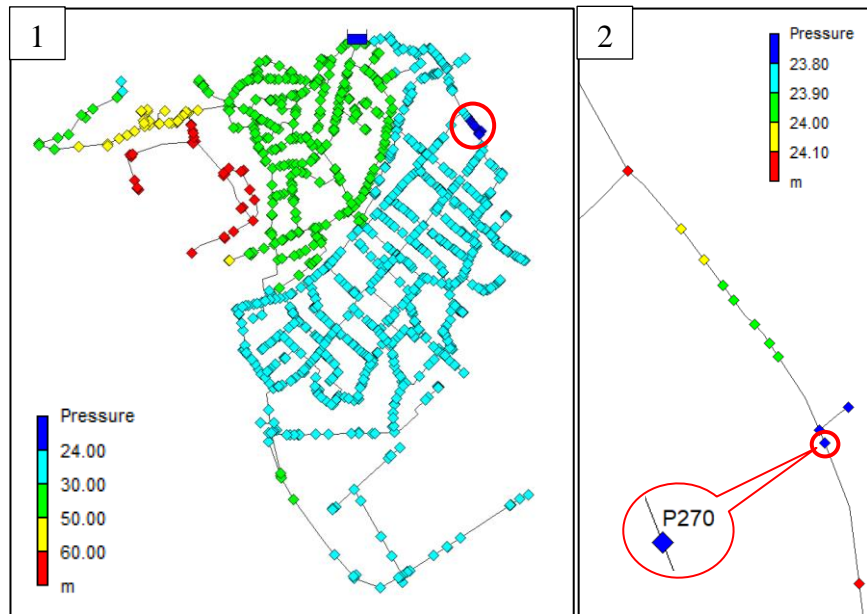
Figure 4.46. The location of the CP related to the least predicted pressure in the PSA (assuming ELL) during summer season. CP (P270), on 22.08.2015 at 10:45 – 11:00 AM; min. pressure = 23.78 m, $\Sigma Q_{(non\text{-}leakage)+(ELL)}$ = 161.35 m^3/h and pressure upstream PRV = 31.93 m
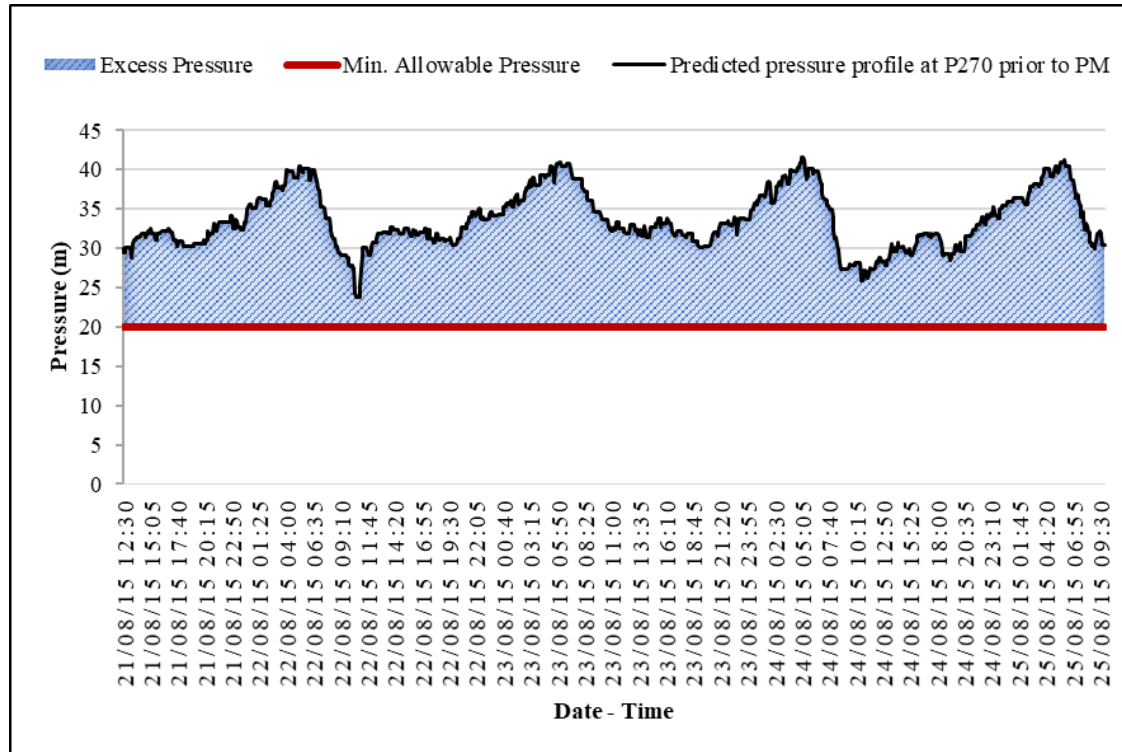
Figure 4.47. The predicted pressure at the CP (P270), the predicted excess pressure, and the minimum allowable pressure level prior to advanced PM application, assuming ELL. (August 21-25, 2015)
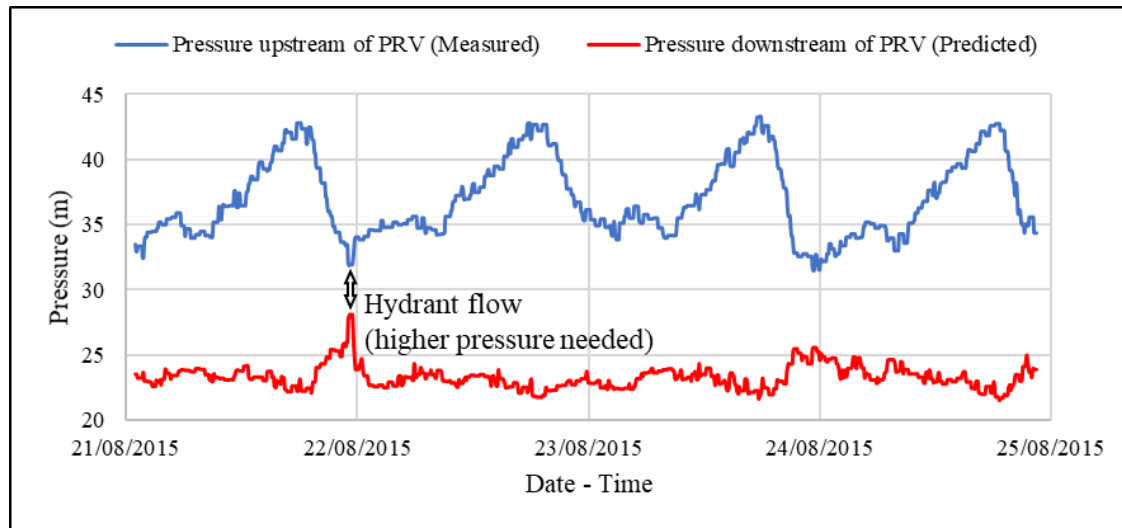
Figure 4.48. The pressure measured upstream of PRV vs. the predicted pressure downstream of PRV, assuming ELL. (August 21 - 25, 2015)
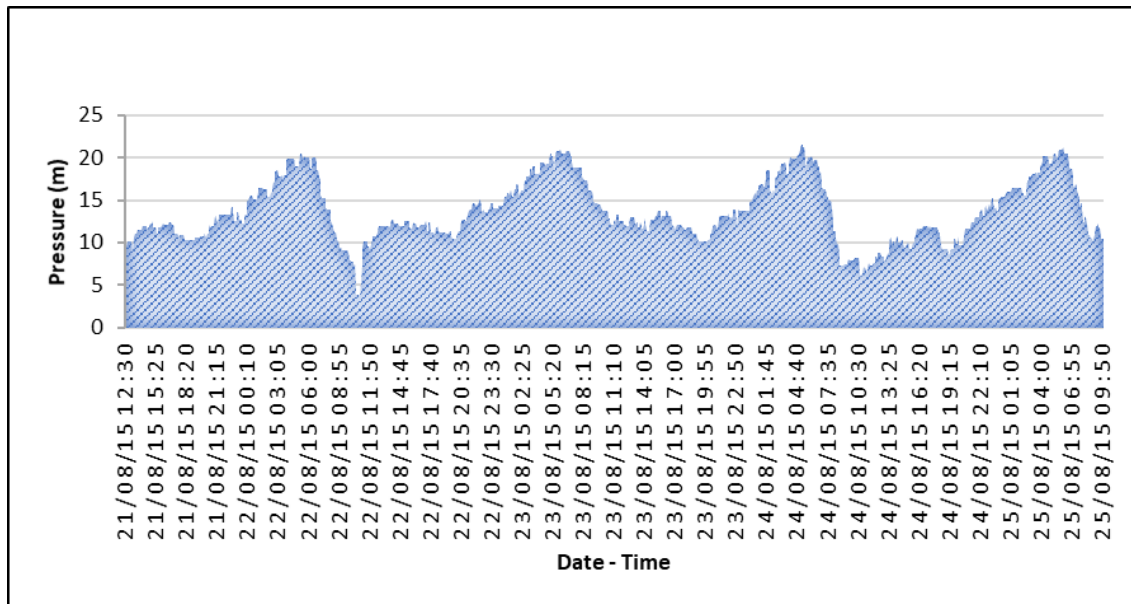
Figure 4.49. The predicted broken pressure by the PRV, assuming ELL. (August 21-25, 2015)

Assuming ELL during the summer simulation period, the maximum predicted pressure at all nodes before and after applying the advanced PM is shown in Figure 4.50. The maximum pressure was predicted as 80.57 m at node (P253) before applying advanced PM, while the maximum predicted pressure at (P253) after applying advanced PM is 60 m. The predicted reduction of the average network pressure and average leakage due to advanced PM application are presented in Table 4.11.
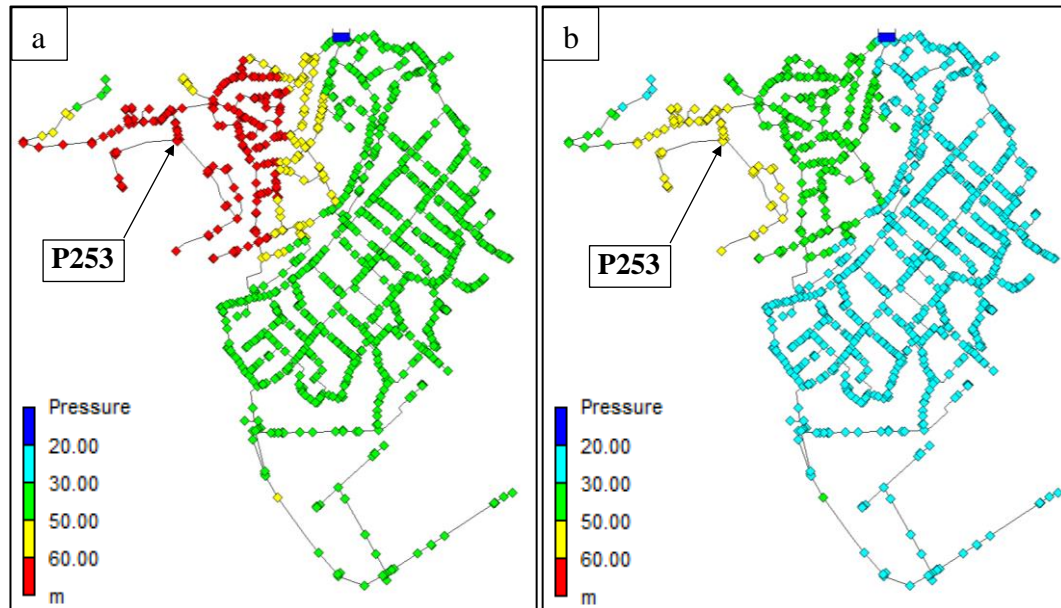
Figure 4.50. The maximum predicted pressure at all nodes in Kaleiçi WDN a) before advanced PM application, b) after advanced PM application, assuming ELL. (August 21-25, 2015)

Table 4.11. The predicted average network pressure reduction and the average leakage reduction, assuming ELL. (August 21 – 25, 2015)

Status		Before Advanced PM Application	After Advanced PM Application
Average Network Pressure (m)		41.89	28.32
Average Pressure reduction (m)		13.57	
Min. Network Pressure (m)		23.78	20
Min. Pressure reduction (m)		3.78	
Max. Network Pressure (m)		80.57	60
Max. Pressure reduction (m)		20.57	
Average $\Sigma Q_{(non\text{-}leakage)+(ELL)}$ (m^3/h)		95.64	92.72
Average Leakage Reduction	m^3/h	2.92	
	m^3/month	2172.48	

4.8.2. In the winter season (January 15 – 19, 2016)

The $\Sigma Q_{(non\text{-}leakage)+(ELL)}$ versus the pressure measured at the inlet of Kaleiçi WDN are presented in Figure 4.51. The model determined the location of the CP which has the least predicted pressure in Kaleiçi WDN as illustrated in Figure 4.52 at node number 270, CP (P704). The predicted pressure at the CP (P704), the predicted excess pressure, and the minimum allowable pressure (20 m) prior to advanced PM application are shown in Figure 4.53. The predicted pressure downstream of PRV versus the pressure measured upstream of PRV at the inlet of Kaleiçi WDN are presented in Figure 4.54. The predicted broken pressure by the PRV is shown in Figure 4.55.
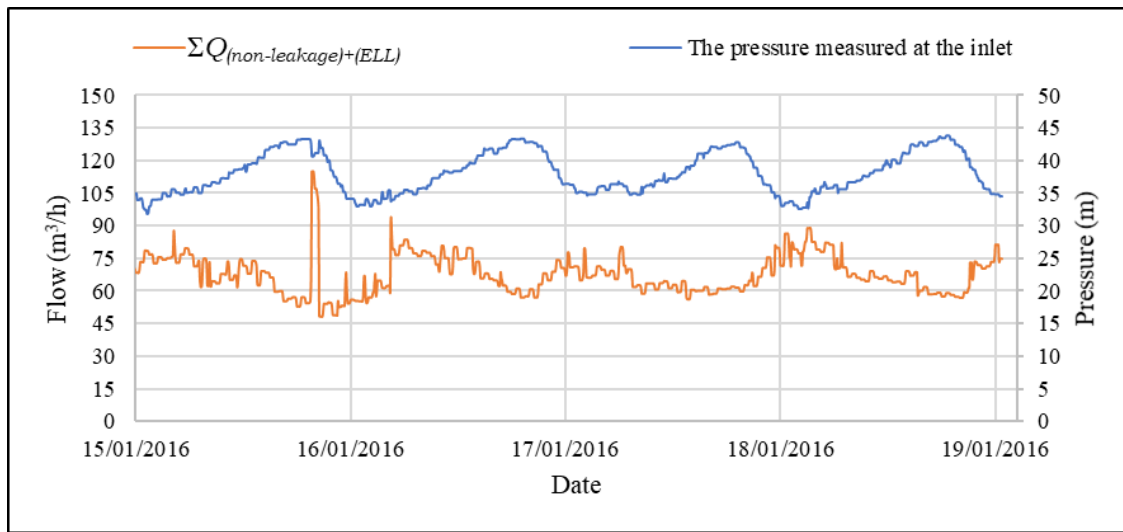
**Figure 4.51.** The pressure measured at the inlet vs. $\Sigma Q_{(non\text{-}leakage)+(ELL)}$, (January 14 – 16, 2016)
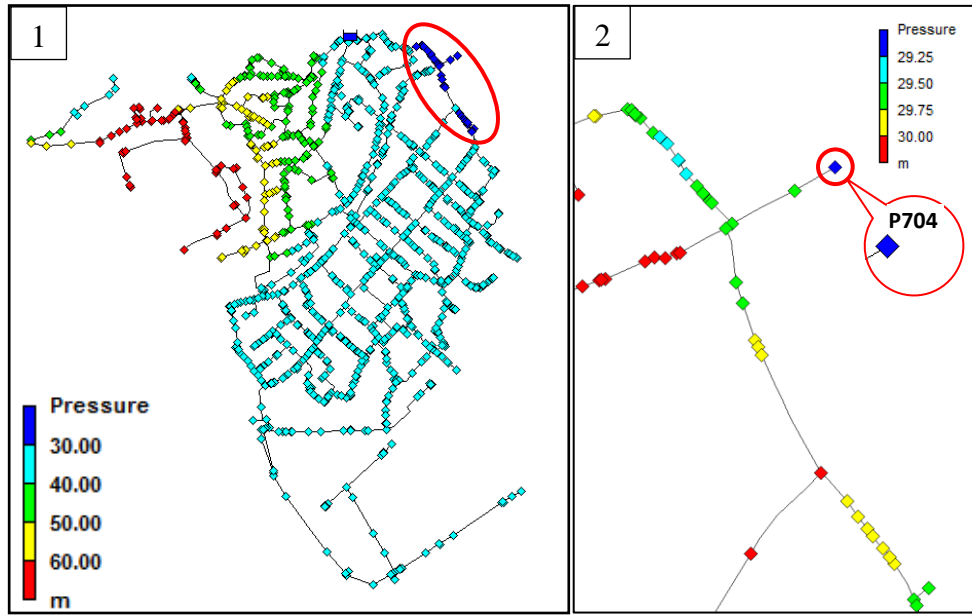
Figure 4.52. The location of the CP related to the least predicted pressure in the PSA (assuming ELL) during winter season. CP (P704), on 15.01.2016 at 12:00 AM; min. pressure = 29.22 m, $\Sigma Q_{(non\text{-}leakage)+(ELL)}$= 78.03 m³/h and pressure upstream PRV = 32.05 m
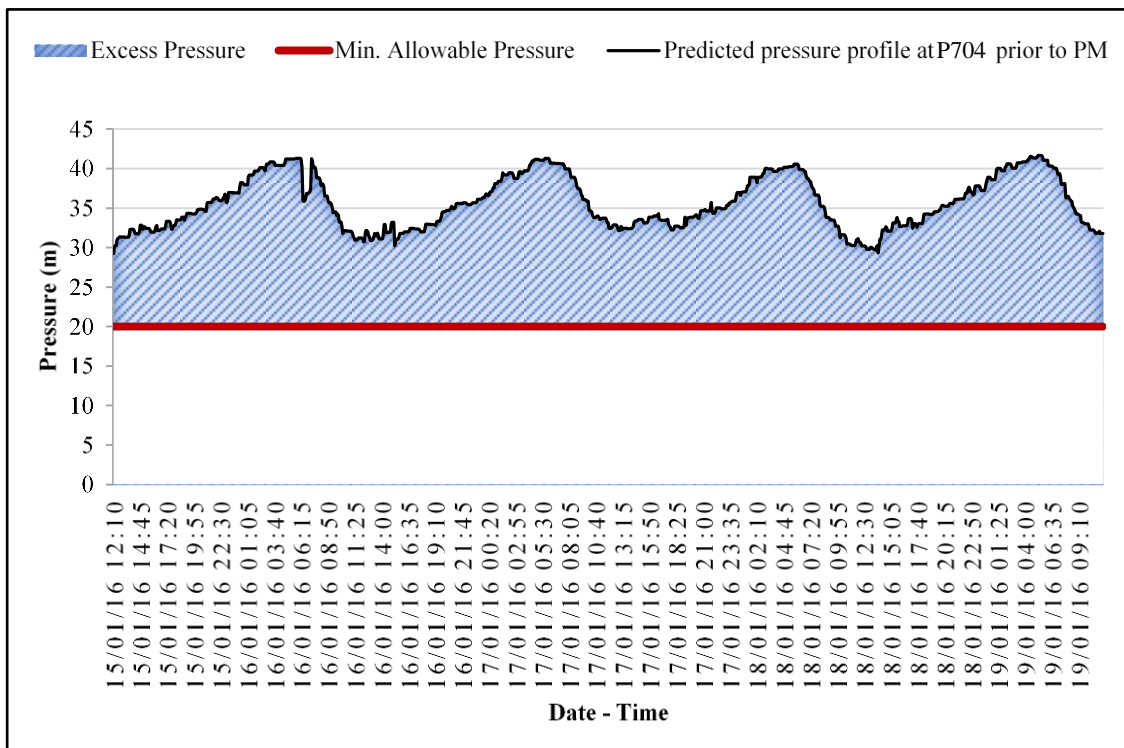

Figure 4.53. The predicted pressure at the CP (P704), the predicted excess pressure, and the minimum allowable pressure level prior to advanced PM application, assuming ELL. (January 15 – 19, 2016)
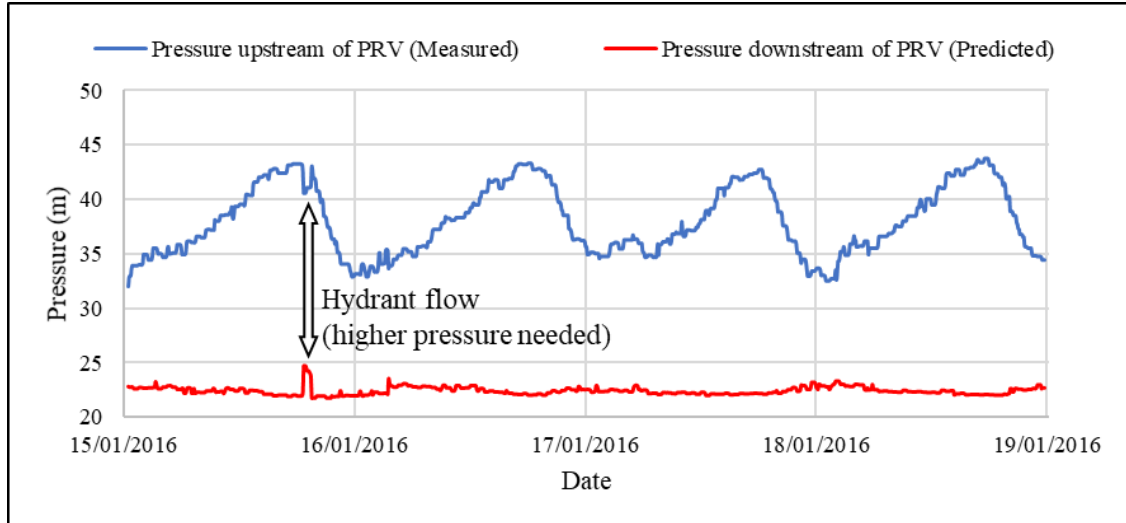
Figure 4.54. The pressure measured upstream of PRV vs. the predicted pressure downstream of PRV, assuming ELL. (January 15 - 19, 2016)
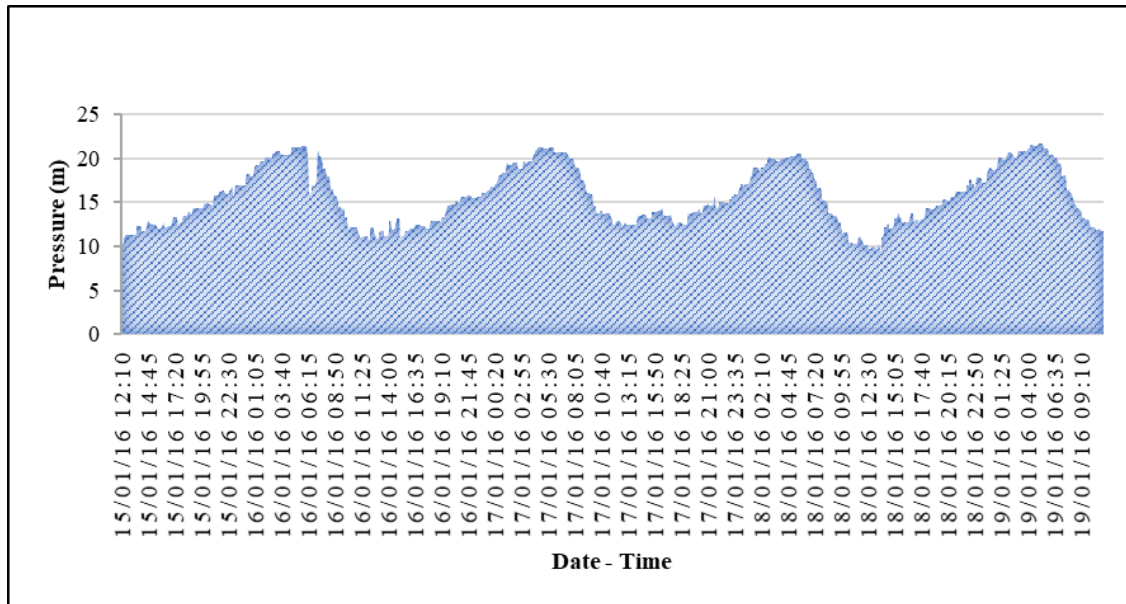

Figure 4.55. The predicted broken pressure by the PRV, assuming ELL. (January 15 – 19,2016)

Assuming ELL during the winter simulation period, the maximum predicted pressure at all nodes before and after applying the advanced PM is shown in Figure 4.56. The maximum pressure was predicted as 81.08 m at node (P253) before applying advanced PM, while the maximum predicted pressure at (P253) after applying advanced PM is 59.83 m. The predicted reduction of the average network pressure and average leakage due to advanced PM application are presented in Table 4.12.
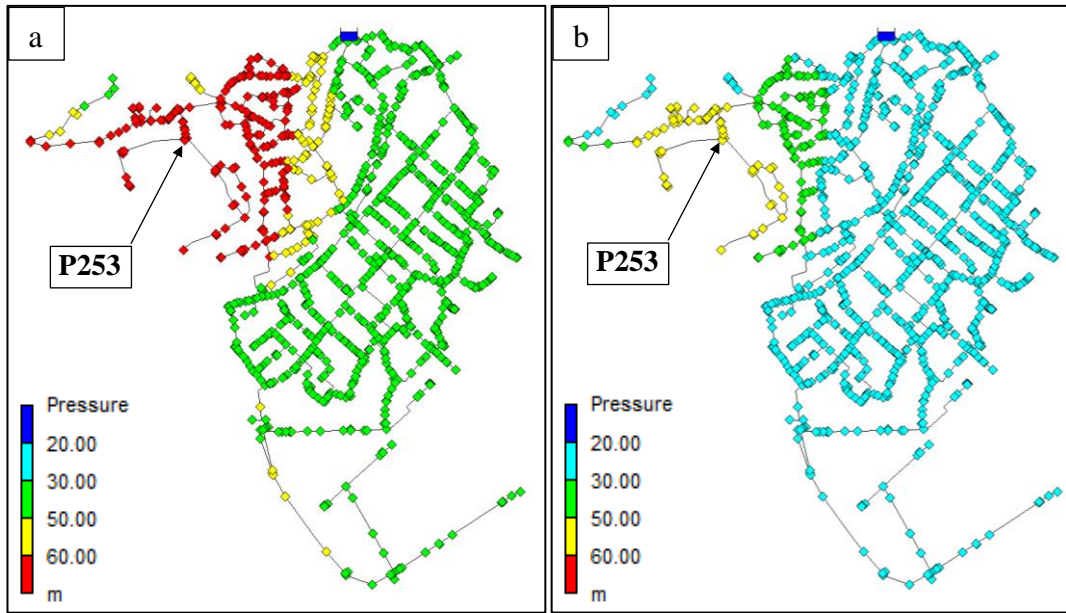
Figure 4.56. The maximum predicted pressure at all nodes in Kaleiçi WDN a) before advanced PM application, b) after advanced PM application, assuming ELL. (January 15 – 19,2016)

Table 4.12. The predicted average network pressure reduction and the average leakage reduction, assuming ELL. (January 15 – 19, 2016).

Status		Before Advanced PM Application	After Advanced PM Application
Average Network Pressure (m)		44.19	28.76
Pressure reduction (m)		15.43	
Min. Network Pressure (m)		29.22	220
Min. Pressure reduction (m)		9.22	
Max. Network Pressure (m)		81.08	59.83
Max. Pressure reduction (m)		21.25	
Average $\Sigma Q_{(non\text{-}leakage)+(ELL)}$ (m^3/h)		67.58	65.18
Average Leakage Reduction	m^3/h	2.4	
	m^3/month	1785.6	

4.9. Discussing the results of applying advanced PM

Generally, there are common results appear after applying the advanced PM in Kaleiçi WDN are summarized as:

- The predicted pressure downstream the PRV shows a noticeable jump during the time of artificial high flow events (fire-hydrant), this jump indicates the PRV reaction to the extraordinary water demand by increasing the pressure.

- All the junctions where the predicted pressure was above 60 m before applying advanced PM showed a predicted pressure after the application of advanced PM less than or equal 60 m.

By applying advanced PM, the predicted pressure reduction during summer season was less than the predicted pressure reduction during winter season. On the contrary, the average predicted leakage reduction during summer season was more than the average predicted leakage reduction during winter season (Tables 4.6 & 4.7). The higher predicted pressure reduction in winter is interpreted through the less system input flow in winter. The higher average predicted leakage reduction (as a flow) in summer season is due to the higher average leakage calculated by SWB before applying advanced PM.

4.10. Prediction of Leakage Flow Spatially

A very important result out of the thesis is that leakage flows could be predicted spatially, i.e. the leakage at any junction within Kaleiçi WDN can be predicted over the simulation period. For example, Figure 4.57 shows the average pressure of all nodes Kaleiçi network in summer simulation period. The red color indicates the highest pressure of the system, above 60 m, while aqua color indicates the lowest, with no pressure under 20 m. Leakage is predicted for each junction in the system. Figure 4.58 and Figure 4.59 exhibit the leakage of sample junctions belongs to different pressure with a convergent leakage coefficient, which are shown in Figure 4.57, during summer and winter simulation periods, respectively.
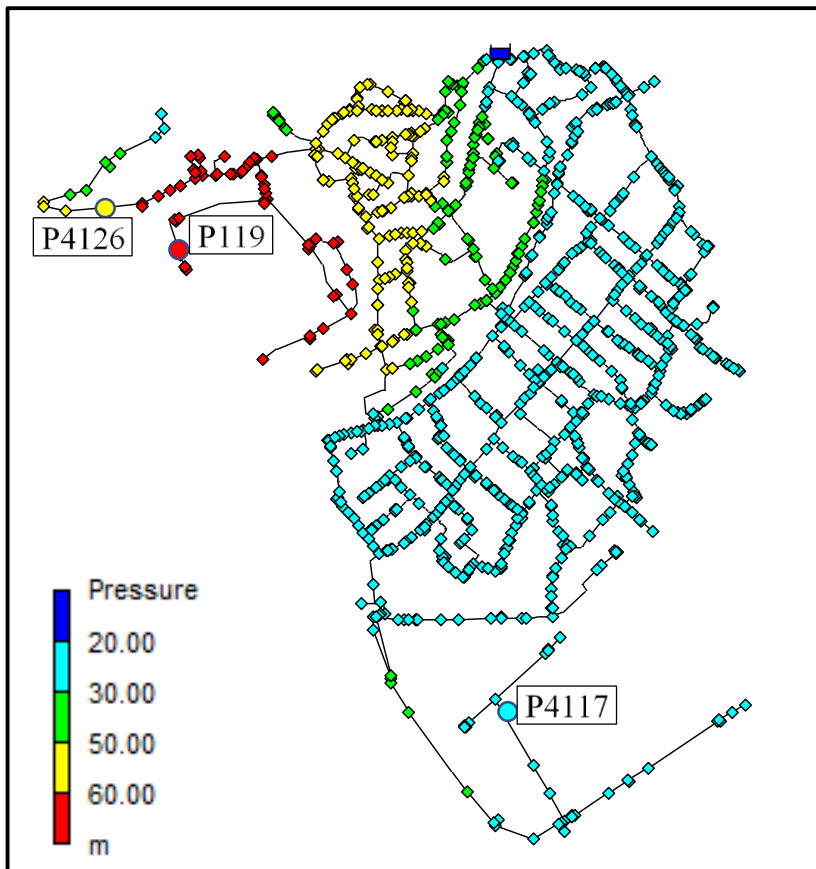
Figure 4.57. Average nodal pressure. (August 20-25, 2015)
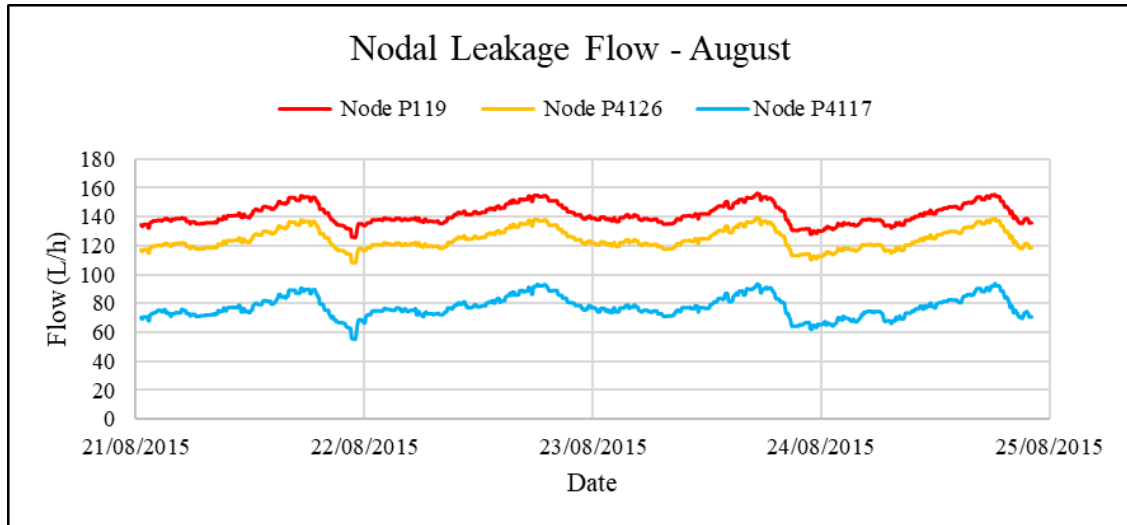
Figure 4.58. The nodal leakage flow of P119, P4126, and P4117. (August 21 - 25, 2015)
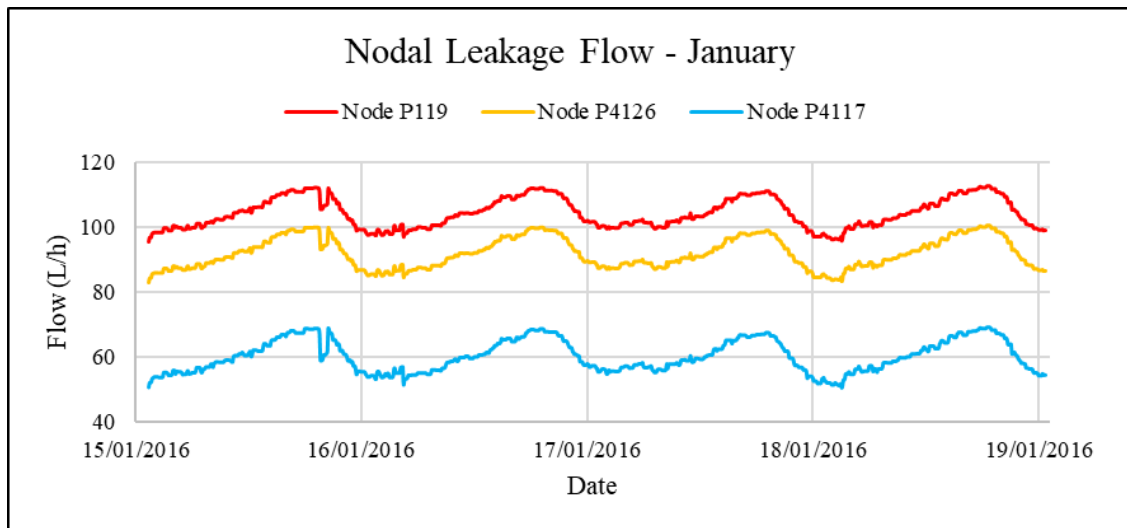
Figure 4.59. The nodal leakage flow of P119, P4126, and P4117. (January 14 - 19, 2016)

4.11. The Effect of The Adopted Scenarios on The Excess Pressure

The total of leakage and non-leakage flow distributed by the model ($\Sigma Q_{(non\text{-}leakage)+(leakage)}$) has been influenced throughout each scenario of changing the non-leakage flow or reducing the leakage to the ELL.

The $\Sigma Q_{(non\text{-}leakage)+(leakage)}$ is inversely related to the pressure throughout the junctions. A comparison between the base simulation of Kaleiçi WDN and each scenario in terms of the excess pressure predicted at the CP during summer simulation period is presented in Figure 4.60 and Figure 4.61. As shown in Figure 4.60, the pressure increases if the non-leakage flow reduced by 25% and conversely decreases when the non-leakage flow increased by 25%. While in Figure 4.61, the predicted excess pressure increased in the scenario of reducing leakage to the ELL. Similar impacts are also valid for the winter simulation period. Increasing the pressure in the network leads to increasing the leakage

and hence applying pressure management leads to significant leakage reduction. The reverse is also correct when the pressure of the network reduces leading to less leakage.
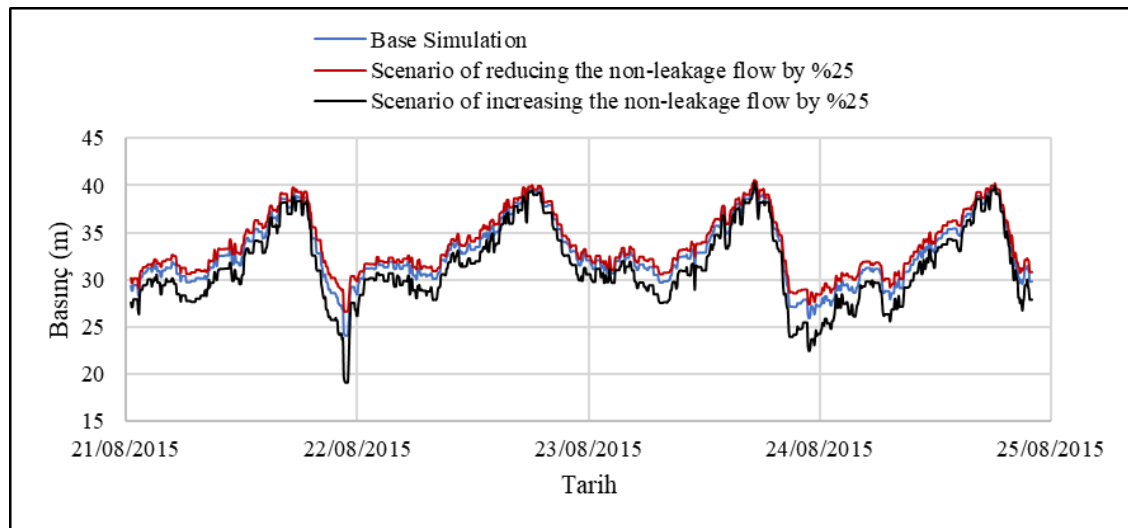
Figure 4.60. The excess pressure at the CP in the base simulation and the scenario of changing the non-leakage flow by ± %25, (August 21 - 25, 2015)
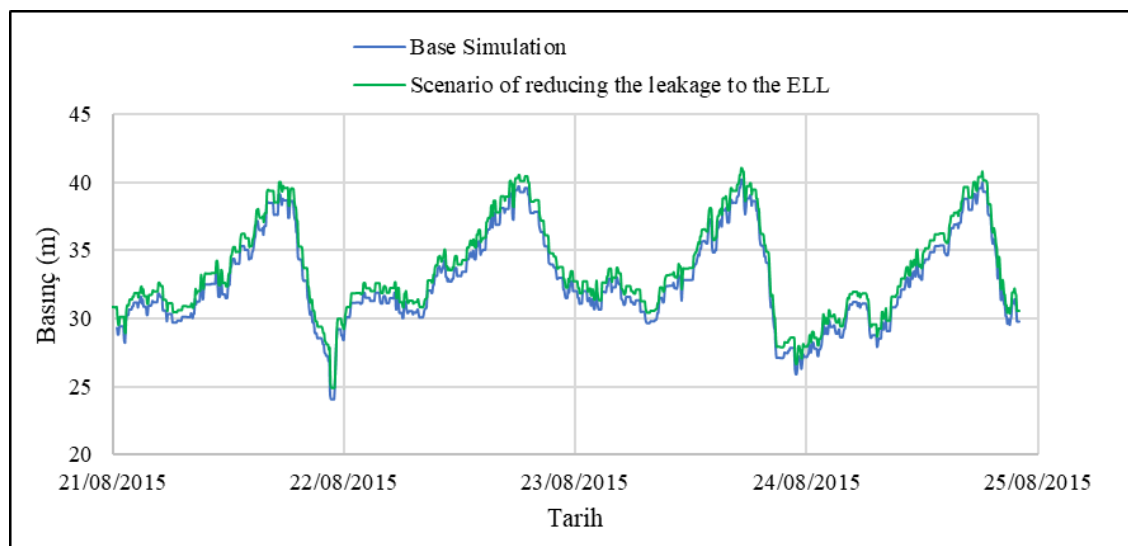
Figure 4.61. The excess pressure at the CP in the base simulation and the scenario of reducing leakage to the ELL, (August 21 - 25, 2015)

5. CONCLUSIONS

The water supply system is one of the fundamental infrastructures for all cities. Each water utility aims at delivering the freshwater of adequate quality and pressure to the customers. But the water loss that occurs in the WDN is an essential challenge encounters the freshwater suppliers. Reducing water losses in any WDN avails in reducing the needed energy for pumping, treating water, and enlarging the capacity of the WDN. Therefore, each water supplier must develop water loss management plans to reduce water loss or maintain it at definite levels. The water loss management programs begin by determining the SWB components periodically to investigate the components and the percentages of water consumption against water losses. The physical water losses (i.e. leakage) constitutes a crucial part of the water losses occurs in any WDN. Leakage is a pressure-dependent flow and its levels are affected by the water pressure in the WDN. Therefore, modeling leakage is vital for the management of water losses.

One of the most useful economic techniques for solving the leakage problem in any water supply system is pressure management (PM). It is applied in both classical and advanced forms to maintain the pressure at the minimum allowable level at all nodes in the WDN. The advanced PM starts by detecting the CP, then the pressure is broken at the inlet of the WDN by which the pressure at the CP is lowered to the minimum allowable limit all the time. Localizing the CP necessitates a calibrated hydraulic model. EPANET is a simple flexible free domain software for hydraulic modeling of WDNs. It has been used in this thesis work to model Kaleiçi WDN as a PSA using Hazen-William equation. The system input flow has been distributed to the junctions by dividing it into leakage through emitters and non-leakage flow through nodal-demand. An approach of spatial and temporal modeling of leakage by EPANET software has been investigated within this thesis methodology, then it is applied to predict the distribution of the total leakage to the junctions in Kaleiçi WDN. The approach depends essentially on the determination of leakage in the study area. This is usually determined through the SWB. According to the Turkish water losses legislations, all water authorities in Turkey are required to determine the SWB yearly. Moreover, the increasing use of smart meters such as AMR enables the establishment of the SWB more accurately and over relatively short periods. The model has been calibrated and verified for a single value of the roughness coefficient (57.6). Then, the model has been used for predicting leakage reduction by applying advanced PM. Finally, the application of advanced PM for two scenarios has been performed; the first scenario assumes that the non-leakage flow changes by ±25%, whereas the other scenario assumes that leakage is reduced to the ELL. The results proved that the hydraulic modeling is an essential tool to control leakage. In this research study, hydraulic modeling was an indispensable tool used for predicting the leakage spatially at each junction in the PSA.

The Kaleiçi WDN is a continuous water supply system. The non-leakage flow follows a definite demand profile with time pattern while leakage is directly dependent on the pressure of water in the network. Both of leakage and non-leakage flow have been distributed to the junctions assuming that they occur uniformly along the pipe length except for two users where the non-leakage flow was determined based on the measured flowrate. Each of the calibration process, application of advanced PM, and investigation of the scenarios has been carried out over two different simulation periods representing summer and winter seasons. The calibrated roughness coefficient of R= 57.6 has revealed

acceptable MAE of pressure at all PMPs over the two simulation periods and verified during another different third simulation period. It was predicted that the application of advanced PM in Kaleiçi WDN by modeling resulted in a significant leakage reduction (4307.76 & 5074.08 m^3/month). This made the hydraulic modeling an important tool in predicting the leakage reduction by advanced PM.

The inverse relation between pressure in the WDN and flow rate appeared through the scenarios. For example, the predicted excess pressure is higher in the scenario of reducing leakage to the ELL than the base simulation (reducing leakage means reducing the system input flow). The non-leakage flow forms the main part of system input flow in Kaleiçi WDN, thus, any change in that flow leads to change the system input flow and accordingly changes the network pressure. Since leakage is a pressure-dependent flow, it will be affected by any change of the non-leakage flow in Kaleiçi WDN. Based on this, in the scenario that assumes changing the non-leakage flow by ±25%, the higher the non-leakage flow, the lower the WDN pressure, and hence, the lower the predicted leakage and vice versa. Additionally, applying advanced PM on this scenario by modeling has predicted lower leakage reduction at higher non-leakage flow as shown in Figure 5.1 (advanced PM was not applicable in scenario of +25% increase of non-leakage flow during summer season). This indicates that less flow leads to less pressure and so less leakage reduction.
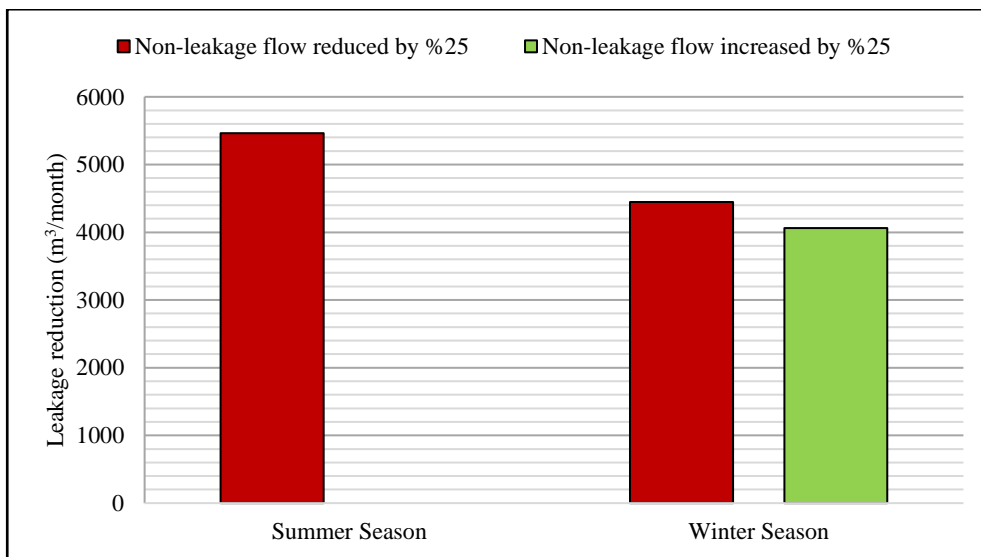
Figure 5.1. The predicted leakage reduction by applying advanced PM on the scenario of changing the non-leakage flow by ±%25

The approach used for spatial and temporal simulation of leakage enables the model of Kaleiçi WDN to predict the leakage as a pressure dependent flow. Additionally, the temporal and spatial variations of the pressure levels all over the WDN are predicted using the same approach. Consequently, the advanced PM can be applied successfully.

For applying the advanced PM in the field, the PRV is setup at the inlet of the PSA and the pressure sensors at the localized CPs by the model as shown in Figure 5.2. Based on that, the closed-loop pressure control can maintain the pressure at the minimum level all over the time and respond to the extraordinary water demand like the fire

accidents. However, different alternatives of the location of the PRV could be investigated.

Despite the good results of the approach used for simulating the leakage, it still can be applied in definite cases and also has some disadvantages. The definite case is that the leakage must be known to be distributed to the junctions of the WDN, for example, SWB tables have been determined at each month within a period of one year for Kaleiçi WDN. This provided us the leakage flow which has been distributed over the nodes. On the other hand, the approach assumes that the cracks and pipe bursts (leakage holes) are uniformly distributed along the pipe length, which is not the reality. This assumption leads to a non-full fitting of the total of leakage and non-leakage flow with the measured system input flow in the field. Both of these points are considered as disadvantage aspects of using this approach.
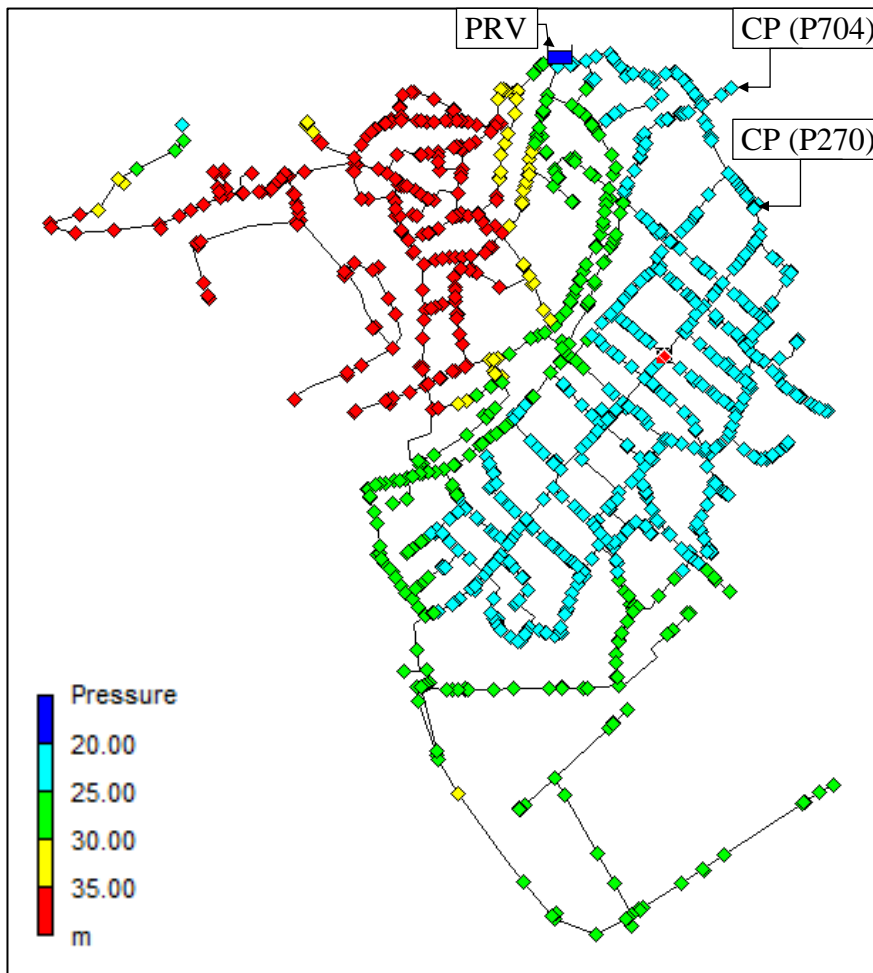
Figure 5.2. The location of the PRV and the CPs where the pressure sensors are suggested to be installed in Kaleiçi WDN.

Recommendations for Future Research Studies

The location of the PRV could be optimized and/or an additional PRV could be added in order to keep the maximum pressure head not to exceed 60 m, as suggested by the water losses regulations issued in 2014. Within this aspect, the related optimum leakage reduction could be investigated together with the location and number of PRV. Additionally, energy production could be investigated together with pressure/leakage reduction.

It is recommended to install a PRV at the entrance of the PSA, and a pressure sensor at the specified CP point, as suggested in this study. After that, the maximum and minimum pressure levels should be monitored, and the broken pressure could be verified.

It is suggested to establish the SWB and use the model for predicting the leakage within a short period of time (e.g. 24 hours), then the model can be helpful for detecting the spatial and temporal variation of leakage to be minimized as much as possible.

The used leakage modeling approach necessitates knowing the total leakage volume. Therefore, it can be useful if this can be accurately determined by using the AMR systems. Then, it is recommended to study connecting the model directly to the SCADA and AMR systems so that the model can be developed to a near real-time modeling to predict the leakage spatially as well as temporally online instead of past-data modeling. This can be achieved by connecting the toolkits of EPANET software using programming languages with SCADA systems (Cheng et al. 2014).

6. REFERENCES

Anonymous 1: BBC, 2017. Dramatic Ukraine water pipe explosion captured on CCTV. [Online] Available at: https://www.bbc.com/news/av/world-europe-40101394/dramatic-ukraine-water-pipe-explosion-captured-on-cctv [Last Accessed 06 August 2018].

Anonymous 2: Danish Environmental Protection Agency, 2018. *Identify sources of water loss.*[Online] Available at: https://eng.mst.dk/nature-water/water-at-home/water-loss/ [Last Accessed 04 August 2018].

Anonymous 3: TÜİK, 2018. Türkiye İstatistik Kurumu - Çevre İstatistikları. [Online] Available at: http://www.tuik.gov.tr/PreTablo.do?alt_id=1019 [Last Accessed 06 August 2018].

Anonymous 4: USEPA, 2000. EPANET Application for Modeling Drinking Water Distribution Systems. [Online] Available at: https://www.epa.gov/water-research/epanet [Last Accessed 04 August 2018].

Anonymous 5: Water And Waste Water International, 2018. Western Europe Poised For Major Investment. [Online] Available at: https://www.waterworld.com/articles/wwi/print/volume-26/issue-1/regulars/creative-finance/western-europe-poised-for-major-investment.html [Last Accessed 03 August 2018].

Anonymous 6: WHO, 2015. World Health Organization - Drinking water. [Online] Available at: http://www.who.int/news-room/fact-sheets/detail/drinking-water [Last Accessed 03 August 2018].

Anonymous 7: Worldmeters, 2018. World population. [Online] Available at: http://www.worldometers.info/world-population/ [Last Accessed 03 August 2018].

Akdeniz, T. & Muhammetoğlu, H., 2016. Chlorine residual management for water utilities using GIS, SCAD Aand modeling tools. Desalination and Water Treatment, 21 June, p. 9.

Armand, H., Stoianov, I. & Graham, N., 2015. Investigating the impact of sectorized networks on discoloration. ELsever science direct , pp. 407 - 415.

Armand, H., Stoianov, I. & Graham, N., 2018. Impact of network sectorisation on water quality management. International Water Association (IWA), pp. 1 - 16 .

ASAT, 2017a. İçmesuyu Temin Ve Dağitim Sistemlerindeki Su Kayiplari Yıllık Raporu, Antalaya: Antalya Su ve Atıksu İdaresi.

ASAT, 2017b. 2017 Yılı Faaliyet Raporu, Anyalya: Antalya Su ve Atıksu İdaresi.

ASAT, 2018. İçmesuyu Temin Ve Dağitim Sistemlerindeki Su Kayiplari Yıllık Raporu, Antalaya: Antalya Su ve Atıksu İdaresi.

ASAT, 2019. İçmesuyu Temin Ve Dağitim Sistemlerindeki Su Kayiplari Yıllık Raporu, Antalaya: Antalya Su ve Atıksu İdaresi.

AWWA, 2009. Water Audits and loss control programs: Manual of water supply practices M36. west quincy ave. denver, CO 80235: American Water Works Association.

Celik, E. & Muhammetoglu, H., 2007. Improving public perception of tap water in Antalya city, Turkey. IWA Journal of Water Supply: Research and Technology— AQUA, September September, p. 5.

Cheng, W. P., Yu, T. C. & Xu, G., 2014. Real-Time Model of a Large-Scale Water Distribution System. Science Direct, Volume 89.

Cobacho Jordán, R., Arregui De La Cruz, F., Soriano Olivares, J. & Cabrera Rochera, E., 2015. Including leakage in network models: an application to calibrate leak valves in EPANET. Journal of Water Supply: Research and Technology - Aqua., pp. 64(2):130-138..

Costanzo , F., Morosini, A. F., Veltri, P. & Savić, D., 2014. Model Calibration as a Tool for Leakage Identification in WDS: A Real Case Study. Elsever ScienceDirect, pp. 672 - 678.

Delgado, D. . M., 2007. Infrastructure Leakage Index (ILI) as a Regulatory and Provider Tool, s.l.: University of Arizona.

Dighade, R. R., Kadu, M. S. & Pande, . A. M., 2014. Challenges in Water Loss Management of Water Distribution Systems in Developing Countries, s.l.: International Journal of Innovative Research in Science, Engineering and Technology.

EurEau, 2017. Europe's water in figures: An overview of the European drinking water and waste water sectors, EU: The European Federation of National Associations of Water Services..

Falls, P. et al., 2011. Guidelines for water loss reduction: A focus on pressure management. Germeny: www.waterlossreduction.com.

Fanner, P., Thornton, J., Sturm, R. & Liemberger, R., 2007a. Evaluating Water Loss and Planning Loss Reduction Strategies.. Denver, Colorado.: AwwaRF and AWWA.

Fanner, P. V. et al., 2007b. Leakaeg Management Technologies. US: AwwaRF and Awwa.

Fontana, N., Giugni, M. & Glielmo, L., 2017. Real-Time Control of a PRV in Water Distribution Networks for Pressure Regulation: Theoretical Framework and Laboratory Experiments. Journal of Water Resources Planning and Management, (ASCE), 26 October, p. 14.

Gomes, R., Sousa, J. & Marques, A. S., 2013. The influence of pressure/leakage relationships from existing leaks in the benefits yielded by pressure management. Water Utility Journal 5, pp. 25 - 32.

Gülaydın, O., 2017. İçme Suyu Dağitim Şebekelerinde Ekonomik Su Kayiplari Seviyesinin Belirlenmesi: Antalya Kaleiçi Örneği. Antalya: Akdeniz Üniversitesi.

IWA, 2007. Water loss Task Force Leak Location and Repair: Guidance Notes, s.l.: March.

Karadirek, . İ. E., 2016. Urban Water Losses Management In Turkey: The Legislation And Challenges. Anadolu University Journal of Science and Technology A-Applied Sciences and Engineering, 04 August, p. 13.

Karadirek, I. E. et al., 2012. Implementation of Hydraulic Modelling for Water-Loss Reduction Through Pressure Management. Research Gate, 7, p. 15.

Kara, S., Karadirek, I. E., Muhammetoglu, A. & Muhammetoglu, H., 2015. Real time monitoring and control in water distribution systems for improving operational efficiency. Desalination and Water Treatment, 24 July, p. 15.

Kara, S., Karadirek, I. E., Muhammetoglu, A. & Muhammetoglu, H., 2016. Hydrayulic modeling of water distribution network in a tourism area with highly varying characteristics. ELSEVIER SCIENCE DIRECT .

Kartakis, S., Abraham, E. & McCann, J. A., 2015. WaterBox: A Testbed for Monitoring and Controlling Smart Water Networks, CySWater'15.

Kingdom, B., Liemberger, R. & Marin, P., 2006. The Challenge of Reducing Non-Revenue Water (NRW) in Developing Countries How the Private Sector Can Help: A Look at Performance-Based Service Contracting. Washington, DC: The World Bank .

Köker, E. & Altan-Sakarya, A., 2015. Chance Constrained Optimization of Booster Chlorination in Water Distribution Networks. Clean, Soil, Air Water, pp. p. 717-726.

Koker, E. & Altan-Sakarya, A., 2016. Optimization of Leakage in Water Distribution Networks Using Pressure Reducing Valves. Poznan, Poland, EURO 2016, 28th European Conference on Operational Research.

Kouchi, D. H. et al., 2017. Sensitivity of Calibrated Parameters and Water Resource Estimates on Different Objective Functions and Optimization Algorithms. MDPI WATER, 30 May, p. 16.

Lambert, A., 2003. Assessing Non-Revenue Water and its Components: A Practical Approach. The IWA water loss task force, 1st(Article No 2).

Lambert, A. O., Brown, T. G., Takizawa, M. & Weimer, D., 1999. A Review of Performance Indicators for Real Losses from Water Supply Systems. AQUA, December.

Liu, J. & Yu, G., 2014. Analysis of Demand and Leakage Distribution Uniformly Along Pipes.. Elsevir ScienceDirect, pp. 603 - 612.

Makaya, E. & Hensel, O., 2015. Water loss management strategies for developing countries: Understanding the dynamics of water leakages.. Kassel: s.n.

Mckenzie, R. S. & Wegelin, W., 2009. IMPLEMENTATION OF PRESSURE MANAGEMENT IN MUNICIPAL WATER SUPPLY SYSTEMS, South Africa: IWA.

Mpiana, L., Hamam, Y. & Abu-Mahfouz, A. M., 2017. Graph based Hydraulic Modelling of Pressure in Water Distribution Networks. IEEE, pp. 1558 - 1563.

Muhammetoğlu, H., 2017. Turistik Bölgelerde Otomatik Okuma Sayaçları Kullanarak Fiziki Su Kayıplarının Yüksek Hassasiyetle Belirlenmesi ve Yönetimi: Antalya-Kaleiçi Uygulaması, ANTALYA: TÜBİTAK.

Muhammetoglu, H. & Muhammetoglu, A., 2017. Içme Suyu Temin ve Dağitim Sistemlerindeki Su Kayiplarinin Kontrolü El Kitabi. Antalya: Menister of forests and water works.

Mutikanga, H. E., Sharma, S. K. & vairavamoorthy, K., 2010. Assessment of apparent losses in urban water systems, s.l.: Water and Environment Journal.

Öztürk, İ., Uyak, V., Çakmakcı, M. & Akça, L., 2007. Dimension Of Water Loss Through Distribution System and Reduction Methods in Turkey, s.l.: research gate.

Puust, R., Kapelan, Z., Savic, D. & Koppel, T., 2010. A review of methods for leakage management in pipe networks. Urban Water Journal, 24 February , p. 22.

Ramon, P. et al., 2014. Leak Localization in Water Networks. Model-Based Methodology Using Pressure Sensors Applied to a Real Network in Barcelona. IEEE, 14 July, pp. 24 - 36.

Rossman, L. A., 2000. EPA/600/R-00/057 EPANET 2 USERS MANUAL. Cincinnati, OH 45268: Water Supply and Water Resources Divisio, Environmental Protection Agenci (EPA).

Schwaller, J. & van Zyl, J. E., 2014. Modeling the Pressure-Leakage Response of Water Distribution Systems Based on Individual Leak Behavior. ASCE.

Thornton, J., Sturm, R. & Kunkel, G., 2008. Water Loss Control. s.l.:The McGraw-Hill Campanies.

Trifunovic, N., 2006. Introduction to Urban Water Distribution. 1st Edition ed. London: CRC Press.

Vicente, D. J., Garrote, L., Sánchez, R. & Santillán, D., 2015. Pressure Management in Water Distribution Systems: Current Status, Proposals, and Future Trends. American Society of Civil Engineers (ASCE).

Wright, R. et al., 2014. Adaptive water distribution networks with dynamically reconfigurable topology. International Water Association (IWA) , 16 June, pp. 1280 - 1301.

Xu, Q., Liu, R., Chen, Q. & Li, R., 2014. Review on water leakage control in distribution networks and the associated environmental benefits. Journal of Environmental Sciences, 11 February, p. 7.

ÖZGEÇMİŞ

Mustafa S. M. BOLBOL

Mustafa.bolbol.1992@gmail.com

ÖĞRENİM BİLGİLERİ

Yüksek Lisans 2015 – 2019	Akdeniz Üniversitesi Fen Bilimleri Enstitüsü, Çevre Mühendisliği Bölümü, Antalya
Lisans 2010 – 2015	Islamic University of Gaza (IUG) Faculty of engineering, department of civil engineering, Gaza, Palestine

MESLEKİ VE İDARİ GÖREVLER

GIS specialist 2015	Palestinian Land Authority Department of surveying, Gaza, Palestine
Teacher Assistant 2015	Islamic University of Gaza (IUG) Faculty of engineering, department of civil engineering, Gaza, Palestine

ESERLER

Uluslararası bilimsel toplantılarda sunulan ve bildiri kitaplarında basılan bildiriler

1- Bolbol, M., Muhammetoğlu H., Muhammetoğlu A. (2019). Smart Water Management for Smart Cities, May 3 – 4, 2019, Third International Students Science Congress. (Abstract/Oral Presentation/Full Paper)

2- Bolbol, M., Muhammetoğlu H., (2018). Modelling of Leakage Flow in Water Supply System, Antalya – Kaleiçi Case Study (Muhammetoğlu H., 2017), May 4 – 5, 2018, Second International Students Science Congress.
(Abstract/Oral Presentation)